UiT The Arctic University of Norway

Faculty of Science and Technology
Department of Geosciences

Seismic characterization and source rock evaluation of Lower Cretaceous organic-rich units on the Norwegian Continental Shelf

An integrated approach for understanding their occurrence and potential across different tectonic settings.

Andreas Hallberg Hagset

A dissertation for the degree of Philosophiae Doctor

February, 2023

Seismic characterization and source rock evaluation of Lower Cretaceous organic-rich units on the Norwegian Continental Shelf

An integrated approach for understanding their occurrence and potential across different tectonic settings

Andreas Hallberg Hagset
ARCEx – Research Centre for Arctic Petroleum Exploration
Department of Geoscience
Faculty of Science and Technology
UiT – The Arctic University of Norway
P.O. box 6050 Langnes
9037 Tromsø, Norway

A dissertation for the degree of Philosophiae Doctor

Supervisors:

Associate Professor Dr. Sten-Andreas Grundvåg

ARCEx – Research Centre for Arctic Petroleum Exploration
Department of Geoscience
Faculty of Science and Technology
UiT – The Arctic University of Norway
P.O. box 6050 Langnes
9037 Tromsø, Norway

Dr. Balazs Badics

Wintershall Dea Norge AS
Jåttåflaten 27
4020 Stavanger
Norway

Dr. Roy Davies

Wintershall Dea Norge AS
Jåttåflaten 27
4020 Stavanger
Norway

Professor Dr. Atle Rotevatn

Department of Earth Science
Faculty of Mathematics and Natural Sciences
UiB – University of Bergen
P.O. box 7803
5020 Bergen, Norway

Front page image: Outcrop picture of the Helvetiafjellet Formation (Barremian – Aptian) at Ullaberget, Svalbad (77°36'43.4"N, 15°12'18.1 "E).

Abstract

The Norwegian Continental Shelf (NCS) is a prolific petroleum province where exploration has been successfully conducted since the late 1960s. Most of the discoveries are sourced from widespread and highly prolific Upper Jurassic black shales. However, as exploration is maturing on the shelf, petroleum originating from these shales becomes continuously harder to find. Large areas of the shelf host deep Cretaceous basins where these traditional source rock units are too deeply buried. Here, the occurrence of a stratigraphically shallower source rock unit could potentially renew exploration strategies and reduce risk. Such source rocks may potentially be present in Cretaceous strata in multiple basins across the NCS. Although, research on Cretaceous organic-rich deposits has been conducted over several decades, their lateral extent and potential remain uncertain. By combining regional 2D reflection seismic data, wireline logs from numerous exploration wells, and a geochemical database, this study aims to broaden our understanding of key factors controlling the deposition and preservation of Cretaceous organic-rich units, establish their stratigraphic occurrence and lateral distribution, and finally elucidate their petroleum potential. In the Lower Cretaceous succession on the SW Barents Shelf, organic-rich units are associated with negative amplitude reflectors, which typically conform to regionally extensive maximum flooding surfaces (Paper I). These negative amplitude reflectors are tied to wireline logs and geochemical data, which together indicate the presence of four potential source rock units in this region of the NCS. These are the: (1) upper Hauterivian, (2) Barremian, (3) lower Aptian, and (4) upper Cenomanian organic-rich units. The deposition and preservation of these organic-rich units are confined to localized, fault bounded depocenters, which mainly formed during a well-known rifting event in the Late Jurassic – Early Cretaceous. Overall, most of these units display a limited petroleum potential, as they are of low quantity and quality. However, some localized potential occurs, particularly in the lower Aptian unit. In the Vøring Basin, on the mid-Norwegian margin, the oldest part of the Cretaceous succession is deeply buried, thus exhibiting a very limited potential (Paper II). Here, our findings indicate the upper Cenomanian organic-rich unit, which previously has been postulated to hold some potential, have been subjected to severe sedimentation rates, causing a dilution effect, and experienced recurring oxygenated conditions. Globally, the Cenomanian is associated with the occurrence of an Oceanic Anoxic Event (OAE II) and widespread deposition of prolific source rocks. Despite the inferred development of a mid-water oxygen minimum zone on the mid-Norwegian margin during this time, most of the exploration wells on the terraces and intra-basinal highs on this part of the NCS, indicate that the upper Cenomanian organic-rich unit have a limited and very localized petroleum potential at best due to the above-mentioned reasons. In Svalbard, at the exhumed NW corner of the NCS, the potential of open marine and paralic strata of Hauterivian – Barremian/early Aptian age is investigated (Paper III). Particularly coals and coaly shales in the Barremian paralic deposits show some potential. If similar deposits are present in the topsets of time-equivalent clinoforms elsewhere on the northern Barents Shelf, this may represent a hitherto unexplored source rock model in this part of the NCS.

Acknowledgements

First, I want to express my gratitude to my main supervisor Sten-Andreas Grundvåg. Your invaluable guidance, constructive criticism and support has been a pillar in this PhD project. I also want to say thank you for your patience and understanding, as this has not been an ordinary PhD journey. Your knowledge and expertise have helped me shape, navigate and complete this project. Thank you for supporting me and for the opportunity to start this PhD, and for all the opportunities that came with it.

I also would like to thank my co-supervisors Balazs Badics, Roy Davies and Atle Rotevatn. Although large parts of this PhD project have been affected by the pandemic, your support and guidance have been constant. I am grateful for your input and constructive criticism which has been paramount for the completion of the project. Many thanks to Wintershall-Dea who funded this PhD project.

Thank you to all my colleagues at the department of geosciences at UiT. It has truly been wonderful to have such eager and motivated colleagues around me. A special thanks to all my officemates at the department, who provided a fun and supporting work environment, you have all made my time here terrific and highly enjoyable.

I also want to express my gratitude to my family. My beloved Camilla, I am deeply grateful for everything you have done for me and our boys during this hectic time. Without you, this time-consuming endeavor would not have been possible to complete. Finally, words cannot express my appreciation to Johannes and Arthur, our dear boys, who fill our days with laughter and excitement. I'm for ever grateful.

Preface

This work is the result of a three-year PhD project that started in September 2018. The project was fully funded by Wintershall-Dea Norway and was associated with the former Research Centre for Arctic Petroleum Exploration (ARCEx). UiT – The Arctic University of Norway is the degree-awarding institution. The project was supervised by representatives both from academia and the petroleum industry. The supervisors were Associate Professor Dr. Sten-Andreas Grundvåg (ARCEx, UiT, UNIS), Dr. Balazs Badics (Wintershall-Dea), Roy Davis (Wintershall-Dea) and Professor Atle Rotevatn (UiB).

The main objective of this study is to establish the presence, spatial variations, depositional conditions, and petroleum potential of Cretaceous organic-rich units on the Norwegian Continental Shelf. To do this, the project combines regional 2D seismic data with wireline logs and geochemical data to map and evaluate the organic-rich units. In addition, conceptual models for the SW Barents Shelf and the mid-Norwegian margin have been established to elucidate key controls for the relevant units. These models take into consideration the paleodepositional conditions and processes necessary for organic-rich units to form and be preserved. The lateral distribution of the organic-rich units is discussed, and their potential is established through traditional source rock evaluation. Parts of this work have been presented at national conferences through oral presentations and posters.

The following ECTS-accredited courses have been completed in order to fulfill the educational component in the PhD degree: SVF- 8600 “Philosophy of science and ethics” (UiT, 6 ECTS), GEO-8126 “Practical seismic processing” (UiT, 5 ECTS), GEO-8144 Marine geology and geophysics cruise (UiT, 5 ECTS), GEO-8145 Arctic marine geology and geophysics workshop (UiT, 5 ECTS), AG-823 Sequence stratigraphy – a tool for basin analysis (UiT, 10 ECTS).

This thesis starts with an introduction and moves on to motivation and geological background (Chapters 1 and 2). Following, the thesis outlines the scientific approach (Chapter 3) and summary of the three research papers (Chapter 4). Then, the three research papers are discussed in the final synthesis (Chapter 8).

The three research articles are as follows:

I. Hagset, A., Grundvåg, S. A., Badics, B., Davies, R., & Rotevatn, A., 2022. **Tracing Lower Cretaceous organic-rich units across the SW Barents Shelf.** Mar. Petrol. Geol. 140, 105664. https://doi.org/10.1016/j.marpetgeo.2022.105664.

II. Hagset, A., Grundvåg, S. A., Badics, B., Davies, R., & Rotevatn, A., 2023. **Deposition of Cenomanian – Turonian organic-rich units on the mid-Norwegian Margin: controlling factors and regional implications.** Mar. Petrol. Geol. 149, 106102. https://doi.org/10.1016/j.marpetgeo.2023.106102

III. Hagset, A., Grundvåg, S. A., Wesenlund, F., Badics, B., Thieβen, O., 2023. **Source rock evaluation of Hauterivian-Barremian (Early Cretaceous) paralic deposits in Svalbard.** *Manuscript prepared for submission to journal of Petroleum Geoscience.*

Contents

1 Introduction

1.1 Rational and relevance

The current energy crisis and geopolitical situation in Europe have made petroleum resources from the Norwegian Continental Shelf (NCS) essential to maintain necessary energy supply to the continent. A recent report from the International Energy Agency (IEA) states that the European Union faces a shortfall of c. 27 billion cubic of natural gas in 2023 (IEA, 2022). The shortage of energy has made prices extremely volatile, and many communities and energy intensive sectors are now experiencing rising poverty and slowing economics. At the same time, governments are moving towards renewable energy sources which are less dependable, but necessary to help bridge the energy gap and reach the goals of the Paris Agreement (Way et al., 2022). In this context, new knowledge on the gas prone source rocks situated in the marginal basins on the NCS, could lead to the discovery of untapped resources that could help ensure a predictable and reliable energy supply. These resources could also help ensure a gentle transition to a society based on renewable energy, while maintaining stability and security (e.g. Way et al., 2022).

In the deep marginal basins along the mid-Norwegian and SW Barents shelves, the traditional Upper Jurassic source rock unit is overmature and spent due to deep burial (Doré et al., 1999; Ohm et al., 2008; Brekke, 2000; Zastrozhnov et al., 2020; Cedeño et al., 2021). Thus, to find new resources, exploration success depends on the occurrence of a stratigraphically shallower source rock units in these basins. Such alternative source rock units may occur in the Cretaceous succession (e.g. Leith et al., 1993; Brekke, 1999; Seldal, 2005; Ohm et al., 2008; Lerch et al., 2017; Sattar et al., 2017; Matapour and Karlsen, 2017).

This study document the stratigraphic occurrence, lateral distribution, and regional variations in the source rock characteristics of Cretaceous organic-rich units across the NCS. The main study areas are confined to the Cretaceous basins on the mid-Norwegian margin, the SW Barents Shelf, and Svalbard, the exhumed NW corner of the NCS. This study utilizes regional high quality 2D reflection seismic data, wireline logs, and an extensive geochemical database, to assess and elucidate the petroleum potential of the recognized organic-rich units. This integrated dataset form the basis for conceptual models made specifically for each region hosting organic-rich units which exhibit petroleum potential. These models emphasize the depositional conditions and controlling factors during development of the various organic-rich units.

The PhD project was fully funded by Wintershall-Dea,

and was partly affiliated to the former Research Center for Arctic Petroleum Exploration (ARCEx). The overall goal of the research center was to increase our understanding of the subsurface geology of the Barents Shelf and adjacent basins, assess geological risk, and thus mitigate environmental risk connected to exploration in frontier regions.

1.2 Formation of source rocks and its controlling factors – an introduction

The formation and preservation of source rocks is generally attributed to three controlling factors. These are: organic primary productivity, preservation potential, and sedimentation rate (Pedersen and Calvert, 1990; Demaison and Moore, 1980; Demaison et al., 1983; Bohacs et al., 2005; Katz, 2005). The following subchapters briefly describe the importance of these factors and how they operate and vary in time and space, ultimately governing source rock potential.

1.2.1 Primary production

To form a source rock, enough organic matter must be produced and incorporated into the sedimentary system. Primary production is thus considered the main controlling factor for organic-matter preservation (Pedersen and Calvert, 1990). Essentially, all organic matter is originally produced by photosynthesis in either the marine or terrestrial environment. In the marine environment, the photosynthesizes are pelagic phytoplankton and benthic algae. The productivity of these is dependent on both physical and chemical factors. Temperature and light are assumed to be the most important physical factors, where the amount of light is affected by the depth, latitude, and turbidity of the basinal waters. Hence, the highest amount of organic productivity takes place in the shallow photic zone and decrease rapidly towards deeper waters. The abundance and availability of nutrients (e.g. phosphates and nitrates) are essential to promote organic productivity, and are the most important chemical aspect. The availability of these nutrients is controlled by either upwelling of nutrient-rich waters from deep basins, or by fluvial input (e.g. Pedersen and Calvert, 1990; Katz, 2005). Organic matter derived from terrestrial sources, including wood, spores, pollen and leaves etc. are mostly transported to the basin through fluvial runoff, but may also be brought into deep marine basins by sediment gravity flows (e.g. Saller et al., 2006). In general, terrestrial sourced organic matter is often a significant contributor to the amount of organic matter occurring and being preserved in nearshore to marine environments (Pedersen and Calvert, 1990).

1.2.2 Preservation of organic matter

The benthic conditions where organic matter is deposited and subsequently buried, are important for source rock development. The main control is the concentration of dissolved oxygen in the water, as oxidizing environments allow bacteria to oxidize organic compounds to CO_2 and water, thus effectively degrading the organic matter (Demaison et al., 1983; Bohacs et al., 2005). This process will reduce the amount of organic matter and can continue until all organic matter is destroyed (Tissot and Welte, 1984). In contrast, anoxic water conditions only allow sulfate-reducing or methanogenic bacteria, which are less efficient in degradation of organic matter (Demaison and Moore, 1980; Demaison et al., 1983). Hence, the oxygen content has direct implications for the quantity and quality of organic matter preserved in the sediments (Demaison and Moore, 1980; Demaison et al., 1983; Tissot and Welte, 1984).

The occurrence of anoxic conditions and its implications towards preservation of organic matter in different basin settings have previously been demonstrated by Demaison and Moore (1980) and Demaison et al. (1983) (Fig. 1.1). These models indicate that anoxic conditions can occur when the oxygen demand exceed the supply in basins of different configurations. The bathymetric confinement of a basin might obstruct water circulation and the supply of oxygen, which may result in thermal and density water stratification (Fig. 1.1A). This is often the case in restricted basins, such as lakes and in silled basins such as fiords and rotated half grabens (e.g. Demaison et al., 1983; Fig 1.1A). As such, the basin configuration and bathymetric conditions have an overall control on water stratification and circulation, and thus deposition and preservation of organic matter. Moreover, in the open marine environment, high organic productivity in the photic zone attributed to high supply of nutrients from fluvial runoff and coastal upwelling, can lead to the development of an oxygen minimum zone (OMZ) with an anoxic core (Fig. 1.1B). Anoxia related to for example an OMZ can be significantly enhanced during times of global Oceanic Anoxic Events (OAEs: e.g. Arthur et al., 1987; Schlanger and Jenkyns, 1976; Jenkyns, 1980) which is further discussed in papers I – II, and the synthesis in particular.

Once the organic matter is incorporated into the sediments, it begins a transformation from biological organic matter into geological organic matter (Dembicki, 2016). During this process the organic matter is subjected to chemical alteration processes such a hydrolysis, reduction, oxidation and even biodegradation, which breaks down larger molecules into smaller organic compounds (Dembicki, 2016). These compounds either form kerogen (solvent-insoluble) or bitumen (solvent-soluble) during diageneses. Kerogen has traditionally been divided into four types based the composition of organic matter and the type of organisms it was derived from, but also based on how well the kerogen was preserved in the basin. As such, the various kerogen types reflect the primary source and depositional conditions in which the organic matter was subjected to during deposition and preservation (Peters and Cassa, 1994). The amount of hydrogen and the type of structure of the organic matter has the overall control on whether the kerogen is oil prone (kerogen Type I-II), gas prone (kerogen Type III), or inert (kerogen Type IV) (e.g. Tissot and Welte, 1984; Peters and Cassa, 1994; Dembicki, 2016).

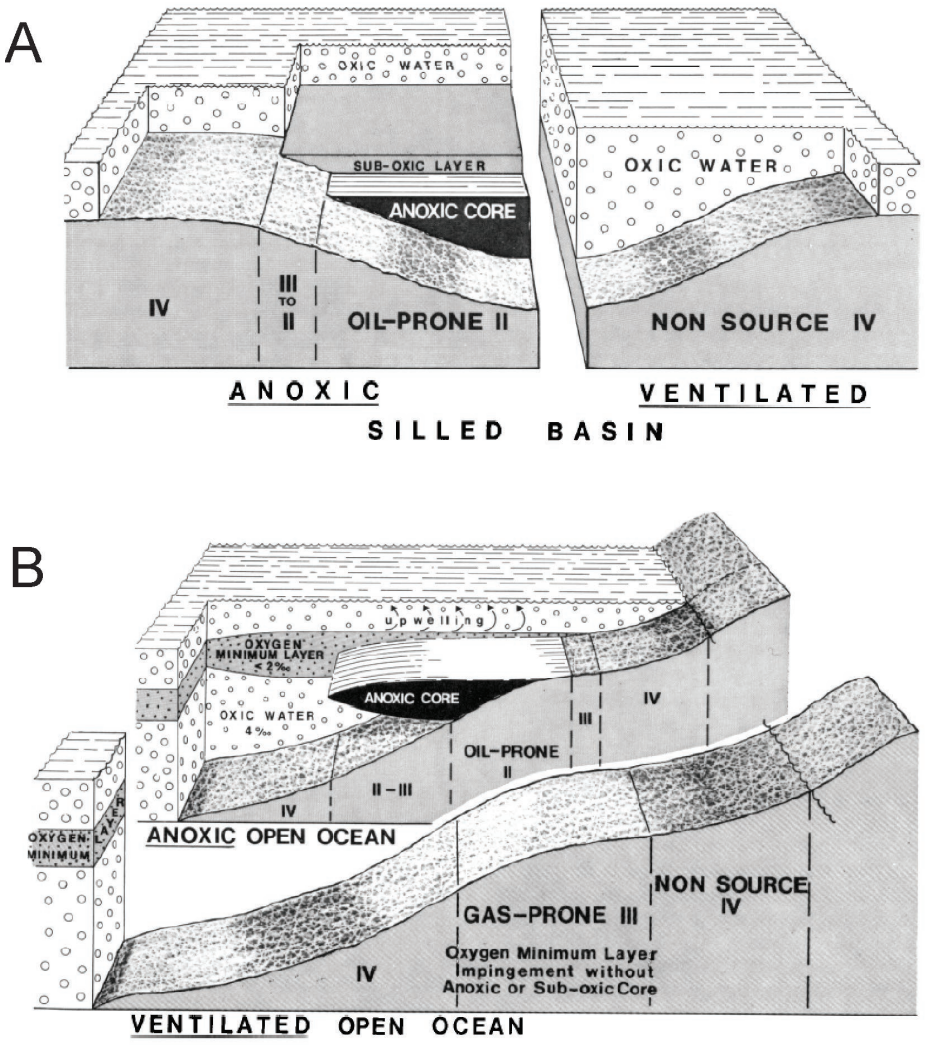

Fig.1.1 A) Deposition of organic matter in lakes and silled basins. Anoxic and sub-oxic water conditions occur when water circulation becomes stagnant due to a permanent density stratification in the water column. B) Deposition of organic matter in open marine environments. The development of an oxygen minimum layer/zone with and anoxic core is attributed to high marine productivity, which can be enforced by coastal upwelling. This can lead to the deposition of prolific source rocks. Kerogen type is annotated I - IV. The figure is attained from Demaison et al. 1983.

1.2.3 Sedimentation rate

Sedimentation rate is a critical factor for preservation of organic-rich sediments. The sedimentation rate should be below a threshold for organic matter to be preserved without experiencing a dilution effect cf. Ibach (1982) and Bohacs et al. (2005). The sedimentation rate should also be high enough to prevent prolonged exposure to biodegradation, and oxidants in porewater (Bohacs et al., 2005). Long exposure also makes them prone to erosion and transport (Bohacs et al., 2005). In most sedimentary basins, particularly those in tectonically active settings such as rift basins, sedimentation rate can vary over short distances. This is due to variable distance and connection to sediment source areas, the nature of sediment delivery systems (e.g. point sourced versus line sourced feeder systems),

tectonically controlled relative sea-level fluctuations and variations in sediment supply, as well as climatic factors (e.g. Prosser, 1993; Færseth and Lien, 2002; Gawthorpe and Leeder, 2002).

2 Geological background

The study areas in this thesis are located on the SW Barents Shelf (Paper I), the mid-Norwegian continental margin (Paper II), and Spitsbergen at the exhumed and exposed NW corner of the NCS (Paper III). Figure 2.1 gives a complete overview of the study areas, seismic data and exploration wells used in this study.

Characteristic for the Cretaceous period is a warm, greenhouse climate (Scotese et al., 2021), apparently with no polar ice caps, and the progressive and continued fragmentation of Pangaea during recurrent and widespread rifting events in the Late Jurassic – Early Cretaceous. In addition, this was associated with supra-regional volcanic activity emplacing multiple Large Igneous Provinces (LIPs) around the globe. The eustatic sea-level was historically high worldwide with extensive, shallow shelf seas bordering most of the continents, and as a response to igneous activity, oceanic anoxia and stagnation was a recurring phenomenon. The deep rifted basins on the NCS formed and evolved during this period and display structurally complex geometries and configurations. The following subchapters briefly outlined the geological settings of the main regions central to this study, starting in the south.

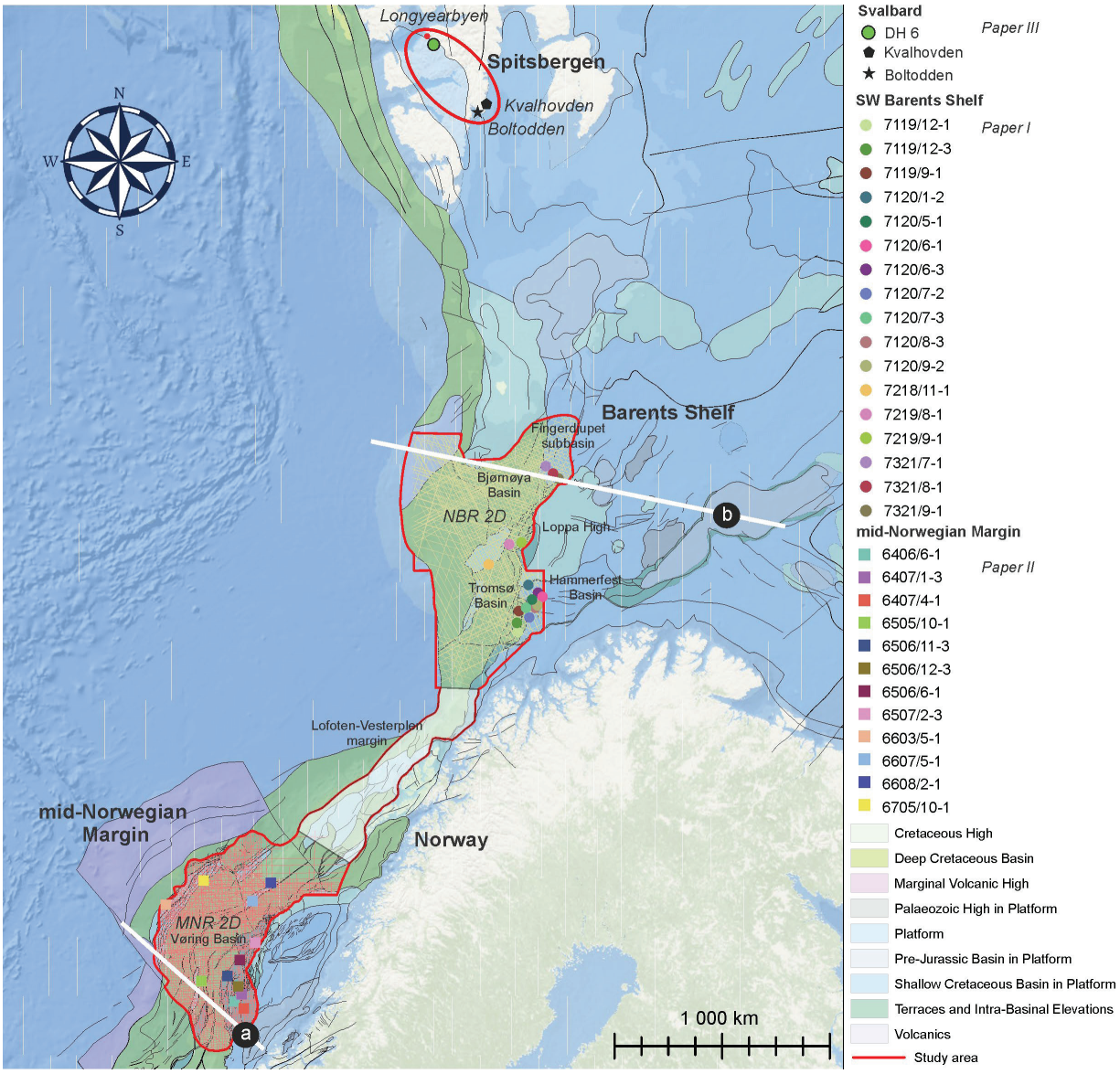

Fig. 2.1 Geographic and structural map indicating the extent of the study area, together with seismic and well data utilized in this PhD-project. This project has three main regions of focus: the SW Barents Shelf (Paper I), the mid-Norwegian Margin (Paper II), and Spitsbergen (Paper III). The location and orientation of the regional transects (a and b) are shown. The red polygon indicates the extent of the study area. The white area along the Lofoten-Vesterålen margin is not included in the study. Structural elements after Blystad et al. (1995).

2.1 The mid-Norwegian margin

The mid-Norwegian margin consist of three main regions, which are separated by fracture zones or lineaments (Brekke, 2000; Faleide et al., 2015; Zastrozhnov et al., 2020). These are the Møre, Vøring and Lofoten-Vestrealen regions. The Vøring Basin is a deep rift-basin and comprise several intrabasinal highs and have complex bathymetry (Fig. 2.1). The basin was mainly formed during the Late Jurassic – earliest Cretaceous regional extension event, which involved strike slip adjustment along the old lineaments. Thus, the preexisting structural grain influenced the overall geometry and segmentation of this deep rifted basin (Rotevatn et al., 2018; Zastrozhnov et al., 2020). In many places

the base of the Cretaceous succession is deeper than 7s two-way-travel time (Brekke, 2000). As such, the thickness of the Vøring Basin succession record the combination of high rates of thermal and load induced subsidence and high influx of sediments derived from the conjugated margins of Fennoscandia and East Greenland (e.g. Gawthorpe and Leeder, 2002; Færseth and Lien, 2002; Zastrozhnov et al., 2020). Consequently, much of the structural relief in the Vøring Basins was healed by mid-Cretaceous times (Fig. 2.2) (Faleide et al., 2015).

The Lower Cretaceous succession on the mid-Norwegian margin consist of the Lyr (Late Berriasian – early Aptian), Langebarn (Berriasian – Late Albian) and Blålange formations (Early Cenomanian – earliest Coniacian), cf. Dalland et al. (1988) revised by Gradstein et al. (2010). These formations were deposited under predominantly open marine conditions. As evident my the dark grey to brown mudstones which dominate the succession. Marls interbedded with carbonates (i.e. Lyr Formation), limestone stringer and turbidite sandstones also occur in the succession (Dalland et al., 1988).

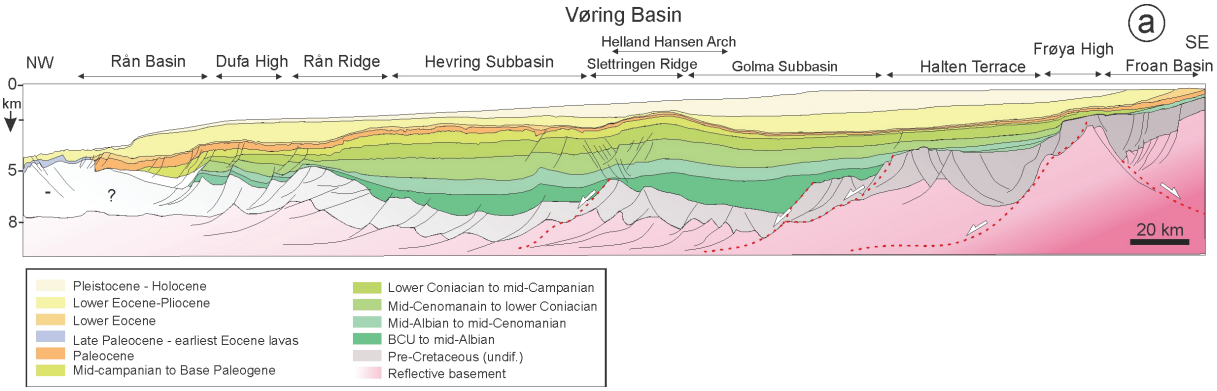

Fig. 2.2 Regional profile "a" extending from the Froan Basin in the SE, to the Rån Basin in the NW, showing the general configuration of the deep Cretaceous Vøring Basin on the mid-Norwegian Margin. The location and orientation of the regional profile is indicate in figure 2.1. Modified after Zastrozhnov et al. (2020).

2.2 SW Barents Shelf

The SW Barents Shelf is an epicontinental platform situated between the Norwegian mainland in the south and the Svalbard archipelago in the north which represent the exhumed and exposed NW corner of the shelf (Fig. 2.3). The most important basins for this study include the Fingerdjupet Subbasin, the Bjørnøya Basin, the Hammerfest Basin, the Tromsø Basin (Figs. 2.1 and 2.3). In general, the evolution of these basins is related to the Late Jurassic – Early Cretaceous extensional event which influenced the entire region (Gabrielsen et al., 1990; Doré, 1995; Faleide et al., 1984; 1993a, b; Kairanov et al., 2021).

The Tromsø and Bjørnøya basins are both deep marginal basins that formed during this extensional event (Fig. 2.3). These basins have similar rift and pull-apart configuration as the Vøring Basin. In contrast, the Hammerfest Basin and Fingerdjupet Subbasin are shallow extensional basins or failed-rift basins that formed during the same rifting event, but which also experienced local reactivation and

uplift (Faleide et al., 1993a, b; 2015; Marín et al., 2020). These basins are situated in the transition zone or along the margins of the deeper Tromsø and Bjørnøya Basins, respectively (Fig. 2.1 and 2.3).

The Lower Cretaceous succession on the Barents Shelf consist of the Knurr (Berriasian – Early Barremian), Kolje (Barremian – Early Aptian) and Kolmule (Aptian – Cenomanian) formations, all belonging to the Adventdalen Group (Parker, 1967; Dalland et al., 1988). During deposition of these mudstone dominated formations the conditions were predominantly open marine with well oxygenated water circulation (Dalland et al., 1988).

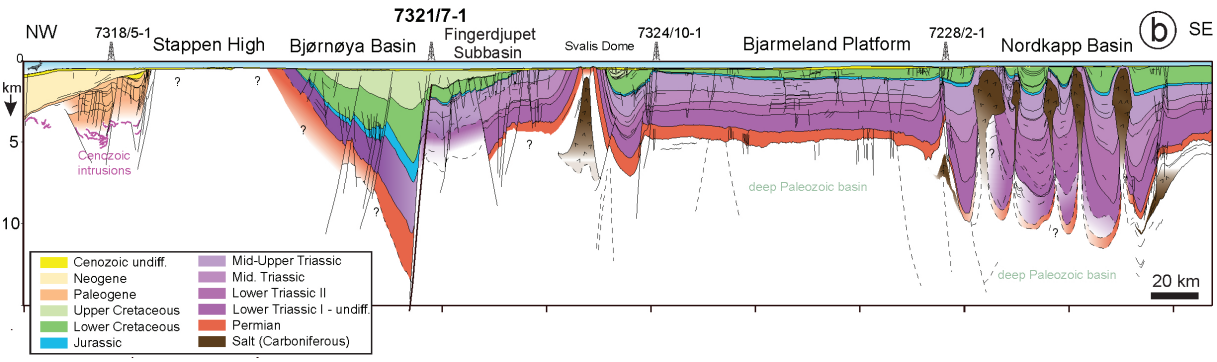

Fig. 2.3 Regional profile "b" extending from the Nordkapp Basin to the Stappen High, displaying the main structural features of the Barents Shelf. The orientation and location of this profile is shown in figure 2.1. Modified after Smelror et al. (2009).

2.3 Svalbard

The Svalbard archipelago is the uplifted and exposed northwestern corner of the Barents Shelf. The study area is situated on Spitsbergen, the largest island of the Svalbard archipelago (Fig. 2.1). In the Early Cretaceous, Svalbard formed part of a regional epicontinental basin (Steel and Worsley, 1984; Grundvåg et al., 2017). Shallow marine and paralic deposits belonging to the Rurikfjellet (Valanginian to Hauterivian) and Helvetiafjellet (Barremian to lower Aptian) formations was deposited along the western to northern margin of the subsiding epicontinental basin and was distributed by shelf processes across a southwards-sloping ramp shelf (Midtkandal and Nystuen, 2009; Grundvåg et al., 2020; Jelby et al., 2020). This fluvial to paralic system hosted amongst others lagoons, estuaries and marshes. Substantial amounts of terrestrial organic matter accumulated in these environments and its preservation led to the formation of coals and shales with high organic content. The Spitsbergen part of the platform experienced significant southward tilting in the Barremian (Gjelberg and Steel, 1995), which was accompanied by some minor fault activity and reactivation of older Paleozoic lineaments in eastern Spitsbergen (Nemec et al., 1988; Onderdonk and Midtkandal, 2010; Olaussen et al., 2018)

3 Scientific approach

This study utilizes three main datasets. These are: i) regional 2D reflection seismic data, ii) well data, attached with full sets of wireline logs, and iii) a geochemical database with Rock-Eval and GC-FID results. This chapter outlines the scientific approach and its limitations.

3.1 Aim and objectives

Identifying the thickness, organofacies, and overall quality of the organic-rich units by combining and integrating various data types provides new knowledge that could decrease risk in exploration on the NCS and elsewhere. Hence, the main aim of this project is to improve our understanding of various Cretaceous basins on the NCS and document the lateral distribution and potential of Cretaceous organic-rich units in the basin fill successions.

The key objectives of this project are to:

- Interpret seismic and well data in the deep to shallow marginal basins along the SW Barents and mid-Norwegian shelves, with the aim to map the presence/absence and spatial variations of potential source rocks, both on a supra-regional and basinal scale. As such, source rock evaluation of core and outcrop samples from the Lower Cretaceous succession of Svalbard are included.

- Establish and elucidate the depositional conditions and factors that were controlling the formation of Cretaceous organic-rich units across the NCS from south to north.

- Integrate all datasets to establish the organofacies and potential of recognized units, and ultimately develop conceptual models for the distribution of particularly the Lower Cretaceous source rocks in the studied marginal, offshore basins.

3.2 Data and Methods

3.2.1 Seismic data and interpretation

The overall approach follows the principals of seismic stratigraphic mapping (Mitchum et al., 1977; Vail, 1987; Veeken, 2007). The seismic horizons recognized and mapped in the SW Barents Shelf correspond to Cretaceous flooding surfaces which bounds a series of genetic sequences (Færseth and Lien, 2002; Marín et al., 2017). The surfaces was interpreted using the Petrel software. These seismic horizons are further tied to specific wireline signals typical for organic-rich sediments, following the methods outlined by Rider and Kennedy (2011) and Løseth et al. (2011). Interpretation of each specific seismic horizon was first conducted in the shallow basins and terraces (e.g. Fingerdjupet Subbasin, Hammerfest Basin and Halten Terrace). This allowed for high confidence in our interpretations given the high resolution and quality of the seismic data on relative shallow depths. It also made it possible with high confidence in our seismic to well ties. Subsequently, the seismic horizon was traced to the deeper basin and more frontier areas (e.g. Bjørnøya, Tromsø and Vøring Basins).

The Rock-Eval data was digitalized and implemented into Petrel, making it possible to better visualize and compare side-by-side with seismic data and wireline signals. Collectively, this approach let us achieve our objectives and confirm the presence/absence of organic-rich units associated with its specific seismic horizons in the subsurface. The Rock-Eval data was collected from the inhouse databased at Wintershall Dea, but the analysis (drill cuttings and core samples) was conducted by various independent consultant companies. Most of the Rock-Eval data is today publicly available in the Diskos database.

Seismic attributes, more specifically the “average negative amplitude” attribute, was generated from specific seismic horizons with a confirmed association with an organic-rich unit from the well and RockEval data. This generation was conducted on most of the 2D seismic surveys and gathered to form distribution maps of average negative amplitudes. This map is based on the principles that organic matter has significant less density than surrounding marine shale and will thus produce a negative acoustic impedance (AI) contrast in the seismic section cf. Løseth et al. (2011). The magnitude of these negative amplitudes can to some degree be correlated with Total Organic Carbon (TOC) cf. Løseth et al. (2011).

3.2.2 Well and Geochemical data

This project utilizes 12 exploration wells located at mid-Norwegian margin, 17 at the SW Barents Shelf and one CO2 research well on Svalbard, in addition to samples from several outcrop sections. The distribution of these exploration/research wells is outlined in Figure 2.1. They are also publicly available through the Norwegian Petroleum Directorate and the Diskos database. Attached to these wells are full setts of wireline logs which assisted in the identification and thickness estimation of the organic-rich units in paper I and II. A brief summary of the typical wireline responses to organic-rich units is provided in Paper I, for details see Rider and Kennedy (2011).

The TOC and Rock-Eval pyrolysis parameters S2, HI and T_{max} was digitalized and imported into the Petrel software in paper I and II. This gave the possibility for a powerful side-by-side comparison with wireline logs in the well section window, but also directly on the 2D seismic data. As such, this method allows for high confidence in establishing the presence of organic-rich units in the exploration wells but also tying the organic-rich units to the correct seismic reflector.

The Svalbard dataset consist of 35 outcrop and core samples. All 35 samples have complete Rock-Eval profiles, but only 5 samples have measured vitrinite reflectance and 11 samples have a full set of GC-FID results. All analysis and measurements of these samples was conducted by Applied Petroleum Technology AS (APT), and belonging results have been made available in the Supplementary files of paper III (Subchapter 7.10).

To evaluate the richness, type and thermal maturity of the organic-rich units, traditional source rock evaluation of the Rock-Eval data, following the principles of Espitalié et al. (1977), Peters (1986) and Peters and Cassa (1994) are applied.

3.2.3 Data uncertainty

The main limiting factor and uncertainty involved in Paper I and II, is deteriorating seismic quality and reflector attenuation with depth. This creates uncertainty in the seismic interpretations in the deeper basins and might lead to the wrong stratigraphic placement of seismic horizons in the seismic section. The interpreter has tried to limit the risk for wrong interpretation by tracing seismic horizons carefully over fault complexes and tying them to the few exploration wells in the deeper basin segments. Seismic mapping of the lateral extent of the organic-rich units, is limited by the vertical resolution of the 2D seismic data, as thin and condenses organic-rich units could fall beneath the vertical resolution (Brown, 2011). Consequently, these units will not appear with an individual reflector in the seismic section (e.g. Løseth et al., 2011) and the seismic horizon will follow the flooding surface. As seismic quality and vertical resolution decrease with depth, mapping of individual reflectors becomes more uncertain in the deeper basins on the NCS (Brown, 2011). In addition, the non-linear relationship between AI and TOC becomes unstable in the deeper basins cf. Løseth et al., 2011. As such, the negative amplitude map presented in Paper I, only gives an indication of the possible distribution of the organic rich units.

Although wireline logs give a higher resolution and more detailed look at the physical subsurface, there could be complications such as drilling mud intrusions that could affect the wireline data. There are also differences in value-standards between some of the exploration wells, giving them different wireline values for equivalent intervals. The change in casing dimensions during drilling operation could also alter and change the wireline logs. Overall, the well data is of high quality and applicable for both detailed and regional studies.

Rock-Eval data is derived from drill cuttings or sidewall cores. As such, they are susceptible to contamination during drilling operations that could alter the chemical signal (e.g. from mud intrusions, drilling mud contamination) (Rider and Kennedy, 2011). Rock-Eval samples could also be subject to other types of contamination and thermal alternation, such as exposure to weathering or too high temperatures when drying the samples. There is also a great variability in the sample spacing in the

Rock-Eval data between exploration wells, which could complicate interpretations. Abnormal values have been checked and removed from the database when appropriate. The outcrop samples collected at Kvalhovden and Boltodden in Svalbard are also prone to weathering, which can severely alter the organic composition (Clayton and Swetland, 1978; Forsberg and Bjorøy, 1983).

4 Summary of research papers

4.1 Paper I

Hagset, A., Grundvåg, S.-A., Badics, B., Davies, R. & Rotevatn, A., 2022. ***Tracing Lower Cretaceous organic-rich units across the SW Barents Shelf.*** *Mar. Petrol. Geol. 140, 105664.* https://doi.org/10.1016/j.marpetgeo.2022.105664.

In paper I, the Lower Cretaceous succession was investigated by combining regional 2D seismic data, wireline logs, and Rock-Eval data. The main aim for the paper was to document the presence of Lower Cretaceous organic-rich units and map their lateral extent on the SW Barents Shelf. In addition, the paper aim to establish the petroleum potential and the depositional conditions during formation of these organic-rich units. The mapped seismic horizons associated with organic-rich units corresponds to regionally extensive flooding surfaces, previously documented by Marín et al. (2017). Paper I thus builds on the sequence stratigraphic framework established by Marín et al. (2017, 2018a, 2018b) and Serck et al. (2017) in the shallow Hammerfest Basin and Fingerdjupet Subbasin. In the deeper Tromsø Basin, the seismic interpretation and sequence stratigraphic sub-division builds on the recent work of Kairanov et al. (2021).

In seismic data, the flooding surfaces appear as negative amplitude reflectors which can be traced from the shallow basins on the platform into the deeper basins along the western shelf margin. Moreover, these negative amplitude reflectors can be tied to intervals exhibiting increased organic carbon contents in numerous exploration wells. Four potential source rock units seems to occur in the Lower Cretaceous succession on the SW Barents Shelf. These are the: (1) upper Hauterivian, (2) Barremian, (3) lower Aptian, and (4) upper Cenomanian units. Negative amplitude maps was generated for the lower Aptian and upper Cenomanian units. This map gives a first-hand indication on the lateral distribution of the organic-rich units. The lower Aptian unit is confined to fault-bounded depocenters.

The source rock potential of each specific unit was assessed using traditional Rock-Eval data. Our findings indicate that the Barremian and Hauterivian organic-rich units have a local potential in the Hammerfest Basin. These units exhibit a kerogen Type II organofacies in this structurally restricted, fault-bounded depocenter. However, these units cannot be traced further towards the deeper Tromsø Basin. The most prolific organic-rich units were encountered in the Fingerdjupet Subbasin. Here, a lower Aptian unit, exhibit a clear kerogen Type II organofacies and high Hydrogen index (HI) values, typical for prolific oil-generating source rocks. This prolific unit was also deposited in a fault bounded depocenter. The upper Cenomanian unit appear to have a semi-regional distribution and displays a clear negative amplitude that could be easily traced across the basins. However, from the available well and RockEval data, no source rock potential was established to be associated with the corresponding seismic horizon. Thus, we suggest that the deposition and preservation of the prolific organic-rich units on the SW Barents Shelf margin are coupled to localized, fault bounded depocenters, mainly controlled by Late Jurassic – Early Cretaceous rifting and local reactivation events.

4.2 Paper II

Hagset, A., Grundvåg, S.-A., Badics, B., Davies, R., & Rotevatn, A., 2023. ***Deposition of Cenomanian – Turonian organic-rich units on the mid-Norwegian Margin: controlling factors and regional implications.*** *Mar. Petrol. Geol. 149, 106102. https://doi.org/10.1016/j.marpetgeo.2023.106102*

In paper II, the Lower to middle Cretaceous succession was investigated on the mid-Norwegian margin, using similar methodology as in paper I. The main aim was to document the presence of the organic-rich units, evaluate their source rock potential and map their lateral extent on the mid-Norwegian margin. Our findings indicate that Hauterivian, Barremian, and lower Aptian organic-rich units are present on the Halten and Dønna Terraces but are severely eroded or condensed elsewhere in the study area. These units cannot not be tied to the deeper Vøring Basin succession due to the lack of well data, diminishing seismic quality and uncertainty. As such, our investigation focus on an organic-rich unit corresponding to the Cenomanian/Turonian boundary interval which is associated with the global anoxic event OAE II (e.g. Arthur et al., 1987; Leckie et al., 2002; Schlanger and Jenkyns, 1976; Jenkyns, 1980) and deposition of prolific source rock units elsewhere (Doré et al., 1997).

The seismic reflector associated with this upper Cenomanian organic-rich unit is regionally distributed and can be tied to many of the exploration wells situated in the outer part of the Vøring Basin. Source rock evaluation indicate that the organic-rich unit have an elevated potential on the Halten Terrace. Here, samples display increased TOC and S2 values, and a kerogen Type III-II composition in exploration wells 6507/2-3 and 6506/11-3. However, although the organic-rich unit was demonstrated to be early mature and record increased organic content, the low hydrogen index values unfortunately indicate a limited source rock potential.

In the deeper segments of the Vøring Basin, the seismic reflector corresponding to the upper Cenomanian organic-rich unit can be traced and tied to a few key exploration wells. In these wells there are limited amount of datapoints across the Cenomanian/Turonian boundary interval. However, one sample from the Vigrid Syncline (Well 6705/10-1) which display elevated S2 and HI values and have a kerogen Type II composition, may suggest that there could be a localized potential along the margins of the syncline.

Moreover a conceptual model outlining the variable depositional environments and the controlling factors is presented and discussed. The model highlights the basin configuration and the influence of upwelling, as well as the inferred influence and contribution of the OAE II. Finally, we discuss the extreme sedimentation rates along the mid-Norwegian margin during the Early Cretaceous, erosion by gravity flows, and periodically oxygenated conditions that hindered preservation of sufficient quantities of organic matter. The combination of these factors appear to effectively have limited the potential of the proposed upper Cenomanian organic-rich source rock unit on the mid-Norwegian margin.

4.3 Paper III

Hagset, A., Grundvåg, S.-A., Wesenlund, F., Badics, B. & Thießen, O., 2023. ***Source rock evaluation of Hauterivian-Barremian (Early Cretaceous) paralic deposits in Svalbard.*** *Manuscript prepared for submission to journal of Petroleum Geoscience.*

In paper III, the uppermost part of the Rurikfjellet (Hauterivian) and the Helvetiafjellet formations (Barremian –lower Aptian) on Spitsbergen is investigated, aiming at evaluating the source rock potential of inferred organic-rich intervals within this overall paralic succession. The study combines outcrop samples from Kvalhovden and Boltodden in eastern Spitsbergen and core samples from the DH6 well in Adventdalen, central Spitsbergen (Fig. 2.1). As these paralics are of no commercial interest, the motivation for the study is linked to the possible presence of analogous deposits in time-equivalent clinoform packages on the Barents Shelf south of Spitsbergen. The paper investigates organic-rich units related to certain depositional environments established by previous workers including sediments deposited in lagoons, interdistributary bays, coastal plain lowlands, and prodelta settings. Special attention is paid to a retreating barrier-lagoonal system associated with the transgressive development of the Helvetiafjellet Formation. This system, which deposits occur in the uppermost marine influenced part of the formation, might theoretically have fostered restricted and oxygen deficient conditions promoting the accumulation and preservation of organic matter. Moreover, the samples from Kvalhovden represent prodelta fines deposited in a large slump scar, which developed close to the Lomfjorden Fault Zone in eastern Spitsbergen. This slump scar mini-basin, which hosts a series of partly rotated slump blocks and in-situ buttress blocks, may have promoted restricted conditions, in similar fashion as rotated fault blocks in the rift basins on the SW Barents Shelf, albeit at an order of magnitude smaller.

By combining TOC, Rock-Eval, GS-FID and vitrinite data we have established that samples belonging to the Rurikfjellet Formation, which consists of silty shales deposited in an open marine, prodelta setting, yield the poorest petroleum potential of all the samples in the dataset. Thus, the organofacies was established to be Type III – IV, which is consistent with the GC-FID results that indicates a distinct terrestrial signature for the organic matter. This interpretation is in line with previous work and confirms the deltaic origin of this unit. Furthermore, samples from the uppermost part of the Helvetiafjellet Formation in central Spitsbergen, which consists of mudstones deposited in a lagoonal setting, display low TOC and S2 and HI values, like the silty shale samples from the Rurikfjellet Formation. Thus, our results suggests that the hypothesized retreating barrier-lagoonal system did not provide favorable conditions for preserving organic matter in central Spitsbergen. The prodelta mudstone samples from the Kvalhovden locality, which was deposited in a slump scar mini basin, all have organic matter of a kerogen Type IV composition. Furthermore, they exhibit low TOC, Rock-Eval S2 and HI values, and the GC-FID results indicate that the organic matter was of terrestrial origin, deposited in an oxidizing environment As such, the prodelta deposits yield a low petroleum potential, which indicate that the slump scar was well ventilated and did not foster favorable conditions for source rock development.

The most prolific samples all belong to the Helvetiafjellet Formation and were collected in well DH6, the Kvalhovden, and the Boltodden localities. These samples, which consists of coal to coaly shale

deposited in coastal plain lowlands and interdistributary bays, contains organic matter of kerogen Types II/III – III composition. However, intermediate HI values, typical of coal, is effectively limiting the potential of these deposits and suggest that they are a mixture of oil and gas prone units. Vitrinite reflectance, T_{max} and sterane isomerization ratios indicate that these source rocks are peak mature. The GC-FID results confirm that the organic matter in all the samples is mostly of terrestrial origin, deposited in an oxidizing environment which was highly susceptible to biodegradation.

To conclude, our analyses indicate that the organic-rich deposits of the Rurikfjellet and Helvetiafjellet formations appear to have a low potential. Consequently, their importance with respect to regional exploration seems limited.

5 Paper I

Tracing Lower Cretaceous organic-rich units across the SW Barents Shelf

Hagset, A.[1,] *, Grundvåg, S.-A.[1,2], Badics, B.[3], Davies, R.[3], Rotevatn, A.

[1] Department of Geosciences, UIT The Arctic University of Norway, Tromsø, Norway

[2] Department of Arctic Geology, University Centre in Svalbard, PO Box 156, N-9171 Longyearbyen, Norway

[3] Wintershall DEA, Stavanger, Norway

[4] Department of Geosciences, University of Bergen, Bergen, Norway

*Corresponding author e-mail: aha155@uit.no)

Marine and Petroleum Geology 140 (2022) 105664

Contents lists available at ScienceDirect

Marine and Petroleum Geology

journal homepage: www.elsevier.com/locate/marpetgeo

Tracing Lower Cretaceous organic-rich units across the SW Barents Shelf

A. Hagset [a,*], S.-A. Grundvåg [a,b], B. Badics [c], R. Davies [c], A. Rotevatn [d]

[a] Department of Geosciences, UIT the Arctic University of Norway, Tromsø, Norway
[b] Department of Arctic Geology, University Centre in Svalbard, PO Box 156, N-9171, Longyearbyen, Norway
[c] Wintershall DEA, Stavanger, Norway
[d] Department of Geosciences, University of Bergen, Bergen, Norway

ARTICLE INFO

Keywords:
Lower Cretaceous stratigraphy
SW Barents Shelf
Source rock evaluation
Seismic attributes
Rock-Eval data analysis
Wireline logs
Source rock characteristics
Fault-bounded depocenters

ABSTRACT

On the Barents Shelf, the northernmost and least explored hydrocarbon province of the Norwegian Continental Shelf, Upper Jurassic organic-rich shales have traditionally been given most attention as these represent the most prolific source rock unit of the region. However, in the western frontier areas of the Barents Shelf, the Upper Jurassic is too deeply buried. By combining high-resolution 2D seismic data, well logs, and digitalized Rock-Eval data, this study documents the lateral distribution and variability of alternative source rock units within the Lower Cretaceous succession on the SW Barents Shelf. Negative high-amplitude anomalies are traced from shallow basins on the platform westward into deeper basins along the western shelf margin. The anomalies are tied to intervals of increased total organic carbon contents in several exploration wells, and we thus establish the presence of four potential source rock units; these are the (1) upper Hauterivian, (2) Barremian, (3) lower Aptian, and (4) upper Cenomanian units. Based on the distribution of the associated seismic anomalies, we infer that the deposition and preservation of these organic-rich units are coupled to localized, fault bounded depocenters, mainly controlled by Late Jurassic – Early Cretaceous rifting and local reactivation events. The lower Aptian stands out as the most significant source rock unit, particularly in the Fingerdjupet Subbasin, where it displays a kerogen Type II composition. The distribution and development of this oil-prone source rock unit is linked to an early Aptian fault reactivation event. Due to increased sediment influx in combination with high subsidence rates during the Albian to Cenomanian, potential pre-Aptian source rock units appear to have undergone too deep burial in the Tromsø and Bjørnøya basins to be presently generative. Furthermore, organic matter dilution due to increased sedimentation rates seems to have reduced the overall potential of the upper Cenomanian unit.

1. Introduction

The presence of a thermally mature and viable source rock unit is one of the key risk factors in oil and gas exploration (White, 1993; Katz, 2005). Several factors may influence the development of a potential source rock unit, including primary organic production, preservation environment, and sedimentation rate (Pedersen and Calvert, 1990; Arthur et al., 1994; Calvert et al., 1996; Bohacs et al., 2005; Katz, 2005). In addition, the tectonic setting of a basin may represent an important first-order control on processes such as accommodation development (e.g. subsidence and burial) and water mass circulation that are vital for source rock development (Demaison et al., 1983; Gawthorpe et al., 2000). Across the Norwegian Continental Shelf (NCS), Upper Jurassic organic-rich shales have traditionally been given the most attention, as these represent the main source rock unit charging most of the largest producing oil and gas fields (Demaison et al., 1983; Cooper et al., 1984; Isaksen et al., 2001; Marín et al., 2020). This has left alternative source rock units to be considered as insignificant or even neglected (Ohm et al., 2008). This is also the case for the Barents Shelf, the northernmost and least explored hydrocarbon province of the NCS. Across large parts of the NCS, the widely distributed Upper Jurassic source rock unit was generally deposited during a period characterized by active faulting forming structurally restricted basins that were ideal sites for the accumulation and preservation of organic matter (e.g. Faleide et al., 1984; Leith et al., 1993; Jongepier et al., 1996; Langrock et al., 2003; Marín et al., 2020). However, despite its extensive distribution across the SW Barents Shelf, the traditional Upper Jurassic source rock unit only appears to be mature in a narrow belt along the western margin of the Hammerfest Basin and on the margins of the Loppa High (Dore, 1995; Marín et al., 2020). In the deeper marginal basins further to the

* Corresponding author.
E-mail address: aha155@uit.no (A. Hagset).

https://doi.org/10.1016/j.marpetgeo.2022.105664
Received 14 January 2022; Received in revised form 22 March 2022; Accepted 23 March 2022
Available online 28 March 2022

west, the Upper Jurassic source rock unit has been buried very deeply and is over-mature (Ohm et al., 2008). Documenting the presence of alternative source rock units at stratigraphic shallower intervals is, therefore, crucial for exploration success in these frontier areas.

Such alternative source rock units may occur in the Lower Cretaceous and Paleogene successions (Leith et al., 1993; Øygard and Olsen, 2002; Seldal, 2005; Lerch et al., 2017; Sattar et al., 2017). Several exploration wells have confirmed the presence of Lower Cretaceous source rock units in the Fingerdjupet Subbasin (e.g. 7321/9–1) and in the western part of the Hammerfest Basin (e.g. 7120/6-3 S) (NPD Factpages, 2021). Moreover, some petroleum discoveries have previously been linked to Lower Cretaceous source rocks by biomarkers (e.g. wells 7120/10–1, 7120/1–2, 7120/2-3 S, 6706/12–2, 6305/8–1, and 6405/7) (Lerch et al., 2017; NPD Factpages, 2021), and on the Mid-Norwegian Shelf are several oil discoveries identified as sourced by Cretaceous source rocks (Matapour and Karlsen, 2017). A regionally extensive, gas condensate-prone source rock unit of early Aptian age have been identified onshore Svalbard at the northwestern corner of the Barents Shelf (Midtkandal et al., 2016; Grundvåg et al., 2019). In addition, oil stains discovered in sandstones onshore northeastern Greenland indicate the presence of a Cretaceous-age source rock (Bojesen-Koefoed et al., 2020). However, there are large uncertainties

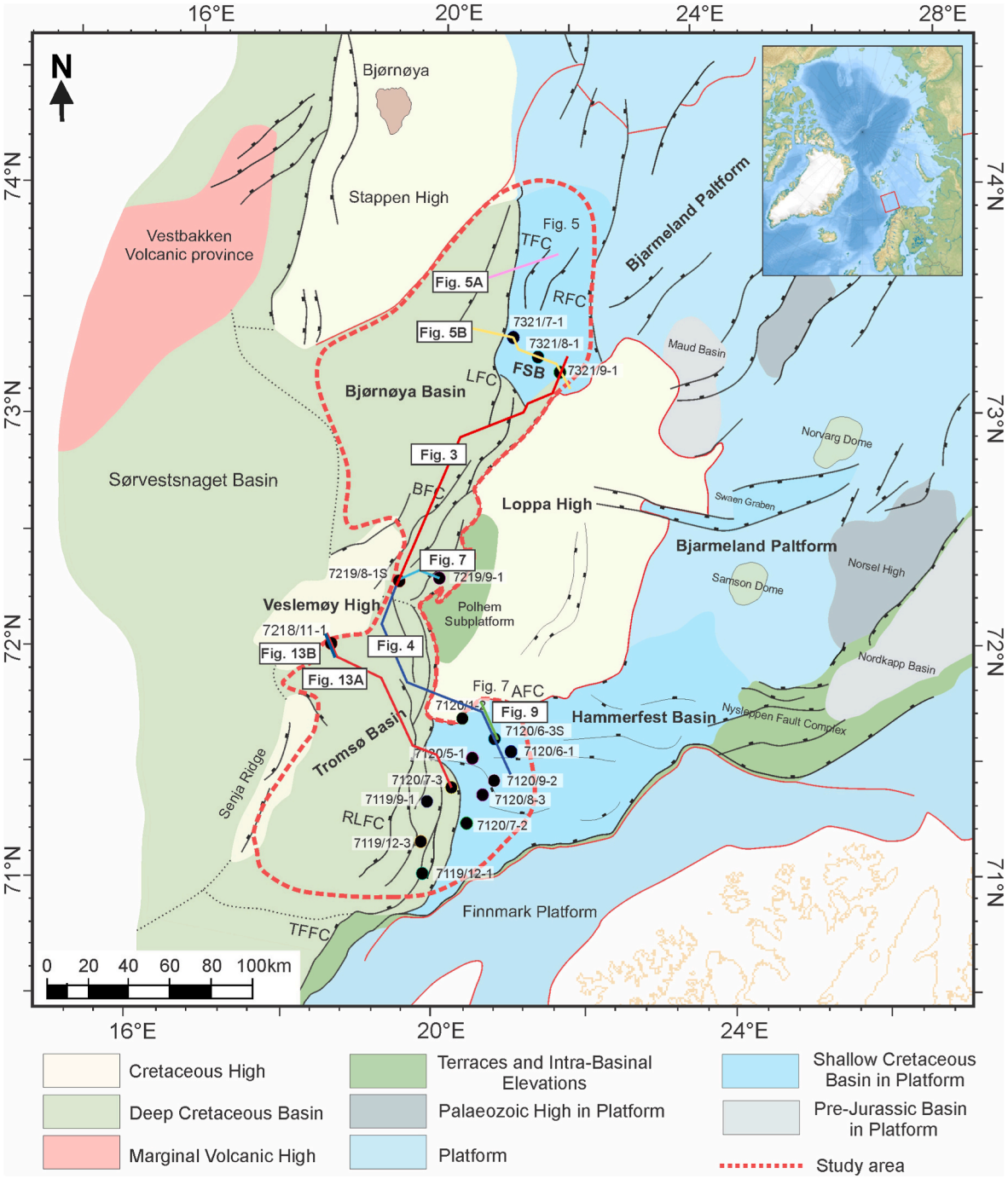

Fig. 1. Structural map of the SW Barents Shelf. The study area includes the western part of the Hammerfest Basin, the Tromsø Basin, the Bjørnøya Basin and the Fingerdjupet Subbasin. Key wells and seismic lines are annotated. TFFC: Troms Finnmark Fault Complex, RLFC: Ringvassøy Loppa Fault Complex, BFC: Bjørnøyrenna Fault Complex, AFC: Asterias Fault Complex, FSB: Fingerdjupet Subbasin, LFC: Leirdjupet Fault Complex, RFS: Randi Fault Set. Modified after NPD Factpages (2021).

related to the presence, stratigraphic position, and lateral distribution of Lower Cretaceous source rock units offshore, particularly in the deep basins along the western shelf margin. The regional significance of Lower Cretaceous source rocks is, therefore, still largely unclear (Dore, 1995; Mann et al., 2002; Øygard and Olsen, 2002; Seldal, 2005; Lerch et al., 2017). Thus, a detailed investigation of organic-rich units exhibiting source rock potential within the Lower Cretaceous succession seems essential in developing new play models and reducing exploration risk in the western frontier areas of the Barents Shelf.

By combining high-resolution regional 2D seismic data, well logs, and a digitalized Rock-Eval database, this study documents the lateral and stratigraphic distribution and variability of potential source rock units within the Lower Cretaceous succession on the southwestern Barents Shelf (Fig. 1). In particular, this study applies traditional source rock evaluation methods (sensu Peters and Cassa, 1994) to establish the potential and quality of the recognized potential source rock units in the shallow basins located on the interior platform part of the shelf (e.g. the Fingerdjupet Subbasin and Hammerfest Basin). This analysis will further aid in mapping the lateral and stratigraphic distribution of potential source rock units in the deeper marginal basins (e.g. the Tromsø and Bjørnøya basins). Finally, various factors that controlled the development and distribution of the investigated organic-rich intervals, such as the tectono-sedimentary evolution of the various basins, are evaluated and discussed.

2. Geological framework

2.1. Structural setting

The Barents Shelf is an epicontinental platform situated between the Norwegian mainland in the south, the Svalbard archipelago and Franz Josef Land to the north, and Novaya Zemlya to the east/southeast (Fig. 1). Following the Caledonian orogeny in the Late Silurian – Early Devonian, the shelf has undergone multiple phases of extension and subordinate compression, which have resulted in a complex pattern of fault-bounded basins and highs, as well as platform areas and smaller inversion-related structures (Faleide et al., 1984, 1993a, 1993b, 2008; Riis et al., 2014). The main extensional, basin-forming phases occurred during i) the Late Devonian associated with the collapse of the Caledonian orogenic belt, ii) the Late Carboniferous, iii) the Late Permian – Early Triassic, iv) the Late Jurassic – Early Cretaceous, and v) finally during the complete opening of the NE Atlantic rift system during the Late Cretaceous – Early Paleogene (Faleide et al., 2008, 2015).

The most important basins for this study include: 1) the Fingerdjupet Subbasin; 2) the Bjørnøya Basin; 3) Hammerfest Basin; and 4) the Tromsø Basin (Fig. 1). In general, the evolution of these basins is related to the Late Jurassic – Early Cretaceous extensional event. A brief outline of their structural development is given below.

2.1.1. Fingerdjupet Subbasin

The Fingerdjupet Subbasin is considered to be the shallow northeastern extension of the Bjørnøya Basin. Its southern and western boundaries are defined by the Leirdjupet Fault Complex (LFC) (Gabrielsen et al., 1990; Faleide et al., 1993a), whereas the Bjarmeland Platform and the Loppa High defines its eastern and southeastern boundaries (Gabrielsen et al., 1990, Fig. 1). The Fingerdjupet Subbasin is characterized by a horst and graben configuration, with a series of faults that developed during Late Jurassic extension and local reactivation during the Early Cretaceous (Faleide et al., 1993b). This includes the Randi Fault Set (RFS), situated in the eastern transition to the Bjarmeland Platform (Serck et al., 2017). Furthermore, an Aptian extensional event is well documented in the Fingerdjupet Subbasin (Faleide et al., 1993a; Clark et al., 2014; Blaich et al., 2017; Serck et al., 2017). This fault activity initiated the formation of localized wedges and contributed to the uplift of the northern parts of Loppa High (Indrevær et al., 2017; Marín et al., 2017). Because of Cenozoic uplift and erosion (Henriksen et al., 2011; Lasabuda et al., 2018, 2021) only the lowermost part of the Lower Cretaceous succession is preserved in the basin.

2.1.2. Bjørnøya Basin

The NE–SW-oriented Bjørnøya Basin is bounded by the LFC to the east, by the Bjørnøyrenna Fault Complex (BFC) to the southeast, and by the faulted margin of the Stappen High to the northwest (Fig. 1), cf. Gabrielsen et al. (1990). Structuring of the Bjørnøya Basin is also attributed to the Late Jurassic – Early Cretaceous extensional event (Faleide et al., 1993a, 1993b). Consequently, most of the basin infill is of Early Cretaceous age (Gabrielsen et al., 1990; Faleide et al., 1993a). The basin was affected by faulting and local inversion in association with the BFC and uplift of the Stappen High during the Late Cretaceous and Paleogene (Faleide et al., 1993a).

2.1.3. Hammerfest Basin

The Hammerfest Basin is an elongated ENE – WSW oriented basin, located south of the Loppa High (Fig. 1). The Ringvassøy-Loppa Fault Complex (RLFC) separates it from the deeper Tromsø Basin to the west, while the Asterias Fault complex (AFC) separates it from the Loppa High (Gabrielsen et al., 1990). Its southern border is defined by the Troms-Finnmark Fault Complex (TFFC), which separates the basin from the Finnmark Platform (Gabrielsen et al., 1990). Structuring of the Hammerfest Basin is mainly attributed to extension in Triassic and Late Jurassic to Early Cretaceous times (Berglund et al., 1986; Gabrielsen et al., 1990; Faleide et al., 1993a). Local compression has also been documented (Sund, 1984; Gabrielsen et al., 1997; Indrevær et al., 2017). Uplift and doming along the central basin axis started in the Middle Jurassic (Berglund et al., 1986) and extended into the Early Cretaceous (Berglund et al., 1986; Faleide et al., 1993a). Consequently, new depocenters formed along the boundaries of the Hammerfest Basin (Marín et al., 2017). The uplift ceased in the early Barremian (Faleide et al., 1993a), leaving most of the Barremian – Aptian succession confined within the faulted boundaries of the basin (Marín et al., 2017, 2018b).

2.1.4. Tromsø Basin

The Tromsø Basin is an NNE – SSW-oriented basin that transitions southwards into the Harstad Basin, eventually terminating against the TFFC (Fig. 1). The BFC and the Veslemøy High define its northern boundary, separating it from the Bjørnøya Basin. The RLFC delineates the eastern boundary towards the Hammerfest Basin, while the Senja Ridge marks its western boundary (Gabrielsen et al., 1990). As the North Atlantic rift system advanced northward during the Middle Jurassic – Early Cretaceous, deep basins formed along the southwestern Barents Shelf margin (Faleide et al., 1993a, 1993b). The Early Cretaceous extensional event in the Tromsø Basin was focused along the NE-SW trending RLFC and the BFC. Consequently, the Tromsø Basin experienced rapid subsidence, creating immense accommodation space for Cretaceous sediments, preserved as an up to ca. 8 km thick succession (Rønnevik et al., 1982; Gabrielsen et al., 1990; Faleide et al., 1993a, 2008; Clark et al., 2014; Indrevær et al., 2017; Kairanov et al., 2021). A total of three Early Cretaceous extensional phases have been documented for the Tromsø Basin (Berriasian – Valanginian, Hauterivian – Barremian and Aptian – Albian) (Faleide et al., 1993a; Kairanov et al., 2021). In addition, Late Palaeozoic salt deposits were mobilized by rapid subsidence and differential loading during Albian times, triggering

diapirism in the central parts of the basin (Kairanov et al., 2021).

2.2. Lower Cretaceous stratigraphy and depositional systems

The Lower Cretaceous succession on the Barents Shelf is divided into the Knurr (Berriasian – Early Barremian), Klippfisk (Late Berriasian – Hauterivian), Kolje (Barremian – Early Aptian) and Kolmule (Aptian – Cenomanian) Formations (Fig. 2), collectively assigned to the Adventdalen Group (Parker, 1967; Dalland et al., 1988). Because there are some age-related uncertainties in correlating these units across the various basins, the Lower Cretaceous succession was recently subdivided into seven genetic sequences (S0 – S6; Fig. 2) bounded by regionally extensive flooding surfaces (Marín et al., 2017). Sequences S0 and S1 corresponds to the Knurr and Klippfisk formations, whereas sequence S2 correspond roughly to the Kolje Formation, and sequences S3 to S6 represents the Kolmule Formation (Marín et al., 2017, Fig. 2).

On the SW Barents Shelf, the Lower Cretaceous succession was generally deposited in open marine shelf environments, affected by periods of restricted bottom circulation (Dalland et al., 1988). The dominant lithology of the succession is grey-brown mudstones with interbeds of siltstone, limestone, and local sandstones (e.g. Worsley et al., 1988; Bugge et al., 2002; Seldal, 2005). The up to 285 m thick (as measured in well 7120/12–1) mudstone-dominated Knurr Formation (Valanginian–early Barremian), and the laterally equivalent carbonate-dominated Klippfisk Formation (Valanginian–Hauterivian) on the eastern platform areas constitute the lowermost part of the Lower Cretaceous succession (Dalland et al., 1988; Smelror et al., 1998). These are both condensed units containing multiple stratigraphic gaps (Smelror et al., 2009). Sandstone units emplaced by gravity-flow process occur locally near structural highs (Seldal, 2005; Sattar et al., 2017; Marín et al., 2018a).

The up to 437 m thick (as measured in well 7119/12–1) mudstone-dominated Kolje Formation (Barremian – earliest Aptian) was deposited in a shelf setting under generally well-oxygenated, open marine conditions (Dalland et al., 1988). A large-scale delta system prograding from the NW, reached the Fingerdjupet Subbasin in Barremian – Aptian times, as evident by the presence of several clinoform-bearing sequences in the upper part of the Barremian succession (Grundvåg et al., 2017; Marín et al., 2017; Midtkandal et al., 2019). A regionally extensive flooding surface, which caps the clinoforms, separates the Kolje Formation from the overlying Kolmule Formation (Grundvåg et al., 2017; Serck et al., 2017; Marín et al., 2018b).

The up to 950 m thick (as measured in well 7119/12–1) mudstone-rich and sandstone-bearing Kolmule Formation (Aptian–Middle Cenomanian) was deposited in response to significant uplift of the northeastern Barents Shelf, particularly during the Albian. Large amounts of sediments were shed off uplifted terranes and transported towards the rapidly subsiding basins along the southwestern shelf margin, such as the Harstad, Tromsø and Bjørnøya basins (Faleide et al., 1993a, 1993b; Smelror et al., 2009). Consequently, a large delta system prograded from the E to NE onto the SW Barents Shelf in the Aptian – Cenomanian (Grundvåg et al., 2017; Marín et al., 2017; Midtkandal et al., 2019). At these times, the shelf was generally characterized by well-oxygenated, open marine conditions (Smelror et al., 2009).

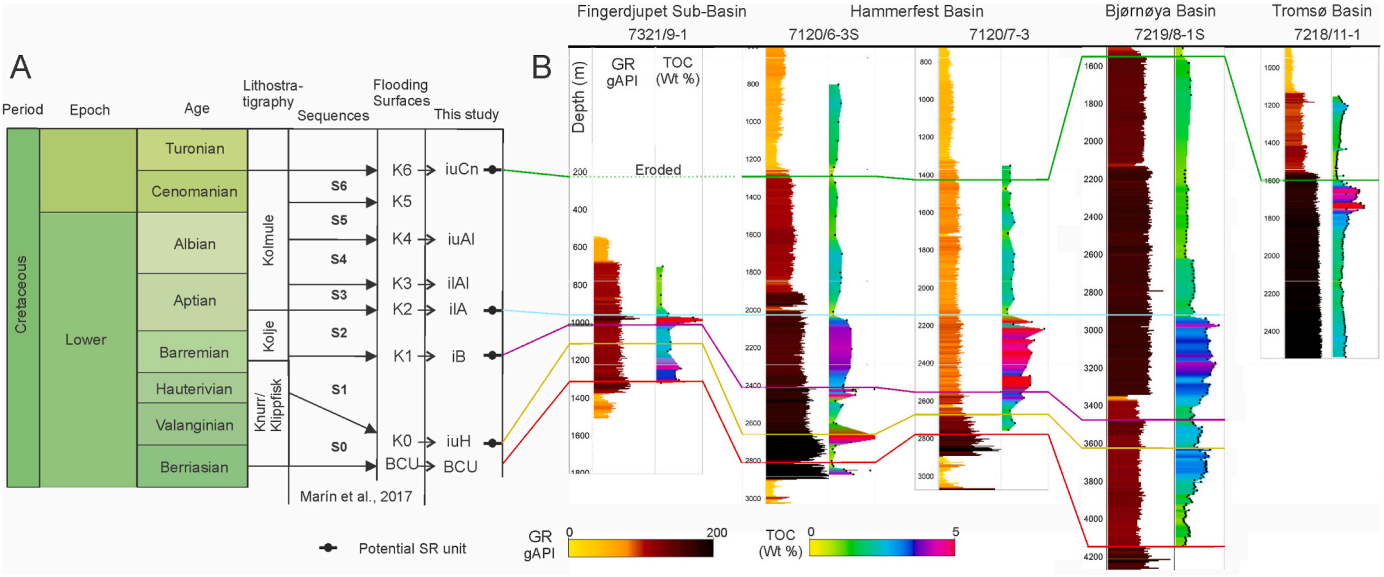

Fig. 2. (A) Lithostratigraphic overview of the Lower Cretaceous succession on the SW Barents Shelf. Marín et al. (2017) subdivided the succession into seven genetic sequences (S0 to S6) bounded by regionally extensive flooding surfaces (K0 to K6). This study conform to this sequence stratigraphic framework, but applies its own nomenclature for the flooding surfaces which refer more accurately to their stratigraphic position (similar to the naming convention of Serck et al., 2017). The chronostratigraphic chart has been modified after Cohen et al. (2013). (B) Correlation of four selected wells showing the distribution of the sequences and the extent of the flooding surfaces across the study area. In this study, four of the flooding surfaces are linked to potential source rock units (marked by source rock symbol in Fig. 2A), which are associated with increased total organic carbon (TOC) contents in the wells. The TOC logs are based on Rock-Eval data from either sidewall cores or drill cuttings. Well locations is displayed in Fig. 1. Abbreviations: iuCn: intra upper Cenomanian, iuAl: intra upper Albian, ilAl: intra lower Albian, ilA: intra lower Aptian, iB: intra Barremian, iuH: intra upper Hauterivian, BCU: Base Cretaceous Unconformity (which defines the base of the entire succession), GR: Gamma ray.

3. Data and methods

3.1. Seismic data

This study includes several high-resolution regional 2D seismic surveys (NBR, 2006–2012). The different orientation and spacing (1–8 km) of the 2D lines make up a grid that spans the study area, thus forming a regional pseudo 3D-grid. The acquisition of these surveys took place over a period of several years, resulting in varying quality between the surveys. In general, frequencies are in the range of 10–50 Hz, while the polarity convention for the dataset is zero-phase normal polarity, following the nomenclature of Sheriff (2002). The description of reflection configurations and seismic geometries follow the terminology established by Mitchum et al. (1977).

Confidence of the seismic interpretations within the deeper basins is strongly affected by a decreasing seismic quality with depth. In addition, no well data were available for either the central parts of the Tromsø or the Bjørnøya basins.

3.1.1. Seismic response to organic-rich intervals and mapping of potential source rock units

Mudrocks with total organic carbon (TOC) contents >3 – 4% typically have significantly lower acoustic impedance and higher intrinsic anisotropy than mudrocks with lower amounts of organic content. The general density of kerogen is typical in the range of 1.1–1.4 g/cm^3, while mudrocks generally have a density of 2.7 g/cm^3 (Løseth et al., 2011; Rider and Kennedy, 2011). Organic matter will, therefore, influence the seismic response trough compressional velocity (Vp), shear velocity (Vs), bulk density, anisotropy, and attenuation (Løseth et al., 2011). A potential source rock unit may thus result in a high amplitude reflection characterized by a negative top and a positive base (Løseth et al., 2011). Furthermore, the acoustic impedance contrast is relatively stable down to a depth of c. 4500 m and decreases nonlinearly with increasing TOC content (Løseth et al., 2011). This has clear implications for the Lower Cretaceous succession, which is buried at depths down to 5–7 s two-way-travel time, in the deep Bjørnøya and Tromsø basins (Gabrielsen et al., 1990; Kairanov et al., 2021).

The seismic mapping thus specifically targets the top of potential source rock units as these are displayed as negative high-amplitude anomalies in the data. Biostratigraphic age determination of the mapped reflectors are guided by well tops from the publicly available database of the Norwegian Petroleum Directorate (NPD Factpages, 2021) and from in-house data provided by Wintershall-Dea Norway. In the deep Tromsø and Bjørnøya basins, well 7219/8-1 S is a key reference point in providing age-control of the Lower Cretaceous succession. In most cases, the targeted reflectors seem to correspond to regionally extensive maximum flooding surfaces documented by previous studies (e.g. Marín et al., 2017). Thus, for regional stratigraphic context, the genetic sequence subdivision of Marín et al. (2017, 2018a, 2018b), and partly that of Serck et al. (2017), is used for guidance in the Hammerfest Basin and Fingerdjupet Subbasin, respectively (with some minor modifications). In the Bjørnøya Basin, the stratigraphic subdivision builds largely on that of the Fingerdjupet Subbasin by correlating the seismic horizons across the LFC and TFC (Fig. 1). In the Tromsø Basin, the stratigraphic framework used in this study, builds largely on the recent work of Kairanov et al. (2021), and by linking it to the stratigraphic framework established by Marín et al. (2017) for the Hammerfest Basin.

To investigate lateral variability and distribution of potential source rock units, average negative amplitude maps have been generated for two of the high-amplitude reflectors following the workflow of Løseth et al. (2011). The negative amplitude map is not very reliable in the deep basins because of deteriorating seismic quality and reflector dimming, making a lateral correlation from the shallow basins a difficult and time-consuming task. Consequently, amplitude maps have only been generated for two of the mapped reflectors. The generation of the amplitude map uses a search window of 5 ms above and 20 ms below the interpretation of the reflector.

3.2. Well data

Seventeen exploration wells have been selected and investigated for this study (Fig. 1 and Table 1). All the wells have an established time-depth relationship trough calibration of check shots. Most of the wells exhibit a common suite of wireline-logs including gamma ray (GR), sonic (AC/DT), density (DEN), and deep resistivity (RDEP). Wireline logs are generally regarded to be a good supplement to seismic data when evaluating the presence of potential source rock units, Thus, to confirm the presence of potential source rock units mapped in the seismic data, wireline log signals are integrated with digitalized TOC logs derived from the Rock-Eval data. The thicknesses of the potential source rock units are estimated from the wireline data and subsequently, TOC samples within the interval, or from stratigraphically nearby intervals, are evaluated (Table 1). The typical wireline response to organic rich units is briefly outlined below.

Table 1
Overview of sample intervals and thickness of units sampled for total organic carbon (TOC) contents and Rock-Eval data. Intervals with no data are marked with "No samples" and the stratigraphically/spatially closest sample points have been used when applicable. Intervals with no potential source rock unit is marked with "N/A".

Exploration wells	Hauterivian sample interval and thickness	Barremian sample Interval and thickness	Lower Aptian sample Interval and thickness	Cenomanian sample interval and thickness
7321/7-1	1498–1520 m (22 m)	1328–1348 m (20 m)	1060–1112 m (52 m)	N/A
7321/8-1	1250–1289 m (39 m)	N/A	859–861 m (2 m)	N/A
7321/9-1	1103–1114 m (11 m)	N/A	961–985 m (24 m)	N/A
7219/8-1 S	3619–3751 m (132 m)	3469–3548 m (79 m)	2929–3088 m (159 m)	1573–1616 m (43 m)
7219/9-1	N/A	N/A	N/A	1467–1599 m (132 m)
7218/11-1	N/A	N/A	N/A	1626–1747 m (121 m)
7120/1-2	N/A	N/A	1815–1825 m (10 m)	N/A
7120/6-3 S	2662–2686 m (24 m)	2403–2451 m (48 m)	2032–2084 m (52 m)	1303–1346 m (43 m)
7120/6-1	2204–2226 m (22 m)	2063–2106 m (43 m)	1912–1953 m (41 m)	N/A
7120/9-2	1870–1880 m (10 m)	1770–1809 m (39 m)	1647–1693 m (46 m)	N/A
7120/8-3	2052–2070 m (18 m)	1960–1988 m (28 m)	1749–1806 m (57 m)	1121–1174 m (53 m)
				No samples
7120/7-2	1986–2002 m (16 m)	1939–1970 m (31 m)	1782–1835 m (53 m)	1067–1096 m (29 m)
7120/5-1	N/A	2148–2170 m (22 m)	N/A	N/A
7120/7-3	2699–2720 m (21 m)	2561–2580 m (19 m)	2142–2283 m (141 m)	1423–1474 m (51 m)
7119/9-1	2647–2656 m (9 m)	2526–2559 m (33 m)	2257–2370 m (113 m)	1562–1587 m (25 m)
7119/12-3	2954–2976 m (22 m)	2738–2768 m (30 m)	2378–2446 m (68 m)	1670–1707 m (37 m)
7119/12-1	2437–2461 m (24 m)	2282–2327 m (45 m)	1909–1992 m (83 m)	1050–1094 m (44 m)

3.2.1. Wireline responses to organic-rich units

3.2.1.1. Gamma ray log (GR). Organic-rich mudrocks commonly show high GR values because of elevated concentrations of uranium. However, this is not always the case as uranium can be a highly mobile element under the right conditions (Bowker and Grace, 2010; Helleren et al., 2020). In addition, the GR-signal may be subject to various interference from the well casing.

3.2.1.2. Sonic log (AC/DT). The presence of organic matter in mudrocks will lower the sonic travel time (Rider and Kennedy, 2011). This response is evidently more apparent in mature source rocks. However, using the sonic log independently to identify organic rich intervals is problematic, because it is impossible to separate low sonic values caused by the presence of organic matter from low sonic values caused by porosity changes (Rider and Kennedy, 2011).

3.2.1.3. Resistivity log (RDEP). The resistivity logs response to a source rock depends on the maturity of the organic matter (Rider and Kennedy, 2011). In immature organic matter, the response will be small due to high conductivity. In mature source rocks where, free petroleum are present in voids and fractures, the resistivity will increase significantly (Rider and Kennedy, 2011).

3.2.1.4. Density log (DEN). Mudrocks containing low amounts of organic matter have a higher density matrix (2.67 – 2.72 g/cm^3) compared to pure organic matter (1.1 – 1.2 g/cm^3). The density log will consequently read lower values in organic rich mudrocks (Rider and Kennedy, 2011). The presence of organic matter thus has a distinct effect on the overall mudrock density, which also shifts the acoustic impedance in the seismic data towards negative amplitudes (Løseth et al., 2011).

3.3. Rock-Eval data

In order to establish the richness, type, and thermal maturity of the source rock units identified in the seismic and wireline data, traditional source rock evaluation following the principles of Espitalié et al. (1977), Peters (1986) and Peters and Cassa (1994) are used. The Rock-Eval data presented here are based on samples derived from either sidewall cores or drill cuttings from the 17 wells. The sample spacing varies between each well (ranging from samples collected every 2–100 m; see Table 1 for sampling interval details), which consequently makes it difficult to achieve a good representation of thin source rock units occurring between the sampled intervals. In these cases, the nearest samples to the interval have been used where applicable. To establish the thermal maturity of the potential source rock units, emphasis has been given to T_{max} values as these are numerous throughout the dataset, while the scarce vitrinite reflectance (R_o) data supplement the interpretation when applicable.

The Rock-Eval database has been digitalized and implemented into Petrel for each corresponding well. This makes it possible for a direct correlation between the source rock reflections and the Rock-Eval data at any of the well locations. The complete Rock-Eval database, including TOC content, is given in the online supplementary file SF1.

4. Results

4.1. Seismic sequences and bounding surfaces

Seven genetic sequences (S0 – S6) and their bounding surfaces (i.e., the BCU, iuH, iB, ilA, ilAl, iuAl, IuCn reflectors of this study, see detailed descriptions below) are recognized within the Lower Cretaceous succession in the study area (Figs. 3 and 4), conforming to the well-established sequence stratigraphic framework of Marín et al. (2017, 2018a, 2018b). Thus, apart from the Base Cretaceous Unconformity (BCU), which defines the base of the Lower Cretaceous succession, the sequence-bounding surfaces represent regionally extensive maximum flooding surfaces that may be correlated from the Hammerfest Basin and the Fingerdjupet Subbasin westward into the Tromsø and Bjørnøya basins (Figs. 3 and 4; Marín et al., 2017). Bellow follows a seismic description of the genetic sequences and their bounding surfaces.

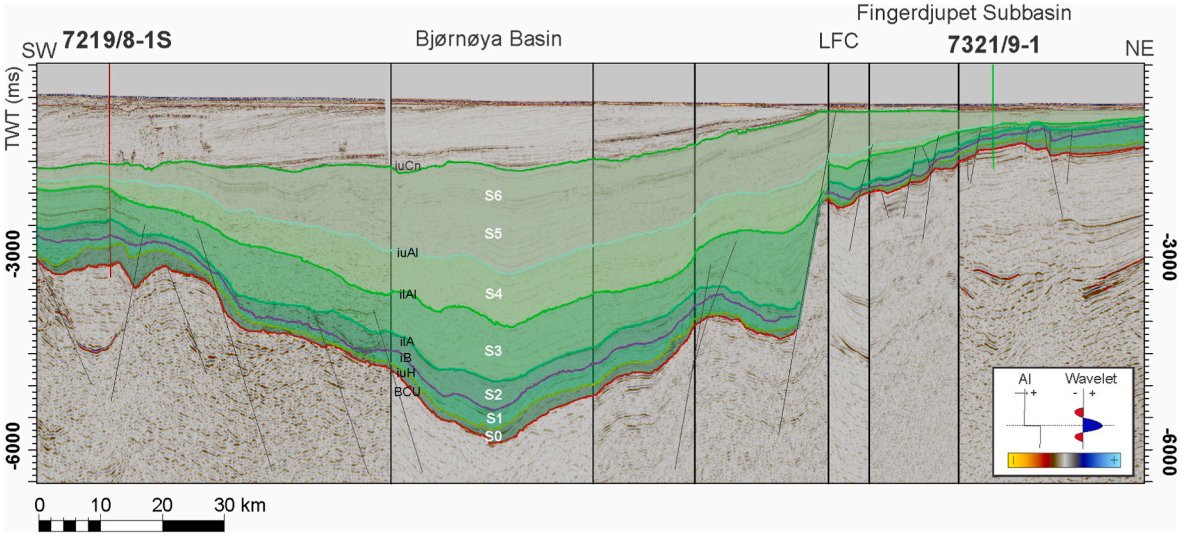

Fig. 3. Interpreted composite seismic line of the southern parts of Fingerdjupet Subbasin and the NE Bjørnøya Basin showing the seven genetic sequences comprising the Lower Cretaceous succession (S0 – S6; see Fig. 2). Location and orientation of the seismic line is shown in Fig. 1. Abbreviations: iuAl: intra upper Albian, ilAl: intra lower Albian, ilA: intra lower Aptian, iB: intra Barremian, iuH: intra upper Hauterivian, BCU: Base Cretaceous Unconformity. Seismic data courtesy TGS and Spectrum.

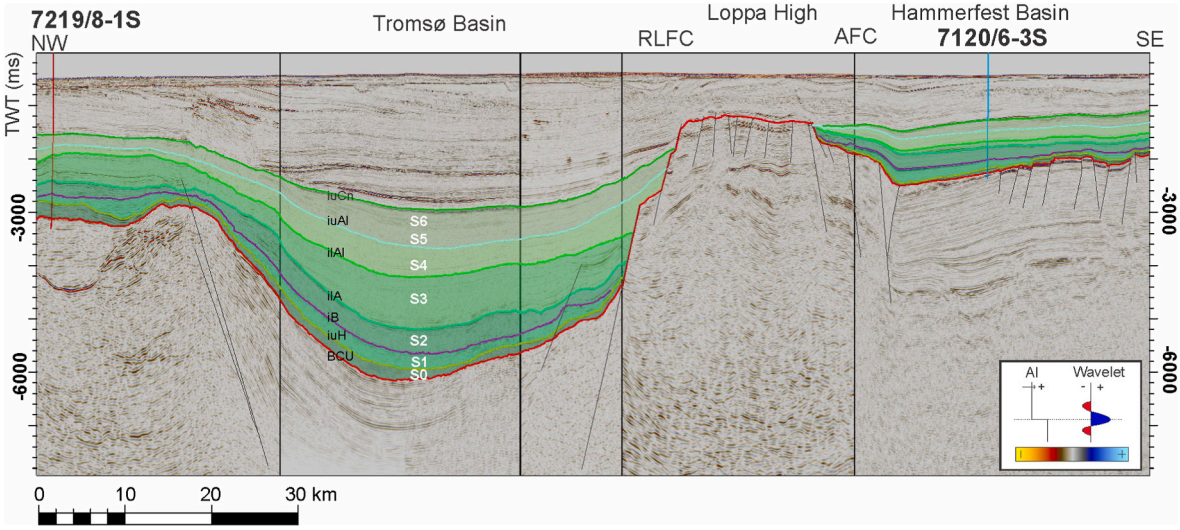

Fig. 4. Interpreted composite seismic line of the Tromsø Basin and the NW corner of the Hammerfest Basin, showing the seven genetic sequences comprising the Lower Cretaceous succession (S0 – S6; see Fig. 2). Location and orientation of the seismic line is shown in Fig. 1. Abbreviations: iuAl: intra upper Albian, ilAl: intra lower Albian, ilA: intra lower Aptian, iB: intra Barremian, iuH: intra upper Hauterivian, BCU: Base Cretaceous Unconformity. Seismic data courtesy TGS and Spectrum.

4.1.1. Sequence 0 (Berriasian – Hauterivian)

Sequence 0 is bounded at the base by the regionally extensive BCU, and atop by the intra upper Hauterivian reflector (iuH). The BCU appears as a high amplitude reflector. The iuH reflector has a negative amplitude with variable magnitude and continuity. In the shallow Fingerdjupet Subbasin and the Hammerfest Basin, sequence 0 has a subparallel to divergent reflection configuration with good continuity and strong amplitudes (Figs. 3 and 4). The sequence has a wedge-shaped geometry, were there is a distinct thickness increase towards the main depocenters. In the deeper Bjørnøya and Tromsø basins, the reflectors are typically subparallel and discontinuous with low amplitude.

4.1.2. Sequence 1 (Hauterivian – Early Barremian)

Sequence 1 is bounded at the base by the iuH reflector, and atop by the intra Barremian reflector (iB). The iB reflector has a medium negative amplitude with relatively good continuity. The sequence is present in the shallow Hammerfest Basin and Fingerdjupet Subbasin, as well as in the deep Tromsø and Bjørnøya basins, though exhibiting varying thickness and seismic characteristics. In the shallow basins, reflectors are usually parallel to subparallel with strong amplitudes and good continuity. The sequence has a sheet and wedge geometry, where thickness variations are controlled by normal faults. In the Tromsø and Bjørnøya basins, reflectors are subparallel and discontinuous with low amplitude.

4.1.3. Sequence 2 (Barremian – Early Aptian)

Sequence 2 is bounded at the base by the iB reflector and above by the intra lower Aptian reflector (ilA; Fig. 2). Reflectors within sequence 2 are subparallel and continuous with medium amplitude in the Hammerfest Basin. In the Fingerdjupet Subbasin, the sequence is represented by sigmoidal clinoforms with medium to high amplitudes. In the Bjørnøya and Tromsø basins, reflectors have a subparallel to divergent configuration, where wedges are located close to the fault complexes (e.g. LFC, BFC and RLFC). These reflectors have low – medium amplitude and are discontinuous towards the deeper basin segments.

4.1.4. Sequence 3 (Aptian – Early Albian)

Sequence 3 is bounded at the base by the ilA and atop by the intra lower Albian reflector (ilAl). Reflectors within the sequence are subparallel to chaotic and amplitudes are generally low to medium. In places, the sequence has a wedge-shaped geometry, typically thickening towards basin bounding faults, but generally have a sheet-like geometry in the deep basins. No visible negative high-amplitude anomalies have been detected within this sequence.

4.1.5. Sequence 4 (Early Albian – Late Albian)

Sequence 4 is bounded at the base by the ilAl reflector and atop by the intra upper Albian (iuAl) reflector. Reflector configurations range from continuous and parallel to chaotic in the shallow basins, while they are typically subparallel in the deeper basins. The amplitudes are often medium to low. The external geometry of the sequence has sheet to sheet drape external form.

4.1.6. Sequence 5 and 6 (Late Albian – Cenomanian)

Sequence 5 and 6 are grouped together due to similarities in internal seismic characteristics and the internal lack of extensive and significant negative high-amplitude anomalies. Note however, that these sequences are seismically distinguishable from each other as demonstrated by previous workers (e.g. Marín et al., 2017, Figs. 3 and 4). The composite sequence 5 and 6 are bounded at the base by the iuAl reflector and atop by the intra upper Cenomanian reflector (iuCn). The sequences and their corresponding lower and upper bounding surfaces are widespread in the Hammerfest and Tromsø basins and partly in the Bjørnøya Basin but are missing/eroded in the Fingerdjupet Subbasin (Fig. 3). Internally, the reflectors of sequences 5 and 6 are typically parallel to subparallel continuous, with medium amplitude. These sequences generally have a 'basin-infill' geometry, where the greatest thicknesses occur in the deepest parts of the respective basins.

4.2. Potential Lower Cretaceous source rock units

Four negative high-amplitude reflectors have been recognized and mapped in detail within the study area. These are the: i) intra upper Hauterivian (iuH; corresponding to flooding surface K0 of Marín et al., 2017), ii) intra Barremian (iB; corresponding to flooding surface K1 of Marín et al., 2017), iii) intra lower Aptian (ilA; corresponding to

Table 2
Summary of seismic expression and distribution of the negative amplitude reflectors which are coupled to potential source rock units with elevated TOC values, and their typical wireline signal in key wells across the SW Barents Shelf. The wells marked in bold record source rock units with an increased potential.

Reflector	Seismic expression	Occurrence	Key wells	Typical wireline signal GR, DEN, AC, RDEP.	TOC range (average)
Intra upper Hauterivian (iuH)	Continuous, low – medium negative amplitudes	Fingerdjupet Subbasin	7321/7-1	78 gAPI 2.4 g/cm^3 120 us/ft 6.3 Ohm.m	1.48–1.87 wt % (1.68 wt %)
	Continuous, medium – high negative amplitudes	Hammerfest Basin	**7120/8–3** **7120/6-3S** 7120/6-1 **7120/9–2** 7119/9-1 7119/12-1	130–170 gAPI 2.0–2.65 g/cm^3 90–105 us/ft 3–7 Ω m	2.09–5.73 wt % (3.47 wt %)
	Continuous, low negative amplitudes	Bjørnøya Basin	7219/8-1 S	120 gAPI 2.4 g/cm^3 90 us/ft 3.5–5 Ω m	2.58–3.58 wt % (3.17 wt %)
Intra Barremian (iB)	Continuous, low – high negative amplitude characteristics	Hammerfest Basin	**7120/6-3S** **7120/5–1**	115–130 gAPI 2.5–2.6 g/cm^3 90–100 us/ft 3–5 Ω m	1.71–4.88 wt% (3.01 wt %)
	Discontinuous, low negative amplitude characteristics	Bjørnøya Basin	7219/8-1 S	100 gAPI 2.54 g/cm^3 110 us/ft 3–4 Ω m	1.60–2.77 wt % (2.35 wt %)
	Continuous, varying amplitude, low –high negative amplitude characteristics	Fingerdjupet Subbasin	**7321/9–1**	up to 308 gAPI 2.23 g/cm^3 No AC up to 15.7 Ω m	4.00–5.30 wt % (4.50 wt %)
Intra lower Aptian (ilA)	Continuous, medium – high negative amplitude	Hammerfest Basin	**7120/7–3** 7120/6-3 S 7119/9-1	60–85 gAPI 2.3–2.7 g/cm^3 70–100 us/ft 2.5–3 Ω m	0.59–4.56 wt % (2.45 wt %)
	Continuous – discontinuous, low – medium negative amplitude	Bjørnøya Basin	**7219/8-1S**	120–130 gAPI 2.4–2.5 g/cm^3 85–95 us/ft 2.5–4.2 Ω m	3.07–4.42 wt % (3.44 wt %)
Intra upper Cenomanian (iuCn)	Continuous, low – medium negative amplitude	Tromsø Basin	**7218/11–1**	125–140 gAPI 2.2–2.4 g/cm^3 115–130 us/ft 1.9–4.5 Ω m	1.54–3.44 wt % (2.68 wt %)

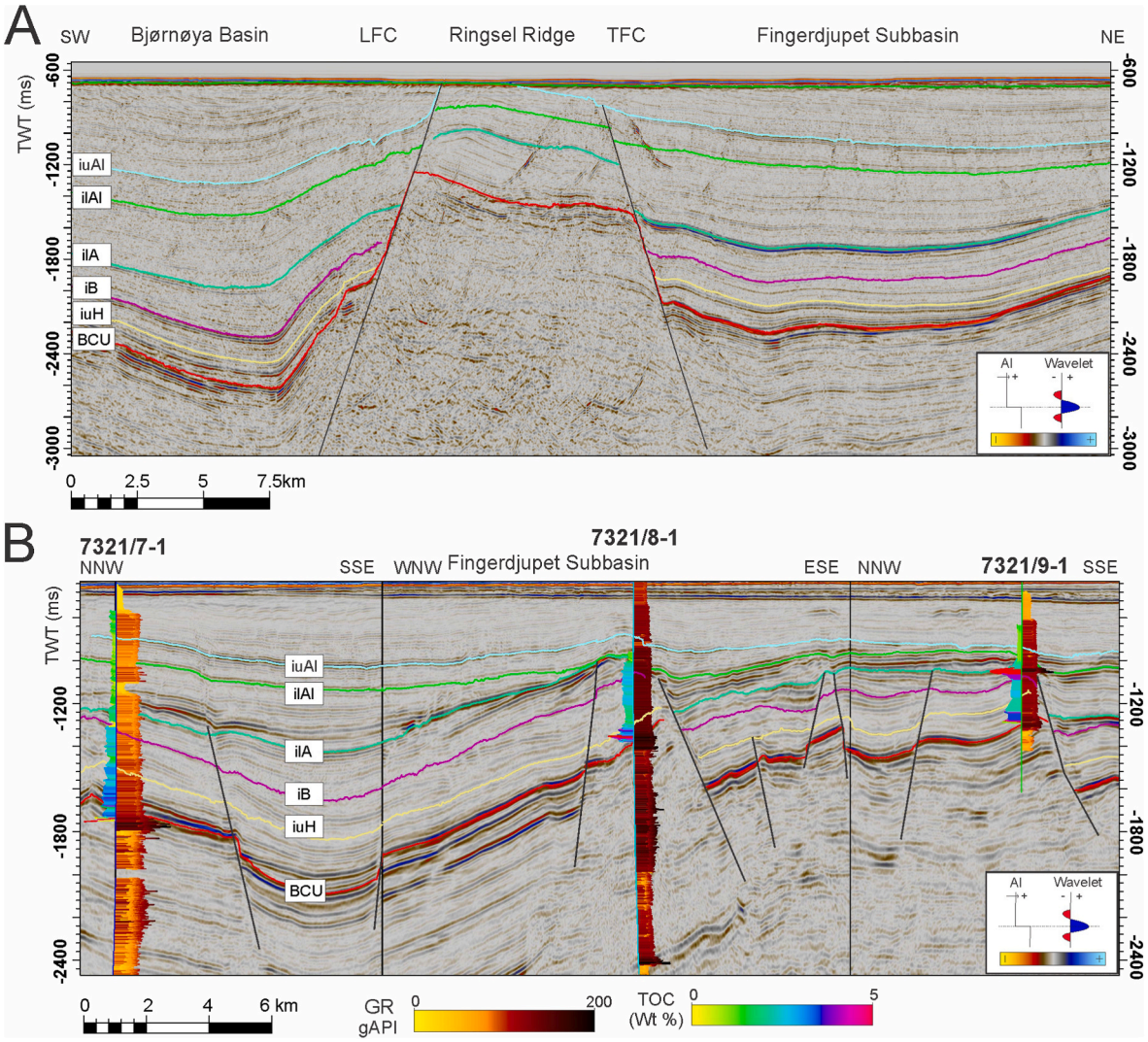

Fig. 5. (A) Seismic section showing the sequence bounding flooding surfaces in the NE part of the Bjørnøya Basin and the main depocenter of the Fingerdjupet Subbasin. Note the prominent negative amplitude associated with the ilA reflector in the Fingerdjupet Subbasin. These basins are separated by the Ringsel Ridge, which is bounded on either side by the Leirdjupet (LFC) and Terningen Fault Complexes (TFC). (B) Composite seismic profile from the Fingerdjupet Subbasin displaying the stratigraphic framework and seismic tie to exploration wells 7321/7–1, 7321/8–1, and 7321/9–1. TOC logs is displayed to the left and GR logs to the right of the individual drill-stems (this is valid for all the following figures). Location of the seismic lines and the wells is shown in Fig. 1. Abbreviations: iuAl: intra upper Albian, ilAl: intra lower Albian, ilA: intra lower Aptian, iB: intra Barremian, iuH: intra upper Hauterivian, BCU: Base Cretaceous Unconformity. Seismic data courtesy TGS and Spectrum.

flooding surface K2 of Marín et al., 2017), and the intra upper Cenomanian (iuCn; corresponding to flooding surface K6 of Marín et al., 2017) reflectors. Each of these reflectors correlate to certain wireline signals in the wells and raised TOC contents, which are typically associated with the presence of organic-rich units. The seismic expression, occurrence, typical wireline signal and TOC range of these units are summarized in Table 2 with a detailed description of each reflector/organic-rich unit given below.

4.2.1. *Intra upper Hauterivian (iuH) reflector*

Fig. 5A shows the stratigraphic framework for the central basin in the Fingerdjupet Subbasin and the transition to the Bjørnøya Basin over the Ringsel Ridge. In addition, a composite seismic profile trough wells 7321/7–1, 7321/8–1 and 7321/9-1 shows the interaction between well, reflector and structural setting in Fig. 5B. The iuH reflector is present across the Fingerdjupet Subbasin and can be traced laterally towards the Bjarmeland Platform (Fig. 5B). The reflector is characterized by continuous low – medium amplitudes, with the strongest amplitudes recorded in the central parts of the basin (see iuH; Fig. 5A). Wells 7321/7–1, 7321/8–1 and 7321/9–1 penetrate the iuH reflector in the Fingerdjupet Subbasin (Fig. 5B). However, the unit corresponding to the reflector has no significant TOC values or wireline signals that would indicate a viable source rock for the area (see iuH; Fig. 6).

The iuH reflector can be traced from the Fingerdjupet Subbasin over the Ringsel Ridge into the Bjørnøya Basin (Fig. 5A). In the Bjørnøya Basin, the iuH reflector has a lower amplitude compared to Fingerdjupet

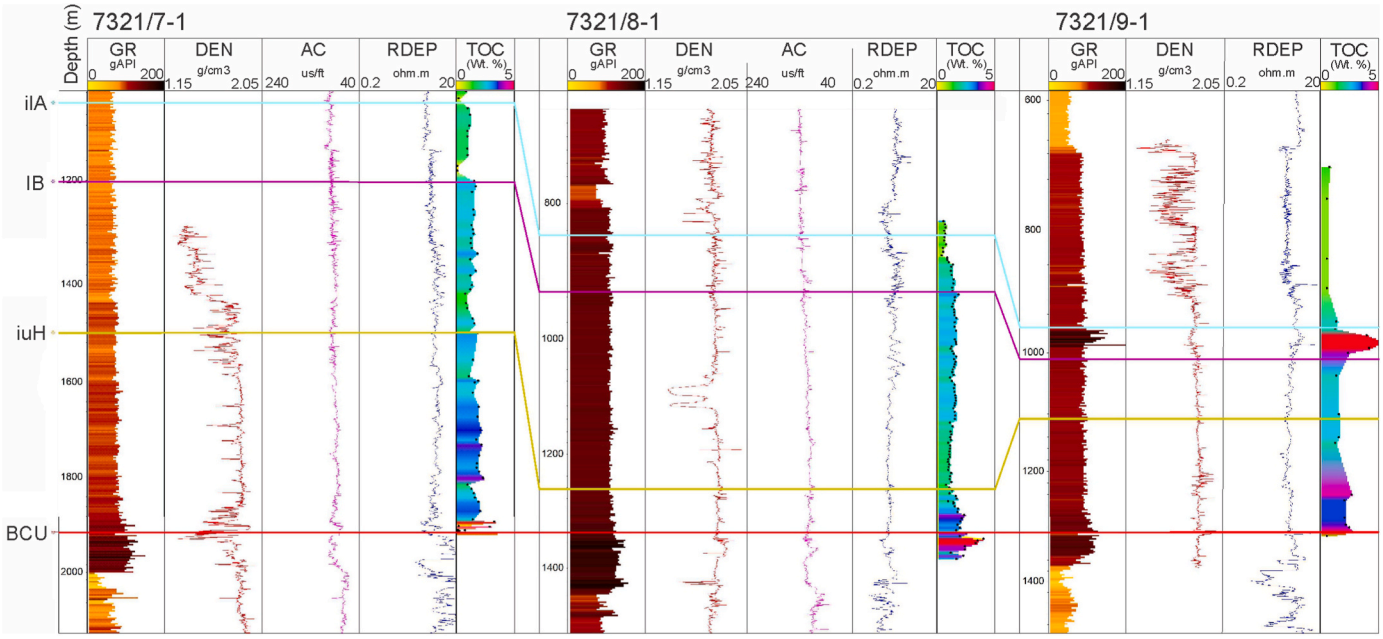

Fig. 6. Correlation of wells 7321/7–1, 7321/8–1 and 7321/9–1 in the Fingerdjupet Subbasin with the BCU (Base Cretaceous Unconformity), iuH (intra upper Hauterivian), iB (intra Barremian), ilA (intra lower Aptian) reflectors annotated. Abbreviations: GR: Gamma ray, DEN: Density, RDEP: Deep Resistivity, TOC: Total organic content. The black circles along the TOC log are sample points. Position of the wells are shown in Fig. 1.

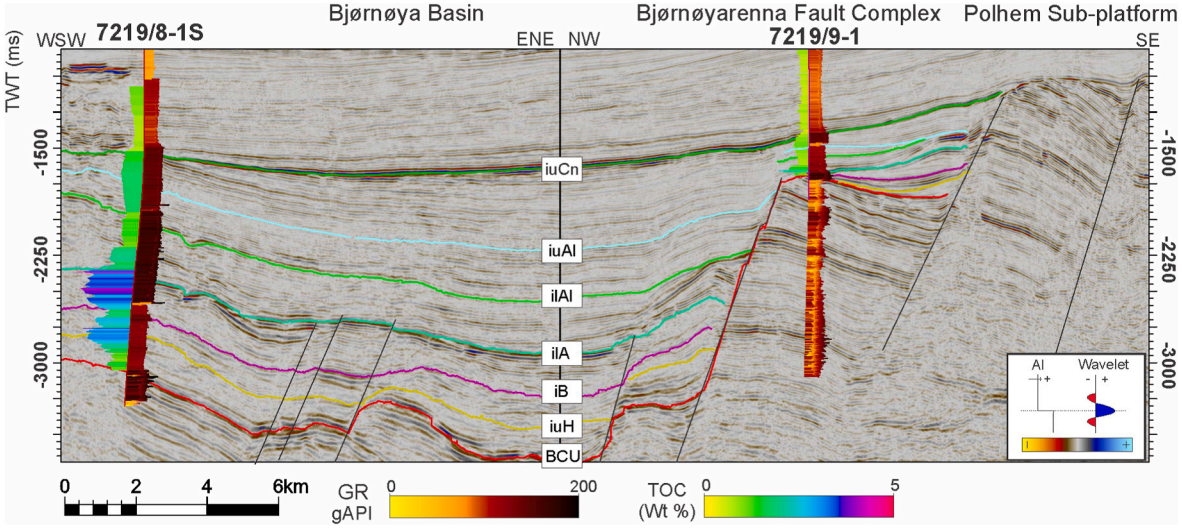

Fig. 7. Seismic composite line displaying the stratigraphic framework in the southern parts of Bjørnøya Basin near the Bjørnøyrenna Fault Complex. The TOC and GR logs is displayed along the left- and right-hand side of the drill-stems, respectively. Note the TOC spikes associated with the iuH and ilA reflectors in the Bjørnøya Basin. Location of the seismic line is indicated in Fig. 1. Abbreviations: iuAl: intra upper Albian, ilAl: intra lower Albian, ilA: intra lower Aptian, iB: intra Barremian, iuH: intra upper Hauterivian, BCU: Base Cretaceous Unconformity. Seismic data courtesy TGS and Spectrum.

Subbasin. However, the reflector remains continuous and can be traced southwards parallel to the BFC. Moving east, towards the deeper parts of the Bjørnøya Basin, the reflector dims to a discontinuous low amplitude reflector. In the southern parts of the Bjørnøya Basin, the iuH reflector is penetrated by well 7219/8-1 S (Fig. 7). Here, the reflector marks the top of a potential source rock unit ranging from 3620 to 3670 m (Figs. 7 and 8). The unit has relatively good TOC content but there is a lack of wireline response to the TOC values (Table 2 and Fig. 8).

In the Hammerfest Basin, the iuH reflector is widely distributed, but onlaps towards the uplifted central high (Fig. 9). The reflector has a medium amplitude with good continuity in the NW corner of the basin but increase in amplitude towards the uplifted central high (see iuH; Fig. 9). In the transition to the Tromsø Basin, the reflector dims but remains continuous until the reflector extends past the RLFC. In wells

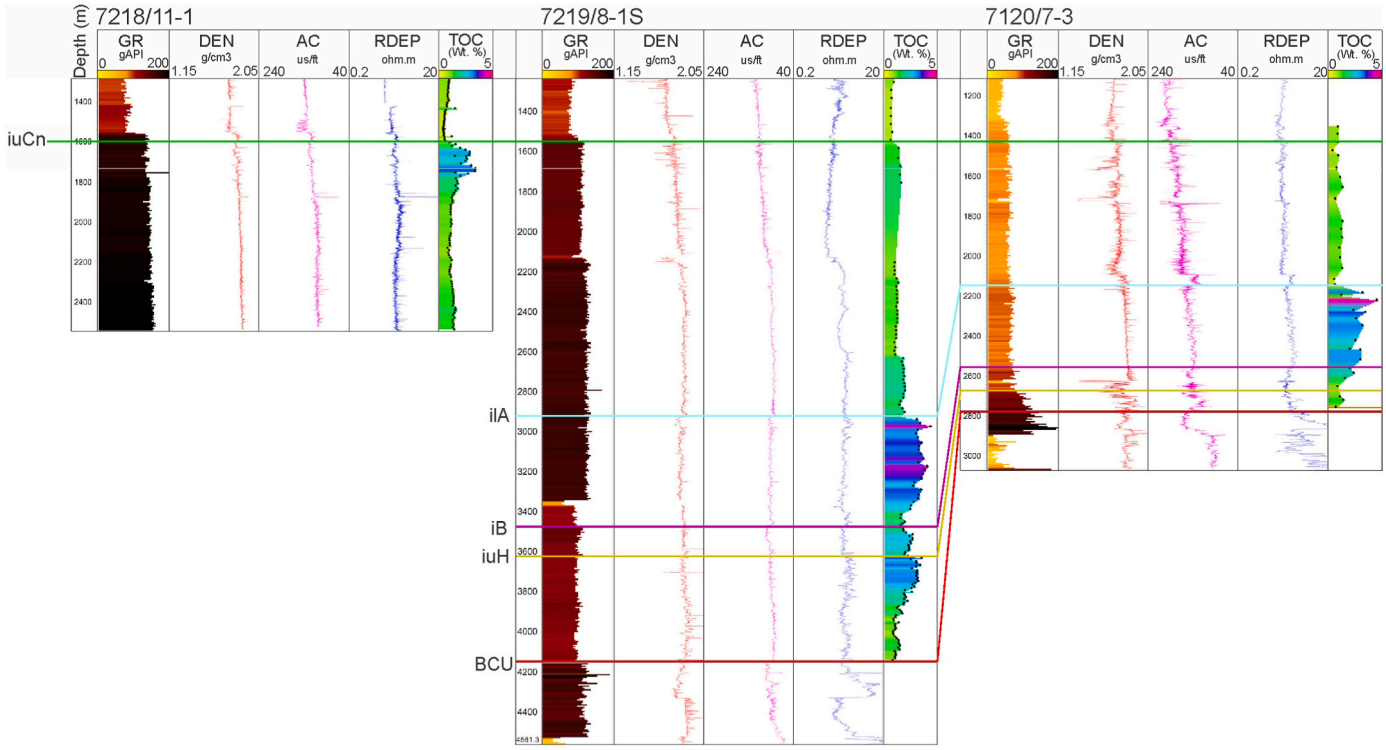

Fig. 8. Correlation panel of wells 7218/11–1, 7219/8-1 S and 7120/7–3 in the Tromsø Basin with the BCU (Base Cretaceous Unconformity), iuH (intra upper Hauterivian), iB (intra Barremian), ilA (intra lower Aptian), and iuCn (intra upper Cenomanian) reflectors annotated. Gamma ray (GR), Density (DEN), deep Resistivity (RDEP) and total organic carbon content (TOC; from Rock-Eval analysis) is included for each well. Note the prominent TOC spike associated with the ilA reflector in well 7120/7-3 located in the faulted transition zone between the Tromsø and Hammerfest Basins. Well location is indicated in Fig. 1.

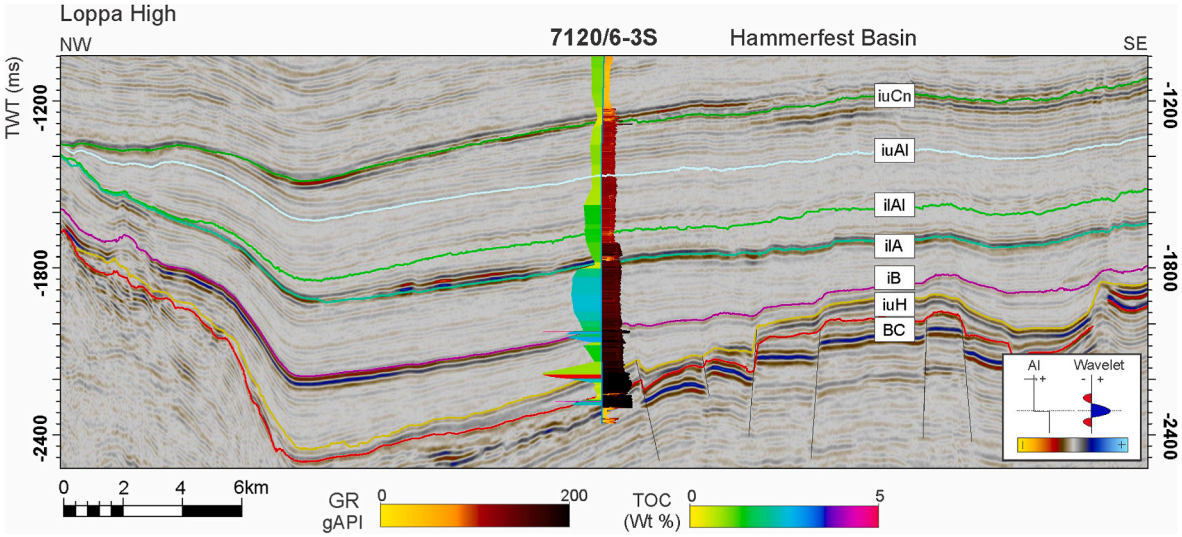

Fig. 9. Seismic section from the Hammerfest Basin showing the NW depocenter and the uplifted central high further to the SE. Here, exploration well 7120/6-3 S is a key well for the Lower Cretaceous succession and record spikes in the TOC-profile associated with the iuH, iB and the ilA reflectors. Abbreviations: iuAl: intra upper Albian, ilAl: intra lower Albian, ilA: intra lower Aptian, iB: intra Barremian, iuH: intra upper Hauterivian, BCU: Base Cretaceous Unconformity. Location of the seismic section is indicated in Fig. 1.

7120/8–3, 7120/6-3 S, and 7119/9–1 the unit corresponding to the iuH reflector have an average thickness of 17 m, and record increased TOC contents (Table 1 and Fig. 10) The wireline logs show a response to the increased TOC values with a drop in DEN values, and increase in both RDEP and AC values (e.g. iuH reflector in well 7120/6-3 S; Fig. 10).

Further towards the west, the iuH reflector is downfaulted along the RLFC into the deeper Tromsø Basin. The reflector quickly loses its seismic characteristics due to deeper burial but can be traced along the NE margin of the Tromsø Basin. At this location, the iuH reflector is discontinuous and characterized by low amplitudes. However, towards the deeper parts of the Tromsø Basin, the reflector is too obscure to be traced with confidence due to the large burial depth and the poorer-quality seismic signal. In addition, there are no well data available from the deep basin.

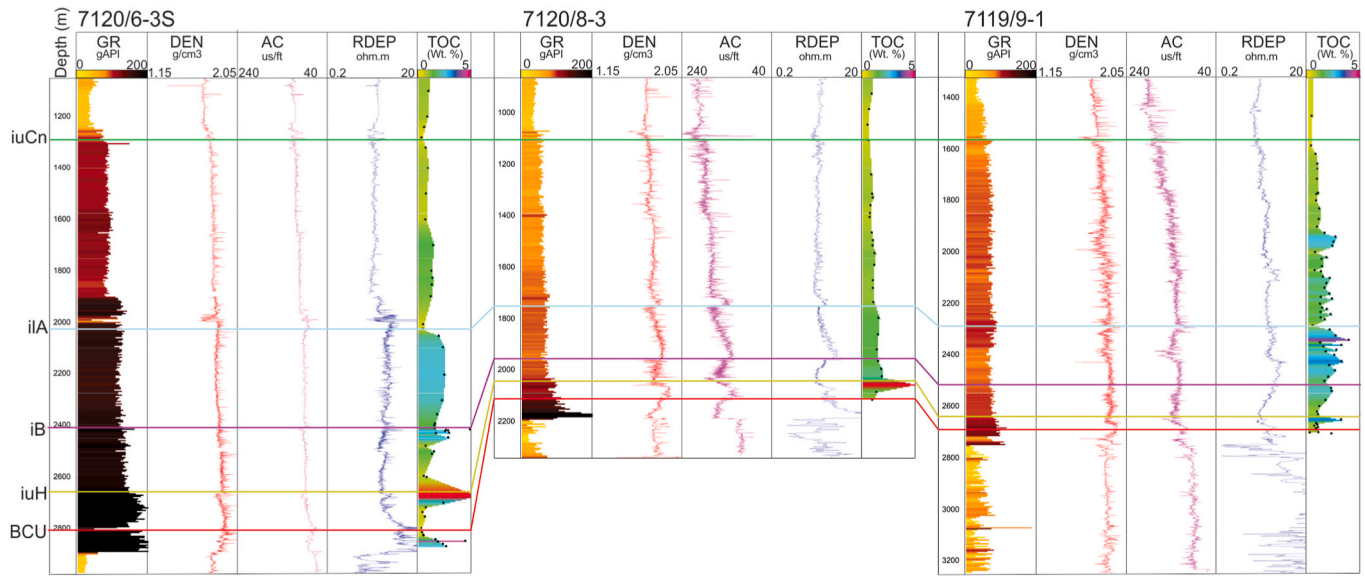

Fig. 10. Well correlation from the Hammerfest Basin including wells 7120/6-3 S, 7120/8–3 and 7119/9–1 with the BCU (Base Cretaceous Unconformity), iuH (intra upper Hauterivian), iB (intra Barremian), ilA (intra lower Aptian), and iuCn (intra upper Cenomanian) reflectors annotated. Prominent TOC spikes is associated with the iuH, iB and ilA reflectors. Well locations are indicated in Fig. 1.

Based on the seismic amplitudes, the wireline signals, and the elevated TOC contents, the iuH reflector is interpreted to represent a potential upper Hauterivian source rock unit in the Hammerfest Basin. The iuH reflector thus marks the top of this unit in well 7120/8–3, 7120/6-3 S, 7119/9–1 and 7120/9–2, which have a clear GR-log trend with associated high TOC values (Fig. 10). Data from well 7120/6-3 S record high TOC values close to the Loppa High and the AFC. However, at this location the amplitude is lower than on the central high. In addition, well 7120/8–3, 7119/9–1 and 7120/9–2 indicate that the organic-rich unit may hold potential in the central parts of the basin. This could indicate that the organic-rich unit is more widely distributed in the Hammerfest Basin, not only occurring in localized depocenters near the Loppa High and the Finnmark Platform.

Despite a small increase in TOC in well 7321/7–1, the low amplitude of the reflector coupled with the unfavorable wireline signals and the generally low TOC values, indicate that there is no potential associated with iuH reflector in the Fingerdjupet Subbasin. In the Bjørnøya Basin, the iuH reflector has a low – medium amplitude associated with the unit in well 7219/8-1 S. This 50 m thick unit has relatively high TOC values. However, the low RDEP values show little to no response to possible liquid petroleum in the unit.

4.2.2. Intra Barremian (iB) reflector

The iB reflector is extending across the entire Fingerdjupet Subbasin as a continuous, but low amplitude negative reflector (Fig. 5A). The reflector is penetrated by three wells in the Fingerdjupet Subbasin and may be correlated to a unit which record a relatively small increase in TOC contents (Fig. 5B; Table 2). However, the TOC levels are relatively low and wireline logs indicate there is no significant response to the slightly increased TOC values (see iB reflector; Fig. 6). From the Fingerdjupet Subbasin, the iB reflector can be traced to the Bjørnøya Basin over the Ringsel Ridge (Fig. 5A) and further south, parallel along the LFC and BFC. The reflector is generally discontinuous and characterized by a low amplitude close to these fault complexes. Towards the deeper parts of the Bjørnøya Basin, the reflector dims significantly and becomes difficult to interpret. The iB reflector intersects well 7218/8-1 S in the southern parts of the Bjørnøya Basin, where the reflector marks the top of an up to 250 m thick unit with elevated GR and moderate TOC values (Table 2 and Fig. 8).

The iB reflector is distributed over the entire western margin of the Hammerfest Basin. The reflector is continuous, has low – high amplitude characteristics, and interacts with all the wells in the area. However, the reflector has its strongest amplitudes in the NW corner of the Hammerfest Basin, and the reflector dims towards the uplifted central high (Fig. 9). Hence, the nearby wells 7120/6-3 S and 7120/5–1 are regarded as key wells for the iB reflector (Table 2). Furthermore, in well 7120/6-3 S the reflector marks the top of a 48 m tick unit, where the highest TOC values are in the uppermost section of the unit (Table 2; Figs. 9 and 10). Laterally, the TOC content in this unit decrease, demonstrated by well 7120/8-3 situated on the central high and well 7119/9-1 located towards the Tromsø Basin (Fig. 10). At the western transition towards the Tromsø Basin, the reflector is downfaulted along the RLFC and becomes impossible to trace in the deeper basin segments. However, the reflector is traced close to the RLFC in the NE parts of the Tromsø Basin. At this location, the reflector is discontinuous and has a low amplitude. There are no wells in the Tromsø Basin that may provide age-control or wireline data.

Based on the wireline logs, TOC values and amplitude characteristics the iB reflector may represent a potential intra Barremian source rock unit in the NW part of the Hammerfest Basin (i.e. wells 7120/6-3 S and 7120/5–1). The negative amplitude of the reflector increases in magnitude towards the Loppa High and the AFC, this might indicate an increased potential. Laterally, the extensive reflector is penetrated by all the wells on the western margin of the Hammerfest Basin, but the TOC contents and wireline values measured in the corresponding unit do not indicate widespread potential. In the Fingerdjupet Subbasin, the iB reflector is of low amplitude and the TOC content is low in wells 7321/7–1, 7321/8–1 and 7321/9–1. In addition, there is no response in the RDEP or GR log. Hence, there is no evidence for an intra Barremian source rock unit in the Fingerdjupet Subbasin. In the adjacent Bjørnøya Basin, the iB reflector marks the top of a unit exhibiting increased GR values in well 7219/8-1 S. However, there are no increases in the TOC values nor do the wireline logs indicate that there is any source rock potential.

4.2.3. Intra lower Aptian (ilA) reflector

The ilA reflector is widespread in the Fingerdjupet Subbasin but is eroded on the local highs (i.e. well 7312/8–1; Fig. 5B). Amplitude characteristics varies laterally, but the reflector has a distinct negative amplitude in the central basin and the southern parts of the Fingerdjupet

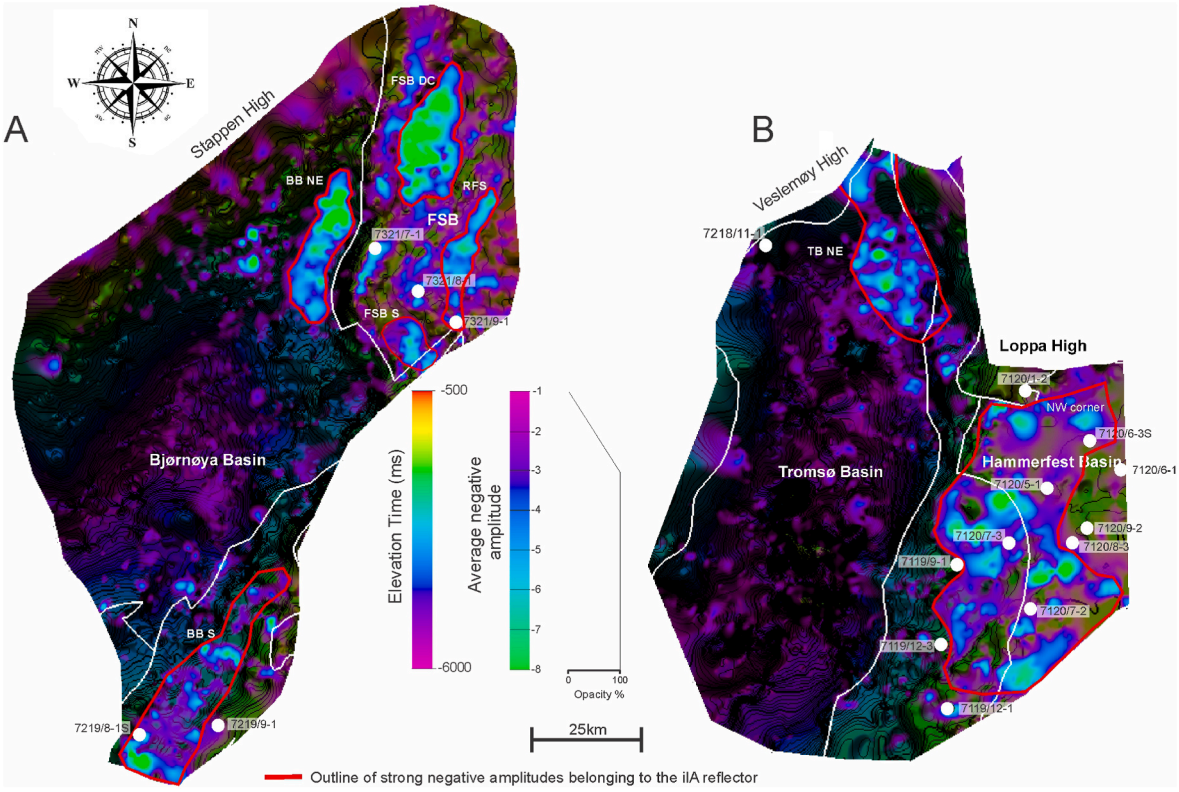

Fig. 11. A) Average negative amplitude and elevation map of the ilA reflector in the Fingerdjupet Subbasin and the Bjørnøya Basin. The negative amplitude map is overlying the elevation map with gradual opacity, in order to highlight the strongest negative amplitudes. B) Average negative amplitude and elevation map of the ilA reflector in the Hammerfest and Tromsø Basins. Outline of structural elements based on maps available at NPD Factpages (2021). Abbreviations: BB: Bjørnøya Basin, FSB; Fingerdjupet Subbasin, RFS: Randi Fault Set, TB: Tromsø Basin, DC: depocenter.

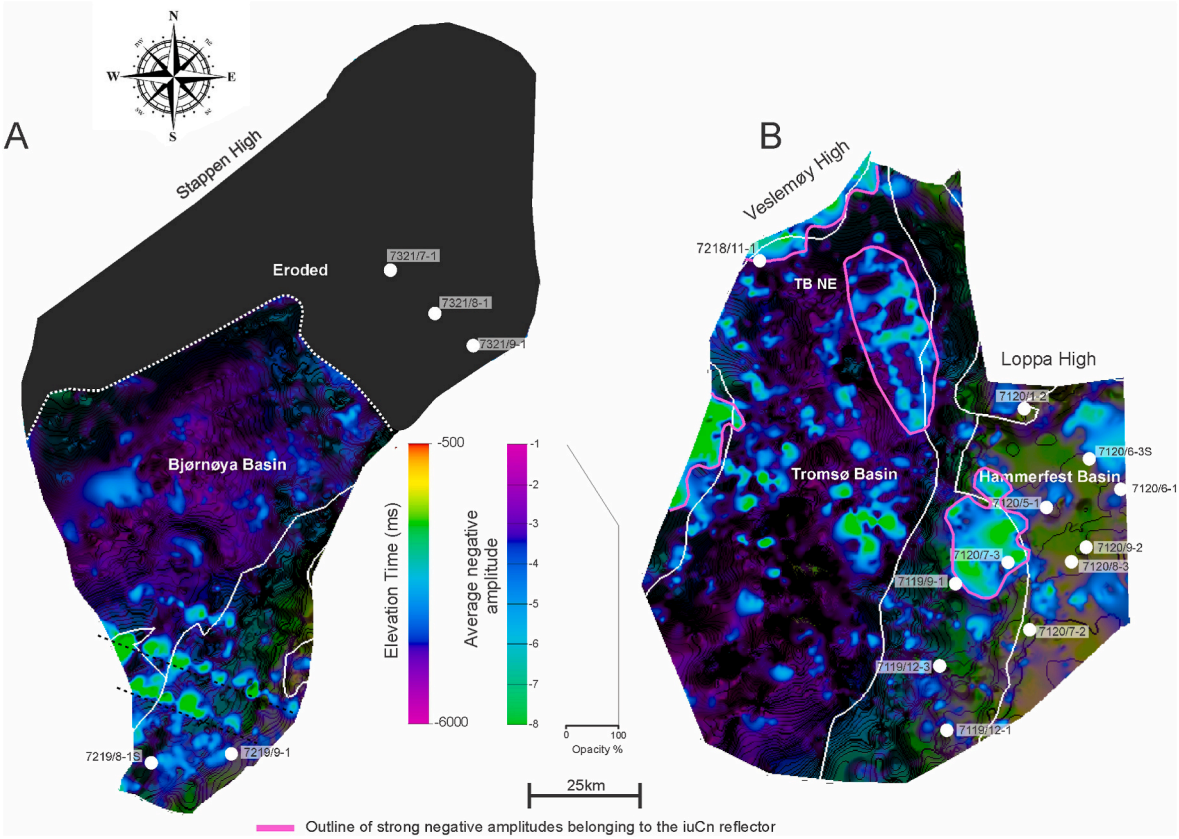

Fig. 12. A) Average negative amplitude and elevation map of the iuCn reflector in the Bjørnøya Basin. The negative amplitude map is overlying the elevation map with gradual opacity, in order to highlight the strongest negative amplitudes. B) Average negative amplitude and elevation map of the iuCn reflector in the Tromsø and Hammerfest Basins. Outline of structural elements based on maps available at NPD Factpages (2021).

Subbasin (Fig. 5A). These negative high amplitudes are illustrated in the negative amplitude map, which show the lateral extent and magnitude of the negative ilA reflector in the Fingerdjupet Subbasin and the Bjørnøya Basin (Fig. 11A). Smaller bright-spots are also sporadically present north of well 7321/9–1 and towards the eastern margin of the Fingerdjupet Subbasin (Fig. 11A). Distribution of these high amplitudes are delimited by local highs controlled by the TFC, LFC and RFS (Figs. 5A–11A).

The ilA reflector is eroded in well 7321/8-1 but it intersects wells 7321/7–1 and 7321/9–1 (Fig. 5B). In well 7321/7–1, there is little indication of a potential source rock unit as the c. 50 m thick unit have low TOC and GR values (Fig. 6). In addition, the RDEP and AC logs do not display any elevated values (Fig. 6). In well 7321/9–1, the ilA reflector marks the top of a 24 m thick unit (levels 961–985 m; Fig. 6), which internally contains five sections of high GR-values and elevated TOC contents (Fig. 6) In addition, the DEN values drop and there is a significant increase in RDEP values (Table 2 and Fig. 6).

The ilA reflector is also mapped in the Bjørnøya Basin. The strongest negative amplitudes are in the NE part of the basin, dimming southwards (Fig. 11A). However, it is still possible to trace it parallel to the LFC and BFC towards well 7219/8-1 S, where the reflector has good continuity and a medium amplitude (Fig. 11A). The reflector is also extending laterally towards the deeper parts of the Bjørnøya Basin, where the reflector dims into a low amplitude reflector of poor continuity (Fig. 11A). Well 7218/8-1 S penetrates the ilA reflector and a 159 m thick unit (Table 1). The unit has a clear increase in TOC values and wireline logs show a small response to the increased TOC values (Table 2 and Fig. 8).

The ilA reflector has a basin-wide distribution in the Hammerfest Basin and typically has a medium to high amplitude with good continuity (Figs. 9–11B). High amplitude patches are sporadically distributed, with some confined to NW part close to the AFC (Fig. 11B). These high amplitude patches are located some distance away from key wells such as 7120/6-3 S and 7119/9–1 (Fig. 11B) but interact with others (e.g. 7120/7–3).

The ilA reflector marks the top of increased TOC values in multiple wells in the Hammerfest Basin (e.g. 7120/6-3 S, 7120/7–3 and 7119/9–1; Figs. 9 and 10). The thickness of these units varies between each

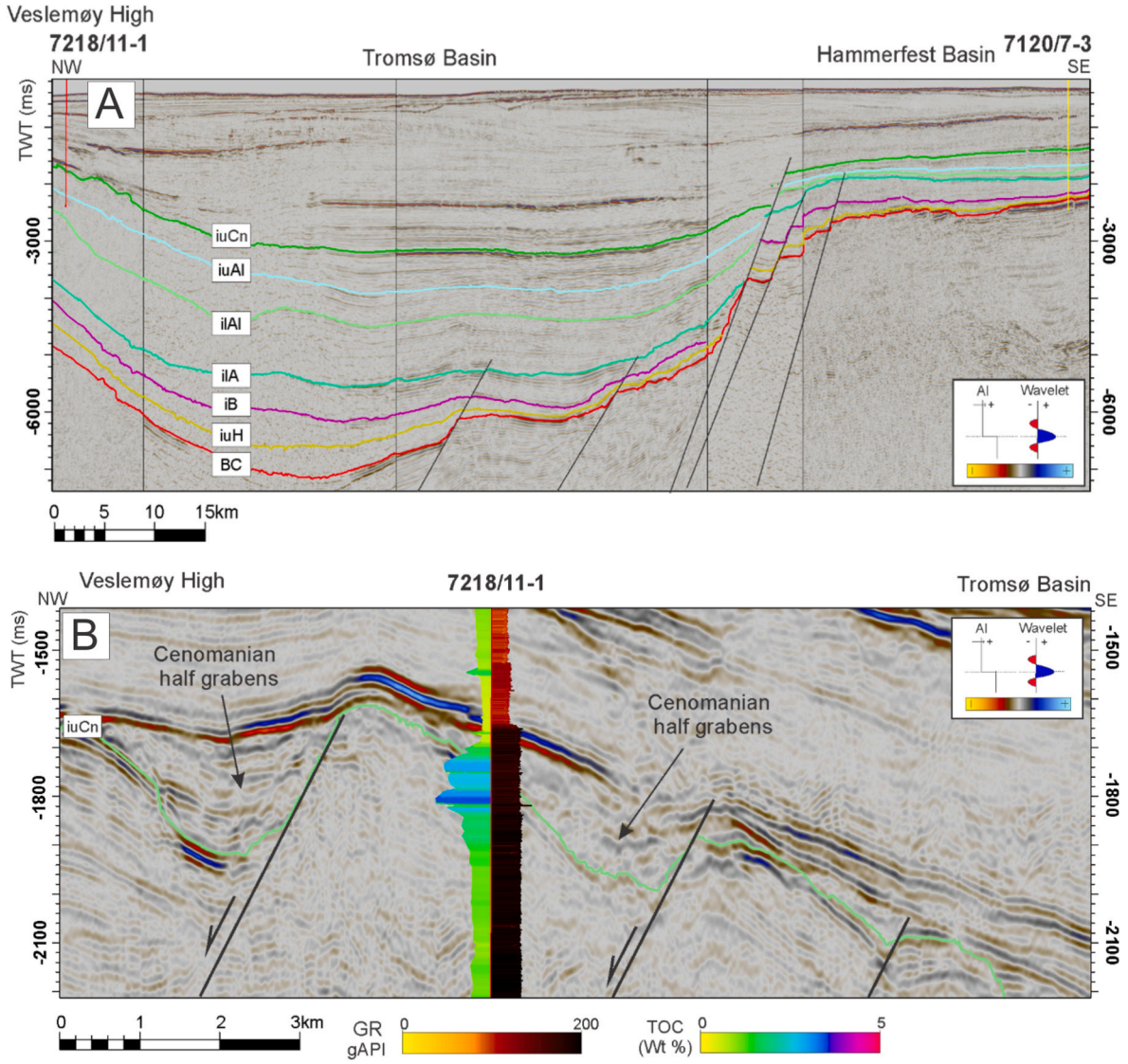

Fig. 13. (A) Seismic composite line covering the NE part of the Tromsø Basin and the western margin of the Hammerfest Basin. Exploration well 7218/11–1 is located in the northern parts of Tromsø Basin and is a key well for the iuCn reflectors which is associated to an inferred upper Cenomanian source rock unit. (B) Seismic section zoomed-in on well 7218/11–1. Here, the iuCn reflector can be traced to the Tromsø Basin across a series of small fault-bound half-graben basins. The TOC-profile shows a pronounced response associated with this reflector. Abbreviations: iuAl: intra upper Albian, ilAl: intra lower Albian, ilA: intra lower Aptian, iB: intra Barremian, iuH: intra upper Hauterivian, BCU: Base Cretaceous Unconformity. Location of the seismic section is indicated in Fig. 1.

Table 3
TOC and Rock-Eval characteristics of the four interpreted source rock units with the highest potential. Average values have been used for each sample interval (Table 1). HI: Hydrogen index, OI: Oxygen index.

Potential source rock unit	Well	Location	TOC wt. %	S2 mg HC/g rock	HI mg HC/g TOC	OI mg CO_2/g TOC	T_{max} °C	Kerogen Type	Vitrinite reflectance (R_o)	Maturity
upper Hauterivian	7120/8-3	Western margin of the Hammerfest Basin	5.02	3.3	67	7	440	III	0.81	Peak mature
	7120/6-3 S		4.07	5.16	130	17	453	II	N/A	Late mature
	7120/9-2		2.09	5.6	265	N/A	N/A	III	N/A	N/A
Barremian	7120/6-3 S	Western margin of the Hammerfest Basin	2.92	8.42	279	11	440	II	N/A	Early mature
	7120/5-1		3.29	3.8	115	11	442	III	0.81	Peak mature
lower Aptian	7321/9-1	Fingerdjupet Subbasin	4.50	19.4	428	11	436	II	N/A	Early mature
	7120/7-3	Western margin of the Hammerfest Basin	3.0	2.9	87	21	446	II-III	0.68	Peak mature
	7219/8-1 S	Southern parts of Bjørnøya Basin,	3.44	3.4	107	63	450	III	0.89	Late mature
upper Cenomanian	7218/11-1	Northern edge of the Tromsø Basin	2.68	7.03	259	35	427	II–III	0.30	Immature

well (Table 1) and common for these units is the lack of wireline response to the elevated TOC values (Table 2). When traced laterally across the RLFC, the ilA reflector changes into a low amplitude reflector with poor continuity, which persists across major parts of the Tromsø Basin. (Fig. 11B). The reflector has medium amplitudes with good continuity in the NE part of the basin (Fig. 11B). Here, the reflector is located at depth of c. 5500 ms, implying that any organic matter has most likely reached very high maturity. In addition, there are no wells in the Tromsø Basin that penetrate the ilA reflector to confirm its potential.

Based on wireline logs, increased TOC values and amplitude characteristics, the ilA reflector is interpreted to represent a potential source rock unit in the Fingerdjupet Subbasin. The potential may extend from well 7321/9–1 towards the deeper parts of the basin in the southern and central parts of the Fingerdjupet Subbasin. In addition, bright spots recorded within the RFS north of well 7321/9–1 may indicate some potential. The reflector also shows favorable amplitude characteristics in the NE part of the Bjørnøya Basin, in proximity to the LFC and the Ringsel Ridge.

Indication of a viable source rock unit is also documented in the Hammerfest Basin. Although there are several wells recording elevated TOC contents, there are no other favorable indications in the wireline data (e.g. well 7120/6-3 S, 7120/7–3 and 7119/9–1). However, the negative amplitude map suggests sporadically distributed bright spots that may indicate an increased potential in the NW part of the basin (i.e., near the AFC). In the NE margin of the Tromsø Basin, the ilA reflector has increased amplitude compared to in the rest of the basin. However, it is positioned at a depth of c. 5500 ms, which implies that any organic matter most likely has reached very high maturity.

4.2.4. *Intra upper Cenomanian (iuCn) reflector*

The iuCn reflector is only present in the deeper parts of the Bjørnøya Basin as it is eroded in the Fingerdjupet Subbasin and across the Stappen High. (Fig. 12A). The iuCn reflector is continuous with low – medium amplitudes, which increases to medium – high further south in the basin towards well 7219/8-1 S (Figs. 7–12A). Elongated high amplitude anomalies are also present in this area (Fig. 12A). The reflector terminates against the BFC on the western margin of the Loppa High but extends across the Veslemøy High to the west of well 7219/8-1 S (Fig. 12A). In well 7219/8-1 S, the corresponding 43 m thick unit records a small increase in TOC values (Table 2). However, the wireline logs indicate that there is no significant response to the TOC content (Fig. 8).

The iuCn reflector is present along the entire western segment of the Hammerfest Basin, delimited by the Loppa High and the Finnmark Platform (Fig. 12B). The reflector is continuous and has a medium – high amplitude, where local high amplitudes occur along the western margin of the basin and towards the Loppa High (Fig. 12B). High amplitude patches are located around key wells such as well 7120/6-3 S near the Loppa High, and well 7120/7–3 towards the Tromsø Basin (Fig. 12B). The iuCn reflector is penetrated by all the wells in the western Hammerfest Basin, but common for these wells is that there is no indication of elevated TOC values associated with this event.

The iuCn reflector is traced from the Hammerfest basin across the RLFC into the Tromsø Basin (Fig. 13A). Here, the amplitude characteristics changes to a lower amplitude, but remains continuous. The reflector extends laterally throughout the basin and the negative amplitude map shows that strong negative amplitudes are present in the central parts and along the basin edges (Fig. 12B). NNE – SSW-oriented, elongated amplitude anomalies are also present across the basin (Fig. 12B).

Well 7218/11–1 is one of few wells that penetrates the iuCn reflector in the Tromsø Basin (Fig. 13A and B). From the seismic data, it is clear that this well is positioned in a half-graben setting near the basin margin (Fig. 13B). At this location, the iuCn reflector has a low – medium amplitude (Fig. 13B). The corresponding 121 m thick unit in the well has elevated TOC values, but wireline logs indicate that there is little to no response to the increased organic matter beneath the iuCn reflector (Table 2 and Fig. 8).

Although the iuCn reflector is penetrated by key wells in the Bjørnøya, Hammerfest and Tromsø basins, there are no TOC values or wireline signals that convincingly demonstrate the presence of a potential upper Cenomanian source rock unit. However, there are some elevated TOC values in well 7218/11–1. The general lack of response in the wireline logs may indicate that the concentration of organic matter is too low to produce a signal characteristic for prolific source rock units.

4.3. *Source rock evaluation of the organic-rich units*

Based on the mapping of the four high-amplitude negative reflectors in the seismic data (i.e. the iuH, IB, ilA, and iuCn reflectors; Table 2) combined with analyses of the wireline and TOC data, four organic-rich units representing potential source rock units are suggested. These includes: 1) upper Hauterivian, 2) Barremian, 3) lower Aptian, and 4) upper Cenomanian units. These potential source rock units occur atop of sequences 0, 1, 2 and 6, respectively (Fig. 2). Source rock characteristics based on the available Rock-Eval data (see Table 1 for sample interval, and the online supplementary file SF1 for the raw data) are given for each of these potential source rock units. The main characteristics of the

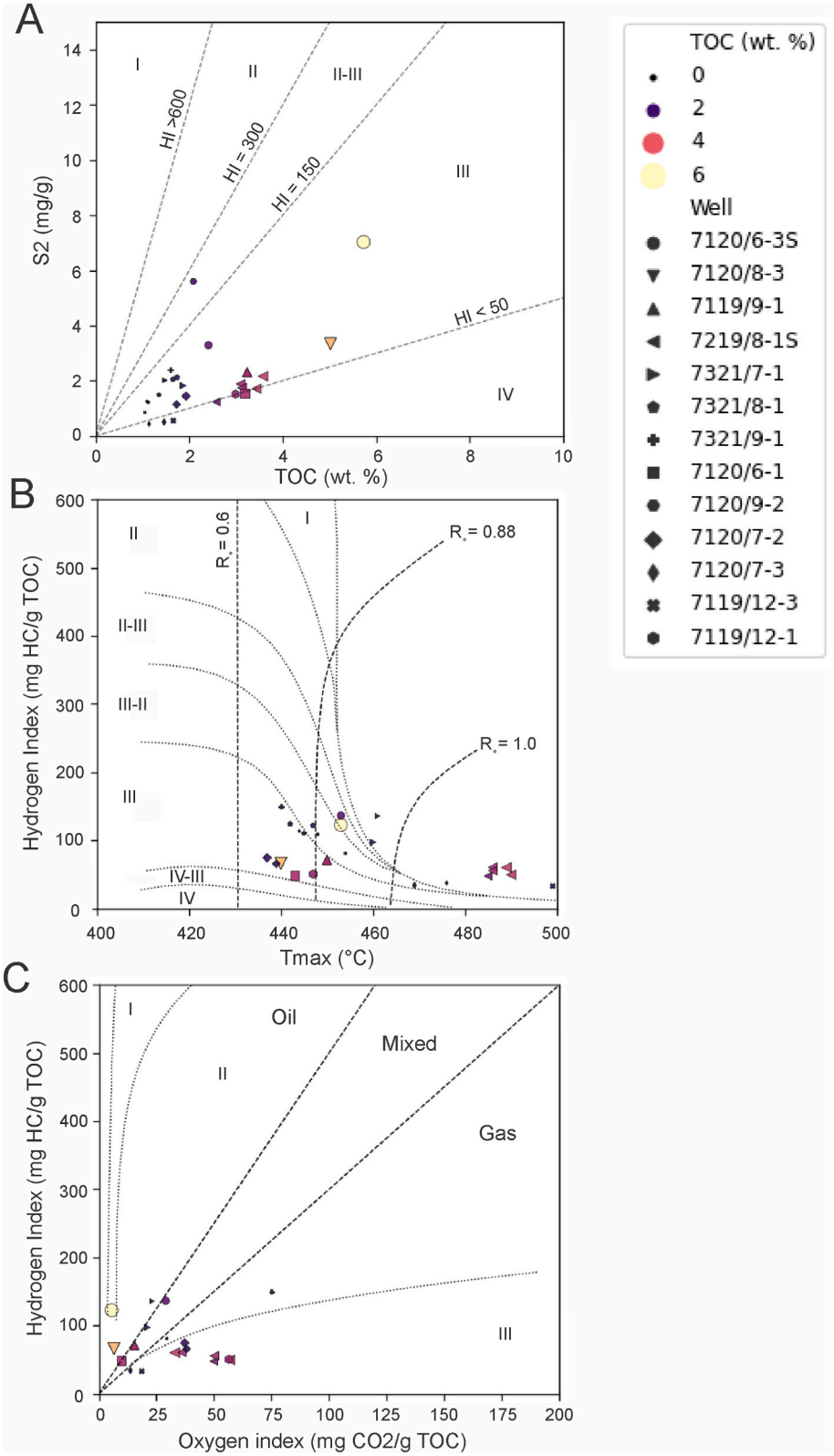

Fig. 14. Plots showing the potential of the Hauterivian source rock unit (corresponding to the iuH reflector) in key wells across the SW Barents Shelf. Sample points increase in size depending on TOC values. Sample points from each well have a specific marker. Location of the wells are shown in Fig. 1. The sample interval and thickness are shown in Table 1 (A) Cross-plot of TOC vs. Rock-Eval S2 values, overlying are the hydrogen index (HI) lines which indicate kerogen type. (B) Plot of T_{max} vs. HI indicating the petroleum potential and maturity of the samples. Overlying are the vitrinite reflectance (Ro) lines after Isaksen and Ledje (2001). (C) van Krevelen diagram of HI vs. OI indicating the quality and maturation level of the samples.

units with highest potential are summarized in Table 3.

4.3.1. Characteristics of the upper Hauterivian organic-rich unit

The characteristics of the upper Hauterivian organic-rich unit is shown in Fig. 14. In general, most of the analyzed samples have poor potential indicated by low S2 values (S2 < 2.5 mg/g) and variable TOC content (1.0–5.7 wt %; Fig. 14A). They also have low HI (50–150 mg HC/g TOC; Fig. 14B) and OI values (1–75 CO_2/g TOC; Fig. 14C). Furthermore, the same samples appear to be mature with T_{max} values of 430–460 °C (Fig. 14B) and near the vitrinite reflectance trend line 0.88%

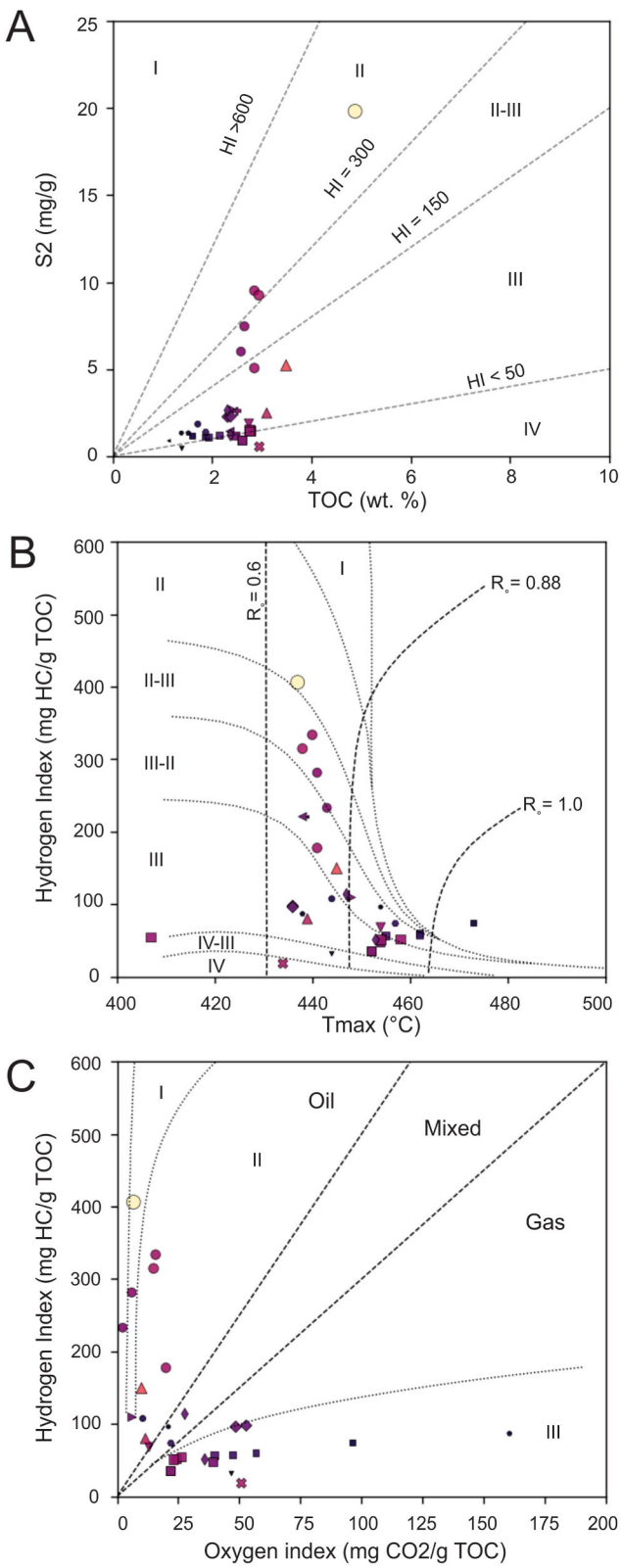

Fig. 15. Plots showing the potential of the Barremian source rock unit (corresponding to the iB reflector) in key wells across the SW Barents Shelf. Sample points increase in size depending on TOC values. Sample points from each well have a specific marker. Location of the wells are shown in Fig. 1. The source rock units thickness and data is shown in Table 1 (A) Cross-plot of TOC vs. Rock-Eval S2 values, overlying are the hydrogen index (HI) lines which are indicating kerogen type. (B) Plot of T_{max} vs. HI indicating the petroleum potential and maturity of the samples. Overlying are the vitrinite reflectance (Ro) lines after Isaksen and Ledje (2001). (C) van Krevelen diagram of HI vs. oxygen index (OI) indicating the quality and maturation level of the samples.

(Fig. 14B). Collectively, the majority of the samples indicate that kerogen Type III dominates the upper Hauterivian organic-rich unit and that gas is the main expelled product (Fig. 14C).

A few sample points deviate from the general trend of the organic-rich unit and may reflect more localized potential. This includes samples from wells 7120/8–3, 7120/6-3 S and 7120/9–2, which all show higher potential (Table 3 and Fig. 14A). However, these units are relatively thin and contain few sample points (Table 1). Well 7120/6-3 S contains the most prolific sample of the Hauterivian organic-rich unit. These samples have higher HI values and plots within the kerogen Type II field (Fig. 14C). No vitrinite reflectance data is available for well 7120/6-3 S.

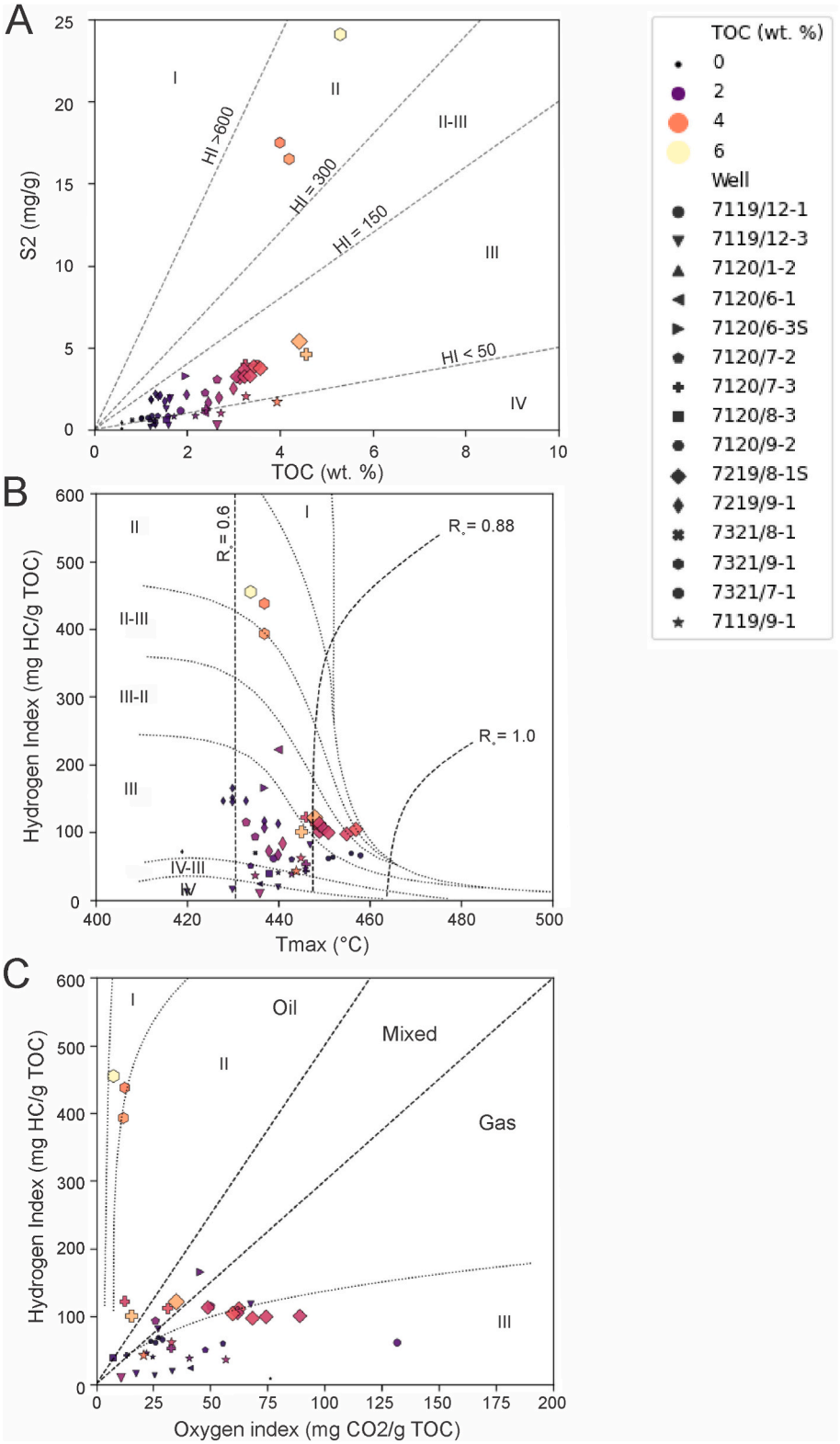

Fig. 16. Plots showing the source rock potential of the Lower Aptian source rock unit (corresponding to the ilA reflector) in key wells across the SW Barents Shelf. Sample points increase in size depending on TOC values. Sample points from each well have a specific marker. Location of the wells are shown in Fig. 1. The source rock thickness and data is shown in Table 1 (A) Cross-plot of TOC vs. Rock-Eval S2 values, overlying are the hydrogen index (HI) lines which are indicating kerogen type. (B) Plot of T_{max} vs. HI indicating the petroleum potential and maturity of the samples. Overlying are the vitrinite reflectance (Ro) lines after Isaksen and Ledje (2001). (C) van Krevelen diagram of HI vs. OI indicating the quality and maturation level of the samples.

4.3.2. *Characteristics of the Barremian organic-rich unit*

Fig. 15 shows the source rock evaluation of the samples from the Barremian organic-rich unit. The general trend shows that most of the samples have a poor potential indicated by low S2 values (S2 < 2.5 mg/g) and a variable TOC content (1.13–4.88 wt %; Fig. 15A). In addition, most of the samples have low HI values (50–150 mg HC/g TOC) and T_{max} values of 430–470 °C (Fig. 15B). The samples also have low OI values (1–100 CO_2/g TOC; Fig. 15C). In total, most of the data indicate a mature (Fig. 15B) kerogen Type III dominated (Fig. 15C) organic-rich unit, with poor potential (Fig. 15A).

The source potential of the Barremian organic-rich unit seems to be very localized demonstrated by samples in wells 7120/6-3 S and 7120/5–1, as these stand out as the most prolific ones (Table 3 and Fig. 15A). The most prolific sample is taken from well 7120/6-3 S and has a S2

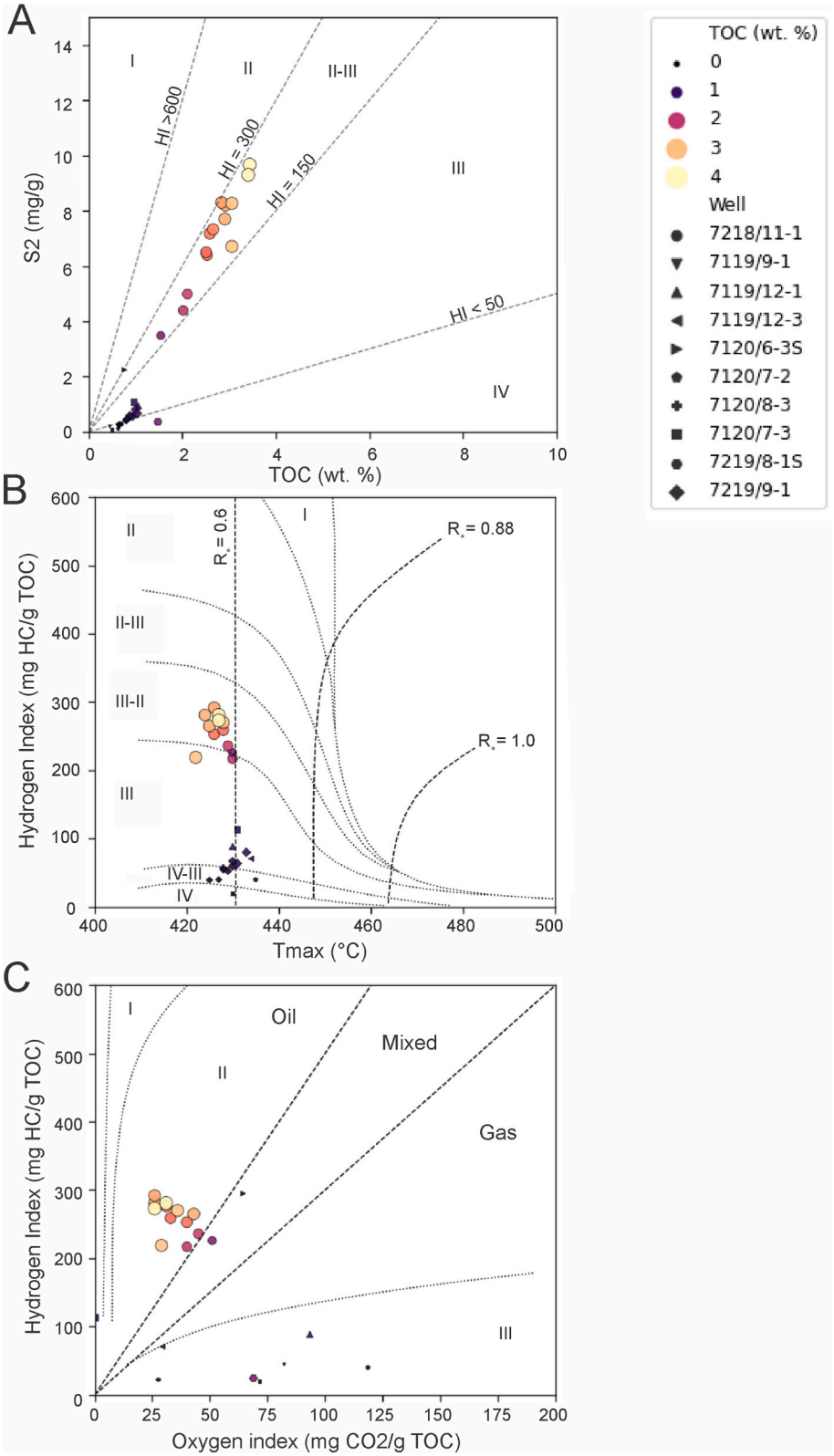

Fig. 17. Plots showing the source rock potential of the Cenomanian source rock unit (iuCn) in key wells across the SW Barents Shelf. Sample points increase in size depending on TOC values. Sample points from each well have a specific marker. Location of the wells are shown in Fig. 1. The source rock units thickness and data is shown in Table 1 (A) Cross-plot of TOC vs. Rock-Eval S2 values, overlying are the hydrogen index (HI) lines which are indicating kerogen type. (B) Plot of T_{max} vs. HI indicating the petroleum potential and maturity of the samples. Overlying are the vitrinite reflectance (Ro) lines after Isaksen and Ledje (2001). (C) van Krevelen diagram of HI vs. OI indicating the quality and maturation level of the samples.

value of 19.82 mg/g and TOC values of 4.88 wt% (Fig. 15A). In general, samples in well 7120/6-3 S exhibit higher hydrogen content (Table 3 and Fig. 15B). In addition, T_{max} values are on average 440 °C, while the vitrinite reflectance (R_o) ranges between 0.6 and 0.88% (Fig. 15B). Collectively, the Barremian organic-rich unit in well 7120/6-3 S has excellent potential with a kerogen Type II composition and is further classified as an early mature to mature oil prone source rock unit.

4.3.3. *Characteristics of the lower Aptian organic-rich unit*

The source rock evaluation on the samples from the lower Aptian organic-rich unit is shown in Fig. 16. Most of the samples are plotting in the poor potential area with low S2 values (S2 < 2.5 mg/g) and

generally low TOC content (1.5–3 wt %; Fig. 16A). These samples have HI values close to 100 mg HC/g TOC and are plotting around T_{max} values of 440 °C to the right of the $R_o = 0.6$ vitrinite reflectance trend line (Fig. 16B). The same cluster also has variable OI values (1–100 CO_2/g TOC) coupled with low HI values (Fig. 16C). Collectively, this indicate that most of the lower Aptian organic-rich samples have a kerogen Type III composition where the expected product would be gas.

A few samples from wells 7321/9–1, 7219/8-1 S, and 7120/7-3 deviate from the general trend and indicate a localized higher potential (Table 3 and Fig. 16A). The most prolific samples for the lower Aptian organic-rich unit are from well 7321/9–1 and have a kerogen Type II composition (Table 3; Fig. 16A and B) No vitrinite reflectance data are available for this source rock unit but based on T_{max} values and the vitrinite reflectance $R_o = 0.6$ trend line, the organic-rich unit is early mature (Fig. 16B). The organic-rich unit has also low OI values and high HI values, implying that the organic-rich unit is high quality and that the main expelled product is oil (Fig. 16C).

Multiple samples from the organic-rich unit in well 7219/8-1 S and 7120/7–3 also indicate elevated potential (Table 3). However, this unit has significantly lower HI values compared to well 7321/9–1 and has a kerogen Type III composition (Fig. 16A and B). The exceptional high T_{max} values in well 7219/8-1 S plot to the right of the $R_o = 0.88\%$ vitrinite reflectance trend line, indicating that the organic-rich unit is mature at this locality (Fig. 16B). Furthermore, based on the OI and HI values the main expelled product is gas from the organic-rich unit in well 7219/8-1 S (Fig. 16C). In contrast, the samples in well 7120/7-3 plots to the left of the $R_o = 0.88$ vitrinite reflectance trend line (Fig. 16B) and within the oil window (Fig. 16C).

4.3.4. Characteristics of the upper Cenomanian organic-rich unit

The source rock evaluation performed on the samples from the upper Cenomanian organic-rich unit is displayed in Fig. 17. Apart from samples in well 7218/11–1, most of the samples show a unimodal distribution with very poor potential, indicated by low S2 (S2 < 2.5 mg/g) and TOC values (0.83–1.49 wt %; Fig. 17A). These samples also have low HI values (20–110 mg HC/g TOC) and variable T_{max} values (422–435 °C; Fig. 17B). This indicates that the small amount of organic matter is most likely of kerogen Type IV–III composition (Fig. 17A and B) and that the main product is gas (Fig. 17C).

The exception is well 7218/11–1 which overall shows a better potential with substantially higher TOC and S2 values (Table 3 and Fig. 17A). Samples from 7218/11–1 also have higher HI values and slightly lower T_{max} values compared to the low potential samples (Table 3 and Fig. 17B). Hence, these samples plot left of the vitrinite reflectance trend line $R_o = 0.6$ (Fig. 17B). In addition, three samples of vitrinite reflectance are available for the unit. These samples have little spread and have an average R_o value of 0.3%. In total, this classifies the organic matter in well 7218/11–1 as a kerogen Type II-III (Fig. 17C) where the main expelled product is oil (Fig. 17C). However, based on the T_{max} values and the vitrinite reflectance samples, the organic-rich unit is classified as immature at the well location.

5. Discussion

The presence of four organic-rich units of variable source rock potential has been documented within the Lower Cretaceous succession on the SW Barents Shelf, these are the: (1) upper Hauterivian (2) Barremian, (3) lower Aptian, and (4) upper Cenomanian organic-rich units (Table 3). These units have different characteristics which result in varying potential across the region. This may reflect variations in depositional environments and oxygen levels, organic productivity, and preservation potential governed by amongst other factors such as sedimentation rate, basin configurations and hydrodynamic conditions.

During the Early Cretaceous, active rifting in the SW Barents Sea resulted in a typical rift configuration with fault-bounded basins separated by structural highs (e.g. Faleide et al., 1984, 1993a, b; Marin et al., 2018a, b). At times when the structural highs were submerged, well-oxygenated hydraulic regimes may have persisted across the highs, whereas stagnant, oxygen deficient conditions may have prevailed in the deeper parts of the basins due to physical restriction and reduced bottom water circulation (e.g. Langrock et al., 2003). Consequently, wells targeting the structural highs that formed during the Early Cretaceous structuring-events, typically sample Lower Cretaceous stratigraphy which most likely exhibit low quantity and quality organic matter. Thus, elevated TOC and HI values, as well as increased source potential are generally expected for the deeper parts of the Early Cretaceous fault-bounded depocenters (e.g. Karlsen et al., 2004: Karlsen and Skeie, 2006). In addition, the data only give an indication of the remaining potential at the prevailing levels of thermal maturity. At early burial, the organic matter was less mature and had higher quality and quantity. Understanding variations in depositional environments and burial history of the potential source rock units is therefore essential. Below, a depositional model for each of the organic-rich units are presented, emphasizing various factors controlling their source potential, particularly focusing on the areas where they have been confirmed by exploration wells and thus hold the greatest potential.

5.1. Controls on source rock distribution and potential

To form a viable source rock unit there must be sufficient primary biological productivity in the depositional environment (Calvert et al., 1996). Primary productivity near continental margins in the marine environment is dependent on nutrient influx either by fluvial run-off or upwelling of deep marine water (Demaison et al., 1983). The Loppa High which is situated in the center of the study area, was subaerially exposed during the Early Cretaceous (Faleide et al., 1993a; Indrevær et al., 2017) and was most likely a crucial source for influx of both sediments and nutrients (e.g. Seldal, 2005; Marín et al., 2017, 2018a; Ärlebrand et al., 2021). In addition, the warm and humid climate characterizing the Cretaceous period, promoted increased organic productivity and biotic changes (Leckie et al., 2002; Scotese et al., 2021) that was crucial for organic matter to be deposited (e.g. Rogov et al., 2020).

Furthermore, the formation of fault bounded depocenters on the SW Barents Shelf and further south along the western margin of the NCS during the Late Jurassic – Early Cretaceous (e.g. Langrock et al., 2003), resulted in restricted circulation and anoxic conditions that ensured optimal preservation conditions, further prohibiting oxidative processes, degradation and consumption of organic matter (Demaison and Moore, 1980). These anoxic to suboxic conditions are also regarded as being the product of climatic variations associated with oceanic anoxic events (OAEs) (Leckie et al., 2002; Midtkandal et al., 2016; Rogov et al., 2020). However, the variations and differences in richness and quality of the organic matter is strongly linked to regional and local paleogeographic factors that affected the basin infill history.

Other controlling factors include grain size and sedimentation rate. Grain size has implications towards preservation of organic matter, as coarse-grained sediments may allow circulation of oxygenated bottom waters into the sediments (Bordovskiy, 1965). In the study area, this could be a localized issue near active sediment source areas such as the Loppa High but for the wider SW Barents Shelf, most of the Cretaceous sediments appear to consist of marine mudrocks with low permeability. Sedimentation rate has a crucial control on the concentration of organic matter, as high rates will cause a dilution effect (Ibach, 1982). According to literature, sedimentation rate should ideally be approximately 1 mm/year (Ibach, 1982; Bohacs et al., 2005). This could be problematic for potential source rock units situated in the Bjørnøya and Tromsø basins, as the Late Jurassic – Early Cretaceous rifting phase caused rapid subsidence and increased sedimentation rates along the RLFC and BFC (Faleide et al., 1984, 1993a, 1993b; Kairanov et al., 2021). In addition, the arrival of large prograding delta systems in the Barremian to early Aptian (from the NW) and in the Albian to Cenomanian (from the E to

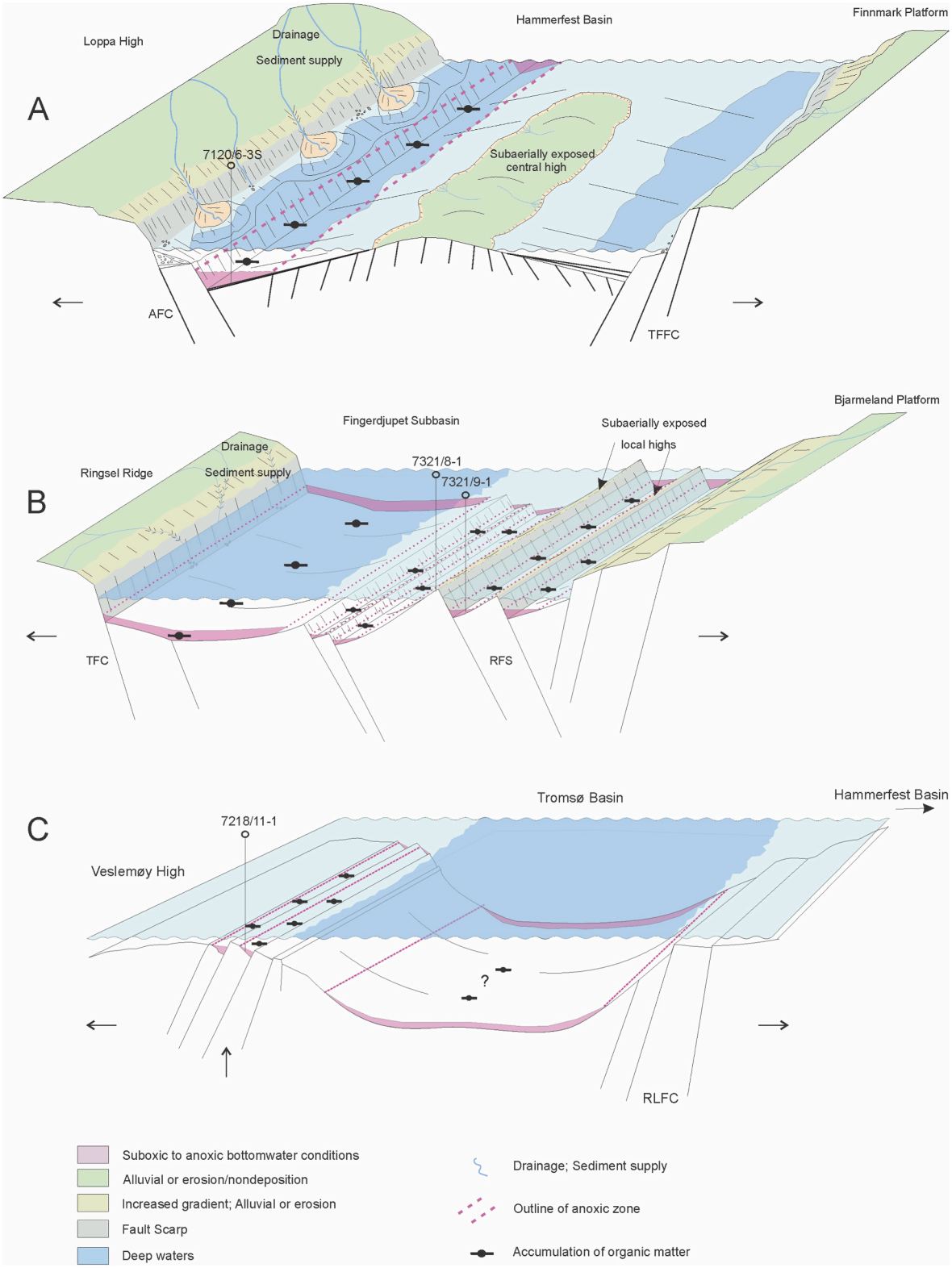

Fig. 18. (A) Depositional model outlining the basin configuration and conditions during deposition of (A) the Hauterivian and Barremian source rock unit in the Hammerfest Basin, (B) the lower Aptian source rock unit in the Fingerdjupet Subbasin, and (C) the upper Cenomanian source rock unit at the transition to the Veslemøy High. Abbreviations: AFC: Asterias Fault Complex, TFFC: Troms Finnmark Fault Complex, RLFC: Ringvassøy Loppa Fault Complex, LFC: Leirdjupet Fault Complex, RFS: Randi Fault Set.

NE) may locally have contributed to increased sedimentation rates and consequently lowered the source rock potential in the receiving basins during these times.

5.1.1. Depositional model and source rock potential of the upper Hauterivian organic-rich unit

The evaluation of the Hauterivian organic-rich unit shows that most of the samples have a kerogen Type III composition with variable TOC content and low S2 values (S2 < 2.5 mg/g). This includes the wells in the Fingerdjupet Subbasin (7321/7–1.7321/8–1, 7321/9–1) and the southern parts of Bjørnøya Basin (7219/8-1 S). The unit was established as mature to overmature in the shallow basins and essentially overmature in well 7219/8-1 S (Fig. 14A). Based on the maturity data in well 7219/8-1 S (Fig. 16) and the lateral mapping of the iuH reflector, we interpret that there is presently no source rock potential for the Hauterivian organic-rich unit in the deep basins, caused by deep burial and compaction. However, a few wells in the Hammerfest Basin (7120/8–3, 7120/6-3 S, 7120/9–2) have higher potential indicated by higher S2 and HI values (Fig. 14A and B). The most prolific samples are taken from well 7120/6-3 S, located close to the NW part of the Hammerfest Basin (Figs. 9 and 10).

The upper Hauterivian organic-rich unit is also present in a more condensed form towards the central high of Hammerfest Basin (e.g. wells 7120/8–3 and 7120/9–2, Fig. 14). The iuH reflector extends further towards the transition to Tromsø Basin. In this transition, the reflector is part of the down-stepping array of normal faults of the RLFC. Source rock evaluation done on samples from wells located in this transition (e.g. 7120/7–2, 7120/7–3, 7119/9–1, 7119/12–3 and 7119/12–1) confirms that the iuH reflector is not associated with a high potential source rock unit (Fig. 14). This supports our interpretation of a localized prolific upper Hauterivian organic-rich unit confined to a restricted depocenter, such as the NW part/segment of the Hammerfest Basin.

According to Ohm et al. (2008) the Knurr Formation (which includes the Hauterivian organic-rich unit of this study; Fig. 2) has a higher potential than the Kolje and Kolmule formations. Their study was predominantly focused on the Hammerfest Basin, where most exploration wells in the SW Barents Sea are located. Their initial findings suggest a low potential for the Knurr Formation, which is in accordance with our source rock evaluation (Fig. 14). However, we emphasize that there is an increased potential in the shallow depocenter of Hammerfest Basin (i.e. in well 7120/6-3 S, NW part). Still, very few exploration wells have drilled the thick sedimentary successions in these depocenters, as most exploration wells typically target structural highs.

The SW Barents Shelf was subject to multiple episodes of rifting during the Late Jurassic – Early Cretaceous extensional event (Faleide et al., 1984, 1993a, 1993b; Gabrielsen et al., 1990; Serck et al., 2017; Kairanov et al., 2021). The elevated potential documented in the NW part of the Hammerfest Basin is clearly linked to the patchy occurrence of smaller fault-bound depocenters that formed during the earliest Cretaceous. It is well known that structural confinement of marine basins may result in restricted water circulation, which eventually lead to oxygen deficient conditions that promote the preservation of organic matter (Demaison and Moore, 1980; Demaison et al., 1983).

We thus envisage that the upper Hauterivian organic-rich unit in the Hammerfest Basin was deposited and preserved in a partly restricted marine setting, between the subaerially exposed Loppa High and the uplifted central arch (Figs. 10–18A). This depocenter formed in response to faulting along the AFC, which was initiated in the Late Jurassic – earliest Cretaceous (Wood et al., 1989; Gabrielsen et al., 1990). The uplifted central arch acted as intrabasinal highs where onlap terminations in sequence S0 and S1 indicate periodic subaerial exposure (Fig. 10) (Indrevær et al., 2017; Marín et al., 2018b). To the north, the Loppa High was subaerially exposed at these times (Faleide et al., 1993a, 1993b) due to periodic and differential uplift that shifted the drainage patterns and promoted the development of incised valleys that routed sediments to the basin (Fig. 18A) (Indrevær et al., 2017; Marín et al., 2018b). In this configuration, the NW corner of the Hammerfest Basin was a partly restricted, bounded between two subaerially exposed structural highs (Marín et al., 2018b). Consequently, this gave the characteristic wedge shape of sequence S0 and S1 in the NW corner but also resulted in increased preservation potential for organic matter. (Fig. 18A). Deep-water conditions prevailed in the central parts of the Hammerfest Basin which was connected to the Tromsø Basin in the west securing better water circulation (Fig. 18A; Marín et al., 2018b).

The kerogen Type III composition characterizing the upper Hauterivian organic-rich unit, suggest that most of the organic matter is of terrestrial origin or of a partly oxidized type possibly including a resedimented fraction (Tissot et al., 1973; Peters, 1986; Peters and Cassa, 1994). The nearby subarial exposed Loppa High was most likely a source for the organic matter, which was transported to the basin by gravitational processes (Fig. 18A). In contrast, the source rock unit in well 7120/6-3 S has a more dominant kerogen Type II composition (Fig. 14C). This may indicate that organic matter accumulated under restricted water circulation which allowed suboxic to anoxic conditions to develop (Demaison and Moore, 1980; Demaison et al., 1983). The nearby sediment source area also ensured high nutrient influx into the marine environment, allowing high productivity under the warm and humid climatic conditions that prevailed during the earliest Cretaceous (Fig. 18A).

5.1.2. Depositional model and source rock potential of the Barremian organic-rich unit

The iB reflector is widely distributed on the SW Barents Shelf and is penetrated by wells in the Fingerdjupet Subbasin, the Bjørnøya Basin and the Hammerfest Basin. Despite its wide distribution, most samples belonging to the Barremian organic-rich unit indicate a mature unit with a kerogen Type III composition yielding low generation potential (Fig. 15; Tables 2 and 3). Similar to the upper Hauterivian organic-rich unit, the most prolific unit occurs in well 7120/6-3 S and 7120/5–1 at the NW corner of the Hammerfest Basin (Fig. 15 and Table 3). At this location, the Barremian organic-rich unit have a kerogen Type II composition (Fig. 15C).

In the Fingerdjupet Subbasin, the iB reflector is located on top a SE-prograding sequence which probably was sourced from the Svalbard Platform that experienced significant uplift in the Barremian (Grundvåg et al., 2017; Marín et al., 2017; Midtkandal et al., 2019). In many prolific basins elsewhere, an elevated source rock potential (i.e. kerogen Type II–I) is commonly reported within the top-set to bottomset of similar large-scale prograding clinoform successions (Barker, 1982; Kosters et al., 2000; Ulmishek, 2003). However, based on the mapping of the iB reflector and the lack of response in the wireline and Rock-Eval data (i.e. 7321/7–1, 7321/8–1 and 7321/9–1), we conclude that the Barremian organic-rich unit does not have any potential in the Fingerdjupet Subbasin.

The source rock evaluation conducted on samples belonging to the Barremian organic-rich unit in well 7219/8-1 S indicate that organic matter is of kerogen Type III and do not hold any potential based on low S2 and HI values (Fig. 15A and B). In addition, the unit is classified as post-mature based on T_{max} values and two vitrinite reflectance samples (Fig. 15A). This has wider implication towards the Bjørnøya and Tromsø basins, as any organic matter that belong to the potential Barremian organic-rich unit is most likely post-mature in the deeper basinal segments.

During deposition of the Barremian organic-rich unit, the NW part of the Hammerfest Basin continued to be an important fault-bound depocenter, and the central arch and the Loppa High were still uplifted, both acting as source areas and exhibiting first-order controls on the basin configuration which was essential for anoxic conditions to be maintained (Fig. 18A).

The long-lived restricted character of the NW depocenter of the Hammerfest Basin governed water circulation and promoted water

stratification and anoxic bottom water conditions (Fig. 18A). Increased fluvial run-off (from the Loppa High) and increased primary productivity influenced by the warm and humid climate and an associated oxygen consumption in the water mass further promoted anoxic bottom water conditions (Fig. 18A). This interpretation is coherent with the kerogen Type II composition of the Barremian organic-rich unit in well 7120/6-3 S (Fig. 15).

5.1.3. Depositional model and source rock potential of the lower Aptian organic-rich unit

The seismic mapping and source rock evaluation of the lower Aptian organic-rich unit indicate that there is an elevated potential in the Fingerdjupet Subbasin and possibly also in the Bjørnøya and Hammerfest basins (Table 3). The unit in well 7321/9–1 was established to be the most prolific and is linked to negative amplitudes occurring in localized fault bounded depocenters in the Fingerdjupet Subbasin (Fig. 11A).

The negative amplitudes concentrated around well 7321/9–1 also extends laterally towards the NNE (Fig. 11A) and appear to be confined to half-grabens (Fig. 5B) that most likely link up with the NNE – SSW-oriented RFS (Fig. 11A), cf. Serck et al. (2017). However, the strongest negative amplitudes are confined to the main depocenter of the Fingerdjupet Subbasin (Fig. 11A, controlled by the N–S and NNE – SSW trending faults belonging the TFC and RFS (Serck et al., 2017). Strong negative amplitudes are also present in the southern part of the Fingerdjupet Subbasin (Fig. 11A). These amplitudes occur in a downfaulted section close to the LFC associated with a distinct thickness increase of the sequence S3 strata. This may indicate a connection to the suggested reactivation event in the early Aptian (Serck et al., 2017).

In the Bjørnøya Basin, the lower Aptian organic-rich unit has kerogen Type III composition and is late mature in well 7219/8-1 S (Table 3). The dim negative amplitudes surrounding well 7219/8-1 S (Fig. 11A) further indicate that this area does not hold any high concentration of organic matter. However, based on the lateral mapping, the unit is most likely extending from well 7219/8-1 S parallel to the nearby fault complexes (i.e. BFC and LFC) and could possibly be associated with the strong negative amplitudes present in the NE corner of the basin (Fig. 11A). It thus appears that the lower Aptian organic-rich unit preferably accumulated along the NE basin margins where conditions were favorable. The amount of TOC in marine sediments is controlled by the abundance and availability of organic matter, preservation and the degree of dilution by sedimentary input (Pedersen and Calvert, 1990). It thus seems that the lower Aptian organic-rich unit was subjected to less dilution effect further north towards the LFC. This may relate to a less active local source area of limited extent (i.e. Ringsel Ridge), possibly coupled with delimited or structurally diverted drainage patterns along the major fault complexes in the area. Consequently, this limited sediment input and the dilution effect in this area. In well 7219/8-1 S, the elevated TOC values of the lower Aptian organic-rich unit are confined to a thick interval (159 m; Tables 1 and 2), possibly indicating that depositional conditions were favorable in places, but were generally negatively affected by high sedimentation rates.

The source rock evaluation and the seismic mapping indicate that the lower Aptian organic-rich unit has less potential in the Hammerfest Basin (Fig. 16). The elevated hydrogen content in wells 7120/6–1 and 7120/6-3 S is coupled to relatively low S2 and TOC values (Fig. 16), indicating a limited potential in the NW part of the basin. Well 7120/7–3 is located in the middle of a cluster of high negative amplitudes. Here, the lower Aptian organic-rich unit is demonstrated to be one of the most prolific intervals of the whole succession (Table 3), indicating that there were favorable conditions for organic matter to accumulate and be preserved in the faulted transition to the Tromsø Basin. These conditions seem to be very localized as no other wells located in this transitional zone contain the lower Aptian organic-rich unit (e.g., wells 7119/12–1, 7119/12–3 and 7119/9–1). This points to organic matter accumulation in depocenters along the RLFC.

The structural development of the Fingerdjupet Subbasin with multiple phases of faulting have clearly governed deposition and preservation of the lower Aptian organic-rich unit. The basin development is attributed to reactivation of the N– S- and NNE– SSW-oriented fault complexes (i.e. LFC, TFC and RFS), which follows the trend of older structural lineaments (Serck et al., 2017). These fault complexes were active during the latest Jurassic – Hauterivian and later reactivated in the early Aptian (Serck et al., 2017).

Considering this development and the distribution of the lower Aptian organic-rich unit, we suggest that it accumulated in restricted shallow, half-graben basins associated with movements along the TFC and RFS (Fig. 18B). The rates of subsidence increased during the latest Jurassic – Hauterivian rifting, eventually creating increased bathymetric relief, and promoting the development of syn-tectonic growth wedges near the TFC and RFS (Serck et al., 2017) (Fig. 5A). The subsequent arrival of the SE-prograding clinoform succession (sequence S2, Marín et al., 2017b) during the Barremian filled much of this relief, but was most likely delimited by uplifted footwall highs (Serck et al., 2017) (e.g. location of well 7321/8–1; Fig. 5B). Fault reactivation during the early Aptian renewed the creation of accommodation space in the half-grabens. Coupled with the eustatic sea-level rise and ocean anoxia in the early Aptian (e.g. Schlanger and Jenkyns, 1976; Jenkyns, 1980), this created an ideal setting which allowed organic matter to be preserved in a localized, structurally restricted marine basin (Fig. 18B). The negative amplitude map supports this interpretation, as the greatest negative amplitudes are observed in the half-grabens along the TFC and RFS (Fig. 11A). In addition, the kerogen Type II composition indicates that the organic-rich unit were deposited in a marine environment under anoxic conditions (Demaison and Moore, 1980; Demaison et al., 1983).

Furthermore, the OAE1a has been recorded on the Svalbard Platform (Midtkandal et al., 2016) and linked to a time-equivalent regional extensive lower Aptian flooding surface (Grundvåg et al., 2019). Here, a lower Aptian source rock unit associated with the flooding surface is located atop of a thick coal-bearing paralic succession, testifying to its proximal position near the northern margin of the Barents Shelf at these times. This unit apparently has a localized wet gas potential (e.g. Grundvåg et al., 2019). Although representing deposition under principle different structural settings (i.e. platform versus half graben), the source rock unit on the Svalbard Platform may represent a lateral equivalent to the unit documented in well 7321/9–1 (e.g. Grundvåg et al., 2019) testifying to the high productivity in this period. However, to confidently establish a link between the lower Aptian source rock unit in the Fingerdjupet Subbasin and the OAE1a, carbon and oxygen isotope methodologies should be implemented in the future (e.g. Herrle et al., 2015; Midtkandal et al., 2016; Vickers et al., 2016). There is also the issue of age uncertainties in well 7321/9–1 (Corseri et al., 2018). However, the time-equivalent deposition of the kerogen Type II-III source rock unit on the Svalbard Platform may indicate that the lower Aptian source rock potential is of regional significance, but dependent on structural confinement to generate an oil-prone source rock unit (Grundvåg et al., 2019).

5.1.4. Depositional model and source rock potential of the upper Cenomanian organic-rich unit

Based on the lateral mapping and evaluation of the upper Cenomanian organic-rich unit, we suggest that this unit has greatest potential in the northern part of Tromsø Basin at the transition to the Veslemøy High (Figs. 13B–17). At this location, well 7218/11–1 penetrated an immature unit with a kerogen Type II–III composition (Table 3). This suggests that the upper Cenomanian unit could have source rock potential in similar restricted settings. In addition, the strong negative amplitudes located in the transition to Veslemøy High and the Senja Ridge could indicate that the upper Cenomanian organic-rich unit has increased potential in relation to these highs (Fig. 12B). The elongated amplitudes seen in the amplitude map (Fig. 12) seem to follow the orientation of the seismic lines and could indicate amplitude differences between the surveys.

One central question is whether this potential can be correlated to the negative amplitudes seen in the Tromsø Basin (Figs. 12B and 13A). The restricted character of the depositional setting of the mudrocks sampled in well 7218/11-1 makes such correlation difficult for a wider basin perspective. In addition, exploration wells drilled on local highs and in association with salt domes do not provide the stratigraphic information needed (i.e. 7219/8-1 S, 7119/9–1, 7119/12–3). The Cenomanian source rock potential is, therefore, still unknown in the Tromsø Basin. This is coupled to the likelihood that the basin was well oxygenated and subject to high sedimentation rates associated with the arrival of the delta system prograding from the E and NE during the late Albian and Cenomanian (i.e. sequences 5 and 6; Marín et al., 2017, Fig. 2).

In the Hammerfest Basin, strong negative amplitudes occur in the proximity of well 7120/7–3, possibly indicating abundant organic matter in this area (Fig. 12B). However, the source rock evaluation conducted on samples from well 7120/7-3 shows that there is no Cenomanian source rock potential here (Fig. 17A). Towards the NW corner of the Hammerfest Basin, well 7120/6-3 S records elevated hydrogen content in the upper Cenomanian unit (Fig. 17C). However, the source rock evaluation shows that the unit has low TOC and S2 values, which limit the potential.

The upper Cenomanian organic-rich unit was deposited in a half-graben situated on the northern edge of the Tromsø Basin, as part of the Veslemøy High (Fig. 18C). The development of this half-graben is attributed to the formation a series of NE–SW-striking faults, possibly belonging to the BFC and RLFC (Kairanov et al., 2021). In this area, Valanginian – late Barremian and Aptian – Albian faulting have been documented (Faleide et al., 1993a; Kairanov et al., 2021). This faulting eventually led to rotation of fault blocks and the formation of localized half-graben basins (Fig. 18C). During the Cenomanian, the Veslemøy High was subject to uplift (Kairanov et al., 2021), further restricting the half-graben basins and limiting oxygenated water circulation. This is supported by the kerogen Type II-III composition of the organic-rich unit, which indicates that anoxic to suboxic conditions must have prevailed during deposition (cf. Demaison and Moore, 1980; Demaison et al., 1983).

5.2. Implications for exploration

Exploration well 7219/8-1 S provides an important stratigraphic control for all the Lower Cretaceous organic-rich units in the deep Tromsø and Bjørnøya basins and adjacent areas (Fig. 2). The source rock evaluation conducted on samples from the four potential source rock units investigated in this study, provides an indication as to the potential in the deeper basinal segments.

Data from well 7219/8-1 S establish the lower Aptian unit to be kerogen Type III dominated and in the late mature stages, still part of the oil window. Hence, we conclude that any organic matter deposited before the early Aptian is most likely post-mature in the deeper basinal areas along the RLFC and BFC. This has implications for hydrocarbon exploration in these frontier areas along the western shelf margin. However, the lower Aptian organic-rich unit is considered to have the greatest potential and should consequently be considered when exploration strategies are discussed for the SW Barents Shelf. The presence of a mature to late mature lower Aptian source rock unit in well 7219/8-1 S, may thus represent a local source for exploration targets in the areas surrounding the RLFC and BFC, as well as towards the flanks of the deep basins (Fig. 11A). Because the traditional Upper Jurassic source rock unit is overmature in these areas (Dore, 1995; Marín et al., 2020), the lower Aptian source rock unit could present a viable alternative. However, as there is limited well control in the deep basins, seismic attributes and lateral mapping is key to understanding the distribution and potential of any source rock units distributed along the fault complexes.

We also demonstrate that the lower Aptian unit in well 7219/8-1 S can be traced laterally into the strong negative amplitudes in the NE corner of the Bjørnøya Basin, confined between the uplifted Stappen High and the LFC (Fig. 11A). This location and similar settings thus seem to be key locations for the occurrence of the lower Aptian source rock unit. Furthermore, the Lower Aptian unit in well 7321/9–1 is established to be the most prolific (Table 3). The patchy occurrence of strong negative amplitudes located in the Fingerdjupet Subbasin (Fig. 11A) could potentially indicate local accumulations of organic matter, with similar characteristics to the source rock unit established in well 7321/9–1. However, the Fingerdjupet Subbasin is also one of the most uplifted areas on the SW Barents Shelf (Lasabuda et al., 2021), which further complicate exploration.

The upper Cenomanian organic-rich unit could potentially be a viable option for the wider Tromsø and Bjørnøya basins. However, this unit is absent in the Hammerfest and Bjørnøya basins. The only documented occurrence is in well 7218/11–1 in the transition to the Veslemøy High (Fig. 13B). We therefore suggest that the greatest potential of the upper Cenomanian organic-rich unit is most likely linked to the development off the structural highs, as faulting along their margins developed half-graben depocenters which promoted the formation of restricted marine basins suitable for organic matter to accumulate. A basin wide distribution thus seems unlikely due to the generally well oxygenated waters prevailing the region at these times (e.g. Smelror, 2009).

6. Conclusions

By combining 2D seismic data, amplitude maps and wireline logs with total organic carbon (TOC) and Rock-Eval data, this study documents the presence of four potential source rock units within the Lower Cretaceous succession on the SW Barents Shelf. These are the: (1) upper Hauterivian (2) Barremian, (3) lower Aptian, and (4) upper Cenomanian units. We demonstrate that the deposition and preservation of these units are coupled to localized and restricted fault bound depocenters which developed during multiple episodes of fault activity, mainly attributed to Late Jurassic – Early Cretaceous rifting and local reactivation events along the western Barents Shelf margin.

The Hauterivian and Barremian organic-rich units exhibit TOC contents in the range of 1.0–5.7 wt % and show the greatest potential in the NW part of the Hammerfest Basin. They do not show any potential in the deeper Tromsø and Bjørnøya basins. This is mainly due to deep burial and dilution effects related to regionally high sedimentation rates associated with progradation and the arrival of a large delta system from the west and northwest during the late Albian to Cenomanian times.

The lower Aptian organic-rich unit exhibits TOC contents in the range of 0.57–5.3 wt % and shows the greatest potential by well 7321/9-1 located in the Fingerdjupet Subbasin. It can be traced laterally from this well towards strong negative amplitudes in the central parts of the Fingerdjupet Subbasin, across the Randi Fault Set and further into the southern part of the Fingerdjupet Subbasin. These negative amplitudes may possibly indicate favorable TOC contents, thus resembling the lower Aptian source rock unit in well 7321/9–1, which exhibits high TOC contents (4.0–5.3 wt %). The negative amplitude reflector associated with the lower Aptian source rock unit in well 7321/9–1 can also be traced across from the Fingerdjupet Subbasin into the Bjørnøya Basin, where the unit appears to be composed of kerogen Type III organic matter in the late mature stages (i.e. well 7219/8-1 S). This indicates that the lower Aptian unit could potentially be a viable source rock unit along the Bjørnøyrenna Fault Complex and the Terningen Fault Complex.

The Cenomanian organic-rich unit only appears as an immature, kerogen II-III dominated unit confined to a half-graben situated in the northern part of the Tromsø Basin, at the faulted transition to the Veslemøy High. Correlation towards negative amplitudes located in the deeper basin segments is difficult due to poor well control. Although, the unit can be traced across the Tromsø Basin, there is no indication of a viable source rock of basinal or regional significance.

Declaration of competing interest

The authors declare that they have no known competing financial interests or personal relationships that could have appeared to influence the work reported in this paper.

Acknowledgments

The first author is grateful to WintershallDea Norway for funding this research through a three-year PhD position at UiT - The Arctic University of Norway. This research is also affiliated with the ARCEx consortium (Research Center for Arctic Petroleum Exploration, ARCEx) which is funded by the Research Council of Norway (grant number 228107) and multiple industry partners. The authors are grateful to TGS for allowing to publish their multiclient data. The authors wish to thank reviewers and editors for improving the paper.

Appendix A. Supplementary data

Supplementary data to this article can be found online at https://doi.org/10.1016/j.marpetgeo.2022.105664.

References

Ärlebrand, A., Augustsson, C., Escalona, A., Grundvåg, S.-A., Marín, D., 2021. Provenance, depositional setting and diagenesis as keys to reservoir quality of the Lower Cretaceous in the SW Barents Sea. Mar. Petrol. Geol. 132, 105–217.
Arthur, M.A., Sageman, B.B., 1994. Marine black shales - depositional mechanisms and environments of ancient deposits. Annu. Rev. Earth Planet Sci. 22, 499–551.
Barker, C., 1982. Oil and gas on passive continental margins. In: Watkins, J.S., Drake, C. L. (Eds.), Studies in Continental Margins Geology, vol. 34. American Association of Petroleum Geologists Memoir, pp. 549–565.
Berglund, L.T., Augustson, J., Færseth, R., Gjelberg, J., Ramberg- Moe, H., 1986. The evolution of the Hammerfest Basin. Habitat of hydrocarbons on the Norwegian continental shelf. Proc. conference, Stavanger 319–338.
Blaich, O.A., Tsikalas, F., Faleide, J.I., 2017. New insights into the tectono-stratigraphic evolution of the southern stappen high and its transition to Bjørnøya basin, SW Barents Sea. Mar. Petrol. Geol. 85, 89–105.
Bohacs, K.M., Grabbowski Jr., G.J., Carroll, A.R., Mankiewicz, P.J., Miskell-Gerhardt, K. J., Schwalbach, J.R., Wegner, M.B., Simo, J.A., 2005. Production, destruction, and dilution - the many paths to source-rock development. In: Harris, N.B. (Ed.), The Deposition of Organic-Carbon-Rich Sediments: Models, Mechanisms, and Consequences. SEPM Special Publication No. 82, pp. 61–101.
Bojesen-Koefoed, J.A., Alsen, P., Bjerager, M., Hovikoski, J., Ineson, J., Nytoft, H.P., Nøhr-Hansen, H., Petersen, H.I., Pilgaard, A., Vosgerau, H., 2020. A mid-Cretaceous petroleum source-rock in the North Atlantic region? Implications of the Nanok-1 fully cored borehole, Hold with Hope, northeast Greenland. Mar. Petrol. Geol. 117, 104414. https://doi.org/10.1016/j.marpetgeo.2020.104414.
Bordovskiy, O.K., 1965. Accumulation of organic matter in bottom sediments. Mar. Geol. 3, 33–82.
Bowker, K.A., Grace, T., 2010. The downside of using GR to determine TOC content: an example from the marcellus shale in SE West Virginia. In: Critical Assessment of Shale Resource Plays, AAPG Hedberg Ressearch Conference, Dec., Austin, TX (2010).
Bugge, T., Elvebakk, G., Fanavoll, S., Mangerud, G., Smelror, M., Weiss, H.M., Gjelberg, J., Kristensen, S.E., Nilsen, K., 2002. Shallow stratigraphic drilling applied in hydrocarbon exploration of the Nordkapp Basin, Barents Sea. Mar. Petrol. Geol. 19, 13–37.
Calvert, S.E., Bustin, R.M., Ingall, E.D., 1996. Influence of water column anoxia and sediment supply on the burial and preservation of organic carbon in marine shales. Geochem. Cosmochim. Acta 60, 1577–1593.
Clark, S.A., Glørstad-Clark, E., Faleide, J.I., Schmid, D., Hartz, E.H., Fjeldskaar, W., 2014. Southwest Barents Sea rift basin evolution: comparing results from backstripping and time-forward modelling. Basin Res 26, 550–566.
Cohen, K.M., Finney, S.C., Gibbard, P., Fan, J.-X., 2013. The ICS international chronostratigraphic chart. Episodes 36, 199–204.
Cooper, B.S., Barnard, P.C., 1984. Source rock and oils of the central and northern north sea. In: Demaison, G., Murris, R.J. (Eds.), Petroleum Geochemistry and Basin Evaluation, vol. 35. AAPG Memoir, pp. 303–315.
Corseri, R., Faleide, T.S., Faleide, J.I., Midtkandal, I., Serck, C.S., Trulsvik, M., Planke, S., 2018. A diverted submarine channel of Early Cretaceous age revealed by high-resolution seismic data, SW Barents Sea. Mar. Petrol. Geol. 98, 462–476.
Dalland, A., Worsley, D., Ofstad, K., 1988. A Lithostratigraphic scheme for the Mesozoic and Cenozoic succession offshore mid- and northern Norway. Norwegian Petrol. Direct. Bull. 4.
Demaison, G.J., Moore, G.T., 1980. Anoxic environments and oil source bed genesis. AAPG (Am. Assoc. Pet. Geol.) Bull. 64, 1179–1209.
Demaison, G.J., Hoick, A.J.J., Jones, R.W., Moore, G.T., 1983. Predictive source bed stratigraphy: a guide to regional petroleum occurrence. In: Proceedings of the 11th World Petroleum Congress, vol. 2. John Wiley & Sons, Ltd., London, p. 17.
Doré, A.G., 1995. Barents Sea geology, petroleum resources and commercial potential. Arctic 48, 207–221.
Espitalié, J., Madec, M., Tissot, B., Mennig, J.J., Leplat, P., 1977. Source rock characterization method for petroleum exploration. Paper OTC (Offshore Technology Conference) 2935, 439–444.
Faleide, J.I., Gudlaugsson, S., Jacquart, G., 1984. Evolution of the western Barents Sea. Mar. Petrol. Geol. 1, 123–150.
Faleide, J.I., Vågnes, E., Gudlaugsson, S.T., 1993a. Late mesozoic-cenozoic evolution of the southwestern Barents Sea. Geol. Soc. Lond. Pet. Geol. Conf. Ser. 4, 933–950.
Faleide, J.I., Vagnes, E., Gudlaugsson, S.T., 1993b. Late mesozoic-cenozoic evolution of the south-western Barents Sea in a regional rift shear tectonic setting. Mar. Petrol. Geol. 10, 186–214.
Faleide, J.I., Tsikalas, F., Breivik, A.J., Mjelde, R., Ritzmann, O., Engen, O., Wilson, J., Eldholm, O., 2008. Structure and evolution of the continental margin off Norway and Barents Sea. Episodes 31, 82–91.
Faleide, J.I., Bjørlykke, K., Gabrielsen, R.H., 2015. Geology of the Norwegian continental shelf. In: Bjørlykke, K. (Ed.), Petroleum Geoscience: from Sedimentary Environments to Rock Physics. Springer Berlin Heidelberg, Berlin, pp. 603–637.
Gabrielsen, R.H., Færseth, R.B., Jensen, L.N., Kalheim, J.E., Riis, F., 1990. Structural elements of the Norwegian continental shelf. Part 1: the Barents Sea region. NPD Bull 6, 33.
Gabrielsen, R.H., Grunnaleite, I., Rasmussen, E., 1997. Cretaceous and tertiary inversion in the Bjørnøyrenna Fault complex, south-western Barents Sea. Mar. Petrol. Geol. 14, 165–178.
Gawthorpe, R.L., Leeder, M.R., 2000. Tectono-sedimentary evolution of active extensional basins. Basin Res 12, 195–218.
Grundvåg, S.A., Marin, D., Kairanov, B., Śliwińska, K.K., Nøhr-Hansen, H., Jelby, M.E., Escalona, A., Olaussen, S., 2017. The lower cretaceous succession of the northwestern Barents shelf: onshore and offshore correlations. Mar. Petrol. Geol. 86, 834–857.
Grundvåg, S.A., Jelby, M.E., Sliwinska, K.K., Nohr-Hansen, H., Aadland, T., Sandvik, S.E., Tennvassas, I., Engen, T., Olaussen, S., 2019. Sedimentology and palynology of the Lower Cretaceous succession of central Spitsbergen: integration of subsurface and outcrop data. Norw. J. Geol. 99, 253–284.
Helleren, S., Marín, D., Ohm, S., Augustsson, C., Escalona, A., 2020. Why does not lithology correlate with gamma-ray spikes in the shaley source rocks of the Upper Jurassic Alge Member (southwestern Barents Sea)? Mar. Petrol. Geol. 121, 104–623.
Henriksen, E., Bjørnseth, H.M., Hals, T.K., Heide, T., Kiryukhina, T., Kløvjan, O.S., Larssen, G.B., Ryseth, A.E., Rønning, K., Sollid, K., Stoupakova, A., 2011. Uplift and erosion of the greater Barents Sea: impact on prospectivity and petroleum systems. In: Spencer, A.M., Embry, A.F., Gautier, D.L., Stoupakova, A.V., Sørensen, K. (Eds.), Arctic Petroleum Geology. The Geological Society of London, pp. 271–281.
Herrle, J.O., Schroder-Adams, C.J., Davis, W., Pugh, A.T., Galloway, J.M., Fath, J., 2015. Mid-cretaceous high arctic stratigraphy, climate, and oceanic anoxic events. Geology 43, 403–406.
Ibach, L.E.J., 1982. Relationship between sedimentation-rate and total organic-carbon content in ancient marine-sediments. AAPG (Am. Assoc. Pet. Geol.) Bull. 66, 170–188.
Indrevær, K., Gabrielsen, R.H., Faleide, J.I., 2017. Early Cretaceous synrift uplift and tectonic inversion in the Loppa High area, southwestern Barents Sea, Norwegian shelf. J. Geol. Soc. 174, 242–254.
Isaksen, G.H., Ledje, K.H.I., 2001. Source rock quality and hydrocarbon migration pathways within the greater utsira high area, viking graben, Norwegian north sea. AAPG (Am. Assoc. Pet. Geol.) Bull. 85, 861–883.
Jenkyns, H.C., 1980. Cretaceous anoxic events - from continents to oceans. J. Geol. Soc. 137, 171–188.
Jongepier, K., Rui, J.C., Grue, K., 1996. Triassic to Early Cretaceous stratigraphic and structural development of the northeastern Møre Basin margin, off Mid-Norway. Nor. Geol. Tidsskr. 76, 199–214.
Kairanov, B., Escalona, A., Norton, I., Abrahamson, P., 2021. Early cretaceous evolution of the Tromsø basin, SW Barents Sea, Norway. Mar. Petrol. Geol. 123, 104–714.
Karlsen, D.A., Skeie, J.E., 2006. Petroleum migration, faults and overpressure, part 1: calibrating basin modelling using petroleum in traps – a review. J. Petrol. Geol. 29, 227–256.
Karlsen, D.A., Skeie, J.E., Backer-owe, K., Bjørlykke, K., Ollstad, R., Berge, K., Cecchi, M., Vik, E., Schaefer, R.G., 2004. Petroleum migration, faults and overpressure. Part II. Case history: the Haltenbanken petroleum province, offshore Norway. In: Cubitt, J. M., England, W.A., Larter, S. (Eds.), Understanding Petroleum Reservoirs: towards an Integrated Reservoir Engineering and Geochemical Approach, vol. 237. Geological Society of London Special Publications, London, pp. 305–372.
Katz, B., 2005. Controlling factors on source rock development—a review of productivity, preservation, and sedimentation rate. Soci. Sed. Geol. 82, 7–16.
Kosters, E.C., VanderZwaan, G.J., Jorissen, F.J., 2000. Production, preservation and prediction of source-rock facies in deltaic settings. Int. J. Coal Geol. 43, 13–26.
Langrock, U., Stein, R., Lipinski, M., Brumsack, H.-J., 2003. Late Jurassic to Early Cretaceous black shale formation and paleoenvironment in high northern latitudes: examples from the Norwegian-Greenland Seaway. Paleoceanography 18, 1–16.
Lasabuda, A., Laberg, J.S., Knutsen, S.M., Hogseth, G., 2018. Early to middle Cenozoic paleoenvironment and erosion estimates of the southwestern Barents Sea: insights from a regional mass-balance approach. Mar. Petrol. Geol. 96, 501–521.
Lasabuda, A.P.E., Johansen, N.S., Laberg, J.S., Faleide, J.I., Senger, K., Rydningen, T.A., Patton, H., Knutsen, S.M., Hanssen, A., 2021. Cenozoic uplift and erosion of the Norwegian Barents Shelf-A review. Earth Sci. Rev. 217, 103609.
Leckie, R.M., Bralower, T.J., Cashman, R., 2002. Oceanic anoxic events and plankton evolution: biotic response to tectonic forcing during the mid-Cretaceous. Paleoceanography 17, 1–29.

Leith, T.L., Weiss, H.M., Mørk, A., Århus, N., Elvebakk, G., Embry, A.F., Brooks, P.W., Stewart, K.R., Pchelina, T.M., Bro, E.G., Verba, M.L., Danyushevskaya, A., Borisov, A.V., 1993. Mesozoic hydrocarbon source rocks of the Arctic region. In: Vorren, T.O., Bergsager, E., Dahl-Stamnes, A., Holter, E., Johansen, Å., Lie, Å., Lund, T.B. (Eds.), Arctic Geology and Petroleum Potential. Elsevier, Amsterdam, pp. 1–25.

Lerch, B., Karlsen, D.A., Seland, R., Backer-Owe, K., 2017. Depositional environment and age determination of oils and condensates from the Barents Sea. Petrol. Geosci. 23, 190–209.

Løseth, H., Wensaas, L., Gading, M., Duffaut, K., Springer, M., 2011. Can hydrocarbon source rocks be identified on seismic data? Geology 39, 1167–1170.

Mann, U., Zweigel, J., Øygard, K., Gjeldvik, G., 2002. Source rock prediction in deepwater frontier exploration areas: an integrated study of the Cretaceous in the Vøring Basin. In: Research, S.P. (Ed.), AAPG Hedberg Conference: Hydrocarbon Habitat of Volcanic Rifted Passive Margins, Stavanger, Norway.

Marín, D., Escalona, A., Sliwinska, K.K., Nohr-Hansen, H., Mordasova, A., 2017. Sequence stratigraphy and lateral variability of Lower Cretaceous clinoforms in the southwestern Barents Sea. AAPG (Am. Assoc. Pet. Geol.) Bull. 101, 1487–1517.

Marín, D., Escalona, A., Grundvåg, S.A., Nohr-Hansen, H., Kairanov, B., 2018a. Effects of adjacent fault systems on drainage patterns and evolution of uplifted rift shoulders: the Lower Cretaceous in the Loppa High, southwestern Barents Sea. Mar. Petrol. Geol. 94, 212–229.

Marín, D., Escalona, A., Grundvåg, S.A., Olaussen, S., Sandvik, S., Sliwinska, K.K., 2018b. Unravelling key controls on the rift climax to post-rift fill of marine rift basins: insights from 3D seismic analysis of the Lower Cretaceous of the Hammerfest Basin, SW Barents Sea. Basin Res 30, 587–612.

Marín, D., Helleren, S., Escalona, A., Olaussen, S., Cedeño, A., Nøhr-Hansen, H., Ohm, S., 2020. The Middle Jurassic to lowermost Cretaceous in the SW Barents Sea: interplay between tectonics, coarse-grained sediment supply and organic matter preservation. Basin Res. 33 (2), 1033–1055. https://doi.org/10.1111/bre.12504.

Matapour, Z., Karlsen, D.A., 2017. Ages of Norwegian oils and bitumen based on agespecific biomarkers. Petrol. Geosci. 24, 92–101. https://doi.org/10.1144/petgeo2016–119.

Midtkandal, I., Svensen, H.H., Planke, S., Corfu, F., Polteau, S., Torsvik, T.H., Faleide, J. I., Grundvåg, S.A., Selnes, H., Kurschner, W., Olaussen, S., 2016. The aptian (early cretaceous) oceanic anoxic event (0AE1a) in svalbard, Barents Sea, and the absolute age of the barremian-aptian boundary. Palaeogeogr. Palaeocl. 463, 126–135.

Midtkandal, I., Faleide, J.I., Faleide, T., Serck, C., Planke, S., Corseri, R., Dimitriou, M., Nystuen, J., 2019. Lower Cretaceous Barents Sea strata: epicontinental basin configuration, timing, correlation and depositional dynamics. Geol. Mag. 157, 1–19.

Mitchum, R.M.J., Vail, P.R., Sangree, J.B., 1977. Seismic stratigraphy and global changes of sea-level, part 6: stratigraphic interpretation of seismic reflection patterns in depositional sequences. In: Payton, C. (Ed.), Seismic Stratigraphy – Applications to Hydrocarbon Exploration, vol. 26. Mem. - Am. Assoc. Pet. Geol., pp. 117–133

NPD Factpages, 2021. [WWW Document]. Norwegian Petroleum Directorate. https://factpages.npd.no. (Accessed 3 November 2021).

Ohm, S.E., Karlsen, D.A., Austin, T.J.F., 2008. Geochemically driven exploration models in uplifted areas: examples from the Norwegian Barents Sea. AAPG (Am. Assoc. Pet. Geol.) Bull. 92, 1191–1223.

Øygard, K., Olsen, R., 2002. Alternative source rock in the north atlantic passive Marin – cretaceous in the møre and vøring basins, offshore Norway. AAPG hedberg conference: "hydrocarbon habitat of volcanic rifted passive margins. Stavanger, Norway 1–4.

Parker, J.R., 1967. The jurassic and cretaceous sequence in spitsbergen. Geol. Mag. 104, 487–505.

Pedersen, T.F., Calvert, S.E., 1990. Anoxia vs productivity - what controls the formation of organic-carbon-rich sediments and sedimentary-rocks. AAPG (Am. Assoc. Pet. Geol.) Bull. 74, 454–466.

Peters, K.E., 1986. Guidelines for evaluating petroleum source rock using programmed pyrolysis. AAPG (Am. Assoc. Pet. Geol.) Bull. 70, 318–329.

Peters, K.E., Cassa, M.R., 1994. Applied source rock geochemistry. In: Magoon, L.B., Dow, W.G. (Eds.), The Petroleum System - from Source to Trap. AAPG, pp. 93–120.

Rider, M.H., Kennedy, M., 2011. The Geological Interpretation of Well Logs, third ed. Rider-French, Scotland.

Riis, F., Halland, E., 2014. CO2 storage atlas of the Norwegian Continental shelf: methods used to evaluate capacity and maturity of the CO2 storage potential. Enrgy. Proced. 63, 5258–5265.

Rogov, M.A., Shchepetova, E.V., Zakharov, V.A., 2020. Late Jurassic – earliest Cretaceous prolonged shelf dysoxic–anoxic event and its possible causes. Geol. Mag. 157, 1622–1642. https://doi.org/10.1017/S001675682000076X.

Rønnevik, H., Bescow, B., Jacobsen, H.P., 1982. Structural and Stratigraphic Evolution of the Barents Sea, vol. 8. Canadian Society of Petroleum Geologists Memoir, pp. 431–440.

Sattar, N., Juhlin, C., Koyi, H., Ahmad, N., 2017. Seismic stratigraphy and hydrocarbon prospectivity of the lower cretaceous Knurr sandstone lobes along the southern margin of Loppa high, Hammerfest basin, Barents Sea. Mar. Petrol. Geol. 85, 54–69.

Schlanger, S.O., Jenkyns, H.C., 1976. Cretaceous oceanic anoxic events: causes and consequences. Geol. Mijnbouw 55, 179–184.

Scotese, C.R., Song, H., Mills, B.J.W., van der Meer, D.G., 2021. Phanerozoic paleotemperatures: the earth's changing climate during the last 540 million years. Earth Sci. Rev. 215, 103–503.

Seldal, J., 2005. Lower Cretaceous: the next target for oil exploration in the Barents Sea? Petrol. Geol. Conf. Proceed. 231–240.

Serck, C.S., Faleide, J.I., Braathen, A., Kjølhamar, B., Escalona, A., 2017. Jurassic to early cretaceous basin configuration(s) in the Fingerdjupet Subbasin, SW Barents Sea. Mar. Petrol. Geol. 86, 874–891.

Sheriff, R.E., 2002. Encyclopedic Dictionary of Applied Geophysics, fourth ed. Society of Exploration Geophysicists, Tulsa, Okla.

Smelror, M., Mørk, A., Monteil, E., Rutledge, D., Leereveld, H., 1998. The Klippfisk formation—a new lithostratigraphic unit of Lower Cretaceous platform carbonates on the Western Barents Shelf. Polar Res 17, 181–202.

Smelror, M., Petrov, O.V., Larssen, G.B., Werner, S., Norway, G.S.o., 2009. Geological history of the Barents Sea: atlas. Geological Survey of Norway 1–135.

Sund, T., 1984. Tectonic development and hydrocarbon potential offshore Troms, northern Norway. AAPG (Am. Assoc. Pet. Geol.) Bull. 68, 1206–1207.

Tissot, B.P., Durand, B., Espitalie, J., 1973. Influence of nature and diagenesis of organic matter in formation of petroleum. AAPG (Am. Assoc. Pet. Geol.) Bull. 58, 499–506.

Ulmishek, G.F., 2003. Petroleum geology and resources of the west Siberian Basin, Russia. USGS Bull 1–49, 2201.

Vickers, M.L., Price, G.D., Jerrett, R.M., Watkinson, M., 2016. Stratigraphic and geochemical expression of Barremian-Aptian global climate change in Arctic Svalbard. Geosphere 12, 1594–1605.

White, D.A., 1993. Geologic risking guide for prospects and plays. AAPG (Am. Assoc. Pet. Geol.) Bull. 77, 2048–2061.

Wood, R.J., Edrich, S.P., Hutchison, I., 1989. Influence of North Atlantic tectonics on the large scale uplift of the stapen high and Loppa high, western Barents shelf. In: Tankard, A.J., Balkwill, H.R. (Eds.), Extensional Tectonics and Stratigraphy of the North Atlantic Margins, vol. 46. Mem. - Am. Assoc. Pet. Geol., pp. 559–566

Worsley, D., Johansen, R., kristensen, S.E., 1988. The mesozoic and cenozoic succession of tromsøflaket. In: Dalland, A., Worsley, D., Ofstad, K. (Eds.), A Lithostratigraphic Scheme for the Mesozoic and Cenozoic Succession Offshore Mid- and Northern Norway, vol. 4. NPD Bull., pp. 42–65

6 Paper II

Deposition of Cenomanian – Turonian organic-rich units on the mid-Norwegian Margin: controlling factors and regional implications

Hagset, A.[1,] *, Grundvåg, S.-A.[1, 2], Badics, B.[3], Davies, R.[3], Rotevatn, A.[4]

[1] Department of Geosciences, UIT - The Arctic University of Norway, Tromsø, Norway

[2] Department of Arctic Geology, University Centre in Svalbard PO Box 156, N-9171, Longyearbyen, Norway

[3] Wintershall DEA, Stavanger, Norway

[4] Department of Geosciences, University of Bergen, Bergen, Norway

*Corresponding author e-mail: aha155@uit.no

Marine and Petroleum Geology 149 (2023) 106102

Contents lists available at ScienceDirect

Marine and Petroleum Geology

journal homepage: www.elsevier.com/locate/marpetgeo

Deposition of cenomanian – Turonian organic-rich units on the mid-Norwegian margin: Controlling factors and regional implications

A. Hagset [a,*], S.-A. Grundvåg [a,b], B. Badics [c], R. Davies [c], A. Rotevatn [d]

[a] Department of Geosciences, UIT - the Arctic University of Norway, Tromsø, Norway
[b] Department of Arctic Geology, University Centre in Svalbard, PO Box 156, 9171, Longyearbyen, Norway
[c] Wintershall DEA, Stavanger, Norway
[d] Department of Geosciences, University of Bergen, Bergen, Norway

ARTICLE INFO

Keywords:
Lower cretaceous stratigraphy
Mid-Norwegian margin
Cenomanian/Turonian boundary
Seismic sequences
Organic-rich units
Source rock evaluation
Rift-basin configuration
OAE 2
Sedimentation rate

ABSTRACT

On the mid-Norwegian margin, extensive rifting and subsequent deposition of thick Cretaceous and Cenozoic sediments have buried the traditional Upper Jurassic organic-rich shales too deep. Consequently, these organic-rich shales are overmature and spent in the deep basins on the mid-Norwegian margin. The absence of well-control, variable seismic quality and in particularly, the great burial depth, makes it difficult to identify alternative Upper Jurassic and Lower Cretaceous organic-rich units. By combining high-resolution 2D seismic data, well logs, and Rock-Eval data, this study documents the presence of alternative organic-rich units in the Cretaceous succession on the Halten Terrace and the Vøring Basin. Multiple seismic horizons which correspond to regional flooding surfaces and define a series of seismic sequences have been mapped across the study area. The regionally extensive upper Cenomanian horizon is associated with wireline log signals and Rock-Eval parameters which imply the presence of a potential source rock unit. Source rock evaluation indicate that this unit contains mainly kerogen Type III on the Halten Terrace, suggesting an organofacies with significant contribution from terrestrial sources. In the Vøring Basin, the unit is sparsely drilled but appears to be mature, thus displaying a relatively limited potential. One well from the Vigrid Syncline demonstrate somewhat higher potential, with Rock-Eval data indicating a kerogen Type II composition. As such, more prolific units seems to exist in the Vøring Basin, albeit exhibiting a patchy distribution. We speculate that the deposition and preservation of this upper Cenomanian organic-rich unit record the development of an extended oxygen minimum zone attributable to increased primary production and sluggish water circulation, linked to the global Oceanic Anoxic Event 2 (OAE 2). However, local physiographic conditions, such as high sedimentation rates, erosion by gravity flows and periodically oxygenated conditions hindered preservation of a significant quantities of organic matter, thus limiting the thickness and quality of the upper Cenomanian organic-rich unit on the mid-Norwegian margin.

1. Introduction

Identifying and mapping the distribution of thermally mature source rock units is important to eliminate risk in hydrocarbon exploration. Whether a viable source rock developed or not, is the outcome of the interaction of many factors and processes across multiple time scales, ultimately recording the environmental and sedimentary response to tectonic, eustatic and climatic forcing (e.g. Arthur and Sageman, 1994; Demaison and Moore, 1980; Demaison et al., 1983; Katz, 2005; Bohacs et al., 2005). The generation and preservation of organic matter, are among other factors, controlled by primary organic production, sedimentation rate, as well as water mass circulation and bottom water oxygen levels, whereas source rock thermal maturity and thus source rock generation potential, is largely governed by the thermal and burial history of the basin (Demaison et al., 1983; Pedersen and Calvert, 1990; Arthur and Sageman, 1994; Peters and Cassa, 1994; Calvert et al., 1996; Katz, 2005). Therefore, the tectono-sedimentary evolution of a basin needs to be carefully assessed during any source rock evaluation program.

In the Vøring Basin, of the mid-Norwegian margin, the traditional Upper Jurassic source rock (i.e. the Spekk Formation) is classified as over-mature due to deep burial caused by extensive rifting and crustal thinning in the Late Jurassic – Early Cretaceous, and subsequent deposition of several kilometers thick Cretaceous and Cenozoic sediments (e.

* Corresponding author.
E-mail address: aha155@uit.no (A. Hagset).

https://doi.org/10.1016/j.marpetgeo.2023.106102
Received 17 November 2022; Received in revised form 4 January 2023; Accepted 7 January 2023
Available online 10 January 2023

g. Doré et al., 1999; Brekke, 2000; Zastrozhnov et al., 2020). In addition, limited well-control and variable seismic quality due to complex fault geometries and, particularly, great burial depths (i.e. 6 – 9 s TWT; Brekke, 2000; Zastrozhnov et al., 2020) make it difficult to identify alternative Upper Jurassic and Lower Cretaceous organic-rich units in the deepest parts of the basin. As a result, exploration strategies in the area have focused on plays with younger source rocks, particularly those of Late Cretaceous and Palaeocene age (e.g. Doré et al., 1997b; Brekke et al., 1999; Mann et al., 2002). Although a thermally mature source rock unit has yet to be proven in the Cretaceous succession in the Vøring Basin, biomarker components found in hydrocarbons from the Ellida, Ormen Lange and Snefrid Nord discoveries strongly suggest the presence of a post-Jurassic source rock (Garner et al., 2017; Matapour and Karlsen, 2018). One such potential source rock unit may be organic rich

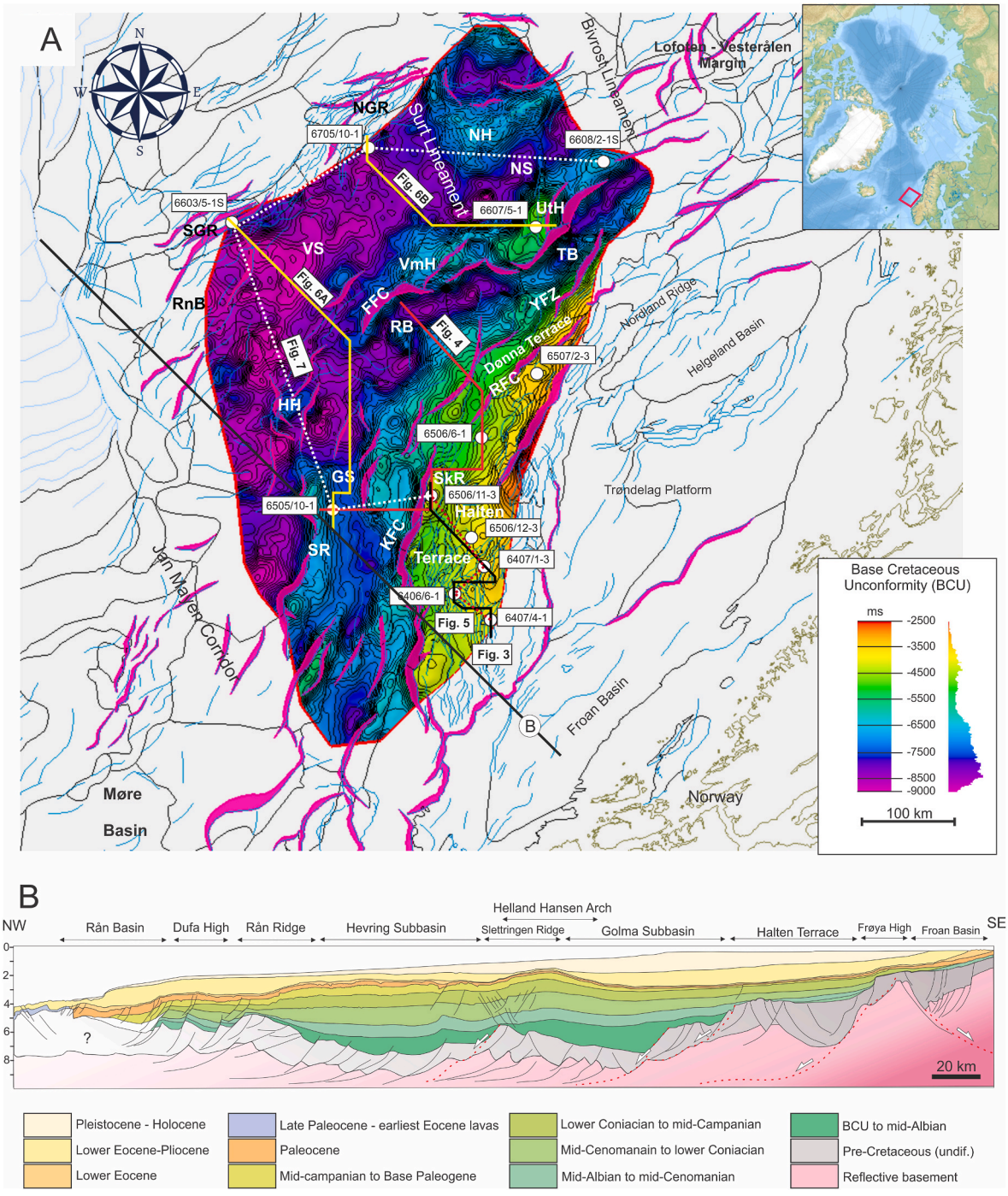

Fig. 1. (A) Time-elevation map of the Base Cretaceous Unconformity indicating the extent of the study area and outlining the main structural elements on the mid-Norwegian Margin. Wells and seismic composite lines utilized in this study are annotated. The structural elements (black lines), minor (light blue lines) and major faults (purple thick lines) are implemented after Gernigon et al. (2021). (B) Simplified geo-seismic profile outlining the structural trend and configuration of the Vøring Basin. The profile is re-drawn (with modifications) after transect "e" in Zastrozhnov et al. (2020) and is annotated "B" herein. Abbreviations after Zastrozhnov et al. (2020): SR – Slettringen Ridge, GsB – Golma Subbasin, TB – Træna Basin, VS – Vigrid Syncline, NS – Någrid Syncline, FFC – Fles Fault Complex, KFC – Klakk Fault Complex, SkR – Sklinna Ridge, SGR -South Gjallar Ridge, NGR – North Gjallar Ridge, RB – Rås Basin, RnB – Rån Basin, UtH – Utgard High, VmH – Vimur High, HH – Hevrig High, NH – Nyk High.

deposits of late Cenomanian – early Turonian age, which has been encountered in an exploration well on the Sklinna High (exploration well 6506/11–3; see NPD Factpages, 2022, Fig. 1 for location). The age-equivalent organic-rich unit, the Blodøks Formation, in the North Sea, reportedly has good source rock qualities despite its thin development there (Isaksen and Tonstad, 1989). On the conjugate margin onshore East Greenland, several outcrop and shallow borehole information give hints to the presence of a potential mid-Cretaceous source rock, including oil stains in younger clastic deposits, as well as isotope and biomarker data compatible with a possible Cretaceous source rock (Bojesen-Koefoed et al., 2020). Age-equivalent organic-rich unit with source rock potential have also been documented in the Kanguk Formation within the Sverdrup Basin, and the Smoking Hills Formation in the Mackenzie Delta area, Arctic Canada (Leith et al., 1993; Lenniger et al., 2014; Herrle et al., 2015; Schröder-Adam et al., 2019). Previous work in the Vøring Basin has also documented the occurrence of organic-rich marine mudstones in Barremian, Aptian and Albian strata (Jongepier et al., 1996; Doré et al., 1997b; Wenke et al., 2021). Regardless of the deep burial, it has been speculated that some of these intervals may hold some source rock potential (Brekke et al., 1999).

It is well known that the Cretaceous period experienced several short-lived Oceanic Anoxic Events (OAEs) which promoted widespread deposition of organic-rich mudstones (Schlanger and Jenkyns, 1976: Arthur and Schlanger, 1979; Jenkyns, 1980; Arthur et al., 1987, 1990; Bralower et al., 1993 Erbacher et al., 1996; Midtkandal et al., 2016). The two most prominent events, the OAE 1a in the early Aptian (i.e. the Selli Event) and the OAE 2 at the Cenomanian – Turonian transition (i.e. the Bonarelli Event), are both attributed to eustatically rising sea level and elevated marine productivity primed by volcanic activity and increased sea surface temperatures (Arthur et al., 1987; Erbacher et al., 1996; Leckie et al., 2002; Turgeon and Creaser, 2008; Adams et al., 2010). Source rocks associated with the OAE 2 are highly prolific and have apparently sourced a quarter of the World's petroleum (Klemme and Ulmishek, 1991).

However, because so few wells penetrate Cretaceous strata in the Vøring Basin, the distribution of potential source rocks in this interval is highly uncertain and the inferred presence of prolific Cretaceous source rocks remains speculative. In this study, we combine high-resolution regional 2D seismic data, available Rock-Eval data, and well logs, to map the distribution of and evaluate the source rock potential of several organic-rich units in the Cretaceous succession in the Vøring Basin. We particularly focus on organic-rich deposits associated with the Cenomanian/Turonian strata, and by applying traditional source rock evaluation methods (*sensu* Peters and Cassa, 1994) the potential of these deposits is meticulously assessed. We also present a depositional model for the Cenomanian – Turonian interval in the Vøring Basin, further arguing that sea-level rise and increased primary productivity during the OAE 2 coupled with extensive rifting fostered favorable conditions for organic-rich units to be deposited. Finally, we discuss our findings in relation to the tectono-sedimentary evolution of the Vøring Basin and its wider implications for the prospectivity of the mid-Norwegian margin.

2. Geological framework

2.1. Lower Cretaceous structural development

The development of the mid-Norwegian margin is related to a series of post-Caledonian rifting phases, which eventually led to the complete separation of Norway and Greenland in the Eocene (Doré et al., 1999; Brekke, 2000; Tsikalas et al., 2005; Lundin et al., 2013; Peron-Pinvidic and Osmundsen, 2018; Zastrozhnov et al., 2020). The preexisting structural grain influenced the segmentation and overall geometry of the subsequent rift basins, and the conjugate margins was from early onset of rifting the fundamental source of sediments (Rotevatn et al., 2018). The Vøring Basin was formed by predominately two rifting phases during the Late Jurassic – earliest Cretaceous, and the Late Cretaceous – Paleocene (Blystad et al., 1995; Tsikalas et al., 2005; Faleide et al., 2008; Zastrozhnov et al., 2020). The western limit of the Vøring Basin is characterized by massive intrusive and extrusive volcanic depositions (Peron-Pinvidic and Osmundsen, 2018; Zastrozhnov et al., 2020). This magmatic activity is linked to the continental breakup and started after the final rift phase in the Late Cretaceous – Paleocene (Planke et al., 2005; Abdelmalak et al., 2016). The eastern limit and proximal regime of the Vøring Basin is defined by the Trøndelag Platform and the Halten and Dønna terraces (Fig. 1). The southern boundary is defined by the Jan Mayen Corridor, which separates it from the Møre Basin. Towards the north, the Vøring Basin is separated from the narrow Lofoten-Vesterålen margin by the Bivrost Lineament (Tsikalas et al., 2019; Brekke, 2000; Zastrozhnov et al., 2020). The Vøring Basin contains several intra basinal highs and subbasins, reflecting a complex structural history. The most important structural elements for this study are in the necking and distal domain which are characterized by hyperextended half-grabens (Peron-Pinvidic and Osmundsen, 2018; Zastrozhnov et al., 2020), and include the (Alphabetically): Gjallar Ridge, Golma Subbasin, Halten Terrace, Rås Basin, Sklinna Ridge, Træna Basin and the Vigrid Syncline (Fig. 1). A brief outline of their structural development is given below.

2.1.1. Gjallar Ridge

The Gjallar Ridge is located in the outer part of the Vøring Basin (Fig. 1) and is bounded by the Vigrid Syncline to the east and by the Fenris Graben to the west. The Gjallar Ridge consists of a series of NE trending rotated fault blocks, formed during the Late Cretaceous – Early Paleocene rift phase, prior to complete continental breakup later in the Cenozoic (Gernigon et al., 2003; Zastrozhnov et al., 2018, 2020).

2.1.2. Golma Subbasin

The Golma Subbasin is a N–S trending subbasin confined between the Halten Terrace and the Slettringen Ridge (Fig. 1). Towards the north, the Golma Subbasin transitions into the Rås Basin and in the south to the Holmen Subbasin. Based on the presence of a thick Lower Cretaceous succession, the Golma Subbasin clearly acted as a prominent depocenter during Early Cretaceous times (Zastrozhnov et al., 2020).

2.1.3. Halten Terrace

The Halten Terrace is a faulted terrace transitionally located between the Trøndelag Platform in the east and the Rås Basin in the west (Fig. 1) The terrace is c. 80 km wide and c. 130 km long, bounded by fault complexes along all its margins (e.g. Blystad et al., 1995; Hansen et al., 2021; Bell et al., 2014; Gernigon et al., 2021). Its formation involves multiple extensional phases during the Palaeozoic, Mesozoic and earliest Cenozoic (Blystad et al., 1995; Doré et al., 1997a; Hansen et al., 2021). The main structural shaping is attributed to the Late Jurassic to Early rifting phase which formed several fault-bound depocenters, that eventually joined into a single depocenter in the Late Cretaceous (e.g. Bell et al., 2014). The Halten Terrace includes a Lower to Upper Cretaceous succession (c. 0.8 S TWT thick, including Cenomanian deposits) which is markedly thinner than the equivalent stratal succession in the Vøring Basin, yet thicker and more complete than the condensed and commonly eroded stratal package sitting on the platform domain further to the east. Deep marine conditions prevailed during deposition of Lower to Upper Cretaceous sediments (Blystad et al., 1995; Doré et al., 1997a; Hansen et al., 2021). These sediments were predominantly sourced from regional highs (e.g. Sklinna High and Frøya High) and the Trøndelag Platform which separated from the Halten Terrace in the Late Cretaceous (Blystad et al., 1995; Brekke et al., 2001).

2.1.4. Rås Basin

The Rås Basin is delimited to the east by the Halten and Dønna Terraces, separating them are the Klakk and Ytreholem Fault Complexes (Blystad et al., 1995; Zastrozhnov et al., 2020). The Fles Fault Complex separates the Rås Basin from the Vigrid Syncline in the west, while the southern and northeastern boundaries are defined by the Jan Mayen and

Surt Lineaments. (Blystad et al., 1995). The Rås Basin contains thick Cretaceous deposits where the greatest thickness (c. 5 S TWT) is reported along the central axis of the basin (Blystad et al., 1995). As such, the basin was a major depocenter for sediments throughout the Cretaceous period (Zastrozhnov et al., 2020).

2.1.5. Sklinna Ridge

The Sklinna Ridge is located on the western margin of the Halten Terrace (Fig. 1). The N–S elongated ridge is c. 140 km long and 13 km wide. The Sklinna Ridge was formed due to uplift along the Klakk Fault Complex during the Late Jurassic – Early Cretaceous rifting event (Blystad et al., 1995). Consequently, the top of the ridge has been subject to erosion since its formation and has been a local sediment source for Lower to Upper Cretaceous sediments (Blystad et al., 1995; Bell et al., 2014; Hansen et al., 2021). Internally, the ridge has a complex fault pattern with a series of intersecting N–S- and NE–SW-striking faults (Blystad et al., 1995).

2.1.6. Træna Basin

The Træna Basin is an elongated NE–SW oriented feature in the northeastern part of the Vøring Basin. It is bounded in the east by the Ytreholmen Fault Zone along the Dønna Terrace in the south and the Revallet Fault Complex along the Nordland Ridge to the north (Fig. 1; Blystad et al., 1995). The western flank is defined by the Fles Fault Complex which bounds the Utgard High. To the south and north the basin is delimited by the Surt and Bivrost lineaments, respectively. The Træna Basin was formed by Late Jurassic – Early Cretaceous crustal extension and faulting, subsequently undergoing significant thermal subsidence. (Blystad et al., 1995; Zastrozhnov et al., 2020). Consequently, the basin contains deeply buried Lower Cretaceous sediments. The Træna Basin was also a prominent depocenter during the Late Cretaceous (Zastrozhnov et al., 2020).

2.1.7. Vigrid Syncline

The Vigrid Syncline is oriented NE–SW and is bounded by the Gjallar Ridge to the west, the Fles Fault Complex to the east, the Surt Lineament to the north and the Jan Mayen Lineament to the south (Fig. 1). Much of the strata in the Vigrid Syncline is made up of Upper Cretaceous deposits, with thicknesses reaching c. 4.5 S TWT, albeit significantly thinning along the western flank (Blystad et al., 1995). Based on the occurrence of Lower Cretaceous strata, the Vigrid Syncline also acted as a depocenter during the Early Cretaceous (Zastrozhnov et al., 2020).

2.2. Lower Cretaceous stratigraphy

The Lower Cretaceous succession on the mid-Norwegian Continental margin has traditionally been divided into the Lyr (Late Berriasian – Early Aptian), Lange (Berriasian – Turonian) and Lysing (Latest Turonian – Early Coniacian) Formations, collectively assigned to the Cromer Knoll Group (Dalland et al., 1988). Recently, however, the original Lange Formation, as defined by Dalland et al. (1988), has been sub-divided into the Langebarn (Berriasian – Late Albian) and the Blålange Formations (Early Cenomanian – earliest Coniacian) (Fig. 2A) cf. Gradstein et al. (2010). Concomitantly, the Blålange Formation has been re-assigned to the Shetland Group, and the renowned turbidite sandstone-dominated Lysing is now ranked as a member of the Blålange Formation (Gradstein et al., 2010) The Lyr and Langebarn Formations are retained within the Cromer Knoll Group (Fig. 2).

The base of the Cretaceous succession is defined by the regional extensive erosive boundary, referred to as the Base Cretaceous Unconformity (BCU) (e.g. Færseth and Lien, 2002; Faleide et al., 2015).

The 0.5–444 m thick Lyr Formation (Late Berriasian -early Aptian) was deposited under open marine conditions and consists of grey to light grey-green marls with interbedded carbonates (Dalland et al., 1988; Gradstein et al., 2010). The Lyr Formation is regionally extensive and stretch across from the Trøndelag Platform to the Halten Terrace. but the unit is eroded or extremely condensed on the Nordland Ridge and has not been penetrated by any exploration wells further west in the Vøring Basin, suggesting that the unit represents a shallow shelf deposit. The upper part of the formation may show a sharp gamma ray response, that may be attributed to the presence of lower Aptian organic-rich mudstones deposited under the OAE1a. See NPD Factpages (2022) for type and reference wells (i.e. 6506/12–1 and 6407/1–2).

The overlying Langebarn Formation (Berriasian – Late Albian) is 3–467 m thick and consists mainly of marine mudstones with some limestone stringers and occasional sandstone units (Dalland et al., 1988;

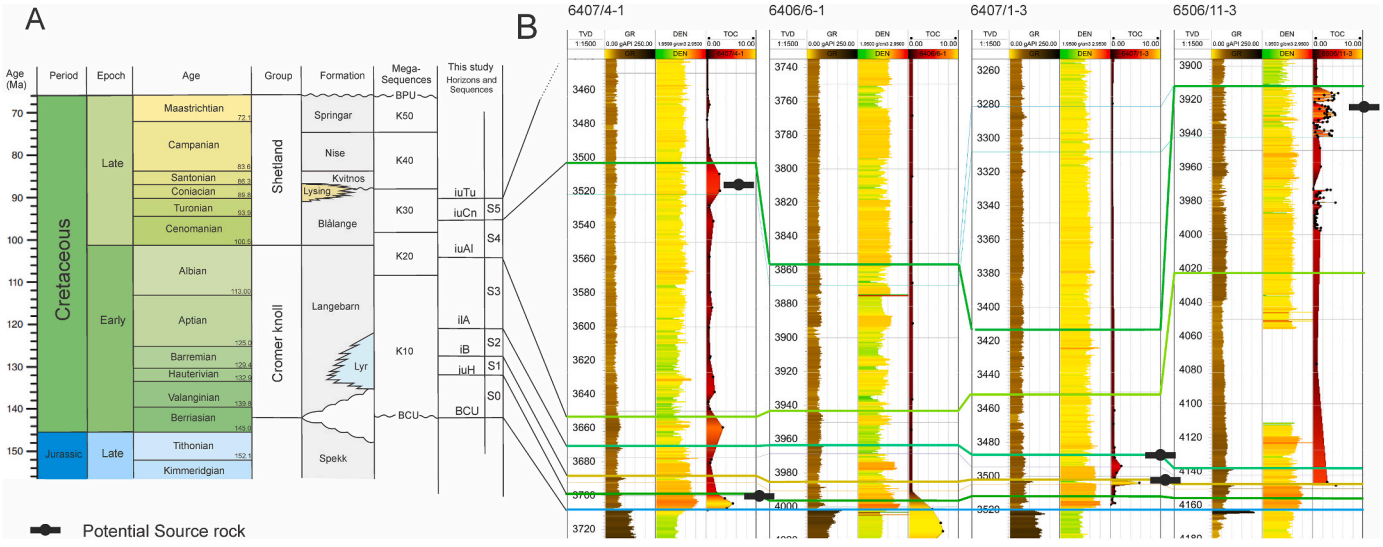

Fig. 2. (A) Lithostratigraphic overview of the Lower Cretaceous succession on the mid-Norwegian Margin. The succession has been subdivided into a series of mega-sequences by Færseth and Lien (2002). The Chronostratigraphic chart has been modified after Cohen et al. (2013). The interpreted seismic horizons and sequences are annotated. B) Well correlation of four selected wells situated on the south-western margin of the Halten Terrace, showing the presence of four organic-rich units with high GR and TOC values: (1) an upper Hauterivian in well 6407/4–1, (2) a Barremian unit in well 6407/1–3 (3) a lower Aptian unit well 6407/1–3 and (4) an upper Cenomanian potential source rock unit in well 6506/11–3 and partly in 6407/4–1. Abbreviations: iuCn: intra upper Cenomanian reflector, iuAl: Intra upper Albian reflector, ilA: intra lower Aptian reflector, iB: intra Barremian reflector, iuH: intra upper Hauterivian reflector, BCU: Base Cretaceous Unconformity, BPU: Base Paleogene Unconformity, GR: Gamma ray log, DEN: Density log, TOC: Total organic carbon (wt. %).

Gradstein et al., 2010). The formation was deposited in shallow to deep marine environments (Dalland et al., 1988; Gradstein et al., 2010). The Langebarn Formation is laterally extending across the Halten and Dønna terraces and the basinal area but is eroded on the Nordland Ridge.

The up to 1573 m thick (well 6505/10–1) Blålange Formation (Early Cenomanian – earliest Coniacian) consists predominantly of dark grey to brown mudstones with limestone stringers, but locally include several tens of meters thick turbidite sandstone units (such as the Lysing Member sandstones) which accumulated in isolated fault-bound basins on the Halten and Dønna terraces and along the Møre margin (e.g. Vergara et al., 2001; Fjellanger et al., 2005; Martinsen et al., 2005; Gradstein et al., 2010; Bell et al., 2014). Most of the mudstones of the Blålange Formation was deposited in a relatively deep, restricted marine environment strongly influenced by the rift-related bathymetry of the region and the limited connection between the various basins of the North Atlantic rift system (Gradstein et al., 1999). Due to limited water circulation, a stratified water column and widespread oxygen deficient bottom water conditions developed. The potential upper Cenomanian–lower Turonian source rock unit investigated in this paper occur within the Blålange Formation (Fig. 2).

3. Data and methods

3.1. Seismic data

Several high-resolution 2D seismic surveys (MNR 2004–2011) have been analyzed to establish and map the seismic horizons used to investigate the organic-rich units in the Cretaceous succession of the Vøring Basin. These surveys have different orientation and variable spacing between seismic lines, ranging from 1 to 8 km. Frequencies typically range between 10 and 50 Hz. The polarity convention for the dataset is zero-phase, normal polarity (*sensu* Sheriff, 2002).

In the Vøring Basin, most of the Lower Cretaceous succession is deeply buried down to depths of 6–9 S TWT, thus confidence in seismic interpretation and reflector correlation towards the deeper segments is strongly affected by decreasing seismic quality with depth. However, the overall quality of the seismic data is good, although there are some noticeable differences between the surveys.

3.1.1. Mapping of potential source rock units

A total of seven seismic horizons of regional to semi-regional extent have been defined and mapped in this study (Fig. 2). These includes the Base Cretaceous Unconformity (BCU; *sensu* Færseth and Lien, 2002), the intra upper Albian (iuAl) and the intra upper Cenomanian horizon (iuCn), which have been interpreted on regional scale and further tied to key wells in the outer Vøring Basin. In addition, the intra upper Hauterivian (iuH), intra Barremian (iB), intra lower Aptian (ilA), and intra upper Turonian (iuTu) seismic horizons have been interpreted at semi-regional scale on the Dønna and Halten terraces. These horizons are not correlated towards the deeper basin segments due to the lack of well data, diminishing seismic quality and the corresponding uncertainty in tracing these reflectors basinwards. In addition, any organic matter associated with these horizons would presumably be classified as overmature in the deeper basin segments. For this reason, these units are treated superficially throughout the remaining part of the paper.

Age determination of the mapped seismic horizons are guided by the works of Gradstein et al. (2010) and Zastrozhnov et al. (2020), together with well tops from the publicly available database of the Norwegian Petroleum Directorate (NPD Factpages, 2022) and in-house data provided by Wintershall-Dea Norway.

3.2. Well data

Wireline data from 12 exploration wells are included in this study, each dataset including Gamma ray (GR), Acoustic (AC/DT), Density (DEN), Neutron (NEU) and deep resistivity (RDEP) logs. We have established the time-depth relationship trough calibration of checkshots. Wireline logs are generally regarded to be a good supplement to seismic data when evaluating the presence of potential source rock units (Løseth et al., 2011; Hagset et al., 2022). As such, to confirm the presence of potential source rock units mapped in the seismic data, wireline log signals are integrated with digitalized total organic carbon (TOC) content logs derived from the Rock-Eval data. The thicknesses of the potential source rock units are estimated from the wireline data and subsequently, TOC samples within the interval, or from stratigraphically nearby intervals, are evaluated. Characteristic wireline responses to organic rich units are described in Hagset et al. (2022).

3.3. Rock-Eval data and interpretation

The Rock-Eval database is based on samples from sidewall cores or drill cuttings from 12 exploration wells. The database is thus based on results from previous geochemical analysis. Data quality control has been conducted to ensure that abnormal values are excluded. Unfortunately, some of the samples are missing values for the oxygen index (OI). In addition, sample spacing varies between each well, making it difficult to evaluate thin, intervening organic-rich deposits. In these cases, the nearest sample to the organic-rich unit have been used where applicable. The Rock-Eval database has been implemented into a Petrel project, making it possible to evaluate the link between seismic character, wireline logs and Rock-Eval data. This also help identify organic-rich units during well correlation and in the seismic section (e.g. Hagset et al., 2022). The complete Rock-Eval database is provided in the online supplementary file SF1.

This study applies traditional source rock evaluation following the principles of Espitalié et al. (1977), Peters (1986) and Peters and Cassa (1994) in order establish the type, richness, and thermal maturity of the organic-rich units. The thermal maturity has been established using T_{max} values, because there are no vitrinite reflectance (R_o) data available.

4. Results

4.1. Lower Cretaceous seismic sequences and bounding surfaces

Six genetic sequences (S0 – S5) and their corresponding bounding surfaces (i.e. the BCU, iuH, iB, ilA, iuAl, iuCn, iuTu reflectors of this study) have been recognized and interpreted in the Lower to lowermost Upper Cretaceous succession in the Vøring Basin (Figs. 3 and 4). Apart from the Base Cretaceous Unconformity (BCU), which defines the base of the Lower Cretaceous succession, and the unconformity related to the iuCn reflector on the Halten Terrace, the sequence-bounding surfaces presumably represent maximum flooding surfaces. Below follows a description of the seismic characteristics of each genetic sequence and their bounding surfaces.

4.1.1. Sequence 0 (Berriasian – Hauterivian)

Sequence 0 is bounded at the base by the BCU and at the top by the intra upper Hauterivian reflector (iuH). The BCU defines the base of the Lower Cretaceous succession and is characterized by a continuous and prominent seismic acoustic impedance contrast. The BCU is regional extensive and can be interpreted with high confidence. The iuH reflector has a variable continuity and negative amplitude character. Sequence 0 is deeply buried in the Vøring Basin and severely condensed on the Halten and Dønna terraces (Fig. 3). Internally, Sequence 0 has a subparallel reflection configuration, where reflectors appear semi-coherent with low to medium amplitudes.

4.1.2. Sequence 1 (Hauterivian – early Barremian)

Sequence 1 is bounded at the base by the iuH reflector and at the top by the intra Barremian reflector (iB). The iB reflector is discontinuous and has a weak negative amplitude. Sequence 1 is present on the Halten Terrace in downfaulted sections and towards the western margin of the

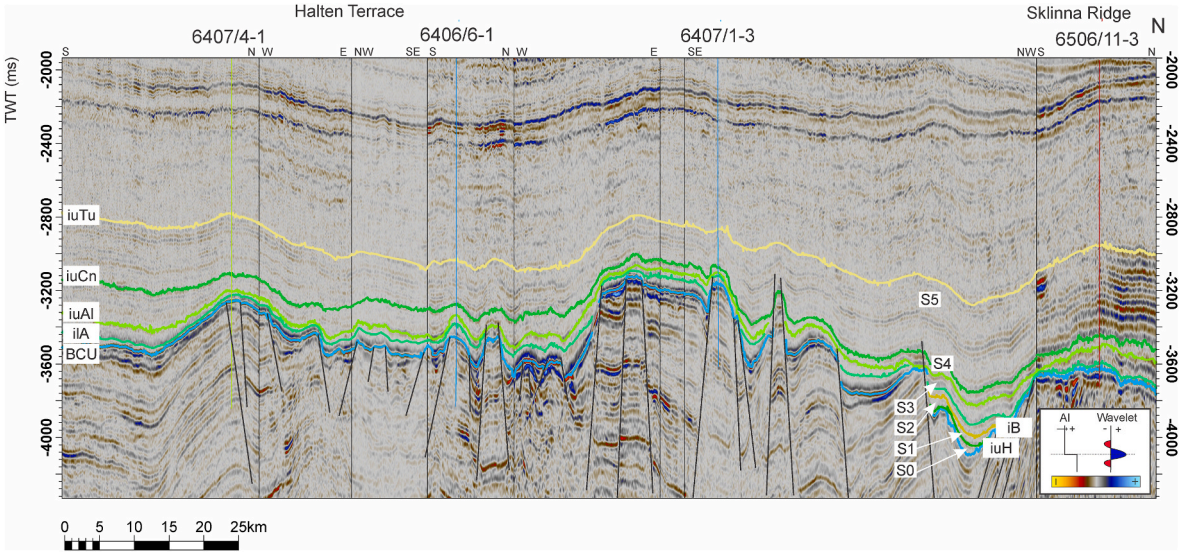

Fig. 3. Composite seismic profile crossing the southern Halten Terrace, displaying the stratigraphic framework of the condensed Lower Cretaceous succession with the sequences of this study indicated (S0–S6). The seismic has been tied to wells 6407/4–1, 6406/6–1, 6407/1–3 and 6506/11–3. The corresponding well-correlation is shown in Fig. 5, whereas location of the composite seismic profile and wells is shown in Fig. 1. Abbreviations for seismic reflectors: iuTu: intra upper Turonian, iuCn: intra upper Cenomanian, iuAl: intra upper Albian, ilA: intra lower Aptian, iB: intra Barremian, iuH: intra upper Hauterivian.

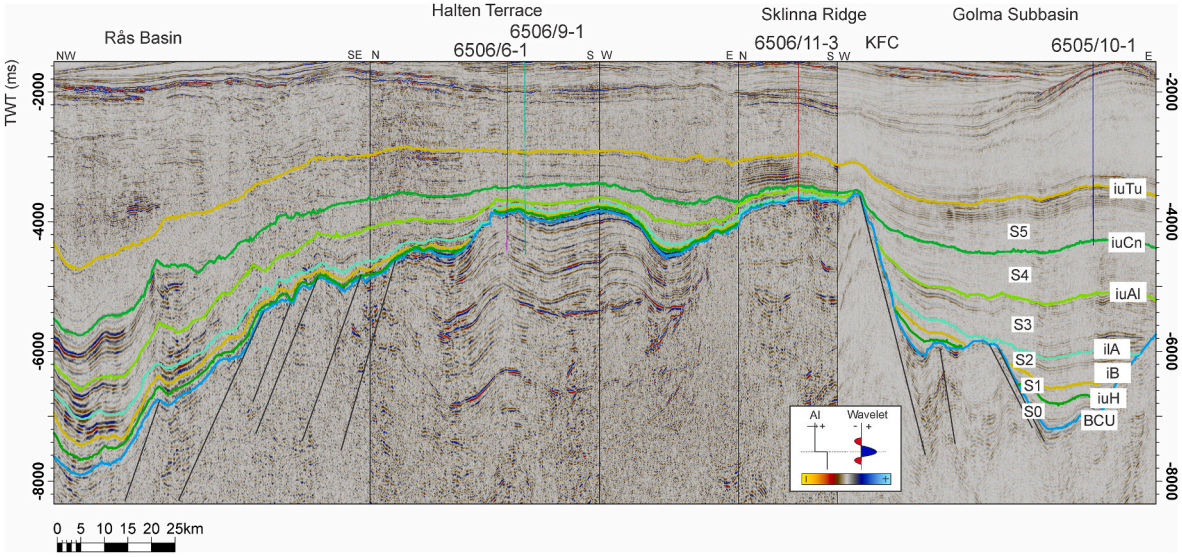

Fig. 4. Composite seismic line crossing the Træna Basin, Halten Terrace, Sklinna Ridge and Rås Basin. The seismic profile is displaying the stratigraphic framework of the Lower Cretaceous succession. Wells 6506/6–1, 6506/9–1, 6506/11–3 and 6505/10–1 are tied to the seismic. Note the deep position and lack of well control of the Lower Cretaceous horizons in the Træna and Rås Basins. Location of the composite seismic profile and wells is shown in Fig. 1. Abbreviations: iuTu: intra upper Turonian, iuCn: intra upper Cenomanian, iuAl: intra upper Albian, ilA: intra lower Aptian, iB: intra Barremian, iuH: intra upper Hauterivian, KFC: Klakk Fault Complex.

terrace (Fig. 3). The sequence is strongly condensed and has semi-coherent, subparallel reflectors with low amplitude characteristics.

4.1.3. Sequence 2 (Barremian – Early Aptian)

Sequence 2 is bounded at the base by the iB reflector and at the top by the intra lower Aptian reflector (ilA). The ilA reflector is continuous over the Halten Terrace and is characterized by low amplitudes (Fig. 3). Locally, sequence 2 is strongly condensed and the ilA reflector is obscured in places. Sequence 2 has a semi-coherent subparallel reflection configuration on the Halten Terrace, highly affected by erosion or non-deposition (Fig. 3).

4.1.4. Sequence 3 (Early Aptian – Late Albian)

Sequence 3 is bounded at the base by the ilA reflector and atop by the intra upper Albian reflector (iuAl). The iuAl reflector has a medium negative amplitude and is continuous across the Halten Terrace and can be traced into the Rås and Træna basins (Fig. 3). The internal reflection configuration of sequence 3 show parallel to subparallel reflectors, which has a low to medium amplitude. These reflectors are discontinuous and have low amplitudes within the deeper segments of the Rås and Træna basins (Fig. 4).

4.1.5. Sequence 4 (Late Albian – latest cenomanian)

Sequence 4 is bounded at the base by the iuAl reflector and atop by the iuCn reflector. The iuCn seismic reflector is continuous with low –

medium amplitude characteristics. The reflector is regionally distributed on the mid-Norwegian margin and penetrated by most of the wells on the Halten Terrace. Internally, Sequence 4 show subparallel discontinuous reflectors with low-medium amplitude characteristics.

4.1.6. Sequence 5 (latest cenomanian – late turonian)

Sequence 5 is bounded at the base by the iuCn reflector and atop by the iuTu reflector. The iuTu reflector has a negative amplitude and appear continuous on the Halten Terrace. The reflector, which marks the end of the Turonian stage, can be interpreted with high confidence across the Vøring Basin. Internally, sequence 5 has subparallel semi-coherent reflectors with variable amplitude characteristics (Fig. 3).

4.2. Potential Lower Cretaceous source rock units

Five negative reflectors have been recognized and mapped in the study area. These are the: i) intra upper Hauterivian (iuH), ii) intra Barremian (iB), iii) intra lower Aptian (ilA), iv) intra upper Albian (iuAl), and v) the intra upper Cenomanian (iuCn) reflectors. These reflectors correlate to wireline signals and raised TOC contents in several of the key exploration wells (Fig. 5; Table 1), presumably indicating the presence of organic-rich units (Løseth et al., 2011; Hagset et al., 2022).

The Lower Cretaceous organic-rich units, in particular those associated with the iB, ilA, and iuAl reflectors, are present on the Halten Terrace, as evident by increased TOC and S2 values in wells 6407/4–1, 6406/6–1, 6407/1–3 and 6506/11–3 (Fig. 5). However, it is generally difficult to tie the wireline signals of these units to distinct reflectors as the thickness of the individual units appear to be below seismic resolution. Occasionally, some of the related reflectors can be recognized in downfaulted blocks on or along the margin of the terrace (Figs. 3 and 4). Nonetheless, due to limited well-control, variable seismic quality and resolution, complex fault geometries, and great burial (i.e. 6 – 8 s TWT), all the reflectors which possibly relate to Lower Cretaceous organic-rich units are difficult to identify and confidently tie to the deeper basinal segments of the mid-Norwegian margin (Fig. 4). Although the thickness and potential of these units may be greater in the adjacent Rås and Træna basins (Fig. 4), we will focus on the organic-rich unit corresponding to the upper Cenomanian reflector in the remaining part of this paper. A detailed description of this organic-rich unit is given below, whereas the sampled intervals, typical wireline signals, TOC contents, and Rock-Eval parameter S2 is summarized in Table 1.

4.2.1. The intra upper cenomanian reflector

4.2.1.1. Lateral distribution and seismic characteristics. The iuCn reflector is traceable across the Halten Terrace and generally appears as a continuous reflector of low to medium negative amplitudes (Fig. 3). Albeit amplitude characteristics can change laterally, the reflector remains coherent over most of the Halten Terrace and the Sklinna Ridge. Towards the southwestern margin of the Halten Terrace, the iuCn reflector is downfaulted along the Klakk Fault Complex into the Golma Subbasin (Fig. 4), where the reflector remains continuous with low to medium negative amplitudes. The iuCn reflector is tied to well 6505/10–1 in the Golma Subbasin (see iuCn and well 6505/10–1; Fig. 4). From this location, the reflector can be traced laterally over the Slettringen Ridge, paralleling the Klakk Fault Complex further into the Rås and Træna Basins.

In the Rås Basin, the iuCn reflector has the same configuration with continuous low to medium negative amplitudes (Figs. 4 and 6A) Towards the more distal domain, the iuCn reflector can be traced past the Fles Fault Complex and into the deeper Vigrid Syncline (Fig. 6A). Here, the reflector remains coherent with low to medium negative amplitude, only segmented by minor down-faulting and doming. The reflector onlaps the uplifted Gjallar Ridge, where the reflector is penetrated by well 6603/5-1 S (Fig. 6A).

The iuCn reflector can also be mapped and traced along the Vigrid Syncline, where it is correlated to well 6705/10-1 situated at the margins of the northern part of the Gjallar Ridge and well 6607/5-1 located at the Utgard High (Fig. 6B). At this location, in the deeper parts of the Vigrid Syncline, the iuCn reflector have low – medium negative amplitudes and appear semi-coherent (Fig. 6B).

4.2.1.2. Well correlation. Fig. 5 shows a well correlation panel from the southern parts of the Halten Terrace and Sklinna Ridge. Here, the iuCn reflector corresponds to the top of an interval exhibiting increased TOC contents and S2 values in wells 6407/4–1, 6407/1–3 and 6506/11–3 (Fig. 5). Concomitantly, wireline logs indicate slightly increased GR and RDEP values in response to the raised TOC content in well 6506/11–3 (Fig. 5). In contrast, wireline logs in well 6407/1–3 and 6407/4-1 do not show any significant response to the increased TOC content (Fig. 5). Increased TOC and S2 levels are also recorded in well 6507/2–3 situated near the Dønna Terrace (Fig. 1 and Table 1).

The correlation panel shown in Fig. 7 includes exploration wells

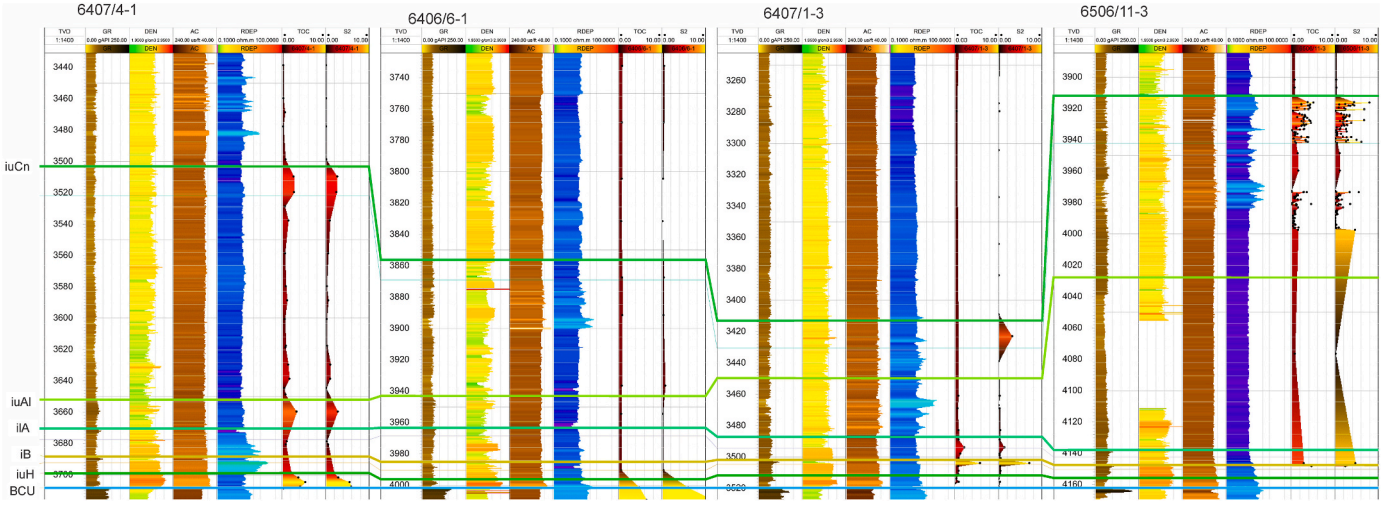

Fig. 5. Correlation of wells 6407/4–1, 6406/6–1, 6407/1–3 and 6506/11–3 on the Halten Terrace and Sklinna Ridge. The seismic reflectors mapped in this study is annotated, including the BCU (Base Cretaceous unconformity), iuH (intra upper Hauterivian), iB (intra Barremian), ilA (intra lower Aptian), iuAl (intra upper Albian) and iuCn (intra upper Cenomanian). Abbreviations: GR. Gamma ray, DEN: Density, AC: Acoustic/Sonic, RDEP: Deep Resistivity, TOC: Total Organic Carbon. S2: Rock-Eval "S2" parameter. Scaling and color schemes are indicated. The Black points along the TOC and S2 log are sample points. Location of wells is indicated in Fig. 1.

Table 1
Interval, wireline log and Rock-Eval values for the upper Cenomanian organic-rich unit in key exploration wells situated on the Halten Terrace and elsewhere in the Vøring Basin. Average values are given in brackets. Single values indicate one sample point for the interval. Rock-Eval values in well 6603/5-1 S are taken close to the sample interval.

Well	Interval (m)	GR (gAPI)	DEN g/cm^3	AC (us/ft)	RDEP (ohm.m)	TOC (Wt %)	S2 (mg/g)
6407/4-1	3503–3521	40–60	2.4–2.6	95–105	1.1–1.6	2.66–2.78 (2.72)	2.46–2.69 (2.58)
6406/6-1	3856–3868	55–70	2.2–2.6	80–95	1.25–1.7	0.84	0.43
6407/1-3	3412–3430	45–70	2.75–2.43	85–105	1.47–4.8	None in interval: 0.8	3.11
6506/6-1	3797–3833	44–85	2.5–2.92	80–100	1.65–2.75	0.68–3.83 (1.83)	0.29–5.13 (2.36)
6506/12-3	3563–3595	35–67	2.3–2.53	78–105	1.29–2.83	0.79–1.86 (1.14)	0.23–13.08 (3.58)
6507/2-3	3253–3263	N/A	2.29–2.56	83–102	1.85–3.32	0.75–11.88 (2.30)	1.12–28.06 (4.11)
6607/5-1	3653–3693	85–250*	2.33–5.7	94–105	1.0–2.2	0.18–0.75 (0.56)	0.06–0.72 (0.41)
6506/11-3	3912–3942	30–75	2.3–2.75	80–110	1.0–6.1	0.19–5.07 (2.53)	0.03–7.89 (2.30)
6505/10-1	4940–4964	80–100	N/A	98–61	1.78–5.5	1.20–1.50 (1.35)	3.08
6603/5-1 S	3825–3848	98–85	2.60–2.70	84–93	2.2–2.85	0.89–1.00 (0.94)	1.24–1.28 (1.26)
6705/10-1	3603–3621	82–95	2.3–2.5	N/A	2.5–3.4	1.97	5.82
6608/2-1 S	3882–2998	80–145	2.4–2.75	80–95	1.6–3.9	N/A	N/A

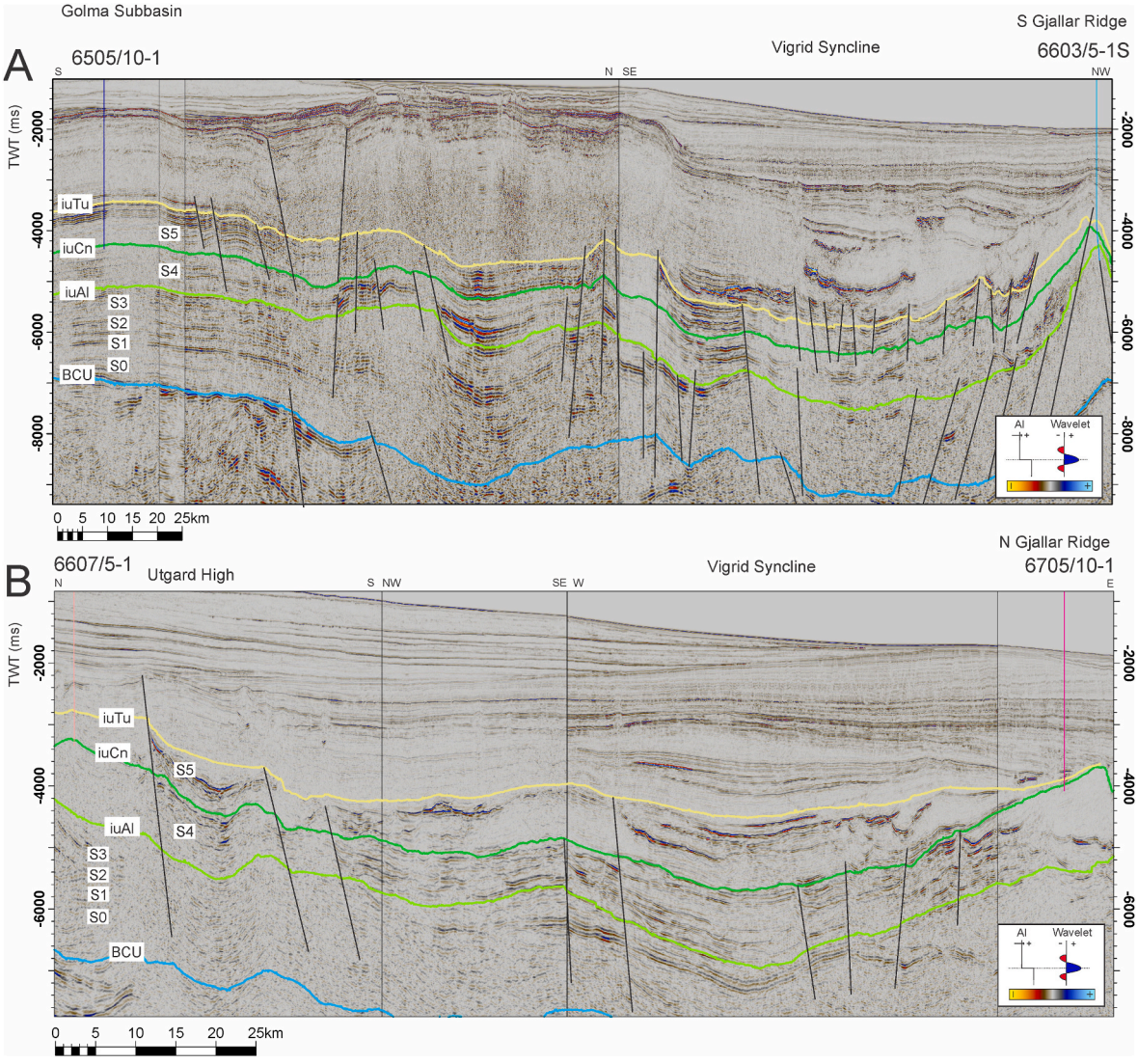

Fig. 6. Composite seismic lines crossing the outer part of the Vøring Basin.(A) Composite seismic section indicating the correlation between well 65005/10–1 in the Golma Subbasin and well 6603/5-1 S at the southern part of the Gjallar Ridge. B) Seismic composite line displaying the correlation between well 66007/5–1 at the Utgard High and well 6705/10–1 at the northern section of the Gjallar Ridge. Seismic reflectors and sequences are annotated. Location and orientation of the composite lines is indicated in Fig. 1. Abbreviations: iuTu: intra upper Turonian, iuCn: intra upper Cenomanian, iuAl: intra upper Albian, ilA: intra lower Aptian, iB: intra Barremian, iuH: intra upper Hauterivian.

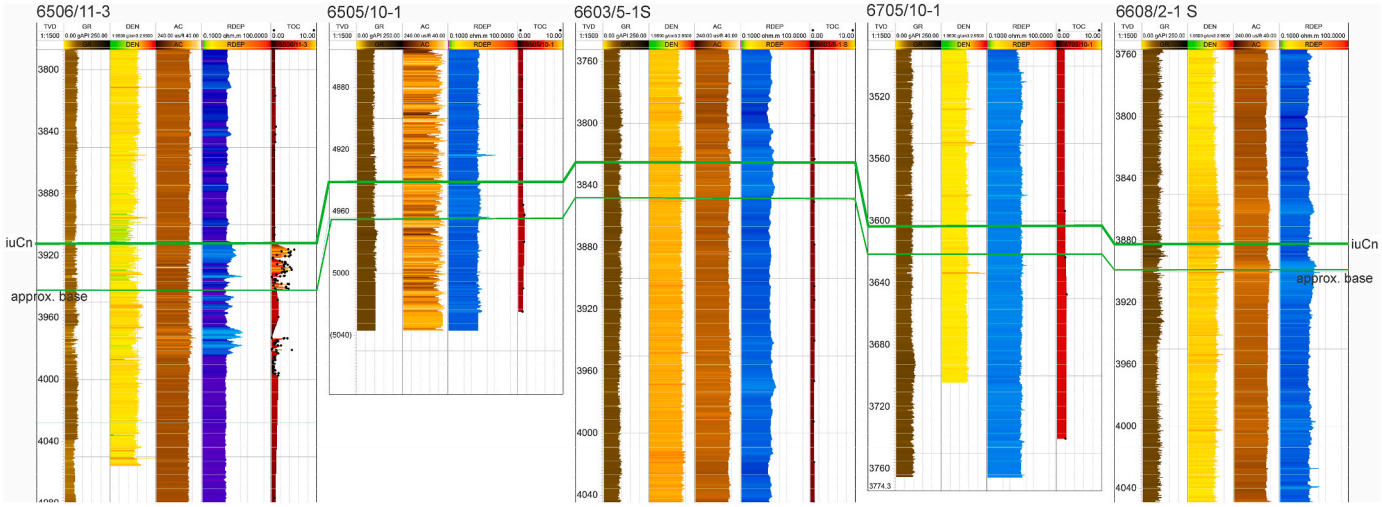

Fig. 7. Correlation of wells 6506/11–3, 6505/10–1, 6603/5-1 S, 6705/10–1 and 6608/2-1 S demonstrating the extent and character of the iuCn reflector (intra upper Cenomanian) and the base of the associated organic-rich unit. Location of wells is indicated in Fig. 1. Abbreviations: GR. Gamma ray, DEN: Density, AC: Acoustic/Sonic, RDEP: Deep Resistivity, TOC: Total Organic Carbon. S2: Rock-Eval "S2" parameter. Scaling and color schemes are indicated. The Black points along the TOC and S2 log are sample points.

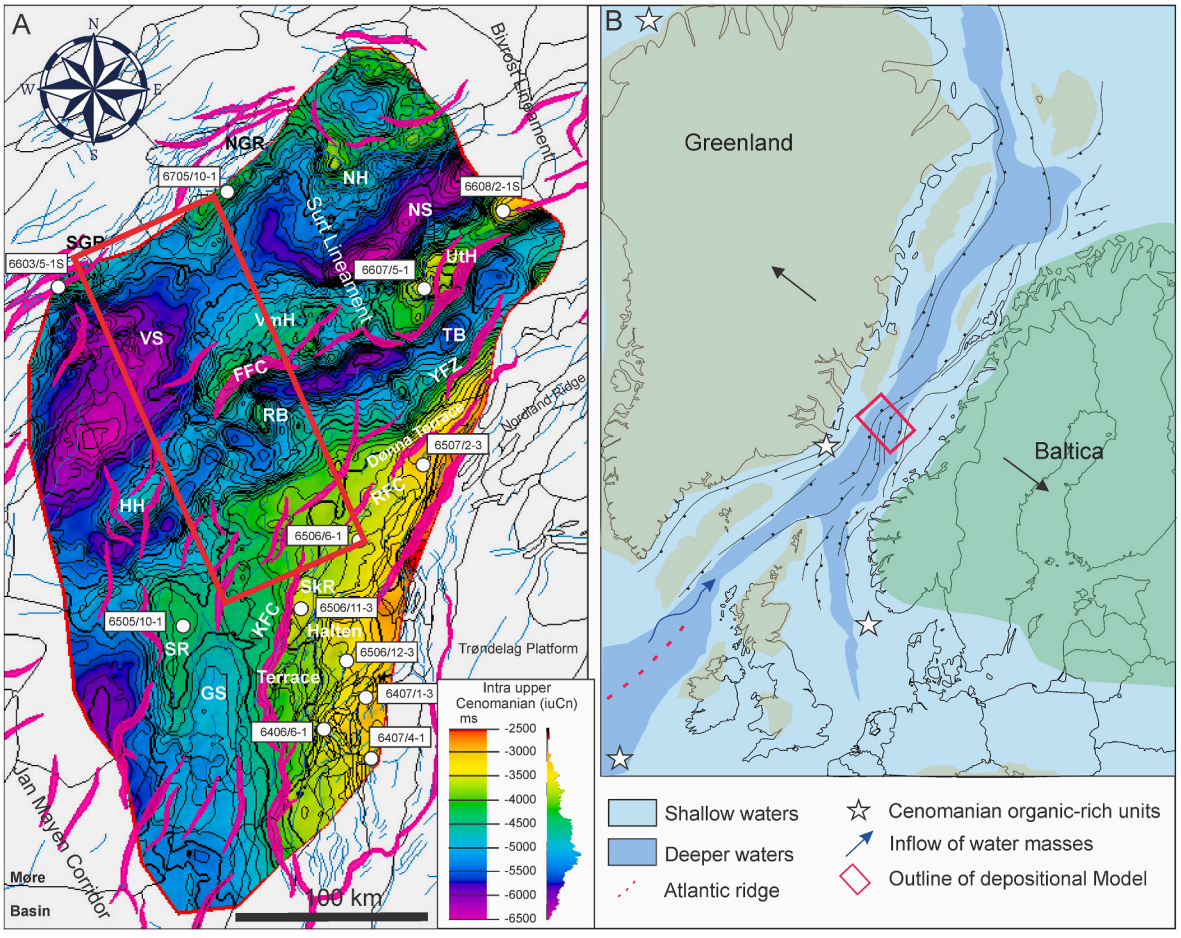

Fig. 8. (A) Time-elevation map of the intra upper Cenomanian reflector (iuCn). The structural elements (black lines), minor (light blue lines) and major faults (purple thick lines) are implemented after Gernigon et al. (2021). Color-scale with value distribution is indicated. Exploration wells of this study are indicated. (B) Paleogeographic map of the mid-Norwegian margin and north Atlantic during the Cenomanian. The map is re-drawn after Gradstein et al. (1999) and include (with modification) some of the major faults in Faleide et al. (2008) The approximated extent of the depositional model presented in Fig. 10 is indicated on the map. The presence of Upper Cenomanian organic-rich units documented in the North Sea, Sverdrup Basin and the NE Greenland is also indicated, after Doré et al. (1997b).

6506/11–3, 6505/10–1, 6603/5-1 S, 6705/10–1 and 6608/2-1 S and document the extent and character of the iuCn reflector. The three latter wells are tied to the iuCn reflector in the outer part of the Vøring Basin. Particularly well 6505/10-1 gives an unequivocal confirmation of the stratigraphic position of the iuCn reflector in a deep basinal setting in the Golma Subbasin west of the Halten Terrace. Common to these outer basin-positioned exploration wells (i.e. 6505/10–1, 66035-1 S, 6705/10–1 and 6608/2-1 S) is the absence of increased TOC values and wireline responses associated with the iuCn reflector (Fig. 7).

4.2.1.3. Evaluation and regional interpretation. A time-elevation map has been generated for the iuCn reflector based on interpretation of the regional 2D seismic data and the well correlations (Fig. 8). The time-elevation map reveals that the iuCn reflector generally parallel the underlying structural elements, albeit commonly being delimited by structural highs (Fig. 8). This is also documented by the onlapping nature of the reflector against for example the Sklinna Ridge and the marked thinning of Sequence 5 onto and across the Halten Terrace (Figs. 4 and 6). As such, the well correlation and regional seismic interpretation, document that the iuCn reflector is laterally extensive

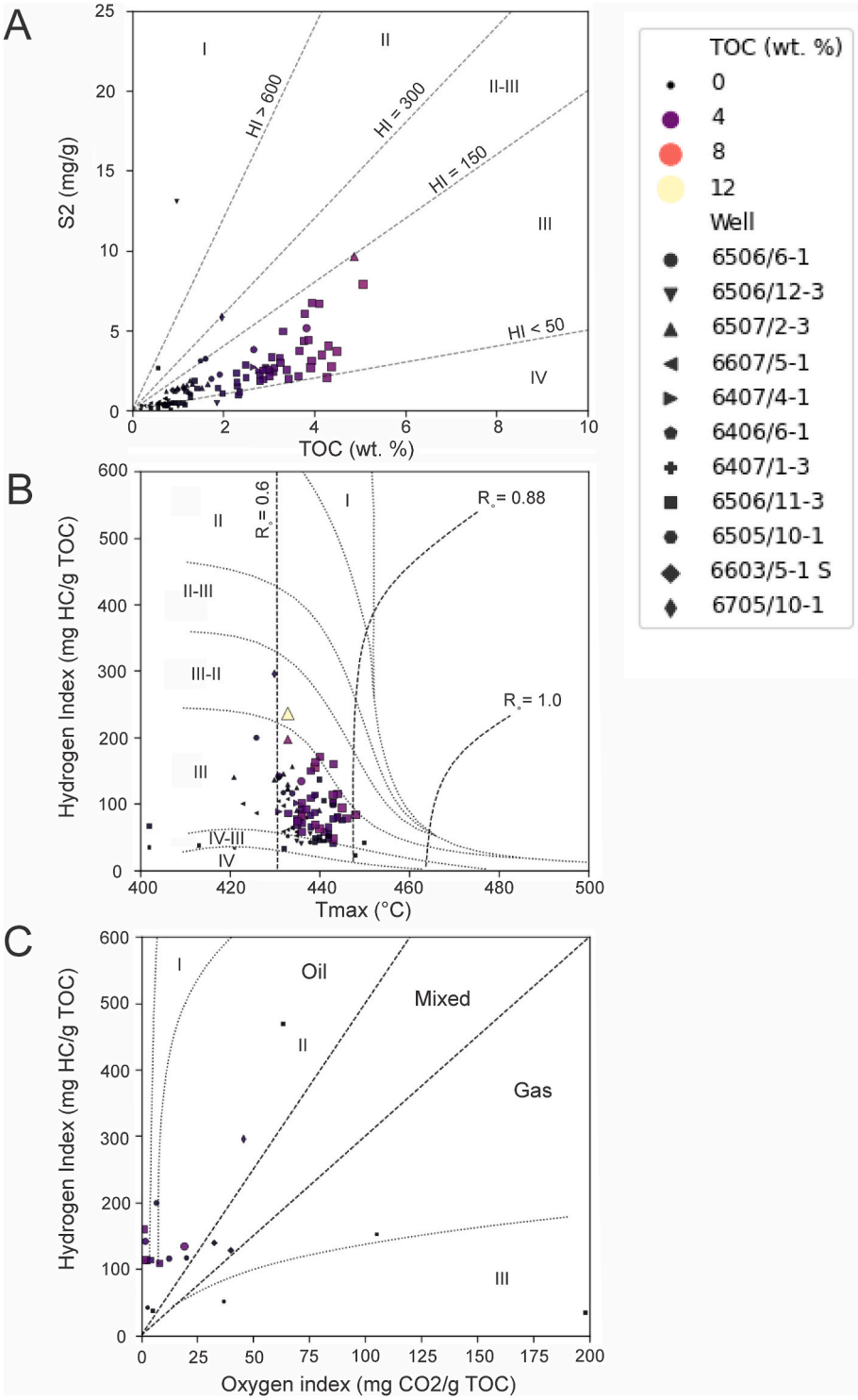

Fig. 9. Diagrams documenting the potential of the upper Cenomanian source rock unit (Corresponding to the iuCn reflector) in key wells on the mid-Norwegian Margin. The sample points increase in size depending on TOC values. Each well have a specific marker. The sample interval and thickness is shown in Table 1. Location of exploration wells is indicated in Fig. 1 (A) TOC content plotted against Rock-Eval S2 values. Kerogen type indicators are overlying the cross plot as Hydrogen index (HI) lines. (B) plot of T_{max} vs. HI indicating the petroleum potential and maturity of the samples. Overlying are the vitrinite reflectance (Ro) lines after Isaksen and Ledje (2001). (C) van Krevelen diagram of HI vs. OI indicating the quality and maturation level of the samples. Unfortunately, very few OI datapoints are available.

over large parts of the Vøring Basin.

Based on the negative amplitude of the reflector, affirmative wireline log responses, increased TOC contents and S2 values, the iuCn reflector is interpreted to represent a potential upper Cenomanian source rock unit on the Halten Terrace, Sklinna Ridge and possibly the adjacent Golma Subbasin, Rås and Træna basins (Figs. 3–5). Similar positive correlations between seismic, wireline and TOC data has been used to infer source rock units elsewhere (e.g. Løseth et al., 2011; Marín et al., 2020; Hagset et al., 2022) However, in the outer Vøring Basin, the localized lack of corresponding wireline responses and variable TOC contents (see wells 6505/10–1, 6603/5-1 S, 6705/10–1 and 6608/2-1 S; Figs. 6 and 7) related to the iuCn reflector, indicates a rather patchy distribution for the upper Cenomanian source rock unit. Consequently, it is problematic to fully assess the unit's regional potential and confidently include it in exploration models. Despite these uncertainties, we evaluate the potential of the upper Cenomanian source rock unit based on the available Rock Eval data to facilitate further discussion and perhaps stimulate future research initiatives.

4.3. Rock eval characteristics of the upper cenomanian source rock unit

The main characteristics of the upper Cenomanian organic-rich unit in the selected key wells are shown in Fig. 9. The overall trend indicates that most of the analyzed samples have poor potential indicated by low S2 values (S2 < 2.5 mg/g) and a highly variable TOC content (0.18–11.88 wt %; Fig. 9A). These samples have low HI values (40–150 mg HC/g TOC; Fig. 9B), and the few OI datapoints available show a widespread value distribution (1–198 CO_2/g TOC; Fig. 9C). Most of the samples are mature with T_{max} values ranging 430–450 °C (Fig. 9B) in proximity to the vitrinite reflectance trend line 0.88% (Fig. 9B). Collectively, most of the samples belonging to the upper Cenomanian organic-rich unit indicate a kerogen Type III composition and that gas would be the main expelled product (Fig. 9C).

Samples belonging to wells situated on the Halten Terrace and Sklinna Ridge indicate localized higher potential compared to the samples from the deeper Vøring Basin (Fig. 9). These samples exhibit increased TOC, S2 and HI values. In this regard, the samples which have a kerogen Type III–II composition in wells 6507/2–3 and 6506/11–3, is very intriguing (Fig. 9C).

Especially the samples from well 6506/11-3 stand out (Table 1 and Fig. 9), with TOC contents and S2 values averaging 2.53 wt % and 2.30 mg/g, respectively. However, these samples have low HI values, averaging 88 mg HC/g TOC, and the few OI datapoints available indicate an average of 48 mg CO_2/g TOC. No vitrinite reflectance data is available from well 6506/11–3. Still, based on the calculated average T_{max} value of 438 °C, the organic-rich unit is early mature. Collectively, this indicate that the upper Cenomanian organic-rich unit is oil-mature and kerogen Type III-dominated on the Sklinna Ridge.

Two samples from well 6507/2–3 indicate elevated potential for the upper Cenomanian – unit on the Halten Terrace (Fig. 9A and B), samples for the whole interval exhibit TOC contents and S2 values averaging 2.30 wt %. and 4.11 mg/g, respectively. The HI is averaging 137 mg HC/g TOC, and there is no OI or vitrinite reflectance data available, but the organic-rich unit have an average T_{max} value of 432 °C, indicating that the organic matter is immature to early mature.

The general trend of the samples from the wells situated in the deeper Vøring Basin (i.e. 6607/5–1, 6705/10–1, 6603/5-1 S), suggest a poor potential indicated by low S2 values and TOC contents (Fig. 9A), as well as low HI values (Fig. 9B). Based on these parameters, the organic-rich unit appear to have a kerogen Type III composition (Fig. 9A and B). The average T_{max} values from samples in these wells (i.e. 432, 430, 407 °C) suggests that the upper Cenomanian organic-rich unit is immature on the eastern margins of the Gjallar Ridge and the Utgard High. The one sample from well 6705/10–1, which deviate from the general trend, exhibit high S2 values (5.82 mg/g), intermediate TOC contents (1.97 wt%) and good HI values (295 mg HC/g TOC). The same sample also have low OI values (46 CO_2/g TOC) indicating higher qualities and a kerogen Type-II composition.

5. Discussion

The presence of an upper Cenomanian organic-rich unit with some source potential on the Halten Terrace and the Sklinna Ridge, as well as locally in the deeper parts of the Vøring Basin, is interesting because of its impact on the prospectivity of area. The apparent patchy and localized distribution and variable potential of the unit, suggests that its development was influenced by the fault-segmented internal configuration of the larger Vøring Basin and lateral variations in depositional environments with superimposed fluctuations in sedimentation rates, oxygen levels, organic productivity, and changing organic-matter preservation potential. Consequently, the most prolific zones are hard to predict. A discussion of the potential of the upper Cenomanian organic-rich unit and our proposed depositional model follows below.

5.1. Controls on source rock distribution and potential

The rift-related paleobathymetric configuration of the Vøring Basin exerted a first-order control on distribution and preservation of organic matter, directly influencing water mass circulation and bottom water oxygenation (e.g. Swiecicki et al., 1998; Fjellanger et al., 2005; Trabucho-Alexandre et al., 2012). The development and distribution of deep, silled basins, ridges and intrabasinal highs was controlled by the many faults and transfer zones which predominantly formed during the Late Jurassic – Early Cretaceous rifting event, and subsequent reactivation in the Late Cretaceous – Palaeocene (Færseth and Lien, 2002; Tsikalas et al., 2012; Zastrozhnov et al., 2020). This includes, amongst others, the Rås and Træna basins, who both experienced accelerated subsidence in the mid-Cenomanian – Turonian (Færseth and Lien, 2002; Lien, 2005; Zastrozhnov et al., 2018, 2020). Similar structural controls on water column circulation are well known from other basins and was crucial during deposition of the renowned Upper Jurassic source rock interval across the Norwegian Continental Shelf (e.g. Demaison et al., 1983; Miller, 1990; Cooper et al., 1995; Isaksen and Ledje, 2001; Marín et al., 2020).

Another critical factor for accumulating potential source rocks is sedimentation rate (e.g. Katz, 2005; Bohacs et al., 2005). Ideally, sedimentation rate should be below a critical threshold for organic matter to be preserved without experiencing a significant dilution effect (Ibach, 1982; Bohacs et al., 2005). Based on lithology, the mudstone dominated Cretaceous succession on the mid-Norwegian Continental shelf (Dalland et al., 1988; Gradstein et al., 2010) has a critical threshold around 21.13 m/m.y. (silty-clay lithology: Ibach, 1982). However, the relationship between sedimentation rate and organic content is complex (Tyson, 2001; Katz, 2005) as sedimentation rate varies across the basin (Færseth and Lien, 2002) due to variable distance and connection to the sediment source, position in relation to sea level, subsidence, climatic factors and sediment source rock composition (Prosser, 1993; Ravnås and Steel, 1998; Færseth and Lien, 2002). In addition to sedimentation rate, primary production and the following destruction of organic matter by biodegradation have a fundamental control on the amount of organic matter preserved cf. Tyson (2001) and Bohacs et al. (2005).

Structural highs which segmented the Vøring Basin during the Late Jurassic – Early Cretaceous rifting event, formed local sediment source areas which promoted high sedimentation rates (e.g. Bell et al., 2014). At a regional scale, rift-shoulder uplift of the conjugate continental landmasses bordering the North Atlantic Rift System (i.e. Western Norway and East Greenland) promoted fast filing of the deep basin bathymetry, presumably diluting the organic matter across the basin. However, the massive influx of continentally derived sediments (as evident by the thickness of the Cretaceous succession in the study area and adjacent basins), including residual material such as plant detritus, and increased fluvial run-off must periodically have enhanced primary

production (e.g. Wakeham and Lee, 1993).

The formation of a marine source rock unit is strongly dependent on nutrient influx to the basin either via fluvial sources or by coastal upwelling, both having the capability of promoting increased primary production of organic matter in the water column (Demaison et al., 1983; Calvert et al., 1996; Wesenlund et al., 2022). Enhanced primary production may also be caused by increased sea surface temperatures, rising sea level and flooding of coastal areas, as well as volcanic activity (Katz, 2005; Leckie et al., 2002; Scotese et al., 2021). The warm and humid climate, which prevailed during the Cretaceous greenhouse period, combined with a historically high eustatic sea-level and wide-spread volcanism related to the emplacement of large igneous provinces (LIPs) promoted increased biological productivity in the ocean (Leckie et al., 2002; Scotese et al., 2021). It may also be that increased chemical weathering and extensive deep weathering of exposed terranes in combination with increased precipitation rates and continental run-off contributed to the favorable conditions for maintaining high rates of primary production (Jenkyns, 1999, 2003; Leckie et al., 2002; Erba, 2004).

The Cenomanian - Turonian OAE 2 is represented by widespread deposition of organic-rich mudstones that imply expansion of anoxic and euxinic water layers on a global scale (Arthur et al., 1987; Leckie et al., 2002). This expansion is coupled to a transgressive development, leading to a global eustatic sea level highstand. The link between the major eustatic sea-level highstand at the Cenomanian – Turonian boundary (Haq et al., 1987; Miller et al., 2005) and deposition of organic-rich mudstones (Arthur et al., 1987, 1988) was established by Schlanger and Jenkyns (1976) and Jenkyns (1980). The increased eustatic sea-level was caused by major volcanism and corresponding active seafloor spreading, volume increase of mid-ocean ridges, thermal uplift of the seafloor, as well as the prevailing greenhouse climate which inhibited the establishment of polar icecaps (Schlanger et al., 1981; Arthur and Sageman, 2005; Pearce et al., 2009). The associated volcanic outgassing increased atmospheric CO_2 concentrations, terrestrial weathering, and nutrient flux (e.g. Sinton and Duncan, 1997; Adams et al., 2010). This development promoted eutrophication of the oceans and enhanced primary production (e.g. Turgeon and Creaser, 2008). The abundance of organic matter increased the consumption of dissolved oxygen by bacteria during decomposition. Eventually, this caused widespread anoxic conditions (i.e. OAE) and led to the deposition of organic-rich mudstones (Schlanger and Jenkyns, 1976; Schlanger et al., 1987; Arthur et al., 1987; Pearce et al., 2009).

The oxygen deficient conditions that characterize the early Aptian OAE1a is represented by an organic-rich unit on the Svalbard Platform (Midtkandal et al., 2016) and possibly also on the SW Barents Shelf (e.g. Hagset et al., 2022). This event was largely subject to the same controlling factors as OAE 2, and has been associated with volcanic outgassing from the Caribbean LIP and the High Arctic LIP (e.g. Maher, 2001; Maher et al., 2004; Corfu et al., 2013; Senger et al., 2014; Polteau et al., 2015; Midtkandal et al., 2016). The volcanism associated with HALIP, together with the Caribbean LIP (e.g. Serrano et al., 2011) is thus part of the larger picture explaining the occurrence of OAE 2 (e.g. Arthur et al., 1985; Adams et al., 2010; Zheng et al., 2013; Eldrett et al., 2014; Scaife et al., 2017).

5.2. Depositional model and source rock potential

It is well known that the fault-controlled topography/bathymetry in rift basins may restrict water circulation which leads to anoxic conditions that eventually favor source rock deposition (e.g. Heilbron et al., 2000). Following the extensive rifting phase in the Late Jurassic – Early Cretaceous, the mid-Norwegian margin developed to become a restricted marine or silled basin, which promoted anoxia and deposition of the renowned Upper Jurassic source rock. We suggest that the Early Cretaceous rift configuration on the mid-Norwegian margin resulted in similar conditions and thus periodically led to hypoxic to anoxic conditions, particularly during the Early Cretaceous pulses of global anoxia (e.g. Beil et al., 2020), as recorded in exploration well 6608/2-1 S (OAE 1a in well 6608/2-1 S; see Zastrozhnov et al., 2020). It is very likely that the deep silled basin on the mid-Norwegian margin hosted a stratified water column controlled by the fault-related bathymetry and influx of fresh water. This physiography in combination with the recurrent global anoxic events promoted favorable conditions for preservation of organic matter (e.g. Demaison et al., 1983) and deposition of the Lower Cretaceous organic-rich units in the rift basins along the mid-Norwegian margin (Jongepier et al., 1996; Doré et al., 1997b) and on the Halten Terrace in particular (Fig. 5).

5.2.1. The upper cenomanian organic-rich unit on the Halten Terrace

The seismic investigation and evaluation of the upper Cenomanian organic-rich unit indicate that there is increased generation potential on the Sklinna Ridge and the northern part of Halten Terrace (i.e. wells 6506/11–3 and 6507/2–3; Table 1), with the organic-rich unit in well 6506/11-3 being recognized as the most prolific (Fig. 9). This unit has a kerogen Type III composition, which indicate significant terrestrial influence, possibly testifying to a proximal paleo-shoreline location for well 6506/11–3. The T_{max} values indicate an early mature source rock unit, whereas the dominant organo-facies, suggest potential for gas expulsion. We propose a depositional model for this unit which involves the development of an extended oxygen minimum zone in combination with significant contributions from terrestrial sources (Fig. 10). This model builds largely on the connection between deep-water circulation and productively as proposed by Arthur et al. (1987).

By Cenomanian times, a rifted seaway, being the precursor of the Norwegian Sea, had already been established for some time (Gradstein et al., 1999; Skogseid et al., 2000) and most likely experienced a steady inflow and exchange of water masses (Figs. 8B and 10). The onset of the OAE 2 greatly extended the oxygen minimum zone and left much of the water column in hypoxic to anoxic conditions (Fig. 10). These oxygen-deficient conditions might have been intensified or prolonged on the Sklinna High and Halten Terrace due to local upwelling (Fig. 10). Coastal upwelling typically forces deep, nutrient-rich water (e.g. nitrates and phosphates) to flow upwards through the water column promoting high biological productivity in the photic zone (Demaison and Moore, 1980; Demaison et al., 1983; Wesenlund et al., 2022, Fig. 10). Consequently, upwelling tends to intensify recycling of organic matter by oxygen-utilizing bacteria, which causes anoxic and hypoxic conditions in the mid to deeper water levels (Demaison and Moore, 1980; Demaison et al., 1983). This eventually promoted preservation of significant amounts of organic matter at the seafloor. Phosphate nodules, which commonly occur in sediments deposited under the influence of upwelling or other high productivity settings (e.g. Papadomanolaki et al., 2022; Wesenlund et al., 2022), have not been recorded in this study due to the lack of core data. However, in many reported cases, phosphate can only be detected as minor components in fossils and microfossils (e.g. Beil et al., 2020).

In the present case, nutrient-rich water was supplied from the deep oceanic realm of the Atlantic Ocean (Fig. 8B). The oceanic water was forced up against the margins of the Halten Terrace (i.e. against the KFC and YFZ) where oxygen minimum zones developed on the shallow marginal areas of the Halten Terrace and Sklinna Ridge due to increased primary production, potentially explaining why the upper Cenomanian organic-rich unit appear along the margins of these positive structural feature (i.e. Sklinna Ridge; Fig. 10). As the upper Cenomanian organic-rich unit only appears in a few wells (i.e. 6506/11–3 and 6507/2–3), its is possible that the anoxic conditions were restricted to specific areas along the margins of the Halten and Dønna Terraces (Fig. 10). Upwelling was most likely controlled by paleobathymetric conditions, water mass circulation, and prevailing winds in relation to the margin. These controlling factors could have restricted the extent and location of the oxygen minimum zone (Fig. 10). This, in combination with high sediment influx which diluted the organic-matter, ultimately hindered the

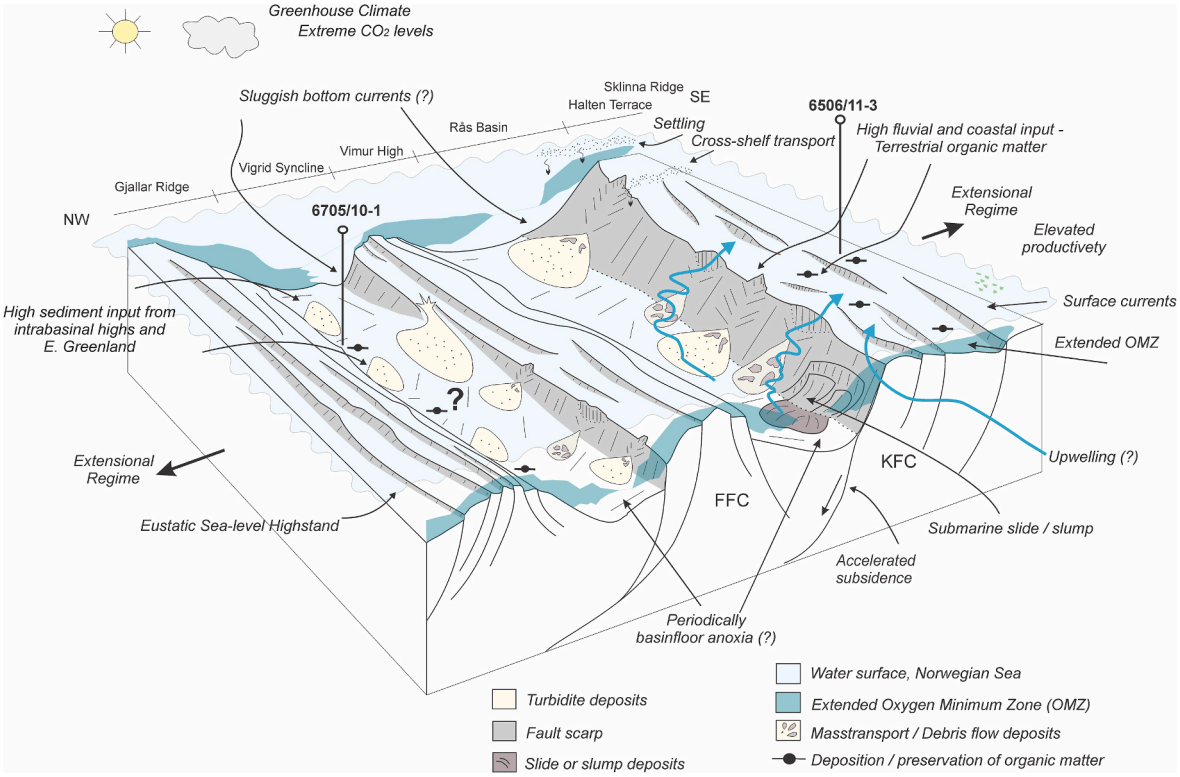

Fig. 10. Conceptual depositional model outlining the basin configuration and conditions during deposition of the upper Cenomanian organic-rich unit on the Sklinna Ridge, Rås Basin and Vigrid Syncline. The light red zone with dotted lines indicate an extended oxygen minimum zone connected to the OAE 2. Abbreviations: FFC: Fles Fault Complex, KFC: Klakk Fault Complex, OMZ: Oxygen minimum zone.

development of a thick, wide-spread prolific source rock at the Cenomanian to Turonian transition (Fig. 10).

The kerogen Type III organo-facies composition suggests that most of the organic matter was derived from terrestrial sources (Tissot et al., 1979; Tissot and Welte, 1984; Demaison et al., 1983). This may indicate that much of the organic matter entered the area via fluvial systems coming off the conjugate margins or via deposition from land-derived sediment gravity flows which promoted rapid burial (Fig. 10) (e.g. de Graciansky et al., 1987). Saller et al. (2006), for example document the presence of turbidites rich in leaves which act as a source rock in the Miocene Kutei Basin in Indonesia. These processes may to some extent explain the uneven vertical and spatial trend seen in the wireline values and TOC contents (well 6506/11–3; Fig. 5).

5.2.2. *The upper cenomanian organic-rich unit in the Vøring Basin*

The iuCn reflector has identical amplitude characteristics on the Sklinna Ridge, Golma Subbasin and in the Rås Basin. Despite similar characteristics, samples from well 6505/10–1 indicate that there is no source rock potential associated with the upper Cenomanian unit in the Golma Subbasin (Figs. 4 and 9). In the deeper Rås Basin and the Vigrid Syncline, the upper Cenomanian unit is confined between intrabasinal highs, being delimited by the FFC and the KFC in the Rås Basin, and the FFC and the Gjallar Ridge in the Vigrid Syncline (Fig. 10). Samples from wells situated in the Vøring Basin (i.e. 6607/5–1, 6705/10–1, 6603/5-1 S) are immature – early mature for the upper Cenomanian organic-rich unit, possibly indicating increasing maturity towards the deeper basin segments. Samples from exploration well 6705/10–1 indicate an elevated petroleum potential with a mixture of kerogen Type II and III (Fig. 9). Collectively, this suggests that there is an increased possibility of a more prolific organic-rich unit locally in the deeper segments of the Vigrid Syncline (Fig. 10).

Sedimentation rates and oxygen levels appear to be the main controls on quantity and quality of organic matter for the upper Cenomanian organic-rich unit (e.g. Arthur et al., 1985; Demaison and Moore, 1980; Demaison et al., 1983). Although hypoxic to anoxic water conditions may have been induced by elevated productively during the OAE 2, the massive sedimented input hindered development of substantial quantities of organic matter (Fig. 10). Færseth and Lien (2002) reported the sedimentation rate to be on average 220 m/m.y. during the Cenomanian – Early Campanian period. Similar values where presented by Kjennerud and Vergara (2005) who indicated a sedimentation rate up to 300 m/m.y. This contrasts the critical threshold for dilution of organic-matter, reported to be 21.13 m/m.y. in silty-clay by Ibach (1982). The development of a high-quality prolific source rock unit therefore seems dependent on local or periodic reduction in sediment input (i.e. well 6705/10–1; Fig. 10), which further is controlled by paleobathymetric conditions and sediment fairways in the basin (Fig. 10).

Due to the well-developed oceanic conditions between Greenland and Norway in the Cretaceous (Gradstein et al., 1999), water mass circulation promoted oxygenated bottom water conditions (Fig. 10). However, during periods of fault-controlled restriction of the basin the bathymetry of the rotated fault blocks promoted reduced water mass circulation and oxygen-deficient bottom water conditions. In addition, biostratigraphic analysis indicate a periodically semi-restricted connection to the central Atlantic oceanic system (Gradstein et al., 1999). Typically, this configuration with a silled basin would create ideal conditions for the preservation of organic matter (Demaison and Moore, 1980; Demaison et al., 1983). However, massive sediment input due to a combination of rift-shoulder uplift of the conjugate margins and increased weathering rates and continental run-off driven by the Cretaceous climate, resulted in severe dilution of the organic matter (Fig. 10). Locally, in areas less affected by sediment dilution, accumulations of organic-rich deposits were preserved (i.e. wells 6603/5-1 S and 6705/10–1), possibly indicating a patchy distribution and moderate potential of the upper Cenomanian source rock unit in the deeper basin segments (Fig. 10). In addition, the Rås Basin has been identified as a

major Cretaceous depocenter during the middle Cenomanian to late Turonian times (Zastrozhnov et al., 2020), and concomitantly experienced accelerated subsidence and increased sedimentation during this period (Færseth and Lien, 2002; Zastrozhnov et al., 2020). High sedimentation rates may thus have impeded the possibility for sufficient and widespread accumulation of organic matter in this and other similar large depocenters on the mid-Norwegian margin (Bohacs et al., 2005).

In a regional perspective, the OAE 2 is represented by prolific organic-rich deposits relatively close to the study area, documented in the Sverdrup Basin, Galicia margin, Porcupine abyssal plain, and the North Sea (Doré et al., 1997b). On the mid-Norwegian margin, the occurrence of OAE 2 is evident by elevated TOC values and Rock-Eval parameters at the Cenomanian/Turonian boundary in several wells (Table 1). This confirms that OAE 2 stretched into the Norwegian – Greenland seaway and possible into the SW Barents Shelf (Fig. 8). However, the units are thin and condensed, making regional correlations problematic, but also indicate that the occurrence of OAE 2 is not enough for a prolific source rock unit to develop (e.g. Bohacs et al., 2005). The lack of a laterally extensive organic-rich unit on the mid-Norwegian margin, indicate that the extreme sedimentation rates and circulation of oxygenated waters were dominant factors. These factors promoted both severe dilution of the organic matter and biodegradation, which ultimately obstructed source rock development during OAE 2 on the mid- Norwegian margin. This contrasts the well-developed source rock units associated with he OAE 2 in the Sverdrup Basin and Arctic Canada (Leith et al., 1993; Lenniger et al., 2014; Herrle et al., 2015; Nøhr-Hansen et al., 2021). The conceptual model (Fig. 10) outlining the basin configuration, could thus be applicable in rift-basin setting where organic-rich units associated with OAEs are underdeveloped due to extreme sedimentation rates and circulation of oxygenated waters.

5.3. Implications for exploration

Although several of the Lower Cretaceous organic-rich units from the mid-Norwegian margin appear to coincide with global OAEs (e.g. Beil et al., 2020), our data demonstrate that most of these units are thin and strongly condensed or eroded on the terraces and local highs, and have been subject to deep burial. In addition, they accumulated during a period characterized by high sedimentation rates and consequently severe dilution of organic matter in the sediment depocenters. Although petroleum from Lower Cretaceous source rocks have been postulated from producing discoveries (Matapour and Karlsen, 2018), the occurrence of a regionally distributed and economically significant Lower Cretaceous source rock unit has not yet been confirmed. However, we cannot rule out the possibility that some of the Lower Cretaceous organic-rich units in the Vøring Basin once acted as potential sources, particularly in localized fault-bounded basins where the dilution effect and erosion had a limited impact on the preservation of organic matter.

The confirmation of a mature, regionally extensive upper Cenomanian source rock unit will have significant impact on the prospectivity of the deep, marginal basins bordering the North Atlantic Rift System (e.g. Bojesen-Koefoed et al., 2020). In the study area, however, our data shows that the unit has a limited thickness and modest quality (Table 1 and Fig. 9), indicating that it only holds a limited and very localized potential in proximity to intra-basinal highs and ridges. The sparsely drilled deep basins may of course contain thicker organic-rich accumulations holding greater source potential, particularly if the depocenters were subject to recurring anoxic conditions and avoided severe sediment dilution. Only continued exploration and drilling may reveal the presence of a prolific Upper Cretaceous source rock unit in the frontier basins on the mid-Norwegian margin.

6. Conclusions

By combining regional 2D reflection seismic data with wireline logs, total organic carbon (TOC) contents, and Rock-Eval data, this study documents the presence of an upper Cenomanian organic-rich unit in the Vøring Basin. The unit exhibits TOC in the range of 0.18–11.88 wt %, S2 in the range of 0.03–28.06 mg/g and Hydrogen content between 4 and 470 mg HC/g TOC. The unit shows the greatest potential in well 6506/11–3 and 6507/2–3 located on the Sklinna Ridge and Halten Terrace. Samples indicate that the organic-rich unit for the most part is characterized by a kerogen Type III–II composition and is in the immature – early mature stages, thus being capable of generating gas.

The corresponding reflector can be traced across the wider Vøring Basin and correlated to distal exploration wells. The upper Cenomanian organic-rich unit is encountered in well 6705/10–1 on the NW flank of the Vigrid Syncline, where the organic-rich unit exhibit a kerogen Type II composition, possibly indicating periods of basin floor anoxic conditions and locally reduced sedimentation rates.

We suggest that the rifted paleo-basin configuration of the Vøring basin in combination with the global anoxic event at the transition between the Cenomanian - Turonian may have resulted in local accumulations of organic material. The configuration of the margin and the shallow character of the Halten Terrace promoted preservation of organic matter attributed to the development of an extended oxygen minimum zone during OAE 2 and local upwelling of deep oceanic water masses from the Atlantic realm. Moreover, the combination of a eustatic seal-level highstand and high input of terrestrial sediments and organic matter, promoted deposition of the upper Cenomanian organic-rich unit. Several other thin and condensed Lower Cretaceous organic-rich units are present on the Halten Terrace. Although these units commonly exhibit elevated TOC contents, they only hold limited potential due to their meagre thickness, localized distribution, and because they were presumably deposited during a time of severe organic matter dilution due to massive sediment flux into the basin.

The well-developed oceanic conditions between Greenland and Norway were parts of the northern Atlantic Ocean where widespread deposition of organic-rich mudstones associated with the OAE 2 occurred. The rift basin configuration with paleobathymetric barriers partly hindered water mass circulation. In combination with OAE 2, this led to hypoxic to anoxic conditions. Thus, establishing favorable circumstances for preservation of organic matter. The close proximity to the conjugate margins ensured high sedimentation rates, diluting much of the organic-matter. However, areas shielded from the highest sedimentation rates, erosion, and gravity flows, could have facilitated conditions suitable for organic-matter preservation. Such areas occur on the Halten Terrace and in the Vigrid Syncline. Hopefully, this could renew interest and research on global anoxic events on the Norwegian Continental Shelf. Once we have a clear understanding about the dynamic and complex distribution of organic-rich sediments, risk involved in exploration could be significantly reduced.

Declaration of competing interest

The authors declare that they have no known competing financial interests or personal relationships that could have appeared to influence the work reported in this paper.

Data availability

Data will be made available on request.

Acknowledgements

The first author is grateful to Wintershall-Dea for funding this research through a three-year PhD position at UiT - The Arctic University of Norway. The authors are grateful to TGS for allowing to publish their multiclient data. Fredrik Wesenlund is thanked for his guidance in Python and for providing the code to the source rock evaluation plots. The Associate Editor and the anonymous reviewers are gratefully

acknowledged for their comments and suggestions which improved the manuscript.

Appendix A. Supplementary data

Supplementary data to this article can be found online at https://doi.org/10.1016/j.marpetgeo.2023.106102.

References

Abdelmalak, M.M., Planke, S., Faleide, J.I., Jerram, D.A., Zastrozhnov, D., Eide, S., Myklebust, R., 2016. The development of volcanic sequences at rifted margins: new insights from the structure and morphology of the Voring Escarpment, mid-Norwegian Margin. J. Geophys. Res. Solid Earth 121, 5212–5236. https://doi.org/10.1002/2015JB012788.

Adams, D.D., Hurtgen, M.T., Sageman, B.B., 2010. Volcanic triggering of a biogeochemical cascade during oceanic anoxic event 2. Nat. Geosci. 3, 201–204.

Arthur, M.A., Sageman, B.B., 1994. Marine black shales - depositional mechanisms and environments of ancient deposits. Annu. Rev. Earth Planet Sci. 22, 499–551.

Arthur, M.A., Sageman, B.B., 2005. sea-level control on source-rock development: perspectives from the holocene black sea, the mid-cretaceous western interior basin of north America, and the late devonian appalachian basin. In: Harris, N.B. (Ed.), The Deposition of Organic Carbon-Rich Sediments: Models, Mechanisms and Consequences. SEPM Special Publication 82. SEPM, Tulsa, Oklahoma, pp. 35–59.

Arthur, M.A., Schlanger, S.O., 1979. Cretaceous "oceanic anoxic events" as causal factors in development of reef-reservoired giant oil fields. AAPG (Am. Assoc. Pet. Geol.) Bull. 63, 870–885.

Arthur, M.A., Dean, W.E., Schlanger, S.O., 1985. Variations in the global carbon cycle during the cretaceous related to climate, volcanism, and changes in atmospheric CO2. In: Sundquist, E., Broecker, W. (Eds.), The Carbon Cycle and Atmospheric CO2: Natural Variations Archean to Present. Geophysical Monograph Series. 32. American Geophysical Union, Washington D.C., pp. 504–529

Arthur, M.A., Schlanger, S.O., Jenkyns, H.C., 1987. The Cenomanian-Turonian Oceanic Anoxic Event, II. Palaeoceanographic controls on organic-matter production and preservation. In: Brooks, J., Fleet, A.J. (Eds.), Marine Petroleum Source Rocks. Geological Society, London, Special Publications. 26. Blackwell Scientific Publications, London, pp. 401–420.

Arthur, M.A., Dean, W.E., Pratt, L.M., 1988. Geochemical and climatic effects of increased marine organic carbon burial at the Cenomanian/Turonian boundary. Nature 335 (6192), 714–717. https://doi.org/10.1038/335714a0.

Arthur, M.A., Jenkyns, H.C., Brumsack, H.-J., Schlanger, S.O., 1990. Stratigraphy, geochemistry, and paleoceanography of organic carbon-rich Cretaceous sequences. In: Ginsburg, R.N., Beaudoin, B. (Eds.), Cretaceous Resources, Events Rhythms: Background and Plans for Research. NATO ASI Series 304. Kluwer Academic Publishers, Dordrecht, pp. 75–119.

Beil, S., Kuhnt, W., Holbourn, A., Scholz, F., Oxmann, J., Wallmann, K., Lorenzen, J., Aquit, M., Chellai, E.H., 2020. Cretaceous Oceanic Anoxic events prolonged by phosphorus cycle feedbacks. Clim. Past 16, 757–782.

Bell, R.E., Jackson, C.A.-L., Elliott, G.M., Gawthorpe, R.L., Sharp, I.R., Michelsen, L., 2014. Insights into the development of major rift-related unconformities from geologically constrained subsidence modelling: Halten Terrace, offshore mid Norway. Basin Res. 26, 203–224.

Blystad, P., Færseth, R.B., Larsen, B.T., Skogseid, J., Tørudbakken, B., 1995. Structural elements of the Norwegian continental shelf. Part II: the Norwegian Sea Region. Norwegian Petroleum Directorate Bulletin 8, 45p.

Bohacs, K.M., Jr, G.J.G., Carroll, A.R., Mankiewicz, P.J., Miskell-Gerhardt, K.J., Schwalbach, J.R., Wegner, M.B., Simo, J.A.T., 2005. Production, destruction and dilution–the many paths to source-rock development. Soc. Sediment. Geol. 82, 61–101.

Bojesen-Koefoed, J.A., Alsen, P., Bjerager, M., Hovikoski, J., Ineson, J., Nytoft, H.P., Nøhr-Hansen, H., Petersen, H.I., Pilgaard, A., Vosgerau, H., 2020. A mid-Cretaceous petroleum source-rock in the North Atlantic region? Implications of the Nanok-1 fully cored borehole, Hold with Hope, northeast Greenland. Mar. Petrol. Geol. 117, 104414 https://doi.org/10.1016/j.marpetgeo.2020.104414.

Bralower, T.J., Sliter, W.V., Arthur, M.A., Leckie, R.M., Allard, D., Schlanger, S.O., 1993. Dysoxic/anoxic episodes in the aptian-albian (early cretaceous). In: Pringle, M., Sager, W.W., Sliter, W.V., Stein, S. (Eds.), The Mesozoic Pacific: Geology, Tectonics, and Volcanism, vol. 77. American Geophysical Union Monograph, pp. 5–37.

Brekke, H., 2000. The tectonic evolution of the Norwegian sea continental margin with emphasis on the Vøring and More basins. Geological Society, London, Special Publications 167 (1), 327–378. https://doi.org/10.1144/gsl.sp.2000.167.01.13.

Brekke, H., Dahlgren, S., Nyland, B., Magnus, C., 1999. The prospectivity of the Vøring and Møre basins on the Norwegian continental margin. In: Fleet, A.J., Boldy, S.A.R. (Eds.), Petroleum Geology of Northwest Europe: Proceedings of the 5th Conference. Geological Society of London, pp. 231–246.

Brekke, H., Sjulstad, H.I., Magnus, C., Williams, R.W., 2001. Sedimentary environments offshore Norway -An overview. In: Martinsen, O.J., Dreyer, T. (Eds.), Sedimentary Environments Offshore Norway -Palaeozoic to Recent. NPF Special Publication, pp. 7–37.

Calvert, S.E., Bustin, R.M., Ingall, E.D., 1996. Influence of water column anoxia and sediment supply on the burial and preservation of organic carbon in marine shales. Geochem. Cosmochim. Acta 60, 1577–1593.

Cohen, K.M., Finney, S.C., Gibbard, P.L., Fan, J.-X., 2013. The ICS international chronostratigraphic chart. Episodes 36 (3), 199–204.

Cooper, B.S., Barnard, P.C., Telnaes, N., 1995. The kimmeridge clay formation of the North sea. In: Katz, B.J. (Ed.), Petroleum Source Rocks. Casebooks in Earth Sciences. Springer, Berlin, Heidelberg. https://doi.org/10.1007/978-3-642-78911-3_6.

Corfu, F., Polteau, S., Planke, S., Faleide, J.I., Svensen, H., Zayoncheck, A., Stolbov, N., 2013. U-Pb geochronology of cretaceous magmatism on svalbard and Franz Josef land, Barents sea large igneous province. Geol. Mag. 150, 1127–1135.

Dalland, A., Worsley, D., Ofstad, K., 1988. A lithostratigraphic scheme for the Mesozoic and Cenozoic succession offshore mid- and northern Norway. NPD Bulletin 4, 63.

Demaison, G.J., Moore, G.T., 1980. Anoxic environments and oil source bed genesis. AAPG (Am. Assoc. Pet. Geol.) Bull. 64, 1179–1209.

Demaison, G.J., Hoick, A.J.J., Jones, R.W., Moore, G.T., 1983. Predictive source bed stratigraphy: a guide to regional petroleum occurrence. In: Proceedings of the 11th World Petroleum Congress, vol. 2. John Wiley & Sons, Ltd., London, p. 17.

Doré, A.G., Lundin, E.R., Flichler, C., Olesen, O., 1997a. Patterns of basement structure and reactivation along the NE Atlantic margin. J. Geol. Soc. 154, 85–92.

Doré, A.G., Lundin, E.R., Birkeland, Ø., Eliassen, P.E., Jensen, L.N., 1997b. The NE Atlantic Margin: implications of late Mesozoic and Cenozoic events for hydrocarbon prospectivity. Petrol. Geosci. 3, 117–131.

Doré, A.G., Lundin, E.R., Jensen, L.N., Birkeland, Ø., Eliassen, P.E., Fichler, C., 1999. Principal tectonic events in the evolution of the northwest European Atlantic margin, 1. In: Geological Society, London, Petroleum Geology Conference Series, vol. 5. Geological Society of London, pp. 41–61.

Eldrett, J.S., Minisini, D., Bergman, S.C., 2014. Decoupling of the carbon cycle during ocean anoxic event 2. Geology 42 (7), 567–570.

Erba, E., 2004. Calcareous nannofossils and Mesozoic oceanic anoxic events. Mar. Micropaleontol. 52, 85–106. https://doi.org/10.1016/j.marmicro.2004.04.007.

Erbacher, J., Thurow, J., Littke, R., 1996. Evolution patterns of radiolaria and organic matter variations: a new approach to identify sea-level changes in mid-cretaceous pelagic environments. Geology 24 (6), 499–502.

Espitalié, J., Madec, M., Tissot, B., Mennig, J.J., Leplat, P., 1977. Source rock characterization method for petroleum exploration. Paper OTC (Offshore Technology Conference) 2935, 439–444.

Factpages, N.P.D., 2022 [WWW Document] Norwegian Petroleum Directorate, Factpages for exploration wells. https://factpages.npd.no/en/wellbore. (Accessed 15 September 2022). Accessed.

Faleide, J.I., Tsikalas, F., Breivik, A.J., Mjelde, R., Ritzmann, O., Engen, O., Wilson, J., Eldholm, O., 2008. Structure and evolution of the continental margin off Norway and Barents Sea. Episodes 31, 82–91.

Faleide, J.I., Bjørlykke, K., Gabrielsen, R.H., 2015. Geology of the Norwegian Continental Shelf. Chapter 25 from the Book. In: second ed. "Bjørlykke, K Petrol. Geosci.: from Sedimentary Environments to Rock Physics", pp. 603–637.

Færseth, R.B., Lien, T., 2002. Cretaceous evolution in the Norwegian Sea – a period characterized by tectonic quiescence. Mar. Petrol. Geol. 19, 1005–1027. https://doi.org/10.1016/S0264-8172(02)00112-5.

Fjellanger, E., Surlyk, F., Wamsteeker, L.C., Midtun, T., 2005. Upper Cretaceous basinfloor fans in the Vøring Basin, mid Norway shelf. In: Wandas, B.T.G., Nystuen, J.P., Eide, E., Gradstein, F. (Eds.), Onshore-offshore Relationships on the North Atlantic Margin. Proceedings of the Norwegian Petroleum Society Conference, October 2002, Trondheim, Norway. Trondheim.

Garner, L.H., Farrimond, P., Nuzzo, M., 2017. Alternative Source Rocks on the Norwegian Continental Shelf: Potential Cretaceous Sourcing in Deepwater Basins. AAPG/SEG International Conference & Exhibition, London, England. Oct 15 – 18, 2017.

Gernigon, L., Ringenbach, J.-C., Planke, S., Jonquet-Kolsto, H., 2003. Extension, crustal structure and magmatism at the outer Vøring Basin, Norwegian margin. J. Geol. Soc. 160, 197–208. https://doi.org/10.1144/0016-764902-055 (London).

Gernigon, L., Zastrozhnov, D., Planke, S., Abdelmalak, M.M., Maharjan, D., Manton, B., Faleide, J.I., Myklebust, R., 2021. A digital compilation of structural and magmatic elements of the Mid-Norwegian continental margin (version 1.0). Norw. J. Geol.

Graciansky, P.C. de, Brosse, E., Deroo, G., Herbin, J.-P., Müller, C., Sigal, J., Schaaf, A., Montadert, L., 1987. Organic-rich sediments and palaeoenvironmental reconstructions of the cretaceous north Atlantic. In: Brooks, J., Fleet, A.J. (Eds.), Marine Petroleum Source Rocks. Geological Society Special Publication No. 26, pp. 317–344.

Gradstein, F.M., Kaminski, M.A., Agterberg, F.P., 1999. Biostratigraphy and paleoceanography of the Cretaceous seaway between Norway and Greenland. Earth Sci. Rev. 46, 27e98. https://doi.org/10.1016/S0012-8252(99)00018-5.

Gradstein, F.M., Anthonissen, E., Brunstad, H., Charnock, M., Hammer, Ø., Hellem, T., Lervik, K.S., 2010. Norwegian offshore stratigraphic lexicon (NORLEX). Newsl. Stratigr. 44, 73–86.

Hagset, A., Grundvåg, S.A., Badics, B., Davies, R., Rotevatn, A., 2022. Tracing lower cretaceous organic-rich units across the SW Barents shelf. Mar. Petrol. Geol. 140, 105664.

Hansen, L.A.S., Hodgson, D.M., Pontén, A., Thrana, C., Obradors Latre, A., 2021. Mixed axial and transverse deep-water systems: the cretaceous post-rift lysing formation, offshore Norway. Basin Res. 33, 2229–2251. https://doi.org/10.1111/bre.12555.

Haq, B.U., Hardenbol, J., Vail, P.R., 1987. Chronology of fluctuating sea levels since the Triassic (250 million years ago to present). Science 235, 1156–1166.

Heilbron, M., Mohriak, W.U., Valeriano, C.M., Milani, E.J., Almeida, J., Tupinamba′, M., 2000. From collision to extension, the roots of the southeastern continental margin of Brazil. In: Mohriak, W.U., Talwani, M. (Eds.), Atlantic Rifts and Continental Margins, vol. 115. AGU Geophysical Monograph, pp. 1–32.

Herrle, J.O., Schröder-Adams, C.J., Davis, W., Pugh, A.T., Galloway, J.M., Fath, J., 2015. Mid-Cretaceous high arctic stratigraphy, climate, and oceanic anoxic events. Geology 43 (5), 403–406.
Ibach, L.E.J., 1982. Relationship between sedimentation-rate and total organic-carbon content in ancient marine-sediments. AAPG (Am. Assoc. Pet. Geol.) Bull. 66, 170–188.
Isaksen, G.H., Ledje, K.H.I., 2001. Source rock quality and hydrocarbon migration pathways within the greater utsira high area, viking graben, Norwegian North Sea. AAPG (Am. Assoc. Pet. Geol.) Bull. 85, 861–883.
Isaksen, D., Tonstad, K., 1989. A Revised Cretaceous and Tertiary Lithostratigraphic Nomenclature for the Norwegian North Sea. NPD-Bulletin. No 5. http://www.npd.no/en/Publications/NPDbulletins/255-Bulletin-5/.
Jenkyns, H.C., 1980. Cretaceous anoxic events - from continents to oceans. J. Geol. Soc. 137, 171–188.
Jenkyns, H.C., 1999. Mesozoic anoxic events and palaeoclimate. Zbl. Geol. Paläontol. 943–949, 1997.
Jenkyns, H.C., 2003. Evidence for rapid climate change in the Mesozoic-Palaeogene greenhouse world. Philosophical Transactions of the Royal Society A 361, 1885. https://doi.org/10.1098/rsta.2003.1240. –1916.
Jongepier, K., Rui, J.C., Grue, K., 1996. Triassic to Early Cretaceous stratigraphic and structural development of the northeastern Møre Basin margin, off Mid-Norway. Nor. Geol. Tidsskr. 76, 199–214.
Katz, B., 2005. Controlling factors on source rock development—a review of productivity, preservation, and sedimentation rate. Soci. Sed. Geol. 82, 7–16.
Kjennerud, T., Vergara, L., 2005. Cretaceous to palaeogene 3D palaeobathymetry and sedimentation in the Vøring basin, Norwegian sea. Geol. Soc. Lond. Petrol. Geol. Conf. ser. 6, 815.
Klemme, H.D., Ulmishek, G.F., 1991. Effective petroleum source rocks of the World: stratigraphic distribution and controlling depositional factors. AAPG Bull. 75, 1809–1851.
Leckie, R.M., Bralower, T.J., Cashman, R., 2002. Oceanic anoxic events and plankton evolution: biotic response to tectonic forcing during the mid-Cretaceous. Paleoceanography 17, 13-1-29.
Leith, T.L., Weiss, H.M., Mørk, A., Århus, N., Elvebakk, G., Embry, A.F., Brooks, P.W., Stewart, K.R., Pchelina, T.M., Bro, E.G., Verba, M.L., Danyushevskaya, A., Borisov, A.V., 1993. Mesozoic hydrocarbon source rocks of the Arctic region. In: Vorren, T.O., Bergsager, E., Dahl-Stamnes, A., Holter, E., Johansen, Å., Lie, Å., Lund, T.B. (Eds.), Arctic Geology and Petroleum Potential. Elsevier, Amsterdam, pp. 1–25.
Lenniger, M., Nøhr-Hansen, H., Hills, L.V., Bjerrum, C.J., 2014. Arctic black shale formation during cretaceous oceanic Anoxic Event 2. Geology 42, 799–802.
Lien, T., 2005. From rifting to drifting: effects on the development of deep-water hydrocarbon reservoirs in a passive margin setting. Norwegian Sea. Nor. J. Geol./Nor. Geol. Foren. 85 (4).
Løseth, H., Wensaas, L., Gading, M., Duffaut, K., Springer, M., 2011. Can hydrocarbon source rocks be identified on seismic data? Geology 39, 1167–1170.
Lundin, E.R., Doré, A.G., Ronning, K., Kyrkjebo, R., 2013. Repeated inversion and collapse in the late cretaceous-cenozoic northern voring basin, offshore Norway. Petrol. Geosci. 19, 329–341. https://doi.org/10.1144/petgeo2012-022.
Maher, H.D., 2001. Manifestations of the Cretaceous high arctic large igneous province in Svalbard. J. Geol. 109, 91–104.
Maher, H.D., Hays, T., Shuster, R., Mutrux, J., 2004. Petrography of the lower cretaceous sandstones of spitsbergen. Polar Res. 23, 147–165.
Mann, U., Zweigel, J., Øygard, K., Gjeldvik, G., 2002. Source rock prediction in deepwater frontier exploration areas: an integrated study of the Cretaceous in the Vøring Basin. In: Research, S.P. (Ed.), AAPG Hedberg Conference: Hydrocarbon Habitat of Volcanic Rifted Passive Margins, Stavanger, Norway.
Marín, D., Helleren, S., Escalona, A., Olaussen, S., Cedeno, A., Nøhr-Hansen, H., Ohm, S., 2020. The Middle Jurassic to lowermost Cretaceous in the SW Barents Sea: interplay between tectonics, coarse-grained sediment supply and organic matter preservation. Basin Res. 33 (2), 1033–1055. https://doi.org/10.1111/bre.12504.
Martinsen, O.J., Lien, T., Jackson, C., 2005. Cretaceous and Paleogene turbidite systems in the North Sea and Norwegian Sea Basins: source, staging area and basin physiography controls on reservoir development. In: Doré, A.G., Vining, B.A. (Eds.), Petroleum Geology: Northwest Europe and Global Perspectives- Proceedings of the 6th Petroleum Geology Conference, pp. 1147–1164.
Matapour, Z., Karlsen, D.A., 2018. Ages of Norwegian oils and bitumen based on agespecific biomarkers. Petrol. Geosci. 24, 92–101. https://doi.org/10.1144/petgeo2016–119.
Midtkandal, I., Svensen, H.H., Planke, S., Corfu, F., Polteau, S., Torsvik, T.H., Faleide, J.I., Grundvåg, S.A., Selnes, H., Kurschner, W., Olaussen, S., 2016. The aptian (early cretaceous) oceanic anoxic event (0AE1a) in svalbard, Barents Sea, and the absolute age of the barremian-aptian boundary. Palaeogeogr. Palaeocl. 463, 126–135.
Miller, R.G., 1990. A paleoceanographic approach to the kimmeridge clay formation. In: Huc, A.Y. (Ed.), Deposition of Organic Facies, American Association of Petroleum Geologists, Studies in Geology 30, 13–26. https://doi.org/10.1306/St30517C2.
Miller, K.G., Kominz, M.A., Browning, J.V., Wright, J.D., Mountain, G.S., Katz, M.E., Sugarman, P.J., Cramer, B.S., Christie-Blick, N., Pekar, S.F., 2005. The phanerozoic record of global sea-level change. Science 310, 1293–1298. https://doi.org/10.1126/science.1116412.
Nøhr-Hansen, H., Pedersen, G.K., Knutz, P.K., Bojesen-Koefoed, J.A., Sliwinska, K.K., Hovikoski, J., Ineson, J.R., Kristensen, L., Therkelsen, J., 2021. The Cretaceous succession of northeast Baffin Bay: stratigraphy, sedimentology and petroleum potential. Mar. Petrol. Geol. 133 https://doi.org/10.1016/j.marpetgeo.2021.105108.
Papadomanolaki, N.M., Lenstra, W.K., Wolthers, M., Slomp, C.P., 2022. Enhanced phosphorus recycling during past oceanic anoxia amplified by low rates of apatite authigenesis. Sci. Adv. 8 (26) https://doi.org/10.1126/sciadv.abn2370.
Pearce, M.A., Jarvis, I., Tocher, B.A., 2009. The Cenomanian–Turonian boundary event, OAE2 and palaeoenvironmental change in epicontinental seas: new insights from the dinocyst and geochemical records. Palaeogeogr. Palaeoclimatol. Palaeoecol. 280, 207–234. https://doi.org/10.1016/j.pa-laeo.2009.06.012.
Pedersen, T.F., Calvert, S.E., 1990. Anoxia vs productivity - what controls the formation of organic-carbon-rich sediments and sedimentary-rocks. AAPG (Am. Assoc. Pet. Geol.) Bull. 74, 454–466.
Peron-Pinvidic, G., Osmundsen, P.T., 2018. The Mid Norwegian-NE Greenland conjugate margins: rifting evolution, margin segmentation, and breakup. Mar. Petrol. Geol. 98, 162–184.
Peters, K.E., 1986. Guidelines for evaluating petroleum source rock using programmed pyrolysis. AAPG (Am. Assoc. Pet. Geol.) Bull. 70, 318–329.
Peters, K.E., Cassa, M.R., 1994. Applied source rock geochemistry. In: Magoon, L.B., Dow, W.G. (Eds.), The Petroleum System - from Source to Trap. AAPG, pp. 93–120.
Planke, S., Rasmussen, T., Rey, S., Myklebust, R., 2005. Seismic characteriztics and distribution of volcanic intrusions and hydrothermal vent complexes in the Vøring and Møre basins. In: Geological Society, London, Petroleum Geology Conference Series. Geological Society of London, pp. 833–844.
Polteau, S., Hendriks, B.W.H., Planke, S., Ganerød, M., Corfu, F., Faleide, J.I., Midtkandal, I., Svensen, H.S., Myklebust, R., 2015. The early cretaceous Barents sea sill complex: distribution, 40Ar/39Ar geochronology, and implications for carbon gas formation. Palaeogeogr. Palaeoclimatol. Palaeoecol. https://doi.org/10.1016/j.palaeo.2015.07.007.
Prosser, S., 1993. Rift-related Linked Depositional Systems and Their Seismic Expression, vol. 71. Geological Society, London, Special Publications, pp. 35–66.
Ravnås, R., Steel, R.J., 1998. Architecture of marine rift-basin successions. AAPG (Am. Assoc. Pet. Geol.) Bull. 82, 110–146.
Rotevatn, A., Kristensen, T.B., Ksienzyk, A.K., Wemmer, K., Henstra, G.A., Midtkandal, I., Grundvåg, S.-A., Andresen, A., 2018. Structural inheritance and rapid rift-length establishment in a multiphase rift: the East Greenland rift system and its Caledonian orogenic ancestry. Tectonics 37, 1858–1875. https://doi.org/10.1029/2018TC005018.
Saller, A., Lin, R., Dunham, J., 2006. Leaves in turbidite sands: the main source of oil and gas in the deep-water Kutei Basin, Indonesia. AAPG (Am. Assoc. Pet. Geol.) Bull. 90, 1585–1608.
Scaife, J.D., Ruhl, M., Dickson, A.J., Mather, T.A., Jenkyns, H.C., Percival, L.M.E., Hesselbo, S.P., Cartwright, J., Eldrett, J.S., Bergman, S.C., Minisini, D., 2017. Sedimentary mercury enrichments as a marker for submarine large igneous province volcanism? Evidence from the mid-cenomanian event and oceanic anoxic event 2 (late cretaceous). G-cubed 18, 4253–4275.
Schlanger, S.O., Jenkyns, H.C., 1976. Cretaceous oceanic anoxic events: causes and consequences. Geol. Mijnbouw 55, 179–184.
Schlanger, S.O., Jenkyns, H.C., Premoli-Silva, I., 1981. Volcanism and vertical tectonics in the Pacific Basin related to global Cretaceous transgressions. Earth Planet Sci. Lett. 52, 435–449.
Schlanger, S.O., Arthur, M.A., Jenkyns, H.C., Scholle, P.A., 1987. The Cenomanian-Turonian Oceanic Anoxic Event, I. Stratigraphy and distribution of organic carbon-rich beds and the marine δ13C excursion. Geol. Soc. Lond. Spec. Publ. 26 (1), 371–399. https://doi.org/10.1144/GSL.SP.1987.026.01.24.
Schröder-Adam, C.J., Herrle, J.O., Selby, D., Quesnel, A., Froude, G., 2019. Influence of the high arctic igneous province on the cenomanian/turonian boundary interval, Sverdrup Basin, high Canadian arctic. Earth Planet Sci. Lett. 511, 76–88.
Scotese, C.R., Song, H., Mills, B.J.W., van der Meer, D.G., 2021. Phanerozoic paleotemperatures: the earth's changing climate during the last 540 million years. Earth Sci. Rev. 215, 103–503.
Senger, K., Tveranger, J., Ogata, K., Braathen, A., Planke, S., 2014. Late mesozoic magmatism in svalbard: a review. Earth Sci. Rev. 139, 123–144.
Serrano, L., Ferrari, L., Martínez, M.L., Petrone, C.M., Jaramillo, C., 2011. An integrative geologic, geochronologic and geochemical study of Gorgona Island, Colombia: implications for the formation of the Caribbean Large Igneous Province. Earth Planet Sci. Lett. 309 (3–4), 324–336.
Sheriff, R.E., 2002. Encyclopedic Dictionary of Applied Geophysics, fourth ed. Society of Exploration Geophysicists, Tulsa, Okla.
Sinton, C.W., Duncan, R.A., 1997. Potential links between ocean plateau volcanism and global ocean anoxia at the Cenomanian-Turonian boundary. Econ. Geol. 92 (7–8), 836–842.
Skogseid, J., Planke, S., Faleide, J.I., Pedersen, T., Eldholm, O., Neverdal, F., 2000. NE Atlantic continental rifting and volcanic margin formation. In: Nøttvedt, A. (Ed.), Dynamics of the Norwegian Margin. Geological Society Special Publications, pp. 295–326.
Swiecicki, T., Gibbs, P.B., Farrow, G.E., Coward, M.P., 1998. A tectonostratigraphic framework for the mid-Norway region. Mar. Petrol. Geol. 15, 245–276.
Tissot, B.P., Welte, D.H., 1984. From kerogen to petroleum. In: Petroleum Formation and Occurrence. Springer, Berlin Heidelberg, pp. 160–198.
Tissot, B., Deroo, G., Herbin, J.P., 1979. Organic matter in Cretaceous sediments of the North Atlantic: contribution to sedimentology and paleogeography. In: Talwani, M., Hay, W.W., Ryan, W.B.F. (Eds.), Deep Drilling Results in the Atlantic Ocean: Continental Margins and Paleoenvironment, Maurice Ewing Ser., vol. 3. Am. Geophys. Union, Washington, pp. 362–374.
Trabucho-Alexandre, J., Hay, W.W., De Boer, P.L., 2012. Phanerozoic environments of black shale deposition and the Wilson Cycle. Solid Earth 3, 29–42. https://doi.org/10.5194/se-3-29-2012.

Tsikalas, F., Faleide, J.I., Eldholm, O., Wilson, J., 2005. Late Mesozoic-Cenozoic structural and stratigraphic correlations between the Conjugate mid-Norway and NE Greenland continental margins. In: Doré, A.G., Vining, B.A. (Eds.), Petroleum Geology: North-West Europe and Global Perspectives—Proceedings of the 6thPetroleum Geology Conference, pp. 785–801.

Tsikalas, F., Faleide, J.I., Eldholm, O., Blaich, O.A., 2012. The NE Atlantic conjugate margins. In: Roberts, D.G., Bally, A.W. (Eds.), Phanerozoic Passive Margins, Cratonic Basins and Global Tectonic Maps, pp. 141–201.

Tsikalas, F., Faleide, J.I., Kalač, A., 2019. New insights into the Cretaceous-Cenozoic tectono-stratigraphic evolution of the southern Lofoten margin, offshore Norway. Mar. Petrol. Geol. 110, 832–855. https://doi.org/10.1016/j.marpetgeo.2019.07.025.

Turgeon, S.C., Creaser, R.A., 2008. Cretaceous oceanic anoxic event 2 triggered by a massive magmatic episode. Nature 454, 323–327. https://doi.org/10.1038/nature07076.

Tyson, R.V., 2001. Sedimentation rate, dilution, preservation and total organic carbon: some results of a modelling study. Org. Geochem. 32 (2), 333–339.

Vergara, L., Wreglesworth, I., Trayfoot, M., Richardsen, G., 2001. The distribution of Cretaceous and Paleocene deep-water reservoirs in the Norwegian Sea basins. Petrol. Geosci. 7, 395–408.

Wakeham, S., Lee, C., 1993. Production, transport, and alteration of particulate organic matter in the marine water column. In: Engel, M., Macko, S. (Eds.), Organic Geochemistry. Springer US. https://doi.org/10.1007/978-1-4615-2890-6_6, 145–169.

Wenke, A., Ferreira, G.B., Bullimore, S.A., Clark, S.A., Dörner, M., Embry, P., et al., 2021. Unlocking the cretaceous petroleum systems of the Norwegian sea. In: 82nd EAGE Annual Conference & Exhibition. European Association of Geoscientists & Engineers, pp. 1–5. https://doi.org/10.3997/2214-4609.202010949, 2021.

Wesenlund, F., Grundvåg, S.-A., Engelschiøn, V.S., Thießen, O., Pedersen, J.H., 2022. Multi-elemental chemostratigraphy of Triassic mudstones in eastern Svalbard: implications for source rock formation in front of the World's largest delta plain. The Depositional Record 1–36. https://doi.org/10.1002/dep2.182, 00.

Zastrozhnov, D., Gernigon, L., Gogin, I., Abdelmalak, M.M., Planke, S., Faleide, J.I., Eide, S., Myklebust, R., 2018. Cretaceous-paleocene evolution and crustal structure of the northern Vøring margin (offshore mid-Norway): results from integrated geological and geophysical study. Tectonics 37 (2), 497–528.

Zastrozhnov, D., Gernigon, L., Gogin, I., Planke, S., Abdelmalak, M.M., Polteau, S., Faleide, J.I., Manton, B., Myklebust, R., 2020. Regional structure and polyphased Cretaceous-Paleocene rift and basin development of the mid-Norwegian volcanic passive margin. Mar. Petrol. Geol. 115.

Zheng, X.-Y., Jenkyns, H.C., Gale, A.S., Ward, D.J., Henderson, G.M., 2013. Changing ocean circulation and hydrothermal inputs during Ocean Anoxic Event 2 (Cenomanian–Turonian): evidence from Nd-isotopes in the European shelf sea. Earth Planet Sci. Lett. 375, 338–348.

7 Paper III

Source rock evaluation of Hauterivian–Barremian (Early Cretaceous) paralic deposits in Svalbard

Hagset, A.[1], Grundvåg, S.-A.[1,2]*, Wesenlund, F.[1], Badics, B.[3], Thießen, O.[4]

[1] Department of Geosciences, UIT - The Arctic University of Norway, Tromsø, Norway

[2] Department of Arctic Geology, University Centre in Svalbard PO Box 156, N-9171, Longyearbyen, Norway

[3] Wintershall DEA, Stavanger, Norway

[4]*Equinor ASA, Harstad, Norway*

**Corresponding author e-mail: sten-andreas.grundvag@uit.no*

Abstract

On the Barents Shelf, the traditional Middle Triassic and Upper Jurassic organic-rich shales have been subjected to deep burial in the marginal basins and significant uplift on the platform areas. These source rock units are thus either spent or immature over large parts of the shelf. The occurrence of organic-rich units in the Lower Cretaceous succession may represent a feasible alternative to these traditional source rocks. However, there are still large uncertainties regarding the distribution and potential of Lower Cretaceous source rock units. This study investigates and evaluates the source rock potential of Hauterivian – early Aptian paralic strata in Spitsbergen, assigned to the Rurikfjellet and Helvetiafjellet formations. Although these paralics are of no commercial interest and despite their location on the far northwest corner of the shelf, they are interesting because analogous deposits may be present in time-equivalent clinoform packages on the shelf south of Spitsbergen. We thus combine TOC, Rock-Eval, GS-FID and vitrinite reflectance data from 10 outcrop and 25 core samples from these units. Our findings indicate that the organic-rich units in Rurikfjellet and Helvetiafjellet formations mostly display a kerogen Type IV – III composition. The organic matter appears to be of mostly terrestrial origin and was deposited under oxic to sub-oxic conditions, and later subjected to severe biodegradation. The coal samples in the upper part of the Helvetiafjellet Formation have the highest potential with a kerogen Type II/III – III composition and overall high organic content. However, these samples have low hydrogen index values, typical of coals. Thus, their potential as feasible source rocks appear limited.

7.1 Introduction

The occurrence of a thermal mature source rock is essential for a working petroleum system, and thus crucial in hydrocarbon exploration (White, 1993). On the Barents Shelf, the traditional Middle Triassic and Upper Jurassic black shales have been subjected to deep burial in the marginal basins to the west and significant uplift on the platform areas to the east (e.g. Rønnevik et al., 1982; Faleide et al., 1993; Doré, 1995; Grogan et al., 1999; Ohm et al., 2008; Kairanov et al., 2021). Consequently, these desirable source rocks are either exhausted or immature over large parts of the Barents Shelf (Cedeño et al., 2021). Previous well-established exploration models, typically derived from early efforts and experiences in the North Sea where prolific Upper Jurassic black shales occur in half-grabens (e.g. Barnard and Cooper, 1981), are therefore less applicable in this frontier region of the Norwegian Continental Shelf (NCS). This have led research and exploration strategies to focus on alternative source rocks, which have previously been regarded as nonsignificant or even neglected on other parts of the NCS (e.g. Leith et al., 1993; Seldal, 2005; Lerch et al., 2017; Sattar et al., 2017; Hagset et al., 2022). In this respect, the Lower Cretaceous succession, which predominantly consists of thick accumulations of marine mudstones across large parts of the Barents Shelf, represent an interval of particular interest because it may contain multiple potential source rock units (e.g. Ohm et al., 2008; Hagset et al., 2022). Several workers have investigated and discussed the occurrence and likelihood of having viable Lower Cretaceous source rocks on the Barents Shelf (e.g. Leith et al., 1993; Øygard and Olsen, 2002; Lerch et al., 2017; Sattar et al., 2017; Ohm et al., 2008; Hagset et al., 2022), as well as on the mid Norwegian margin (Doré et al., 1997; Brekke et al., 1999; Matapour and Karlsen, 2017; Wenke et al., 2021; Hagset et al., 2023). However, there are still large uncertainties with respect to their lateral and stratigraphic distribution and potential across the NCS. Globally, the Cretaceous is known to be one of the most important stratigraphic intervals for source rock units (Doré et al., 1997; Yang et al., 2014).

On the SW Barents Shelf, Hagset et al. (2022) recently documented the presence of Hauterivian to Barremian organic-rich units which may hold some localized generation potential. These units are typically confined to fault-bounded basins which formed during recurrent rifting along the western shelf margin. In addition, Ohm et al. (2008) previously identified organic-rich mudstones of the Knurr Formation (Berriasian – ?early Barremian) as the most prolific unit of the Lower Cretaceous succession in the Hammerfest Basin. The importance of these source rock units on the northern part of the Barents Shelf, which is unavailable for exploration, are poorly resolved due to the sparsity of subsurface data. However, based on the contrasting paleo-geographic settings between the southwestern and northern Barents Shelf (rifted margin vs low-gradient ramp-type shelf), and the severe amount of uplift and erosion that the entire region experienced during the Cenozoic (e.g.

Lasabuda et al., 2021), they are likely to be of neglectable importance. Anyhow, according to Norwegian authorities, large volumes of unexploited hydrocarbons may be present in the subsurface of the northern Barents Shelf, presumably with Triassic black shales being the most important source rock of the region (NPD, 2017; Wesenlund et al., 2021; 2022). Upper Jurassic and younger organic-rich mudstones are largely expected to be immature. Onshore Svalbard, at the exposed NW corner of the Barents Shelf, an organic-rich mudstone unit, identified at the Barremian – Aptian boundary, have surprisingly shown to have some generation potential. The unit presumably accumulated during a regional flooding event in the early Aptian and may be associated with the Ocean Anoxic Event 1a (Midtkandal et al., 2016; Grundvåg et al., 2019; Thießen and Grundvåg, in prep.). This lower Aptian mudstone unit appears to be gas condensate prone in some onshore wells drilled in relation to a CO_2 sequestration project in central Spitsbergen (Midtkandal et al., 2016; Grundvåg et al., 2019). Moreover, coal seams, which was mined for a brief period during the early 1900's, and organic-rich mudstones in the Barremian – Aptian Helvetiafjellet Formation (e.g. Nemec, 1992; Midtkandal et al., 2007; Grundvåg et al., 2019) may have been the source for non-commercial volumes of dry gas reported in a coal exploration well drilled in the early 1980's in central Spitsbergen (Mackenzie et al., 1983). Apart from these limited and random efforts, there are few, if any, previous contributions which attempt to unravel the generation potential and regional significance of these paralic deposits.

In this paper we investigate a Hauterivian- to Barremian/early Aptian-aged fluvio-deltaic succession in Svalbard, assigned to the uppermost Rurikfjellet and Helvetiafjellet formations. We combine analyses of outcrop and core samples from these units to ascertain their petroleum potential by evaluating and interpreting TOC, Rock-Eval, GS-FID and vitrinite reflectance data. The sedimentology and stratigraphy of the two units, as well as the basin paleo-physiography and evolution are well known (Nemec, 1992; Nemec et al., 1988; Midtkandal et al., 2007; Grundvåg et al., 2017, 2019, 2020; Jelby et al., 2020), which enables us to place our findings in the larger, regional stratigraphic framework of the Lower Cretaceous succession of the NW Barents Shelf. Finally, we discuss implications for petroleum exploration on other parts of the Barents Shelf.

7.2 Geological setting

7.2.1 Study area and geological framework

The study area is located on Spitsbergen, which is the largest island of the Svalbard archipelago (Fig. 7.1). The archipelago represents the uplifted and exposed northwestern corner of the Barents Shelf and have a unique stratigraphic record spanning the Devonian to the Cenozoic (Olaussen et al., 2022). In the Early Cretaceous, Svalbard was part of a larger epicontinental sag basin (Steel and Worsley, 1984; Grundvåg et al., 2017; Midtkandal et al., 2019) situated between 63 – 66 °N (Shephard et al., 2013).

Paralic and shallow marine sediments were deposited on the margins of the subsiding epicontinental basin and was distributed by shelf processes across a regional extensive, southwards-sloping ramp shelf (Midtkandal and Nystuen, 2009; Grundvåg et al., 2020; Jelby et al., 2020). Presently, Lower Cretaceous strata is exposed along the margins of the NNW-SSE oriented Central Tertiary Basin, which formed during Paleogene compressional tectonics (Fig. 7.1). Lower Cretaceous strata is thus dipping steeply or near vertically along the western margin of the basin. While at the eastern and southern margin, the strata dips gently (<3°) towards the southeast (Nemec, 1992).
Although syn-sedimentary collapse features have been identified in the Helvetiafjellet Formation near the Lomfjorden Fault Zone in eastern Spitsbergen (Nemec et al., 1988; Onderdonk and Midtkandal, 2010), and compressional features are reported from the subsurface off Kong Karls Land (Kairanov et al., 2018; Olaussen et al., 2019), the Svalbard Platform was mostly dominated by thermal and sediment load-induced subsidence during the Early Cretaceous, thus being a strong contrast to the rift-basin development reported from the SW Barents Shelf margin (e.g. Faleide et al., 1993; Serck et al., 2017; Marín et al 2018a, b; Hagset et al., 2022). However, significant differential uplift in the Barremian and southward tilting of the shelf, led to subaerial exposure of large parts of the Svalbard Platform, as evident by the regionally extensive erosional unconformity at the base of the Helvetiafjellet Formation (Gjelberg and Steel, 1995; Maher, 2001; Midtkandal et al., 2008; Grundvåg et al., 2017). Moreover, the tilting resulted in an immense sediment flux from the uplifted terrains, forcing a series of clinoform successions to prograde southward onto the Barents Shelf (Grundvåg et al., 2017; Midtkandal et al., 2019). The uplift was also accompanied by widespread igneous activity culminating in the emplacement of the High Arctic Large Igneous Province (HALIP) (Maher, 2001; Senger et al., 2014; Corfu et al., 2013; Polteau et al., 2015). Magmatism was short-lived and sporadic, with apparent peak-activity in the late Barremian - early Aptian (Corfu et al., 2013). In addition, subaerial lava flows interfinger with fluvial sandstone bodies of the Helvetiafjellet Formation on Kong Karls Land (Mørk et al., 1999; Olaussen et al., 2019) and volcanic ashes (i.e. bentonites) occur in the upper part of the Helvetiafjellet Formation in central Spitsbergen (Corfu et al., 2013; Midtkandal et al., 2016), all testifying to the HALIP.

Onwards from the Late Cretaceous through large parts of the Cenozoic, the Svalbard Platform have been subject to recurring uplift and glaciations. Consequently, Upper Cretaceous strata are not present on Svalbard (Dörr et al., 2012; Olaussen et al., 2022).

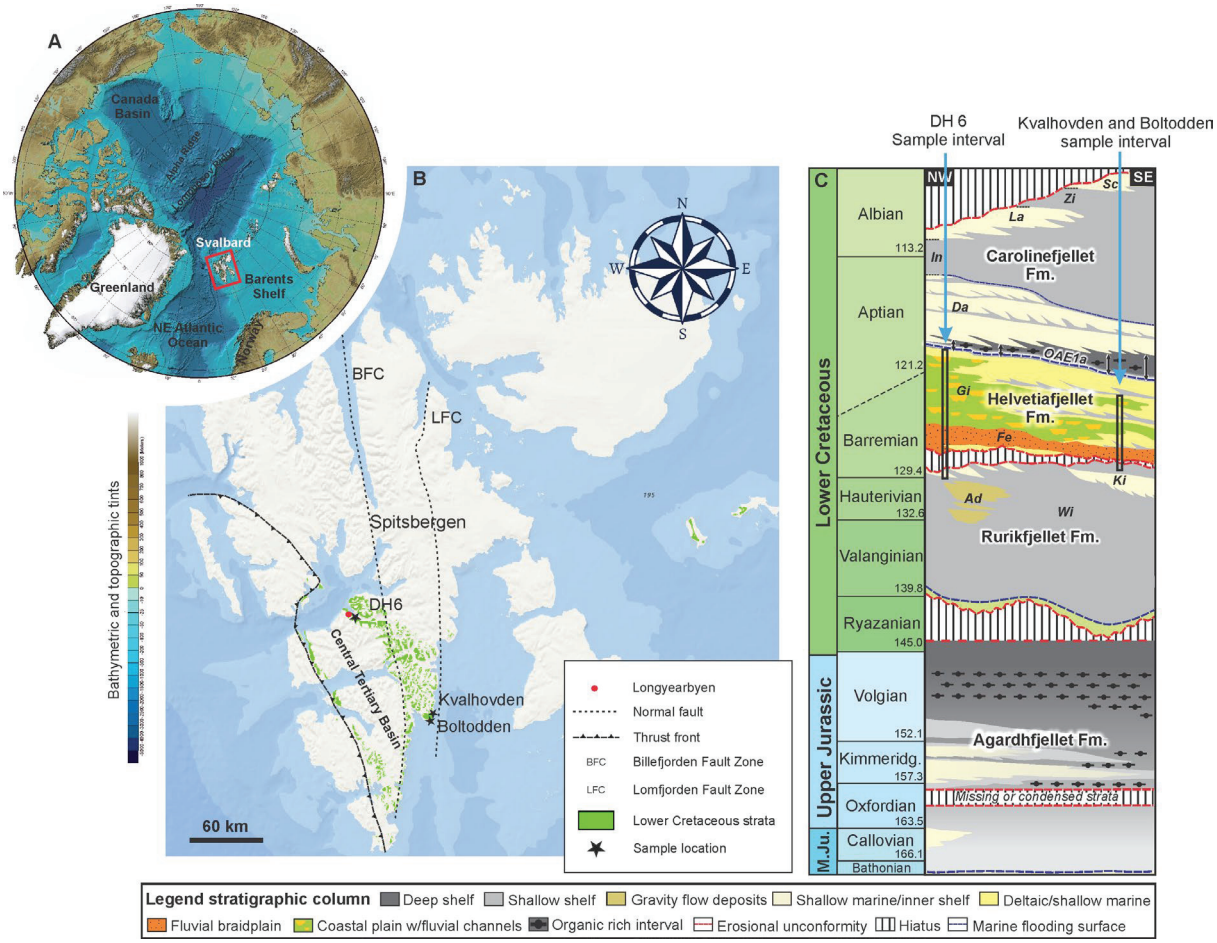

Fig. 7.1 (A) Circumpolar map of the Arctic, indicating the location of the Svalbard archipelago on the northwestern corner of the Barents Shelf (red rectangle). Modified after Jakobsson et al. (2013) (B) Map of Svalbard showing the distribution of Lower Cretaceous strata exposed along the flanks of the Central Tertiary Basin. The location of the DH6 well and the investigated outcrop sections at Kvalhovden and Boltodden is indicated. Modfied from Svalbardkartet Norsk Polarinstitutt (2022). (C) Northwest to southeast-oriented cross-section showing the stratigraphic development of the Lower Cretaceous succession of Spitsbergen. This study only pertains to the uppermost Rurikfjellet Formation and the Helvetiafjellet Formation. Approximate position of the sample interval in well DH6 and the two outcrop locations is indicated in the column. The cross-section is based on Grundvåg et al. (2019, 2020) and modified herein. Abbreviations: Wi: Wimanfjellet Member, Ad: Adventpynten Member, Ki: Kikutodden Member, Fe: Festningen Member, Gi: Glitrefjellet Member, OAE1a: Oceanic Anoxic Event 1a, Da: Dalkjegla Member, In: Innkjegla Member, La: Langstakken member, Zi: Zillerberget member, Sc: Schønrockfjellet member.

7.2.2 Lithostratigraphy and depositional systems

The Lower Cretaceous succession of Svalbard belongs to the Adventdalen Group, which consist of the Middle Jurassic – lowermost Cretaceous Agardhfjellet (see Koevoets et al., 2016; 2019), the Rurikfjellet (Valanginian – lowermost Barremian), the Helvetiafjellet (Barremian – lower Aptian), and the Carolinefjellet (lower Aptian to middle Albian) formations (Parker, 1967; Nagy, 1970; Dypvik et al., 1991a; Mørk et al., 1999; Hurum et al., 2016a; Śliwińska et al., 2020) (Fig. 7.2). This paper focus on the uppermost part of the Rurikfjellet Formation and the overlying Helvetiafjellet Formation.

The up to 200 m thick Rurikfjellet Formation is subdivided into the mudstone-dominated Wimanfjellet Member and the overlying sandstone-rich Kikutodden Member (Midtkandal et al., 2008; Grundvåg et al., 2019, 2020; Jelby et al., 2020). The lower part, which is not dealt with here, was deposited on a moderately deep, open marine shelf, whereas the upper part represents deposition in a storm influenced regressive prodeltaic to shallow marine setting (Dypvik et al., 1991a; Mørk et al., 1999; Grundvåg et al., 2017, 2019; Jelby et al., 2020). A significant lower Barremian subaerial uplift unconformity of regional extent separates the Rurikfjellet Formation from the overlying Helvetiafjellet Formation (Parker, 1967; Steel and Worsley, 1984; Grøsfjeld, 1992; Nemec, 1992; Gjelberg and Steel, 1995; Maher, 2001 Midtkandal and Nystuen, 2009; Grundvåg et al., 2017). As such, the Rurikfjellet Formation represent the early sedimentary response to the uplift event which culminated in the formation of the subaerial unconformity (Grundvåg et al., 2019).

The Helvetiafjellet Formation is 40 – 155 m thick and is subdivided into the lower sandstone-dominated Festningen Member, and the overlying heterolithic and coal-bearing Glitrefjellet Member (Parker, 1967; Midtkandal et al., 2008). The formation is considered to be deposited in a fluvial to paralic setting, and exhibit an upwards increase in marine influence with facies belts showing a retrograding, paleo-landward-stepping (i.e. to the west-northwest) stacking trend (Steel et al., 1978; Nemec et al., 1988; Nemec, 1992; Gjelberg and Steel, 1955; Midtkandal et al., 2007; Grundvåg et al., 2017, 2019).

Of particular interest to this study is the presence of inferred organic-rich lagoonal or interdistributary bay deposits in the uppermost part of the Helvetiafjellet Formation, which is capped by a thick sandstone-dominated barrier sequence in eastern Spitsbergen (Nemec, 1992; Gjelberg and Steel, 1995). The transgressively eroded remnants of this barrier-lagoonal system occur in our study area in central Spitsbergen and is one of the sampled intervals in the investigated well(Grundvåg et al., 2019). In addition, the occurrence of possible organic-rich mudstones restricted to a series of slump scars near the Lomfjorden Fault Zone in eastern Spitsbergen may also be interesting as these mini basins may, theoretically, have promoted restricted, oxygen-deficient conditions (Nemec et al., 1988; Nemec, 1992; Onderdonk and Midtkandal, 2010).

7.3 Material and methods

7.3.1 Data overview

This study includes two sample sets spanning the uppermost Rurikfjellet and the Helvetiafjellet formations. The first set include samples from well DH6 in Adventdalen (central Spitsbergen), which represent Lower Cretaceous strata of the northwestern, inferred proximal (i.e. more paleo-landward)

part of the study area. The second set is from outcrops at Kvalhovden and Boltodden on eastern Spitsbergen, which holds an inferred more distal (basinward) paleo-location (Fig. 7.1). Complete overview and availability of the data is provided in the supplementary files SF1 (Rock-Eval and vitrinite reflectance) and SF2 (Selected GC-FID results). Complete GC-FID and vitrinite reflectance results are available in SF3 on request. In total, 35 samples are included, 25 core samples from well DH6, 8 outcrop samples from Kvalhovden, and 2 from Boltodden. All 35 samples have complete Rock-Eval profiles (Table 1 and SF1). Vitrinite reflectance have been measured for 5 samples (Table 2 and SF1), and 11 samples have a full set of GC-FID results (SF2 and SF3). A summary of key GC-FID results is provided in SF2 and Table 3.

Table 1. Summary of the distribution of the available Rock-Eval data from the uppermost Rurikfjellet and Helvetiafjellet formations at the three specific locations. The Rock-Eval data is available in the supplementary file (SF1) and visualized in Figures 7.4 and 7.5.

Data	Location	Formation (Fm.)	Nr. of plotted samples
Rock-Eval	DH6 (Adventdalen)	Helvetiafjellet Fm.	21
		Rurikfjellet Fm.	4
	Kvalhovden	Helvetiafjellet Fm.	5
		Rurikfjellet Fm.	3
	Boltodden	Helvetiafjellet Fm.	2
		Rurikfjellet Fm.	0

Table 2. Overview of the number of plotted datapoints, including lithology and location for measured and calculated vitrinite reflectance. The dataset is visualized in Figure 7.6 and is available in the online supplementary files SF1 and SF2.

Location	$\%R_o$	%Rc	%Rc (F1)	%Rc (T_{max})
Adventdalen	3 coal	2 coal 1 mudstone	2 coal 1 mudstone	6 coal 4 coaly shale 10 mudstone 4 silty shale
Kvalhovden	1 coal	1 coal 1 silty shale	1 coal 1 silty shale	1 coal 1 coaly shale 1 mudstone 5 silty shale
Boltodden	1 coaly shale	2 coaly shale	2 coaly shale	2 coaly shale

Table 3. Summary of the key GC-FID results from the 11 samples from well DH6, Kvalhovden and Boltodden. See Figures 7.7 to 7.11 for visualization and analysis.

Location	Formation	Sample	Lithology	Pr/Ph ratio	Wax	CPI 2	Pr/n-C17	Ph/n-C18	δ^{13}C-Aro	δ^{13}C-Sat	CV	Ts/(Ts+Tm)	∑(C23tri to C29tri)/30ab	%C27	%C28	%C29	%20S	%ββ
Adventdalen, Well DH6	Helvetiafjellet Fm.	DH6_34	Coal	4.89	0.75	1.09	0.44	0.09	-25	-28.8	5.71	18.93	0.077	23.48	22.28	54.24	60.66	50.14
		DH6_29	Coal	4.8	0.67	1.05	0.76	0.14	-25	-26.5	-0.10	29.30	0.020	7.69	20.42	71.89	53.53	53.71
		DH6_24	Mudstone	3.13	0.55	1.09	0.53	0.16	-25.3	-27.5	1.75	36.72	0.050	17.31	19.60	63.09	58.08	57.72
Kvalhovden	Helvetiafjellet Fm.	S1	Coal	2.02	0.92	1.19	0.33	0.16	-24.7	-27.9	4.10	54.11	2.964	36.44	28.06	35.50	50.38	60.18
		S3	Coaly shale	1.69	0.71	1.03	0.22	0.13	-25.3	-27.5	1.75	N/A	N/A	N/A	N/A	N/A	N/A	N/A
		S4	Mudstone	1.4	0.73	1.05	0.25	0.17	-25.4	-28	2.80	N/A	N/A	N/A	N/A	N/A	N/A	N/A
		S7	Silty shale	2.58	0.73	1.03	0.21	0.08	-24.8	-28.5	5.39	46.81	2.641	38.20	28.50	33.30	55.99	36.52
	Rurikfjellet Fm.	RF1	Silty shale	1.24	0.79	1.05	0.21	0.15	-24.6	-28.9	6.85	N/A	N/A	N/A	N/A	N/A	N/A	N/A
		RF2	Silty shale	1.4	0.78	1.05	0.18	0.11	-24.9	-28.8	5.93	N/A	N/A	N/A	N/A	N/A	N/A	N/A
Boltodden	Helvetiafjellet Fm	S5-FW	Coaly shale	5.66	0.65	1.01	2.48	0.43	-25.5	-28.7	4.35	9.47	0.016	6.48	25.84	67.68	51.61	51.04
		S6-FW	Coaly shale	4.88	0.55	1.12	2.48	0.47	-25	-29.4	7.23	7.17	0.026	6.22	11.94	81.84	52.50	49.58

7.3.2 Outcrop and well data

Outcrop samples S3, S4, S5, S6, and S7 were sampled from a mudstone dominated section in the Helvetiafjellet Formation, immediately above the Festningen Member at the Kvalhovden locality (Fig. 7.2A, B and C). At this location, the sandstones of the Festningen Member have been involved in a paleo-landslide and consequently occur as a series of partly rotated and rafted sandstone blocks (see Nemec et al., 1988; Onderdonk and Midtkandal, 2010). The sampled interval represents prodelta deposits which built into and eventually healed the slump scar (Nemec et al., 1988; Fig. 7.2A and B). Sample S4 is in the central and lowermost exposed part of the mini basin/slump scar infill (Fig. 7.2D), whereas the other samples occur stratigraphically higher where the prodelta deposits onlap and drape a slump block of the Festningen Member. Sample S1 was collected from a thin coal seam (< 30 cm) which prior to the slump event originally capped and defined the top of the Festningen Member at this location (Fig. 7.2E). Samples RF2 and RF3 was collected from mudstone interbeds in the uppermost sandstone rich Rurikfjellet Formation (i.e. the Kikutodden Member), directly below the Festningen Member at the same locality, albeit slightly to the north (Fig. 7.2F). These mudstones occur within a 10 m thick coarsening-upward unit interpreted to represent a prograding prodelta to delta front deposit (see figure 5 of Nemec et al., 1988 for a detailed description of this unit). At Boltodden, Samples S6 FW and S5 FW were collected in the middle of the Glitrefjellet Member in the mudstone-dominated lower part of an 8 m thick coarsening-upward unit which previously have been interpreted to represent a prograding mouthbar deposit (Fig. 7.2G; see Hurum et al 2016b for more information of these deposits). It is therefore inferred that the sampled mudstones accumulated in a sheltered interdistributary bay setting.

Multiple core samples of the Helvetiafjellet Formation have been analyzed from well DH6 located in Adventdalen (Fig. 7.1). The approximate position of some selected samples is indicated in the core-photos in Figure 7.3. The samples consist of mudstones, coaly shales and thin coals, and were largely deposited in various coastal plain/terrestrial sub-environments (i.e. the samples labeled DH6_28 to DH6_43; Grundvåg et al., 2019). The exception is the four uppermost samples of the Helvetiafjellet Formation (samples DH6_24 to DH6_27). These mudstones were collected from an interval (level c. 121–131.5 m; Fig. 7.5) which appears to have been deposited in a more marine-influenced setting and testify to the paleo-landward (W/NW) retreat of a barrier-lagoon system and the final drowning of the Helvetiafjellet Formation coastal plain (Grundvåg et al., 2019). The sample set from well DH6 also includes four mudstone samples from the uppermost part of the Rurikfjellet Formation (samples DH6_44 to DH6_47). In central Spitsbergen, this part of the Rurikfjellet Formation represents open marine, storm-dominated shelf to prodelta deposits (see Jelby et al., 2020).

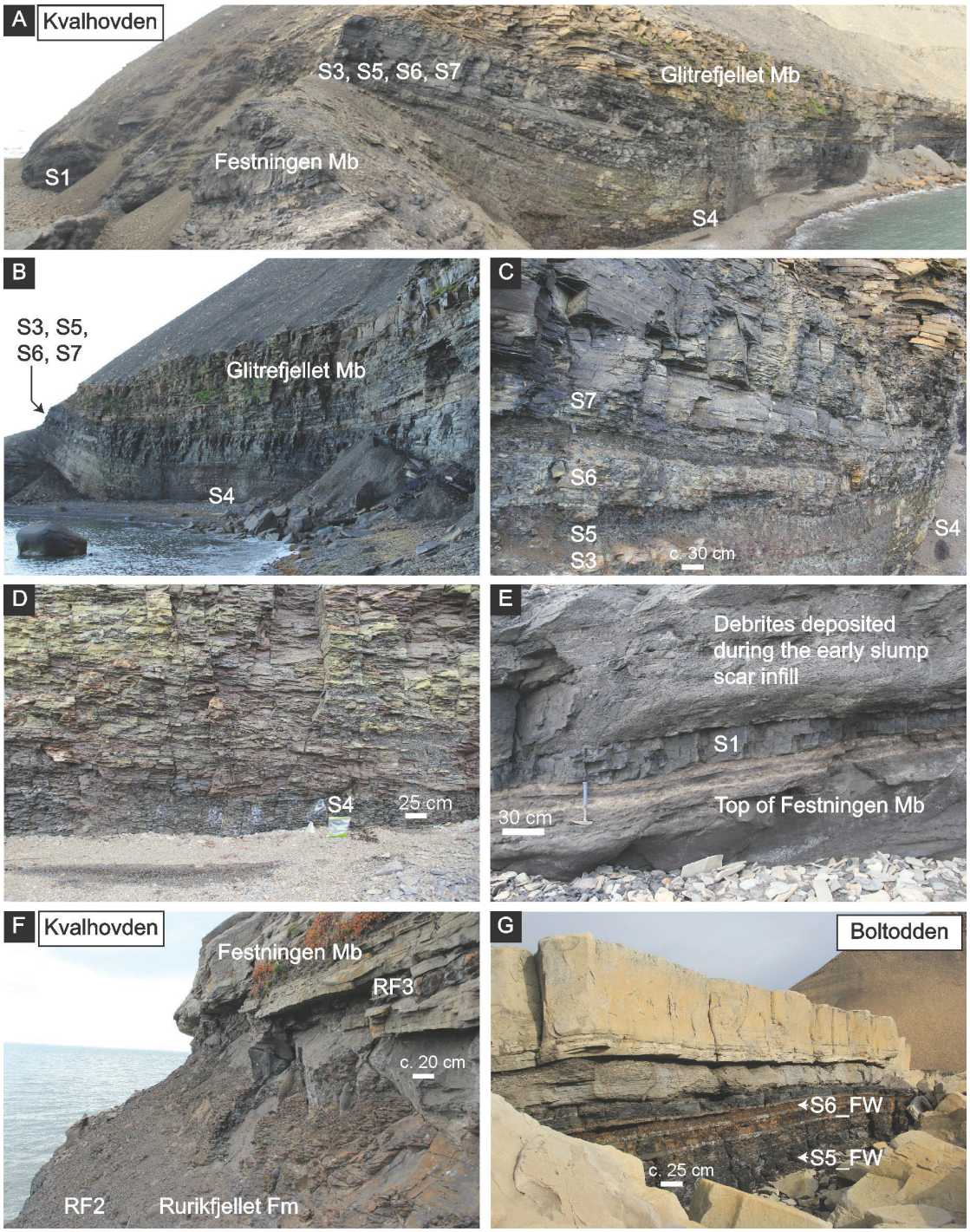

Fig. 7.2 Overview of the outcrop sections and sample locations. (A) Panorama photo of the Kvalhovden locality showing the stratigraphic position of outcrop samples S1, S3, S4, S5, S6, and S7, all collected in the Helvetiafjellet Formation. The onlap relation between a slump block consisting of fluvial sandstones, assigned to the Festningen Member, and deltaic deposits of the Glitrefjellet Member is clearly visible. (B) Photo of the same locality as shown in (A) but from another angle. Note the coarsening upward trend in the Glitrefjellet Member deltaics. These deposits represent a delta system which built into and eventually filled a collapse scar. (C) Close-up photo of the section where samples S3, S5, S6 and S7 was collected. (D) Close-up photo of the section where Sample S4 was collected. This section holds a more central position within the slump scar 'mini basin' and is dominated by silty shales. (E) Photo showing the coal seam where Sample S1 was collected atop the Festningen Member. (F) Photo of the Kvalhovden locality showing the stratigraphic position of samples RF2 and RF3 in the uppermost Rurikfjellet Formation. (G) Photo of the Boltodden locality showing the mouthbar unit in which samples S5_FW and S6_FW was collected. The mouthbar unit is assigned to the middle part of the Glitrefjellet Member and occur stratigraphically above the slump scar infill at Kvalhovden.

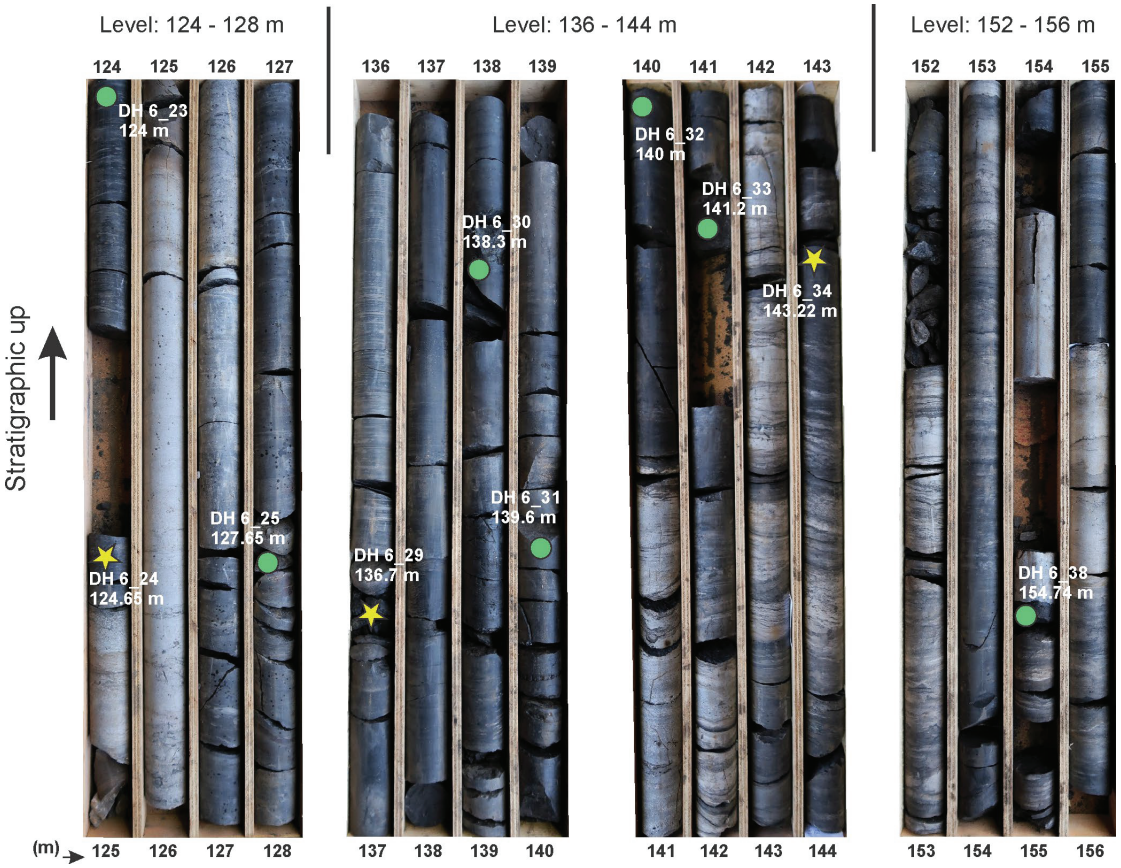

Fig. 7.3 Selected core photos from well DH6, showing the heterolithic character of the Glitrefjellet Member of the Helvetiafjellet Formation. The stratigraphic position for a few selected samples are indicated. Samples indicated by a star have both GC-FID and Rock-Eval data, whereas samples indicated by green circles only have Rock-Eval data.

7.4 Results

7.4.1 Total organic carbon and pyrolysis

The samples show a broad range in kerogen richness, exemplified by the TOC content (1.11–89.40 wt. %) and the S2 parameter acquired from pyrolysis (0.46–211.61 mg HC/g rock) (Fig. 7.4A). These parameters indicate present-day kerogen types III–IV for most samples (Fig. 7.4). This includes all samples from the Kvalhovden and Boltodden locality, and the samples consisting of siltstone or mudstone lithologies in well DH6, independent of which formation the samples were collected from (Fig. 7.4; Table 1). In contrast, samples consisting of coaly shale or coal, all belonging to the Helvetiafjellet Formation in well DH6, display a present-day kerogen Type II/III (Fig. 7.4A and B; Table 1).

The samples from the Kvalhovden locality show a higher average T_{max} value for the Rurikfjellet (484.6 °C) and Helvetiafjellet formations (479.6°C) compared to the average T_{max} values taken from the same formations at the Boltodden (Helvetiafjellet Formation: 442.5°C) and Adventdalen localities

(Rurikfjellet Formation: 453.7 °C. Helvetiafjellet Formation: 449.2 °C) (Fig. 7.4B). Samples belonging to the Rurikfjellet and Helvetiafjellet formations from the Kvalhovden locality display the greatest OI values (4–19 mg CO_2 /g TOC), while the Helvetiafjellet Formation coals from DH6 in Adventdalen show the lowest OI values (0–1 mg CO_2 /g TOC). For all the samples, the oxygen index (OI) parameter generally exhibits an inverse proportional relationship with the hydrogen index (HI) (Fig. 7.4C).

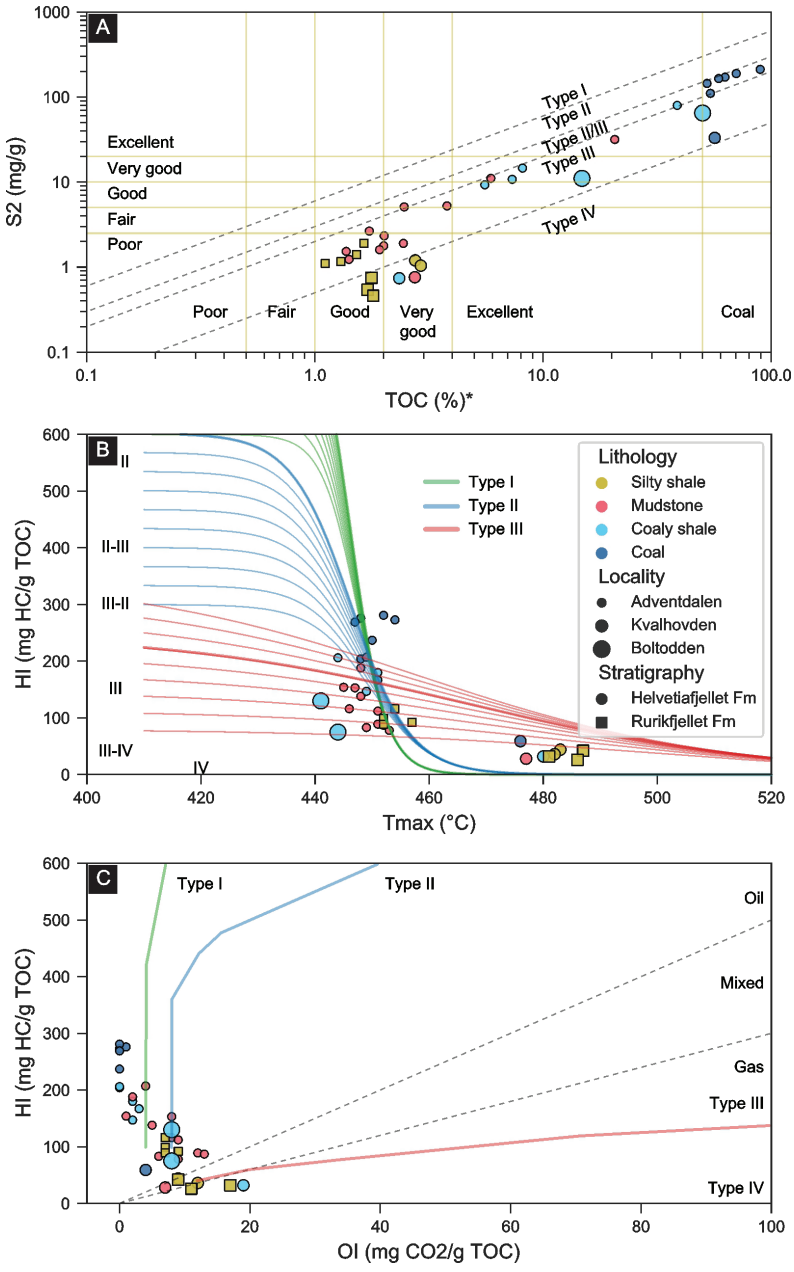

Fig. 7.4 Binary plots of total organic carbon (TOC) and pyrolysis-derived parameters. (A) S_2 vs. TOC. The source potential lines (solid) and kerogen lines (dashed) are adapted from Peters and Cassa (1994). (B) HI vs. Tmax. The thick kerogen lines shown in green, blue and red represent calculated kerogen maturation pathways from Banerjee et al. (1998), fitted from kerogen maturation pathways initially reported by Bordenave (1993). The thinner lines shows varying kerogen maturation pathways variation with varying initial HI. (C) HI vs. OI. The kerogen lines (solid) and resulting petroleum product lines (dashed) are adapted from Dembicki (2009).

Figure 7.5 shows a geochemical log panel of TOC, S2, production index (PI = S1/[S1+S2]), HI and OI correlated with a lithostratigraphic log from Adventdalen (well DH6). The TOC content and the pyrolysis products of the four silty mudstone samples of the Rurikfjellet Formation are similar to those from the mudstone facies of the Helvetiafjellet Formation. The lowermost ~16 m of the Helvetiafjellet Formation consists of sandstones assigned to the Festningen Member. The boundary to the overlying Glitrefjellet Member is defined as the base of the coal bed at ~174 m depth. The Helvetiafjellet Formation thus exhibits an upwards increase in kerogen richness and quality in correspondence to the upwards increase in the abundance of finer-grained lithofacies up until the uppermost ~10 m. The PI values of the sample set range from 0.02–0.22 and vary significantly between lithofacies, being substantially lower in the coal samples (mean 0.02 ± 0.01) relative to the mudstones (mean 0.13 ± 0.04) and the silty shales (mean 0.16 ± 0.04).

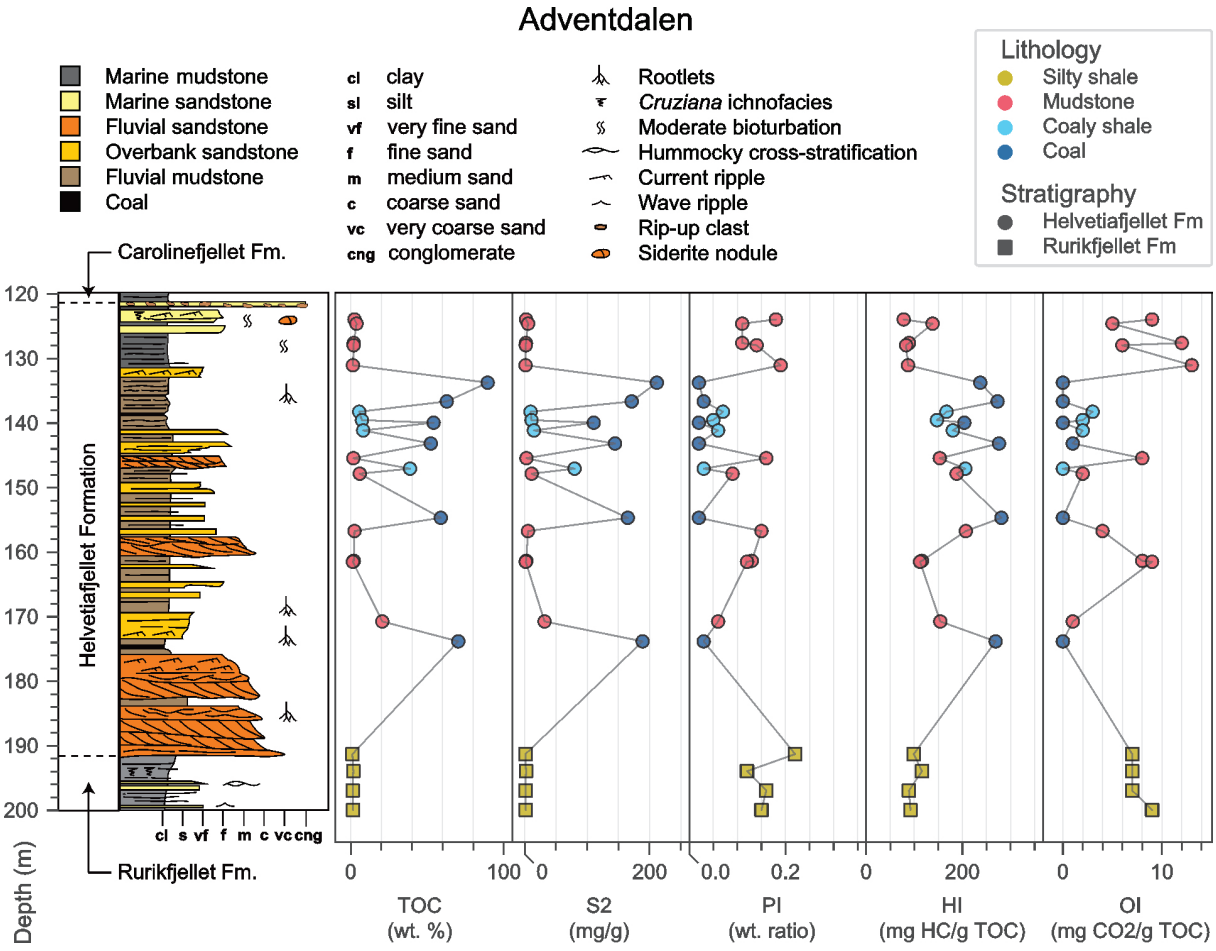

Fig. 7.5 Simplified sedimentary log of the sampled interval in well DH6 (i.e. the uppermost Rurikfjellet and the Helvetiafjellet formations) accompanied by TOC and pyrolysis-derived parameters. The sedimentary log and interpreted depositional environments are adapted from Grundvåg et al. (2019). Note that the uppermost part of the Helvetiafjellet Formation is dominated by shallow to marginal marine deposits (i.e. the uppermost four mudstone samples; interval c. 121-131.5 m).

7.4.2 Measured and calculated vitrinite reflectance

The Adventdalen and Boltodden localities show measured vitrinite reflectance (%Ro) values of 0.75–0.77 and 0.66 respectively, while the sample from the Kvalhovden locality has a notably higher %Ro value of 1.50. Sorted by locality, the calculated vitrinite values (%Rc; after Radke, 1988) from the methylphenantrene ratio (MPR; after Radke et al., 1982), methylphenantrene distribution fraction 1 (F1; after Kvalheim et al., 1987) and T_{max} show a comparable relationship as the measured values (Fig. 7.6). For the Kvalhovden locality, %Rc (MPR), %Rc (F1) and %Rc (T_{max}; after Jarvie et al., 2001) ranges from 1.61–1.62, 1.54–1.54 and 1.41–1.61, respectively, comparable to the measured vitrinite value (%Ro = 1.50). However, the samples from the Adventdalen and Boltodden localities show %Rc (MPR), %Rc (F1) and %Rc (T_{max}) ranging from 0.88–1.08, 0.84–1.00 and 0.78–1.07, respectively, and are thus overestimated relative to the measured vitrinite reflectance values (0.66–0.77) from this locality (Fig. 7.6).

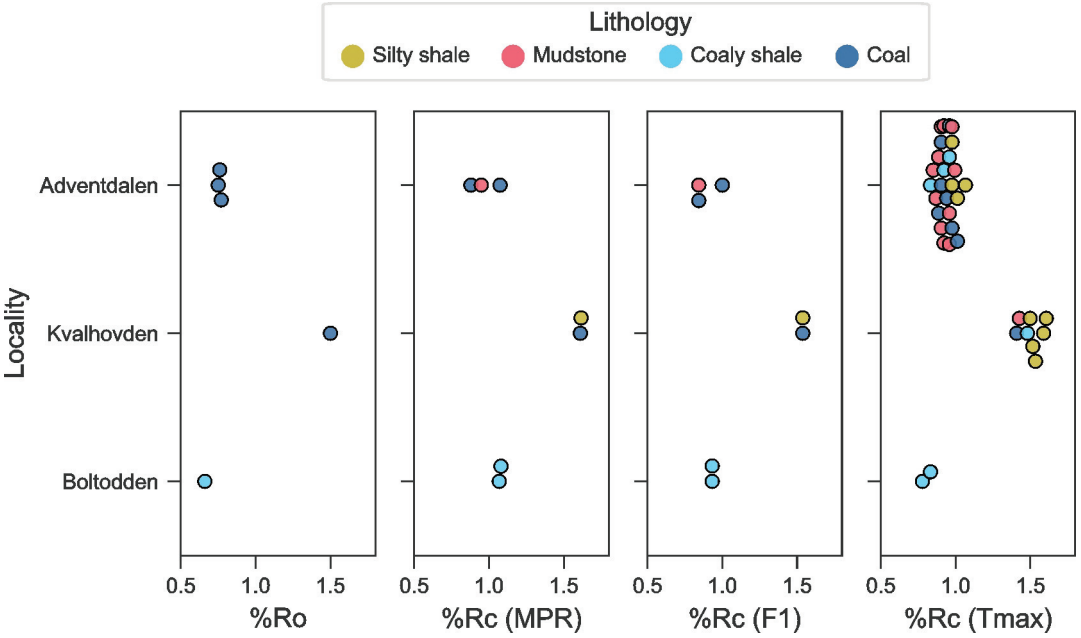

Fig. 7.6. Swarmplots of measured and calculated vitrinite reflectance parameters. (A) Measured vitrinite reflectance (B) Calculated vitrinite reflectance from MPR, adapted from Radke (1988), originally modified from Radke et al. (1982). (C) Calculated vitrinite reflectance from F1, adapted from Kvalheim et al. (1988). (D) Calculated vitrinite reflectance from Tmax, adapted from Jarvie et al. (2001). An overview of the dataset is provided in Table 2. Details are available in the online supplementary files SF1 and SF2.

7.4.3 n-alkanes, acyclic isoprenoids and stable carbon isotopes

The GC-FID chromatograms are generally unimodal with medium chain *n*-alkanes (within the range $C_{12}H_{26}$ to $C_{22}H_{46}$) being the most abundant for each sample (Fig. 7.7). The carbon preference index 2 (CPI2; after Marzi et al., 1993) shows an odd-over-even carbon preference (1.01–1.19, mean 1.07 ± 0.05) with no clear grouping based on lithostratigraphic unit or locality. The samples show variable

waxiness as expressed by the *n*-C_{17}/(*n*-C_{17} + *n*-C_{27}) ratios (0.55–0.92, mean 0.71 ± 0.11) (Fig. 7.7). For the analyzed samples from the Adventdalen and Kvalhovden localities, the Pr/n-C_{17} ratios vs Ph/n-C_{18} ratios indicate that the bitumen was generated from mostly terrigenous sources deposited within oxidizing depositional environments (Fig. 7.8). In contrast, the bitumen in the more mature Kvalhovden appears to have originated from mixed organic sources.

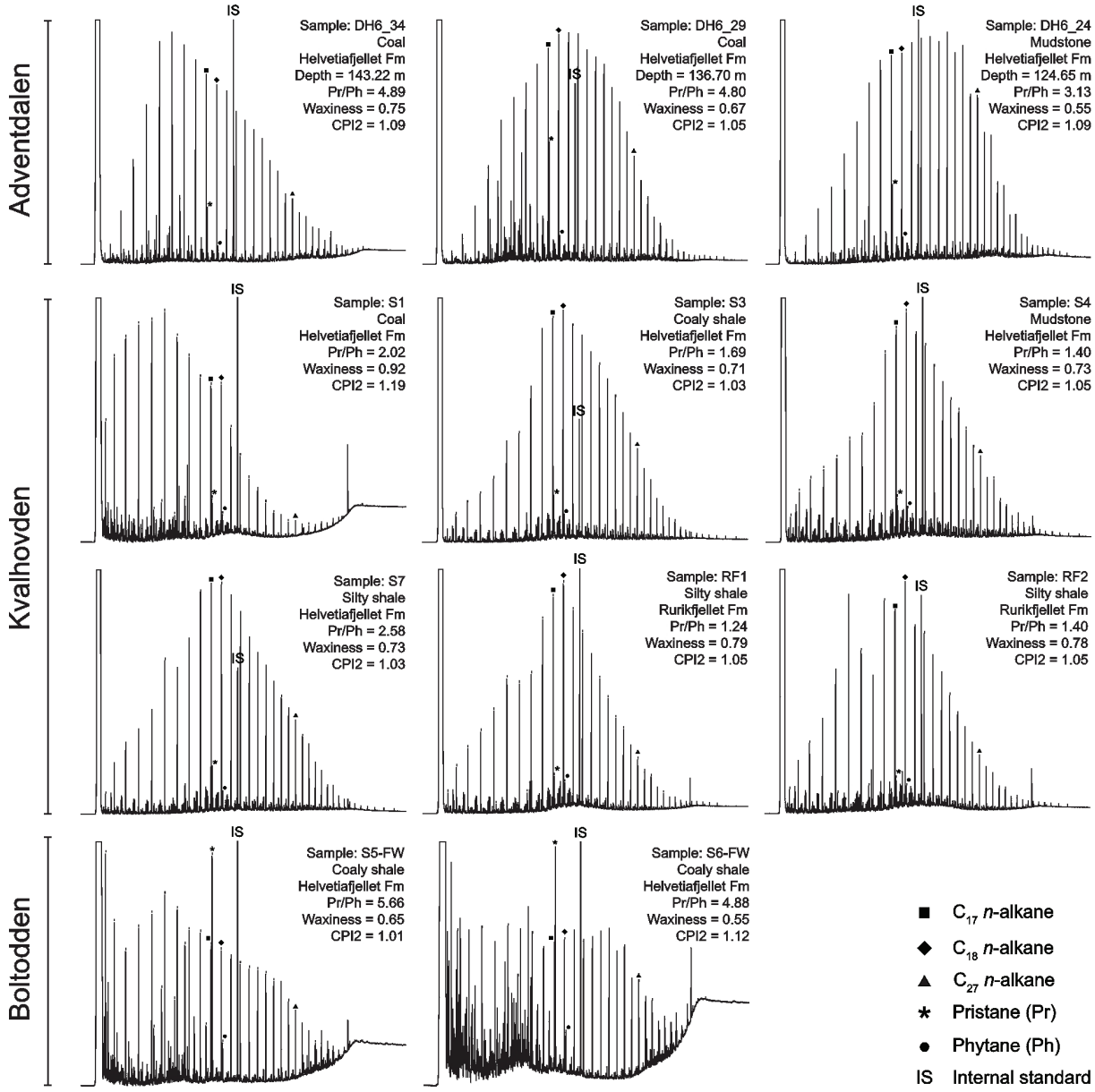

*Fig. 7.7 GC-FID chromatograms of selected samples of various lithologies. Pr/Ph = Pristane/Phytane. Waxiness = n-C_{17}/(n-C_{17} + n-C_{27}), CPI2 = ((C_{23} + C_{25} + C_{27}) + (C_{25} + C_{27} + C_{29}))/(2 * (C_{24} + C_{26} + C_{28})), where C represents the carbon number of the n-alkanes. See main text for discussion.*

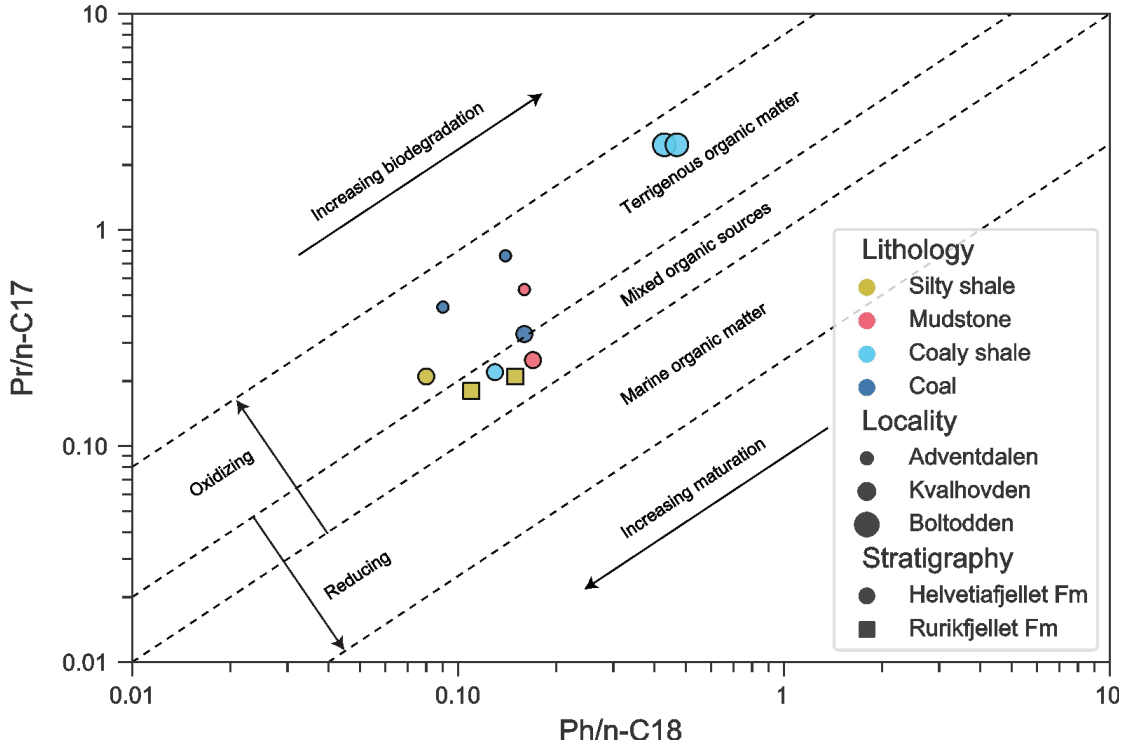

Fig. 7.8 Binary plot of Pr/n-C_{17} vs. Ph/n-C_{18} of selected samples. The data is indicating that the organic matter is mainly of terrestrial origin, deposited in a oxygenated environment. The plot is adapted from Shanmugam (1985).

A plot of $\delta^{13}C_{sat}$ vs $\delta^{13}C_{aro}$ isotope fractions of the extracts is shown in Figure 7.9. The range of these ratios (-29.4 ‰ to -26.5 ‰ and -25.5 ‰ to -24.6 ‰, respectively) indicate that the bitumen was dominantly sourced from terrigenous organic matter (Fig. 7.9A), resulting in a canonical variable (CV) greater than 0.47 for all but one extract (mean 4.16 ± 2.35) (Fig. 7.9B). The Pr/Ph ratios (mean 3.06 ± 1.69) are overall high, however, those derived from the Kvalhovden samples (1.24–2.58) are clearly lower than those from the Boltodden (4.88–5.66) and Adventdalen (3.13–4.89) localities (Fig. 7.9B).

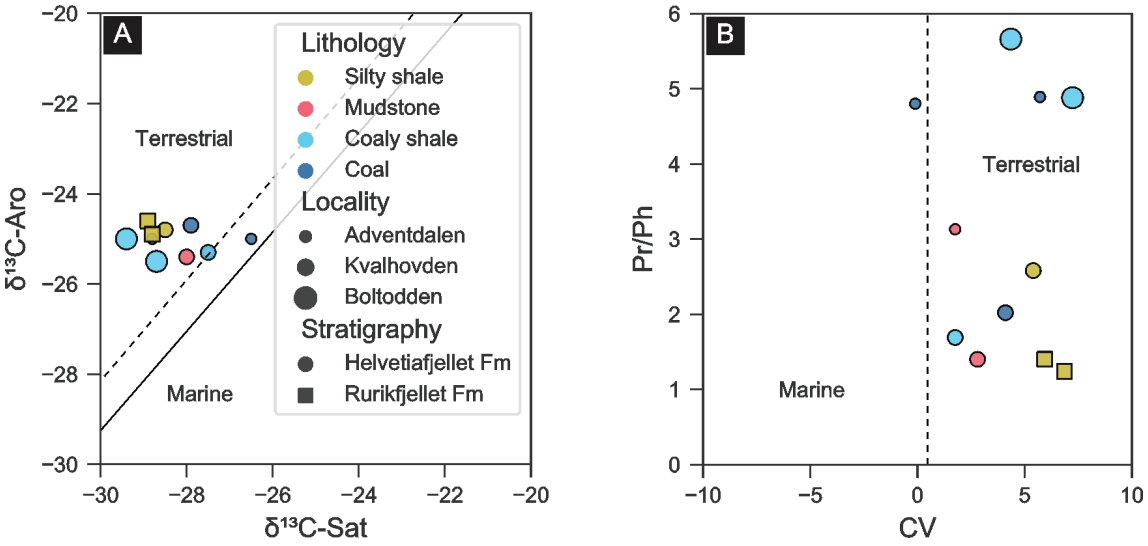

Fig. 7.9 (A) $\delta^{13}C_{Aro}$ vs. $\delta^{13}C_{Sat}$ plot indicating source input. The dashed and solid lines are adapted from Sofer (1984) and are used to demarcate bitumen that have dominantly marine or terrestrial source input. (B) The canonical variable (CV) plotted vs. Pr/Ph. The CV is adapted from Sofer (1984). Both plots demonstrates the predominance of terrestrial sources in both the investigated formations.

7.4.4 Terpanes and steranes

Figure 7.10 shows the m/z 191 fragmentograms for the extracts using a retention time window ranging from 19tri to the C35 homohopanes. These fragmentograms clearly display that 30ab is commonly the tallest peak among the identified biomarkers, yielding a Σ(23tri to 29tri)/30ab ≥ 0.08 for all samples excluding the two from the Kvalhovden locality, which on the other hand show significantly greater ratios (2.64 and 2.96). These two samples express a noisier baseline as a result of lower biomarker signal response (Fig. 7.10). Similarly, the %27Ts (Ts/[Ts+Tm]*100; adapted from Seifert and Moldowan, 1978) ratios of the samples from the Boltodden and Adventdalen localities show notably lower ratios (7.17–36.72%), while the two Kvalhovden samples are notably higher (46.81 % and 54.11 %).

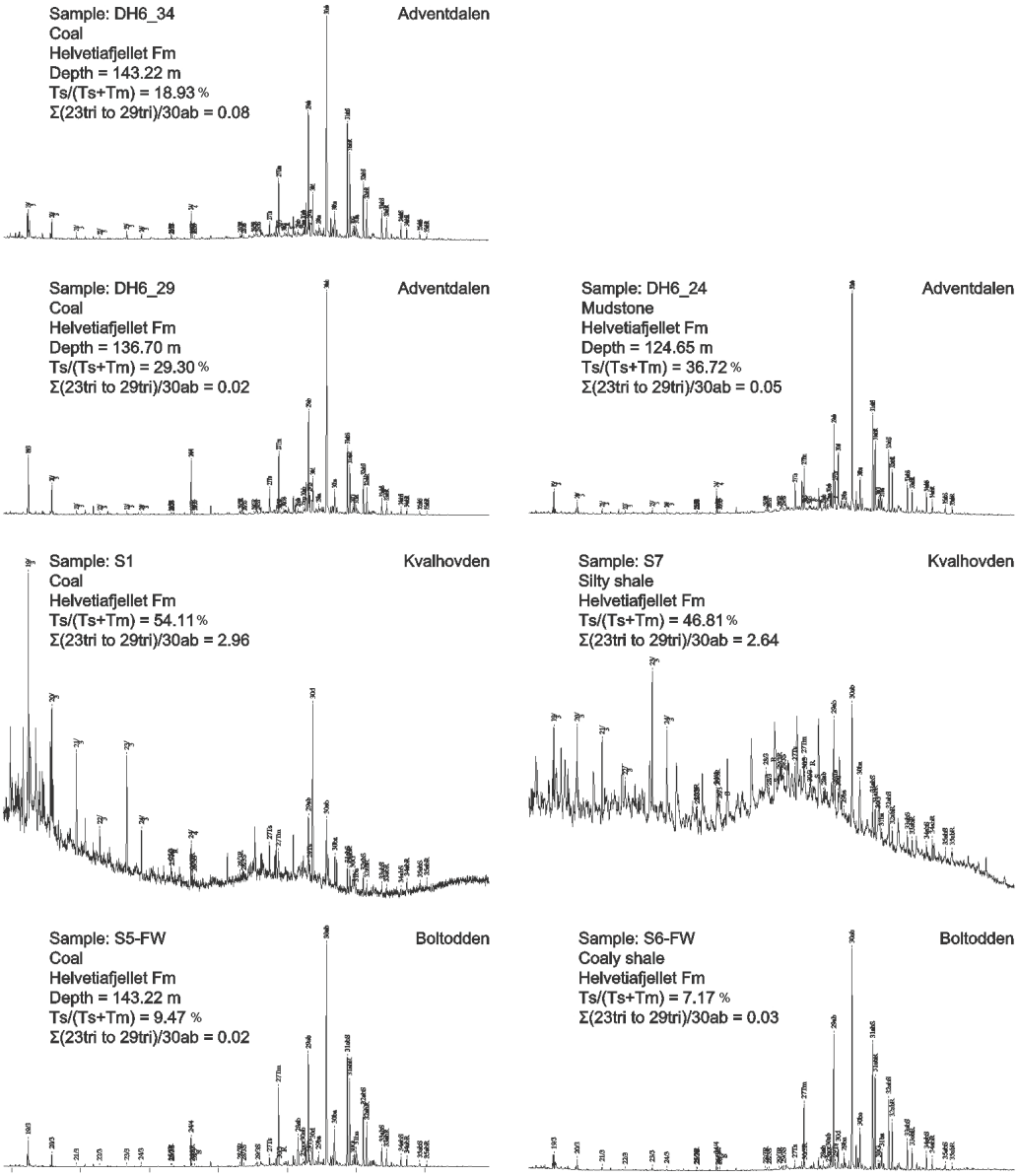

Fig 7.10 m/z 191 fragmentograms of selected samples. Samples S1 and S7 from the Kvalhovden locality have a low biomarker signal response, resulting in generally noisier baselines. See main text for discussion. For a full reference of the abbreviated labels of the biomarker compounds, see Weiss et al. (2000). Ts/(Ts+Tm) is adapted after Seifert and Moldowan (1978). Σ(23tri to 29tri)/30ab is adapted after Peters et al. (2005).

The C_{27}, C_{28} and C_{29} ββ -sterane distribution indicate that terrigenous organic matter has the most important influence on all samples, as expected for coals and coaly shales (Fig. 7.11). However, sample S1 (coal) belonging to the Helvetiafjellet formation from Kvalhovden locality, show an open marine–estuarine signature based on their ββ sterane distribution that does not agree with its lithology (Fig. 7.11). Sample S7 (silty shale) display similar ββ sterane distribution values as S1 (Fig. 7.11). However, an open marine-estuarine setting is more likely for sample S7, as this silty shale originates from the lower part of the slump-scar infill at Kvalhovden. Furthermore, the %20S (50.38–60.67 %)

and %ββ (36.52–60.18 %) maturity ratios show that the isomerization threshold has been reached for all samples, indicating that the bitumen extracted for these samples have reached a minimum thermal maturity corresponding to the early mature oil window (Fig. 7.11).

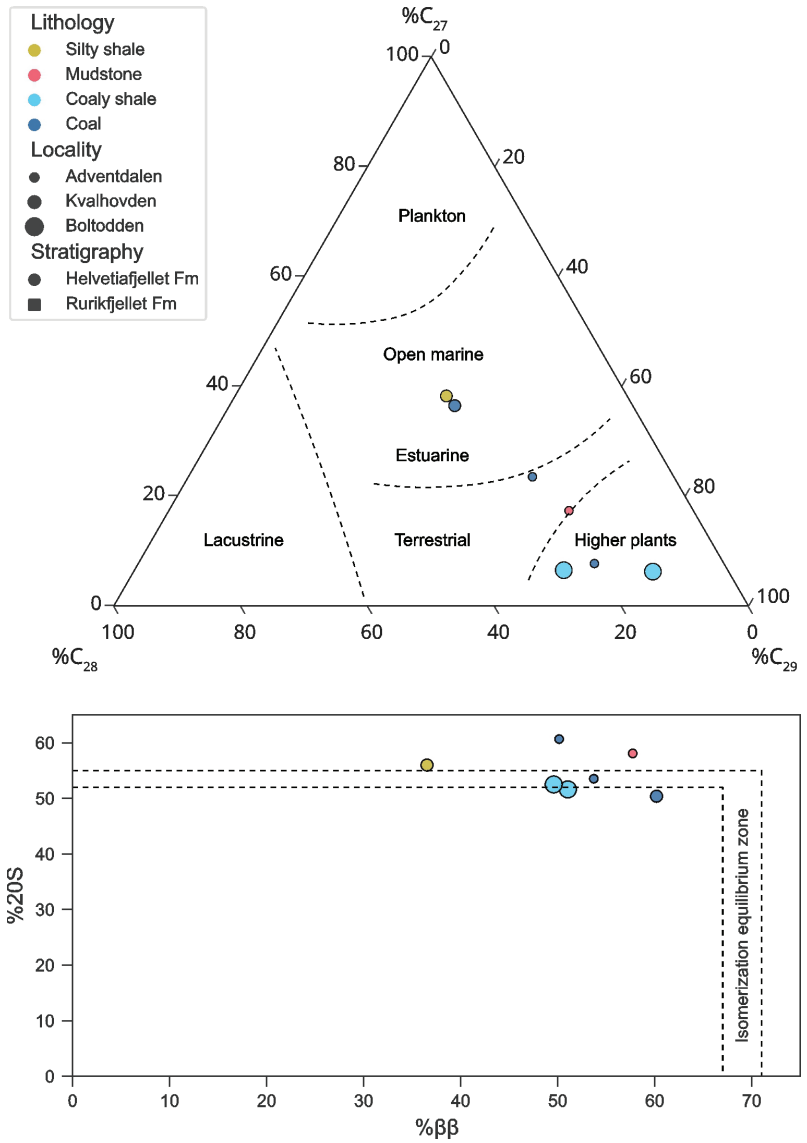

Fig. 7.11 (A) Ternary diagram of %C_{27}, %C_{28} and %C_{29} ββ-steranes indicating the origin of the sampled organic matter. The plot is indicating that organic matter is derived from terrestrial matter and higher plants. Two samples appear to be affected by a more marine signature. Adapted after Huang and Meinschein (1979) and Shanmugam (1985). (B) Sterane isomerization ratios indicating the thermal maturity of the selected samples. The plot is adapted after Peters et al. (2005).

7.5 Discussion

7.5.1 Organofacies and potential of the Hauterivian – Barremian paralic deposits

The Rock-Eval data gives an indication on the remaining potential of the organic-rich units at the current thermal maturities (e.g. Tissot and Welte, 1984; Peters and Cassa, 1994; Peters et al., 2005). During early burial of the investigated paralic deposits, the organic matter was less mature and had substantial higher quality and quantity than at present. Further burial subjected the organic matter to chemical and physical alteration and degradation, eventually reducing its source potential (e.g. Demaison et al., 1983; Tissot and Welte, 1984). Organic productivity, which is vital in the formation of a prolific source rock unit, as well as sedimentation rates, and destruction of organic matter by biodegradation, all have fundamental controls on the quantity and quality of the organic matter (Demaison and Moore, 1980; Demaison et al., 1983; Pedersen and Calvert, 1990; Demaison, 1991; Calvert et al., 1996; Tyson, 2001; Bohacs et al., 2005; Katz, 2005). Below follows a discussion on the geochemical results in relation to depositional environments and controlling factors for source rock development.

Overall, every sample included in this study have high organic carbon contents (TOC > 1 wt.%; Fig. 7.4), indicating relatively high primary productivity and favorable conditions for preservation. Based on the Rock-Eval data and back-calculation lines (Fig 7.4), all the analyzed samples from the Rurikfjellet and Helvetiafjellet formations appear to have had a kerogen Type IV – III composition, prior to the present-day thermal maturity. It must, however, be noted that the current kerogen organofacies are not necessary representative for the organic matter at early burial. This is because increased thermal maturities decrease the hydrogen content and changes the isoprenoid and n-alkanes parameters (e.g. Wesenlund et al., 2022).

7.5.1.1 The Rurikfjellet Formation (Hauterivian)

Our findings indicate that all samples belonging to the investigated Hauterivian part of the Rurikfjellet Formation from DH6 (samples DH6_44 – 47) and Kvalhovden (Samples RF1, RF2 and RF3) have the lowest petroleum potential of all the analyzed samples. All the samples consist of silty shale and display low TOC, S2 and HI values (Figs. 7.4 and 7.5). Hence, the organic matter in these samples are classified to be kerogen Type IV – III. It is thus likely that these deposits were not oil-prone prior to maturation (Fig. 7.5). As such, the remaining discussion will mainly focus on the Helvetiafjellet Formation paralics.

7.5.1.2 The Helvetiafjellet Formation (Barremian – early Aptian)

Most of the samples from the three localities where the Helvetiafjellet Formation was sampled exhibit low S2 and HI values, indicating poor to fair potential (Fig. 7.4) (Peter and Cassa, 1994). In particulate the four uppermost samples of the Helvetiafjellet Formation (samples DH6_24 – 27), which represent mudstones deposited in a marine influenced environment (Figs. 7.3 and 7.5; Grundvåg et al., 2019), yield a low potential similar to the Rurikfjellet Formation samples. As such, the hypothesized source rock unit associated with the landward retreating barrier-lagoonal system in the uppermost Helvetiafjellet Formation, appear to hold a very low petroleum potential, at least in central Spitsbergen. This probably relate to well ventilated conditions presumably governed by wave activity during deposition of these mudstones (see later discussion).

The most prolific samples of the Helvetiafjellet Formation are represented by coal and coaly shale deposits of the Glitrefjellet Member in the interval between c. 130 – 140 m in well DH6 (samples DH6_28 – 34) and two coaly shale samples from Boltodden (samples S6_FW and S5_FW) and one coal sample from Kvalhovden (Sample S1, the coal atop the Festningen Member) (Figs. 7.4 and 7.5). These samples indicate a very good source rock potential with high TOC and S2 values (Fig. 7.4A). However, the relatively low hydrogen content (HI<300), is effectively limiting their ability to generate oil. Collectively, the kerogen Type III – II/III composition is indicating that most of the organic-matter is derived from terrestrial sources, deposited under oxic to sub-oxic conditions (e.g. Demaison et al., 1983; Demaison and Moore, 1980). In general, terrestrial organic matter is often affected by significant reworking and oxygenation promoting severe biodegradation, thus forming less reliable source rock units (Demaison and Moore, 1980; Demaison et al., 1983). Still, the analyzed coal and coaly shale samples, despite having unfavorable HI values, demonstrates some petroleum potential (Figs. 7.4 and 7.5), where the main expelled product would most likely be a mixture of oil and gas at peak maturity (Peter and Cassa, 1994).

7.5.2 Thermal maturity

No measured vitrinite reflectance data was available for the silty shale samples belonging to the Rurikfjellet Formation in well DH6 or Kvalhovden (Fig. 7.6). However, based on the calculated vitrinite reflection data, the samples appear to be in the late mature window in well DH6. This is consistent with the average T_{max} value of 454°C for these samples (Peters and Cassa, 1994). In contrast, the silty shale samples at Boltodden had an average T_{max} of 484°C which was reflected in the calculated vitrinite reflectance that showed that the samples are post-mature.

Based on the classification of Peters and Cassa (1994), the Helvetiafjellet Formation samples in well DH6 are at their maturity peak, with an average vitrinite reflectance of 0.76 $\%R_o$ and average T_{max} values of 445°C. Samples from the Boltodden locality (S6_FW and S5_FW) are early mature, indicated by a low average T_{max} of 442°C and a measured vitrinite reflectance of 0.6 $\%R_o$. As such, the calculated vitrinite reflectance of %Rc (MPR), %Rc (F1) and %Rc (T_{max}) should be excluded, as they appear to overestimate relative to the measured vitrinite reflectance values. Finally, the single coal sample from the Kvalhovden locality (Sample S1), which yields a vitrinite reflectance value of 1.5 $\%R_o$, and the mudstone samples collected from the slump scar infill deposits at Kvalhovden (samples S3 to S7), which exhibit an average T_{max} value of 481.5 °C and average calculated vitrinite reflectance of 1.366 $\%R_C$ (T_{max}), are all classified as post-mature.

Although there is no universal correlation equation between T_{max} and $\%R_o$, they indicate a similar thermal maturity interval for most samples herein. This is consistent with the %20S vs. %ββ maturity ratios which indicated that the isomerization threshold has been reached for all samples, indicating that the bitumen extracted for these samples have reached a minimum thermal maturity corresponding to the early mature oil window (Fig. 7.11). Furthermore, maturity differences that occur between the three localities might be explained by spatiotemporal variations in depositional environments and different burial histories (e.g. Yang and Horsfield, 2020). The major difference in vitrinite reflectance between well DH6 in central Spitsbergen and the Boltodden locality in eastern Spitsbergen coincides with the reported regional maturity trend with R_o values typically decreasing eastward (e.g. Grogan et al., 1999; Abay et al., 2017; Olaussen et al., 2022). The difference between the Boltodden and Kvalhovden localities are harder to explain given the short distance between the two locations (c. 1 km) and the deltaic origin of all the analyzed mudstones. Brekke et al. (2014) suggested that anomalous vitrinite reflectance values in Middle Triassic source rock strata on Edgeøya, some 60 – 70 km east of the Boltoden/Kvalhovden localities, was caused by Early Cretaceous dolerite intrusions in the nearby subsurface. However, volcanic intrusions of Early Cretaceous age, which may have affected the thermal maturities of the samples, appear to be absent in this area (e.g. Senger et al., 2014).

7.5.3 Origin of organic matter and paleoenvironment indicators

The organofacies and limited petroleum potential established through Rock-Eval is further confirmed by the GC-FID results, which indicated that all samples from the Rurikfjellet and Helvetiafjellet formations contain organic-matter that was derived from terrestrial sources. This is particularly evident when comparing the Pr/*n*-C_{17} and Ph/*n*-C_{18} ratios (Fig. 7.8), which indicates that the organic matter from all samples originated from terrestrial and mixed sources typical of transitional terrestrial/marine environments (Shanmugam, 1985). This largely coincides with the open marine to

fluvial and paralic depositional setting previously interpreted for the investigated succession (e.g. Nemec, 1992; Midtkandal et al., 2007, 2008, 2016; Grundvåg et al., 2017, 2019). Plotting of $\delta^{13}C_{Aro}$ vs. $\delta^{13}C_{Sat}$ and Pr/Ph vs. CV also indicate terrestrial source input (Fig. 7.9) and the ternary diagram of $\%C_{27}$, $\%C_{28}$ and $\%C_{29}$ steranes, showed that the origin is higher plants, terrestrial or estuarine (Fig. 7.11). Hence, there is evidence for a sub-oxic to oxic environment susceptible to significant biodegradation. The remaining organic matter was presumably derived from the nearby landmasses, which testifies to the warm greenhouse climate in the Cretaceous period, that fostered high terrestrial and marine organic productivity across large parts of the northern hemisphere (Leckie et al., 2002; Herrle et al., 2015; Hurum et al., 2016b; Scotese et al., 2021).

7.5.4 Depositional controls on source rock potential

7.5.4.1 Rurikfjellet Formation

The Rurikfjellet Formation exhibit a large-scale upwards-coarsening signature, and records the southeastward progradation of a storm-influenced deltaic shoreline onto a low-gradient ramp-type shelf (Dypvik et al., 1991b; Jelby et al., 2020; Grundvåg et al., 2020). In general, terrestrial organic matter that enters the coastal zone by fluvial runoff is deposited in nearshore environments, and rivers may also contribute with a considerable amount of nutrients that may increase primary production in the photic zone (e.g. Petersen and Calvert, 1990; Fahl and Stein, 1999). Given the right circumstances, this combination could elevate the petroleum potential of nearshore sediments by deposition of lipid-rich organic matter (e.g. sporinite and resinite) from both marine and terrestrial sources (Langrock and Stein, 2004). However, the low potential indicate that the organic matter recorded in the Rurikfjellet Formation samples accumulated in well oxygenated, ventilated waters in a high energy, nearshore setting, resulting in fractionation and biodegradation of the organic matter.

Moreover, the coarsening-upward trend, the abundance of sandstones, and the silty character of the mudstone samples from both well DH6 and the Kvalhovden locality, coincide with the overall regressive, shallowing upward development described by previous workers (Dypvik, 1985; Dypvik et al., 1991a, b; Nemec et al., 1988; Grundvåg et al., 2017, 2019, 2020; Jelby et al., 2020). Thus, for the samples from the Rurikfjellet Formation, our geochemical results are largely in line with the findings of Hvoslef et al. (1986), who did a comprehensive organic geochemical assessment of both the Agardhfjellet (Middle Jurassic – lowermost Cretaceous) and the Rurikfjellet formations in central Spitsbergen. They also concluded with a limited source rock potential for the unit.

7.5.4.2 Helvetiafjellet Formation

The Helvetiafjellet Formation exhibit an overall transgressive development with fluvial braidplain deposits of the Festningen Member at its base, which is succeeded by various paralic deposits of the Glitrefjellet Member (Steel et al., 1978; Nemec, 1992; Gjelberg and Steel, 1995; Midtkdandal et al., 2007, 2008; Midtkandal and Nystuen, 2009; Grundvåg et al., 2017, 2019). The Glitrefjellet Member is a very heterolithic unit containing abundant mudstones, coaly shales and thin coals, as well as intercalated sandstones (e.g. Figs. 7.3 and 7.5). Deposition occurred in fluvial distributary channels, interdistributary bays, deltas, estuaries, lagoons, and barriers, and the associated deposits are organized into landward-stepping facies belts, amongst others recorded by an upward increase in marine influence (e.g. Nemec, 1992; Gjelberg and Steel, 1995; Midtkandal and Nystuen, 2009; Grundvåg et al., 2019). Paleo-geographic changes such as transgressive shifts are generally favorable for the deposition and preservation of organic matter (e.g. Mancini et al., 2002).

Barriers and lagoons are depositional systems associated with a landward shoreline migration concomitant with relative sea-level rise (e.g. Storms et al., 2008). The presence of a barrier complex may thus promote ideal conditions for the accumulation and preservation of organic-matter in the sheltered lagoon with stagnant water circulation and limited sedimentation (e.g. Demaison et al., 1983; Oertel et al., 1992; Candido et al., 2019) However, based on the lithology, Rock-Eval and the GC-FID results of the mudstone samples in the uppermost marine-influenced section of the Helvetiafjellet Formation in the well (samples DH6_24 – 27), the presence of organic-rich lagoonal (or interdistributary bay) deposits with generation potential appear to be unlikely in central Spitsbergen. Tidal indicators have been reported in the Glitrefjellet Member at multiple levels in many locations (Gjelberg and Steel, 1995; Midtkandal and Nystuen, 2009; Grundvåg et al.,2019). This includes the presence of double mud drapes in reworked fluvial sandstones (level 132–134 m in well DH6, Fig. 7.5; see FA 9 in Grundvåg et al., 2019) occurring immediately below the interpreted lagoonal/marine mudstone interval (level c. 121–131.5 m in well DH6; Fig. 7.5) in the upper part of the Glitrefjellet Member. This is coherent with a tidally influenced, transgressive coastline, which commonly result in barrier systems dissected by tidal inlet channels which allow water exchange and enhance circulation (e.g. Oertel et al., 1992). We therefore speculate that significant water exchange through tidal inlets promoted oxygenated and well ventilated conditions in the lagoon, resulting in biodegradation which consequently limited the potential for source rock development in the uppermost Glitrefjellet Member, at least in central Spitsbergen. However, because we lack data, we cannot determine or disregard the potential of the lateral equivalent, slightly older lagoonal deposits in eastern Spitsbergen, which there display a much thicker development (up to 30 m of dark-colored mudstone, see Nemec, 1992).

The coals of the Helvetiafjellet Formation have an increased potential with a kerogen Type III - II/III composition. However, according to Nemec (1992), the coals of the Glitrefjellet Member are of very limited thickness and lateral extent reflecting rapidly changing depositional environments and periodically high input of siliciclastic sediments during development of the Helvetiafjellet Formation coastal plain. This naturally limits the source rock potential of individual coal seams. However, the collective thickness of coal seams and coaly shale units suggests that the Glitrefjellet Member coastal plain succession may hold some potential, at least at local scale. Due to their abundance of organic matter, coals commonly represent gas-prone, as well as potentially oil-prone source rock units in prolific basins elsewhere (e.g. Collinson et al., 1994; Wilkins and George, 2002). The coal on top of the Festningen Member at the Kvalhovden locality, represented here by Sample S1 and sample DH6_43 in well DH6, has previously been suggested to be the result of a transgressive event (Grundvåg et al., 2017, see also Midtkandal et al., 2007). During this interpreted transgression, the groundwater table was presumably positioned near the land surface, and the terrestrial organic productivity eventually outpaced the degradation rate. The organic matter was then trapped and subjected to peatification (e.g. Flores, 1993). A similar setting can probably be envisaged for several of the Glitrefjellet Member coals in well DH6, which collectively records the transgressive development of the Helvetiafjellet Formation coastal plain (Grundvåg et al., 2019). Fluctuations and long-term rising of relative sea-level in marginal marine settings often result in trapping of terrestrial material in nearshore and coastal plain environments (Flores, 1993).

The Boltodden section is located c. 100 km to the southeast of well DH6, and thus held a more distal, southeasterly position relative to the sediment source area W and NW of Spitsbergen (Fig. 7.1; Grundvåg et al., 2019; 2017). Here, the analyzed coaly shale samples S6_FW and S5_FW have a kerogen Type III composition, indicating a increased petroleum potential compared to the silty shales and mudstones (Fig. 7.4). The same samples represent the initial, fine-grained deposits of a distributary bay fill/prograding mouth bar sequence in the lower half of the Glitrefjellet Member (Fig. 7.2G; see also Hurum et al., 2016b). Judging from their high TOC contents (14.8% and 50%, respectively; SF1), the distributary bays along the Helvetiafjellet Formation deltaic shoreline offered ideal sites for accumulating organic matter However, their limited potential suggests that the distal reaches of the interdistributary bays were readily influenced by marine processes (e.g. wave action and tidal currents) which promoted water circulation and oxygenation. In addition, approaching mouthbars prograding into and filling the bays presumably caused a dilution effect due to increased sedimentation rates (e.g. Ibach, 1982; Bohacs et al., 2005). As such, the interdistributary bay sediments appear to yield a very limited potential.

7.5.4.3 Possibly Increased potential for deposition and preservation of organic matter in the collapse scars at Kvalhovden

Sub-oxic to anoxic conditions is a prerequisite for preserving high quality organic-matter, and the formation of kerogen Type III – I source rocks (Demaison et al., 1983; Demaison and Moore, 1980). Such conditions are commonly developed in physically restricted (silled) basins, or in basins having stratified water columns (e.g. Demaison et al., 1983). Fault-bounded basins, formed during rifting events, have for example been shown to host Lower Cretaceous source rock units on the SW Barents Shelf (Hagset et al., 2022). The mudstone samples from Kvalhovden (samples S3 to S7), inferred to be pro-delta deposits (Fig. 7.2), are part of a slump scar infill section which developed close to the Lomfjorden Fault Zone in eastern Spitsbergen (Nemec et al., 1988; Onderdonk and Midtkandal, 2010). The downward slump-related displacement of sandstone blocks of the Festningen Member created a series of mini basins which offered accommodation space for pro-delta sediments (Onderdonk and Midtkandal, 2010). Theoretically, these early slump scar infill sediments could have accumulated under sub-oxic or anoxic conditions which developed due the restriction offered by the slump blocks in a similar manner to source rock developments reported in fault-bounded basins elsewhere (e.g. Demaison and Moore, 1980; Demaison et al., 1983; Gawthorpe and Leeder, 2000; Katz, 2005; Hagset et al., 2022).

However, the samples from Kvalhovden slump scar infill were established to have a poor potential due to very low HI and S2 values (Fig. 7.4 and SF1). Collectively, the kerogen Type IV compositions and Pr/*n*-C_{17} vs. Ph/*n*-C_{18} ratios points towards deposition in an oxidizing environment with significant biodegradation of the organic matter (Fig. 7.8). Furthermore, these samples interestingly plot more towards a mixed organic source, reflecting the inferred brackish to marine character of the water which covered the collapse-induced basin (Fig. 7.9). High rates of sedimentation associated with an approaching delta, which eventually filled-in and healed the collapse scar, in combination with significant input of terrestrial organic matter contributed to the limited potential of these sediments (e.g. Nemec et al., 1988; Onderdonk and Midkandal, 2010 Fig. 7.9). Furthermore, we cannot neglect the possibility that the high thermal exposure in this area have altered and overprinted the original bitumen composition in these samples, resulting in incorrect values for the isoprenoid and n-alkane ratio-based interpretation parameters. Thus, the poor source rock quality of these mudstones indicate that the displacements of the slumped sandstone blocks did not create a sufficient barrier or structural confinement to facilitate anoxic conditions (e.g. Demaison and Moore, 1980; Demaison et al., 1983; Katz, 2005). The shallow character of the shelf and the modest scale of the collapse was most likely the limiting factors. Compared to the regional fault systems described from the rifted SW margin of the Barents Shelf (e.g. Grogan et al., 1999; Serck et al., 2017; Hagset et al., 2022), the collapse-generated basins appear to be an order of magnitude smaller and would thus be difficult to correlate

laterally on conventional reflection seismic data. However, the trigger for the collapse have previously been related to movement in either the Lomfjorden or the Billefjorden fault zones (Nemec et al., 1988; Onderdonk and Midtkandal, 2010). As such, it may be speculated that collapse-generated basins like those investigated here represent incipient fault-bounded basins. Thus, given a scenario with continued fault growth and associated subsidence, the collapse-related basins may develop into sites ideal for the trapping and preservation of organic matter, which ultimately facilitate the accumulation of localized source rock units along faults (e.g. Gawthorpe and Leeder, 2000; Katz, 2005).

7.6 Implications for regional exploration

The recognition of new source rock units on the Barents Shelf could potentially have important implications for regional exploration as the traditional Upper Jurassic and Triassic source rocks have either been subjected to deep burial or significant uplift in many parts of the region (e.g. Rønnevik et al., 1982; Doré, 1995; Grogan et al., 1999; Ohm et al., 2008; Henriksen et al., 2011; Kairanov et al., 2021; Lasabuda et al., 2021).

Organic-rich units with localized source potential have been identified in the Hauterivian – lower Aptian succession in various fault bounded depocenters on the rifted SW Barents Shelf (Hagset et al., 2022). The most prolific of these units occur in well 7321/9-1 of the Fingerdjupet Subbasin (Hagset et al., 2022). This Barremian -lower Aptian unit (e.g. Hagset et al., 2022; Serck et al., 2017; Corseri et al., 2018; Bryn et al., 2020) coincides with a regional flooding surface which appears to cap two distinct clinoform packages (Marín et al., 2017; Grundvåg et al., 2017; Midtkandal et al., 2019). As such, it may correlate time- and facies-wise to the lower Aptian organic rich unit present atop of the Helvetiafjellet Formation in Spitsbergen (not considered here, for more details see Midtkandal et al., 2016; Grundvåg et al., 2017, 2019).

These clinoform packages are of high-angle and low-relief and are inferred to be delta-scale clinoforms (Bryn et al., 2020). It may thus be speculated that they contain paralic deposits like those of the Helvetiafjellet Formation in their topsets. However, the clinforms were unfortunately not penetrated during drilling of the recent ‘Scarecrow’ prospect briefly presented by Bryn et al. (2020). Barremian clinoforms of similar scale to those of the ‘Scarecrow’ prospect, displaying a south- to southeastward migration direction, similar to the published paleo-current measurements from the Helvetiafjellet Formation (e.g. Steel et al., 1978; Nemec, 1992; Gjelberg and Steel, 1995; Midtkandal and Nystuen, 2009; Grundvåg et al., 2019), also occur on the Bjarmeland Platform east of the Fingerdjupet Subbasin (Marín et al., 2017; Faleide et al., 2019). Previous workers have noted the similarities in migration directions and consequently linked the migration of these clinoforms to the Barremian uplift event north of Svalbard, further proposing a genetic link between the Helvetiafjellet

Formation paralics and the age-equivalent clinoform units on the shelf (Grundvåg et al., 2017; Midtkandal et al., 2019). This may indicate the presence of a laterally extensive deltaic system across large parts of the northern to central areas of the shelf. Thus, with reference to the source rock data presented here, the potential presence of undrilled paralic strata hosting viable source rock units, as well as reservoirs, over large areas of the Barents Shelf, are intriguing. If this is to be the case, our results from the Helvetiafjellet Formation can be of relevance to future exploration in the region, and it certainly highlights the fact that the link between clinoforms, paralic strata, and the deposition of organic-rich units is still an underexplored play on the Barents Shelf.

7.7 Conclusion

This study investigates the kerogen and bitumen content of the Hauterivian–Aptian uppermost Rurikfjellet and Helvetiafjellet formations onshore Svalbard. Their depositional environments have been assessed through lithostratigraphic and organic geochemical analyses of outcrop and core samples. As these formations are time-equivalent to strata in the offshore parts of the Barents Shelf, this study provides new results and insights into the Lower Cretaceous petroleum potential on Svalbard with inferences for the offshore Barents Shelf.

The Hauterivian part of the uppermost silty shales of the Rurikfjellet Formation exhibit the lowest TOC values and correspondingly low pyrolysis S2 and HI values, indicating present-day kerogen types III – IV. The Pr/*n*-C_{17} vs. Ph/*n*-C_{18} and the $\delta^{13}C_{Aro}$ vs. $\delta^{13}C_{Sat}$ ratios suggest that the *in-situ* bitumen was mainly sourced by terrestrial organic matter. This is likely a result of the nearshore and oxidizing benthic environment that took place during the deposition of the Rurikfjellet Formation, favouring the preservation of land-derived organic matter relative to marine organic matter. Calculated vitrinite reflectance values suggest that the Rurikfjellet Formation is late mature in well DH6 in central Spitsbergen and post mature at Kvalhovden in eastern Spitsbergen.

The Barremian Festningen Member of the lower Helvetiafjellet Formation was not sampled and analyzed for source rock richness and quality as it mainly consists of sandstones, which presumably are void of any significant source rock intervals.

The coals and coaly shales of the Barremian–Aptian part of the middle–upper Helvetiafjellet Formation mainly exhibit present-day kerogen types II/III – III. This is consistent with the Pr/*n*-C_{17} vs. Ph/*n*-C_{18} ratios, the $\delta^{13}C_{Aro}$ vs. $\delta^{13}C_{Sat}$ ratios, and the distribution of %C_{27}, %C_{28} and %C_{29} regular steranes, all indicating that the organic matter is of terrestrial origin and deposited during oxidizing conditions, as expected for coals. Vitrinite reflectance, T_{max} and sterane isomerization ratios indicate

that these coals and coaly shales are peak mature, implying that their original TOC and HI values were higher prior to maturation, possibly with greater original liquid hydrocarbon potential.

The inferred lagoonal/marine mudstones from the uppermost part of the Barremian to lower Aptian Helvetiafjellet Formation display low TOC, S2 and HI values, exhibiting a present-day kerogen Type III. This is consistent with the terrestrial organofacies signatures of the Pr/*n*-C_{17} vs. Ph/*n*-C_{18} and the $\delta^{13}C_{Aro}$ vs. $\delta^{13}C_{Sat}$ ratios. The implied preferential preservation of terrestrial organic matter indicate poorly developed benthic preservation potential during deposition of the lagoonal system in the uppermost part of the Helvetiafjellet Formation.

Consequently, the investigated strata in the Rurikfjellet and Helvetiafjellet formations have dominantly low source rock potential with the underlying Rurikfjellet formation being the poorest. The importance of possible slump scar-basin deposits of Aptian age and the lagoonal/marine mudstones in the upper Helvetiafjellet Formation thus appear limited in respect to regional exploration. The coal-bearing intervals, interpreted to represent coastal plain deposits, show the most promising source rock potential due to the highest organic richness and possibly oil-prone kerogen. If similar deposits occur in Barremian-aged offshore clinoform successions, extending across large areas of the northern and central Barents Shelf, un-discovered source rocks may still be present. Ultimately, continued drilling and exploration efforts targeting the Lower Cretaceous succession could speculatively facilitate the establishment of new exploration plays involving paralic strata comparable to the Helvetiafjellet Formation.

7.8 Acknowledgments

The first author is grateful to Wintershall Dea Norway for funding this research through a three-year PhD position at UiT The Arctic University of Norway. The authors also wish to thank reviewers and editors for improving the paper.

7.9 References

Banerjee, A., Sinha, A.K., Jain, A.K., Thomas, N.J., Misra, K.N., Cahndra, K., 1998. A mathematical representation of Rock-Eval hydrogen index vs. Tmax profiles. Organic Geochem. 28, 43–55. https://doi.org/10.1016/S0146-6380(97)00119-8.

Barnard, P.C., Cooper, B.S., 1981. Oils and source rocks of the North Sea area. Petroleum Geology of the Continental Shelf of North-West Europe. Institute of Petroleum, London, pp. 169–175.

Bordenave, M.L., 1993. Applied Petroleum Geochemistry. Editions Technip, Paris.

Bryn, B.K.L., Ahokas, J., Patruno, S., Schjelderup, S., Hinna, C., Lowrey, C., Escalona, A., 2020. Exploring the reservoir potential of lower cretaceous clinoforms in the fingerdjupet subbasin, Norwegian barents sea. Basin Res. 32, 332–347. https://doi. org/10.1111/bre.12407.

Candido, M., Cagliari, J., Tognoli, F.M.W., Lavina, E.L.C., 2019. Stratigraphic modeling of a transgressive barrier-lagoon in the Permian of Paraná Basin, southern Brazil. J. S. Am. Earth Sci. 90, 377–391.

Calvert, S.E., Bustin, R.M., Ingall, E.D., 1996. Influence of water column anoxia and sediment supply on the burial and preservation of organic carbon in marine shales. Geochem. Cosmochim. Acta 60, 1577–1593.

Cedeño, A., Ohm, S., Escalona, A., Marín, D., Olaussen, S., Demchuck, T., 2021. Upper Jurassic to Lower Cretaceous Source Rocks in the Norwegian Barents Sea, Part I: Organic Geochemical, Petrographic, and Paleogeographic Investigations.

Collinson, M.E., Van Bergen, P.F., Scott, A.C., De Leeuw, J.W., 1994. The oil-generating potential of plants from coal and coal-bearing strata through time: a review of new evidence from Carboniferous plants. In: Scott, A.C., Fleet, A.J. (Eds.), Coal and Coal-bearing Strata as Oil-prone Source Rocks, vol. 77. Geological Society Special Publication, London, pp. 31–70.

Corfu, F., Polteau, S., Planke, S., Faleide, J.I., Svensen, H., Zayoncheck, A., Stolbov, N., 2013. U–Pb geochronology of cretaceous magmatism on svalbard and Franz Josef land, Barents sea large igneous province. Geol. Mag. 150, 1127–1135.

Corseri, R., Faleide, T.S., Faleide, J.I., Midtkandal, I., Serck, C.S., Trulsvik, M., Planke, S., 2018. A diverted submarine channel of Early Cretaceous age revealed by high-resolution seismic data, SW Barents Sea. Mar. Petrol. Geol. 98, 462–476.

Dembicki, H., 2009. Three common source rock evaluation errors made by geologists during prospect or play appraisals. AAPG Bull. 93, 341–356.

Doré, A.G., 1995. Barents Sea geology, petroleum resources and commercial potential. Arctic 48, 207–221.

Doré, A.G., Lundin, E.R., Birkeland, Ø., Eliassen, P.E., Jensen, L.N., 1997. The NE Atlantic Margin: implications of late Mesozoic and Cenozoic events for hydrocarbon prospectivity. Petroleum Geoscience 3, 117–131.

Dörr, N., Lisker, F., Clift, P.D., Carter, A., Gee, D.G., Tebenkov, A.M., Spiegel, C., 2012. Late Mesozoic–Cenozoic exhumation history of northern Svalbard and its regional significance: constraints from apatite fission track analysis. Tectonophysics 514–517, 81–92. http://dx.doi.org/10.1016/j.tecto.2011.10.007.

Brekke, H., Dahlgren, S., Nyland, B., Magnus, C., 1999. The prospectivity of the Vøring and Møre basins on the Norwegian continental margin. In: Fleet, A.J., Boldy, S.A.R. (Eds.), Petroleum Geology of Northwest Europe: Proceedings of the 5th Conference. Geological Society of London, pp. 231–246.

Brekke, T., Krajewski, K.P., Hubred, J.H., 2014. Organic geochemistry and petrography of thermally altered sections of the Middle Triassic Botneheia Formation on south-western Edgeøya, Svalbard. Norwegian Petroleum Directorate Bulletin 11, 111–128.

Dypvik H. 1985: Jurassic and Cretaceous black shales of the Janusfjellet Formation, Svalbard, Norway. Sedimentary Geology 41, 235–248. https://doi.org/10.1016/0037-0738(84)90064-2.

Dypvik H., Nagy J., Eikeland, T.A., Backer-Owe, K., Andresen, A., Haremo, P., Bjarke, T., Johansen, H. & Elverhoi, A. 1991a: The Janusfjellet Subgroup (Bathonian to Hauterivian) on central Spitsbergen: a revised lithostratigraphy. Polar Research 9, 21–43. https://doi.org/10.1111/j.1751-8369.1991.tb00400.x.

Dypvik, H., Nagy, J., Eikeland, T.A., Backer-Owe, K., Johansen, H., 1991b. Depositional conditions of the bathonian to hauterivian janusfjellet subgroup, spitsbergen. Sed. Geol. 72, 55 –78.

Fahl, K., Stein, R., 1999. Biomarkers as organic-carbon-source and environmental indicators in the Late Quaternary Arctic Ocean: problems and perspectives. Marine Chemistry 63 (3–4), 293–309.

Faleide, T.S., Midtkandal, I., Planke, S., Corseri, R., Faleide, J.I., Serck, C.S., Nystuen, J. P., 2019. Characterisation and development of Early Cretaceous shelf platform deposition and faulting in the Hoop area, southwestern Barents Sea-constrained by high-resolution seismic data. Nor. J. Geol. 99 https://doi.org/10.17850/njg99-3-7.

Faleide, J.I., Vågnes, E., Gudlaugsson, S.T., 1993. Late mesozoic-cenozoic evolution of the southwestern Barents Sea. Geol. Soc. Lond. Pet. Geol. Conf. Ser. 4, 933–950.

Flores R. M., 1993. Coal-bed and related depositional environments in methane gas-producing sequences. In Hydrocarbons from Coal. AAPG Stud. Geol. Series. 38, 13–37.

Gawthorpe, R.L., Leeder, M.R., 2000. Tectono-sedimentary evolution of active extensional basins. Basin Res 12, 195–218.

Gjelberg, J., Steel, R.J., 1995. Helvetiafjellet formation (Barremian-Aptian), spitsbergen: characteristics of a transgressive succession. In: Steel, R.J., Felt, V.L., Johannesen, E.P., Mathieu, C. (Eds.), Sequence Stratigraphy on the Northwest European Margin. Elsevier, Amsterdam, pp. 571–593.

Grogan, P., Østvedt-Ghazi, A.-M., Larssen, G.B., Fotland, B., Nyberg, K., Dahlgren, S., Eidvin, T., 1999. Structural elements and petroleum geology of the Norwegian sector of the northern Barents Sea. In: Fleet, A.J., Boldy, A.R. (Eds.), Petroleum Geology of Northwest Europe. Proceedings 5th Conference, pp. 247-259.

Grundvåg, S.A., Marin, D., Kairanov, B., Śliwińska, K.K., Nøhr-Hansen, H., Jelby, M.E., Escalona, A., Olaussen, S., 2017. The lower cretaceous succession of the northwestern Barents shelf: onshore and offshore correlations. Mar. Petrol. Geol. 86, 834–857.

Grundvåg, S.A., Jelby, M.E., Śliwińska, K.K., Nohr-Hansen, H., Aadland, T., Sandvik, S.E., Tennvassas, I., Engen, T., Olaussen, S., 2019. Sedimentology and palynology of the Lower Cretaceous succession of central Spitsbergen: integration of subsurface and outcrop data. Norw. J. Geol. 99, 253–284.

Grundvåg, S.-A., Jelby, M.E., Olaussen, S., Śliwińska, K.K., 2020. The role of shelf morphology on storm-bed variability and stratigraphic architecture, Lower Cretaceous, Svalbard. Sedimentology. 68, 196-237. https://doi.org/10.1111/sed.12791

Grøsfjeld, K., 1992. Palynological age constraints on the base of the Helvetiafjellet formation (barremian) on spitsbergen. Polar Res. 11, 11–19.

Hagset, A., Grundvåg, S. A., Badics, B., Davies, R. and Rotevatn, A. 2022. Tracing Lower Cretaceous organic-rich units across the SW Barents Shelf. Mar. Petrol. Geol. 140, 105664. https://doi.org/10.1016/j.marpetgeo.2022.105664.

Hagset, A., Grundvåg, S. A., Badics, B., Davies, R. and Rotevatn, A. 2023. Deposition of Cenomanian – Turonian organic-rich units on the mid-Norwegian margin: Controlling factors and regional implications. Mar. Petrol. Geol. 149, 106102. https://doi.org/10.1016/j.marpetgeo.2023.106102.

Herrle, J.O., Schröder-Adams, C.J., Davis, W., Pugh, A.T., Galloway, J.M., Fath, J., 2015. Mid-cretaceous high arctic stratigraphy, climate, and oceanic anoxic events. Geology 43, 403–406. http://dx.doi.org/10.1130/G36439.1.

Huang, W.Y., Meinschein, W.G., 1979. Sterols as ecological indicators. Geochem. Cosmochim. Acta 43, 739–745.

Hurum, J.H., Roberts, A.J., Dyke, G.J., Grundvåg, S.-A., Nakrem, H.A., Midtkandal, I., Śliwińska, K.K., Olaussen, S., 2016a. Bird or maniraptoran dinosaur? A femur from the Albian strata of Spitsbergen. Palaeontol. Pol. 67, 137 – 147.

Hurum, J.H., Dyke, G., Roberts, A.J., Grundvag, S.A., Nakrem, H.A., Midtkandal, I., Śliwińska, K.K. & Olaussen, S. 2016b: An
avialan femur from Albian strata on Spitsbergen, Arctic Norway. Palaeontologia Polonica 67, 137–147.

Hvoslef, S., Dypvik, H. & Solli, H. 1986: A combined sedimentological and organic geochemical study of the Jurassic/Cretaceous Janusfjellet Formation (Svalbard), Norway. Organic Geochemistry 10, 101–111. https://doi.org/10.1016/0146-6380(86)90013-6.

Jakobsson, M., Mayer, L., Coakley, B., Dowdeswell, J.A., Forbes, S., Fridman, B., Hodnesdal, H., Noormets, R., Pedersen, R., Rebesco, M., Schenke, H.W., Zarayskaya, Y., Accettella, D., Armstrong, A., Anderson, R.M., Bienhoff, P., Camerlenghi, A., Church, I., Edwards, M., Gardner, J.V., Hall, J.K., Hell, B., Hestvik, O., Kristoffersen, Y., Marcussen, C., Mohammad, R., Mosher, D., Nghiem, S.V., Pedrosa, M.T., Travaglini, P.G., Weatherall, P., 2012. The international bathymetric chart of the Arctic Ocean (IBCAO) version 3.0. Geophys. Res. Lett. 39. http://dx.doi.org/10.1029/2012GL052219.

Jarvie, D. M., Claxton, B. L., Henk, F., Breyer, J. T., 2001. Oil and Shale Gas from the Barnett Shale, Ft. Worth Basin, Texas. Talk presented at the AAPG National Convention, June 3–6, 2001, Denver, CO. American Association of Petroleum Geologists Bulletin A, 100.

Jelby, M.E., Grundvåg, S.-A., Helland-Hansen, W., Olaussen, S., Stemmerik, L., 2020. Tempestite facies variability and storm-depositional processes across a wide ramp: towards a polygenetic model for hummocky cross-stratification. Sedimentology 67, 742–781.

Kairanov, B., Escalona, A., Mordasova, A. Śliwińska, K., Suslova, A., 2018. Early Cretaceous tectonostratigraphic evolution of the north central Barents Sea. J. Geodyn. 119, 183–198. https://doi.org/10.1016/j.jog.2018.02.009.

Kairanov, B., Escalona, A., Norton, I., Abrahamson, P., 2021. Early cretaceous evolution of the Tromsø basin, SW Barents Sea, Norway. Mar. Petrol. Geol. 123, 104–714.

Katz, B., 2005. Controlling factors on source rock development—a review of productivity, preservation, and sedimentation rate. Soci. Sed. Geol. 82, 7–16.

Koevoets, M.J., Abay, T.B., Hammer, Ø., Olaussen, S., 2016. High-resolution organic carbon-isotope stratigraphy of the middle jurassic–lower cretaceous Agardhfjellet Formation of central spitsbergen, svalbard. Palaeogeogr. Palaeoclimatol. Palaeoecol. 449, 266 – 274.

Koevoets, M.J., Hammer, Ø., Olaussen, S., Senger, K., Smelror, M., 2019. Integrating subsurface and outcrop data of the middle jurassic to lower cretaceous Agardhfjellet Formation in central spitsbergen. Norw. J. Geol. 98 (4), 1–34. https://doi.org/ 10.17850/njg98-4-01.

Kvalheim, O. M., Christy, A. A., Telnæs, N., & Bjørseth, A., 1987. Maturity determination of organic matter in coals using the methylphenanthrene distribution. Geochimica et Cosmochimica Acta, 51(7), 1883-1888.

Langrock, U., Stein, R., 2004. Origin of marine petroleum source rocks from the late Jurassic/Early Cretaceous Norwegian Greenland Seaway-evidence for stagnation and upwelling. Mar. Petroleum Geol. 21, 157 – 176.

Lasabuda, A.P.E., Johansen, N.S., Laberg, J.S., Faleide, J.I., Senger, K., Rydningen, T.A., Patton, H., Knutsen, S.M., Hanssen, A., 2021. Cenozoic uplift and erosion of the Norwegian Barents Shelf-A review. Earth Sci. Rev. 217, 103609.

Leith, T.L., Weiss, H.M., Mørk, A., Århus, N., Elvebakk, G., Embry, A.F., Brooks, P.W., Stewart, K.R., Pchelina, T.M., Bro, E.G., Verba, M.L., Danyushevskaya, A., Borisov, A.V., 1993. Mesozoic hydrocarbon source rocks of the Arctic region. In: Vorren, T.O., Bergsager, E., Dahl-Stamnes, A., Holter, E., Johansen, Å., Lie, Å., Lund, T.B. (Eds.), Arctic Geology and Petroleum Potential. Elsevier, Amsterdam, pp. 1–25.

Lerch, B., Karlsen, D.A., Seland, R., Backer-Owe, K., 2017. Depositional environment and age determination of oils and condensates from the Barents Sea. Petrol. Geosci. 23, 190–209.

Mackenzie, A., Leythaeuser, D., Schaefer, R., Bjorøy, M., 1983. Expulsion of petroleum hydrocarbons from shale source rocks. Nature 301, 506–509. https://doi.org/10.1038/301506a0.

Maher, H.D., 2001. Manifestations of the Cretaceous high arctic large igneous province in Svalbard. J. Geol. 109, 91–104.

Mancini, E. A., Markham, P. T., Armentrout, J. M., Rosen, N. C., 2002. Transgressive-Regressive Cycles: Application to Petroleum Exploration for Hydrocarbons Associated with Cretaceous Shelf Carbonates and Coastal and Fluvial-Deltaic Siliciclastics, Northeastern Gulf of Mexico. Sequence Stratigraphic Models for Exploration and Production: Evolving Methodology, Emerging Models and Application Histories. SEPM Society for Sedimentary Geology. Vol. 22.

Marín, D., Escalona, A., Śliwińska, K.K., Nohr-Hansen, H., Mordasova, A., 2017. Sequence stratigraphy and lateral variability of Lower Cretaceous clinoforms in the southwestern Barents Sea. AAPG (Am. Assoc. Pet. Geol.) Bull. 101, 1487–1517.

Marín, D., Escalona, A., Grundvåg, S.A., Nohr-Hansen, H., Kairanov, B., 2018a. Effects of adjacent fault systems on drainage patterns and evolution of uplifted rift shoulders: the Lower Cretaceous in the Loppa High, southwestern Barents Sea. Mar. Petrol. Geol. 94, 212–229.

Marín, D., Escalona, A., Grundvåg, S.A., Olaussen, S., Sandvik, S., Sliwinska, K.K., 2018b. Unravelling key controls on the rift climax to post-rift fill of marine rift basins: insights from 3D seismic analysis of the Lower Cretaceous of the Hammerfest Basin, SW Barents Sea. Basin Res 30, 587–612.

Marzi, R., Torkelson, B. E., Olson, R. K., 1993. A revised carbon preference index. *Organic Geochemistry*, *20*(8), 1303-1306.

Matapour, Z., Karlsen, D.A., 2017. Ages of Norwegian oils and bitumen based on age-specific biomarkers. Petroleum Geoscience, 24(1), 92-101.

Midtkandal, I., Nystuen, J.P., Nagy, J., 2007. Paralic sedimentation on an epicontinental ramp shelf during a full cycle of relative sea-level fluctuation; the Helvetiafjellet Formation in Nordenskiöld Land, Spitsbergen. Nor. J. Geol. 87, 343–359.

Midtkandal, I., Nystuen, J.P., Nagy, J., Mørk, A., 2008. Lower Cretaceous lithostratigraphy across a regional subaerial unconformity in Spitsbergen: the Rurikfjellet and Helvetiafjellet formations. Nor. J. Geol. 88, 287–304.

Midtkandal, I., Nystuen, J.P., 2009. Depositional architecture of a low-gradient ramp shelf in an epicontinental sea: the lower Cretaceous of Svalbard. Basin Res. 21, 655–675. http://dx.doi.org/10.1111/j.1365-2117.2009.00399.x.

Midtkandal, I., Faleide, J.I., Faleide, T., Serck, C., Planke, S., Corseri, R., Dimitriou, M., Nystuen, J., 2019. Lower Cretaceous Barents Sea strata: epicontinental basin configuration, timing, correlation and depositional dynamics. Geol. Mag. 157, 1–19.

Midtkandal, I., Svensen, H., Planke, S., Corfu, F., Polteau, S., Torsvik, T., Faleide, J.I., Grundvåg, S.-A., Selnes, H., Olaussen, S., 2016. The Aptian oceanic anoxic event (OAE1a) in Svalbard and the age of the Barremian-Aptian boundary. Palaeogeogr. Palaeoclimatol. Palaeoecol. 463, 126–135.

Mørk, A., Dallmann, W.K., Dypvik, H., Johannessen, E.P., Larssen, G.B., Nagy, J., Nøttvedt, A., Olaussen, S., P_celina, T.M., Worsley, D., 1999. Mesozoic lithostratigraphy. In: Dallmann, W.K. (Ed.), Lithostratigraphic Lexicon of Svalbard, pp. 127–214. Norsk Polarinstitutt (Tromsø).

Nagy, J., 1970. Ammonite faunas and stratigraphy of lower cretaceous (albian) rocks in southern spitsbergen. Nor. Polarinst. Skr. 152, 1–58.

Nemec, W., 1992. Depositional controls on plant growth and peat accumulation in a braidplain delta environment: Helvetiafjellet Formation (Barremian-Aptian), Svalbard. In: McCabe, P.J., Parish, J.T. (Eds.), Controls on the Distribution and Quality of Cretaceous Coals. Boulder Colorado, pp. 209–226. Geol. Soc. Spec. Paper 267.

Nemec, W., Steel, R.J., Gjelberg, J., Collinson, J.D., Prestholm, E., Øxnevad, I.E., 1988. Anatomy of collapsed and re-established delta front in Lower Cretaceous of Eastern Spitsbergen: gravitational sliding and sedimentation process. AAPG Bull. 72, 454–476.

NPD (Norwegian Petroleum Directorate), 2017. [WWW Document] Geological assessment of petroleum resources in eastern parts of Barents Sea north. Norwegian Petroleum Directorate. https://www.npd.no/globalassets/1-npd/publikasjoner/rapporter/geologivurderingbhn-nett.pdf.

Oertel, G.F., Krafi, J.C., Kearney, M.S., Woo, H.J., 1992. A rational theory for barrier lagoon development. In: Quaternary Coasts of the United States: Marine and Lacus Trine Systems. Society for Sedimentary Geology Special Publication 48, pp. 77–87.

Ohm, S.E., Karlsen, D.A., Austin, T.J.F., 2008. Geochemically driven exploration models in uplifted areas: examples from the Norwegian Barents Sea. AAPG (Am. Assoc. Pet. Geol.) Bull. 92, 1191–1223.

Olaussen, S., Grundvåg, S-A., Senger, K., Anell, I., Betlem, P., Birchall T., Braathen, A., Dallmann, W., Jochmann, M., Johannessen, E. P., Lord G., Mørk, A., Osmundsen, P. T., Smyrak-Sikora, A. and Stemmerik, L., 2022. The

Svalbard Carboniferous to Cenozoic Composite Tectono-Stratigraphic Element. Geological Society, London, Memoirs, 57 (1), M57-2021-36. https://doi.org/10.1144/M57-2021-36

Olaussen, S., Larssen, G.B., Helland-Hansen, W., Johannessen, E.P., Nøttvedt, A., Riis, F., Rismyhr, B., Smelror, M., Worsley, D., 2019. Mesozoic strata of Kong Karls land, svalbard, Norway; a link to the northern Barents Sea basins and platforms. Norw. J. Geol. 98 (4), 1–70. https://doi.org/10.17850/njg98-4-06.

Onderdonk, N., Midtkandal, I., 2010. Mechanisms of collapse of the cretaceous Helvetiafjellet Formation at kvalvågen, eastern spitsbergen. Mar. Petrol. Geol. 27, 2118–2140.

Parker, J.R., 1967. The jurassic and cretaceous sequence in spitsbergen. Geol. Mag. 104, 487–505.

Peters, K.E., Cassa, M.R., 1994. Applied source rock geochemistry. In: Magoon, L.B., Dow, W.G. (Eds.), The Petroleum System - from Source to Trap. AAPG, pp. 93–120.

Peters, K.E., Walters, C.C., Moldowan, J.M., 2005. The Biomarker Guide: Biomarkers and Isotopes in Petroleum Exploration and Earth History, second ed., vol. 2. Cambridge University Press, Cambridge.

Polteau, S., Hendriks, B.W.H., Planke, S., Ganerød, M., Corfu, F., Faleide, J.I., Midtkandal, I., Svensen, H.S., Myklebust, R., 2015. The early cretaceous Barents sea sill complex: distribution, 40Ar/39Ar geochronology, and implications for carbon gas formation. Palaeogeogr. Palaeoclimatol. Palaeoecol. http://dx.doi.org/10.1016/j.palaeo.2015.07.007.

Radke, M., 1988. Application of aromatic compounds as maturity indicators in source rocks and crude oils. Marine and petroleum geology, 5(3), 224-236.

Radke, M., Willsch, H., Leythaeuser, D., Teichmüller, M., 1982. Aromatic components of coal: relation of distribution pattern to rank. Geochimica et Cosmochimica Acta, 46(10), 1831-1848.

Rønnevik, H., Bescow, B., Jacobsen, H.P., 1982. Structural and Stratigraphic Evolution of the Barents Sea, vol. 8. Canadian Society of Petroleum Geologists Memoir, pp. 431–440.

Sattar, N., Juhlin, C., Koyi, H., Ahmad, N., 2017. Seismic stratigraphy and hydrocarbon prospectivity of the lower cretaceous Knurr sandstone lobes along the southern margin of Loppa high, Hammerfest basin, Barents Sea. Mar. Petrol. Geol. 85, 54–69.

Scotese, C.R., Song, H., Mills, B.J.W., van der Meer, D.G., 2021. Phanerozoic paleotemperatures: the earth's changing climate during the last 540 million years. Earth Sci. Rev. 215, 103–503.

Seifert, W. K., & Moldowan, J. M., 1978. Applications of steranes, terpanes and monoaromatics to the maturation, migration and source of crude oils. *Geochimica et cosmochimica acta*, *42*(1), 77-95.

Seldal, J., 2005. Lower Cretaceous: the next target for oil exploration in the Barents Sea? Petrol. Geol. Conf. Proceed. 231–240.

Senger, K., Tveranger, J., Ogata, K., Braathen, A., Planke, S., 2014. Late Mesozoic magmatism in svalbard: a review. Earth-Sci. Rev. 139, 123–144.

Serck, C.S., Faleide, J.I., Braathen, A., Kjølhamar, B., Escalona, A., 2017. Jurassic to early cretaceous basin configuration(s) in the Fingerdjupet Subbasin, SW Barents Sea. Mar. Petrol. Geol. 86, 874–891.

Shanmugam, G., 1985. Significance of coniferous rain forests and related organic matter in generating commercial quantities of oil, Gippsland Basin, Australia. AAPG (Am. Assoc. Pet. Geol.) Bull. 69, 1241–1254.

Shephard, G.E., Miller, R.D., Seton, M., 2013. The tectonic evolution of the Arctic since Pangea breakup: integrating constraints from surface geology and geophysics with mantle structure. Earth Sci. Rev. 124, 148–183.

Śliwińska, K.K., Jelby, M.E., Grundvåg, S.-A., Nøhr-Hansen, H., Alsen, P., Olaussen, S., 2020. Dinocyst stratigraphy of the ValanginianeAptian Rurikfjellet and Helvetiafjellet formations on Spitsbergen, Arctic Norway. Geological Magazine 157, 1693 – 1714. https://doi.org/10.1017/S0016756819001249.

Sofer, Z., 1984. Stable carbon isotope compositions of crude oils: application to source depositional environments and petroleum alteration. AAPG Bull. 68, 31–49. https://doi.org/10.1306/ad460963-16f7-11d7-8645000102c1865d.

Steel, R.J., Gjelberg, J. & Haarr, G., 1978. Helvetiafjellet Formation (Barremian) at Festningen, Spitsbergen – a field guide. Norsk Polarinstitutt Årbok 1978, 111–128.

Steel, R.J., Worsley, D., 1984. Svalbard's post-Caledonian strata e an atlas of sedimentational patterns and palaeogeographic evolution. In: Spencer, A.M. (Ed.), Petroleum Geology of the North European Margin. Norwegian Petroleum Society. Graham and Trotman Ltd, pp. 109–135.

Storms, J. E., Weltje, G. J., Terra, G. J., Cattaneo, A., & Trincardi, F., 2008. Coastal dynamics under conditions of rapid sea-level rise: Late Pleistocene to Early Holocene evolution of barrier–lagoon systems on the northern Adriatic shelf (Italy). Quaternary Science Reviews, 27(11-12), 1107-1123.

Svalbardkartet Norsk Polarinstitutt [WWW Document], 2022. https://geokart.npolar.no/Html5Viewer/index.html?viewer=Svalbardkartet (Accessed 25.11.22).

Tissot, B., Welte, D.H., 1984. Petroleum Formation and Occurrence. Springer-Verlag, Berlin Heidelberg.

Weiss, H.,Wilhelms,A.,Mills,N.,Scotchmer,J.,Hall,P.,Lind,K.,Brekke,T., 2000. NIGOGA—The Norwegian Industry Guide to Organic Geochemical Analysis. [online] Edition 4.0 Published by Norsk Hydro, Statoil, Geolab Nor, SINTEF Petroleum Research and the Norwegian Petroleum Directorate. 102 pp. (accessed 06.02.2023). Available at: http://www.npd.no/engelsk/nigoga/default.htmS

Wenke, A., Ferreira, G.B., Bullimore, S.A., Clark, S.A., Dörner, M., Embry, P., Erdmann, M., Hansen J.O., Inthorn, Johansen, L.M., . Kløvjan, O.S., Kyrkjebø, R., Mann, U., Orlovs, A., Rein, E., Rafaelsen, B., Ryseth, A.E., Roudot, M., Schmidt, B.J., Stavrou, E., Thießen, O., Vandré, C., van Koverden, J.H. and Zweigel, J., 2021. Unlocking the Cretaceous Petroleum Systems of the Norwegian Sea. In: 82nd EAGE Annual Conference & Exhibition. European Association of Geoscientists & Engineers, pp. 1–5. https://doi.org/10.3997/2214-4609.202010949

Wesenlund, F., Grundvåg, S.-A., Sjøholt, V.E. Thiessen, O., Pedersen, J.H. 2021. Linking facies variations, organic carbon richness and bulk bitumen content – a case studyfrom the organic-rich Middle Triassic shales of eastern Svalbard. Marine and Petroleum Geology, 132. https://doi.org/10.1016/j.marpetgeo.2021.105168

Wesenlund, F., Grundvåg, S.-A., Engelschiøn, V.S., Thießen, O. & Pedersen, J.H. 2022. Multi-elemental chemostratigraphy of Triassic mudstones in eastern Svalbard: Implications for source rock formation in front of the World's largest delta plain. The Depositional Record, 00, 1– 36. https://doi.org/10.1002/dep2.182

White, D.A., 1993. Geologic risking guide for prospects and plays. AAPG (Am. Assoc. Pet. Geol.) Bull. 77, 2048–2061.

Wilkins, R.W., George, S.C., 2002. Coal as a source rock for oil: a review. Int. J. Coal Geol. 50 (1–4), 317–361.

Yang, R., Wang, Y., Cao, J., 2014. Cretaceous source rocks and associated oil and gas resources in the world and China: a review. Petrol. Sci. 11 (3), 331–345.

7.10 Supplementary material

7.10.1 Supplementary file SF1

Table SF1. Rock-Eval data from well DH6 in Adventdalen and the two outcrop localities, Kvalhovden and Boltodden.

Rock-Eval data																
Well / Location	Analysis	Sample info	Lithology	Age	Formation	Lower Depth (m)	S1 (mg/g)	S2 (mg/g)	S3 (mg/g)	Tmax (°C)	PP (mg/g)	PI (wt ratio)	HI (mg HC/g TOC)	OI (mg CO2/g TOC)	TOC (%)*	%Rc (Tmax)	%Ro
DH6	RE	DH6_23	Mudstone	Barremian	Helvetiafjellet Fm	124	0.43	1.9	0.22	453	2.33	0.18	78	9	2.44	0.994	N/A
DH6	RE, GC	DH6_24	Mudstone	Barremian	Helvetiafjellet Fm	124.65	0.67	5.24	0.18	448	5.91	0.11	138	5	3.79	0.904	N/A
DH6	RE	DH6_25	Mudstone	Barremian	Helvetiafjellet Fm	127.65	0.22	1.78	0.23	451	2	0.11	89	12	2	0.958	N/A
DH6	RE	DH6_26	Mudstone	Barremian	Helvetiafjellet Fm	128	0.26	1.6	0.12	449	1.86	0.14	83	6	1.92	0.922	N/A
DH6	RE	DH6_27	Mudstone	Barremian	Helvetiafjellet Fm	131.1	0.28	1.23	0.18	452	1.51	0.19	87	13	1.41	0.976	N/A
DH6	RE, Ro	DH6_28	Coal	Barremian	Helvetiafjellet Fm	133.8	3.83	211.61	0.41	450	215.44	0.02	237	0	89.4	0.94	0.77
DH6	RE, GC	DH6_29	Coal	Barremian	Helvetiafjellet Fm	136.7	5.89	171.26	0.29	454	177.15	0.03	273	0	62.7	1.012	N/A
DH6	RE	DH6_30	Coaly shale	Barremian	Helvetiafjellet Fm	138.3	0.69	9.27	0.18	451	9.96	0.07	167	3	5.55	0.958	N/A
DH6	RE	DH6_31	Coaly shale	Barremian	Helvetiafjellet Fm	139.6	0.62	10.78	0.13	449	11.4	0.05	147	2	7.32	0.922	N/A
DH6	RE	DH6_32	Coal	Barremian	Helvetiafjellet Fm	140	1.7	110.42	0.27	448	112.12	0.02	204	0	54.1	0.904	N/A
DH6	RE	DH6_33	Coaly shale	Barremian	Helvetiafjellet Fm	141.2	1	14.58	0.14	451	15.58	0.06	180	2	8.12	0.958	N/A
DH6	RE, GC	DH6_34	Coal	Barremian	Helvetiafjellet Fm	143.22	2.97	144.58	0.31	448	147.55	0.02	276	1	52.3	0.904	N/A
DH6	RE	DH6_35	Mudstone	Barremian	Helvetiafjellet Fm	145.5	0.51	2.65	0.13	447	3.16	0.16	153	8	1.73	0.886	N/A
DH6	RE	DH6_36	Coaly shale	Barremian	Helvetiafjellet Fm	147.9	1.04	11.07	0.09	448	12.11	0.09	188	2	5.9	0.832	N/A
DH6	RE	DH6_37	Mudstone	Barremian	Helvetiafjellet Fm	147.12	2.78	79.73	0.15	444	82.51	0.03	206	0	38.7	0.904	N/A
DH6	RE, Ro	DH6_38	Coal	Barremian	Helvetiafjellet Fm	154.74	2.96	165.05	0.24	452	168.01	0.02	281	0	58.8	0.976	0.75
DH6	RE	DH6_39	Mudstone	Barremian	Helvetiafjellet Fm	156.79	0.9	5.1	0.11	449	6	0.15	207	4	2.46	0.922	N/A
DH6	RE	DH6_40	Mudstone	Barremian	Helvetiafjellet Fm	161.4	0.35	2.33	0.17	446	2.68	0.13	116	8	2.01	0.868	N/A
DH6	RE	DH6_41	Mudstone	Barremian	Helvetiafjellet Fm	161.55	0.2	1.53	0.13	451	1.73	0.12	112	9	1.37	0.958	N/A
DH6	RE	DH6_42	Mudstone	Barremian	Helvetiafjellet Fm	170.8	1.85	31.66	0.26	445	33.51	0.06	154	1	20.6	0.85	N/A
DH6	RE, Ro	DH6_43	Coal	Barremian	Helvetiafjellet Fm	173.88	6.26	188.8	0.29	447	195.06	0.03	269	0	70.2	0.886	0.76
DH6	RE	DH6_44	Silty shale	Hauterivian	Rurikfjellet Fm	191.35	0.31	1.1	0.08	452	1.41	0.22	99	7	1.11	0.976	N/A
DH6	RE	DH6_45	Silty shale	Hauterivian	Rurikfjellet Fm	194	0.27	1.91	0.12	454	2.18	0.12	116	7	1.64	1.012	N/A
DH6	RE	DH6_46	Silty shale	Hauterivian	Rurikfjellet Fm	197	0.22	1.16	0.09	452	1.38	0.16	89	7	1.3	0.976	N/A
DH6	RE	DH6_47	Silty shale	Hauterivian	Rurikfjellet Fm	200	0.24	1.4	0.14	457	1.64	0.15	92	9	1.52	1.066	N/A
Kvalhovden	RE, GC, RO	S1	Coal	Barremian	Helvetiafjellet Fm	N/A	3.61	33.13	2.01	476	36.74	0.1	59	4	56.5	1.408	1.50
Kvalhovden	RE, GC	S3	Coaly shale	Barremian	Helvetiafjellet Fm	N/A	0.19	0.74	0.45	480	0.93	0.2	32	19	2.34	1.48	N/A
Kvalhovden	RE, GC	S4	Mudstone	Barremian	Helvetiafjellet Fm	N/A	0.41	0.76	0.19	477	1.17	0.35	28	7	2.74	1.426	N/A
Kvalhovden	RE	S5	Silty shale	Barremian	Helvetiafjellet Fm	N/A	0.37	1.2	0.24	483	1.57	0.24	44	9	2.75	1.534	N/A
Kvalhovden	RE, GC	S7	Silty shale	Barremian	Helvetiafjellet Fm	N/A	0.41	1.04	0.34	482	1.45	0.28	36	12	2.91	1.516	N/A
Boltodden	RE, GC	S5-FW	Coaly shale	Barremian	Helvetiafjellet Fm	N/A	0.82	11.04	1.17	444	11.86	0.07	75	8	14.8	0.832	N/A
Boltodden	RE, GC, RO	S6-FW	Coaly shale	Barremian	Helvetiafjellet Fm	N/A	2.14	64.88	4.03	441	67.02	0.03	130	8	50	0.778	0.66
Kvalhovden	RE, GC	RF1	Silty shale	Hauterivian	Rurikfjellet Fm	N/A	0.22	0.75	0.16	487	0.97	0.23	42	9	1.77	1.606	N/A
Kvalhovden	RE, GC	RF2	Silty shale	Hauterivian	Rurikfjellet Fm	N/A	0.12	0.54	0.29	481	0.66	0.18	32	17	1.7	1.498	N/A
Kvalhovden	RE	RF3	Silty shale	Hauterivian	Rurikfjellet Fm	N/A	0.1	0.46	0.2	486	0.56	0.18	26	11	1.8	1.588	N/A

7.10.2 Supplementary file SF2

Table SF2. Summary of the key GC-FID results from the 11 samples from well DH6, Kvalhovden and Boltodden.

Location	Formation	Sample	Lithology	Pr/Ph ratio	Waxiness	CPI2	Pr/n-C17	Ph/n-C18	δ^{13}C-Aro	δ^{13}C-Sat	CV	TS (TS+TM)	∑(C23tri to C29tri)/30ab	%C27	%C28	%C29	%20S	%ββ
Adventdalen, Well DH6	Helvetiafjellet Fm.	DH6_34	Coal	4.89	0.75	1.09	0.44	0.09	-25	-28.8	5,714	18.93	0.077	23.48	22.28	54.24	60.66	50.14
		DH6_29	Coal	4.8	0.67	1.05	0.76	0.14	-25	-26.5	-0.105	29.30	0.020	7.69	20.42	71.89	53.53	53.71
		DH6_24	Mudstone	3.13	0.55	1.09	0.53	0.16	-25.3	-27.5	1,759	36.72	0.050	17.31	19.60	63.09	58.08	57.72
Kvalhovden	Helvetiafjellet Fm.	S1	Coal	2.02	0.92	1.19	0.33	0.16	-24.7	-27.9	4,103	54.11	2.964	36.44	28.06	35.50	50.38	60.18
		S3	Coaly shale	1.69	0.71	1.03	0.22	0.13	-25.3	-27.5	1,759	N/A	N/A	N/A	N/A	N/A	N/A	N/A
		S4	Mudstone	1.4	0.73	1.05	0.25	0.17	-25.4	-28	2,802	N/A	N/A	N/A	N/A	N/A	N/A	N/A
		S7	Silty shale	2.58	0.73	1.03	0.21	0.08	-24.8	-28.5	5,399	46.81	2.641	38.20	28.50	33.30	55.99	36.52
	Rurikfjellet Fm.	RF1	Silty shale	1.24	0.79	1.05	0.21	0.15	-24.6	-28.9	6,855	N/A	N/A	N/A	N/A	N/A	N/A	N/A
		RF2	Silty shale	1.4	0.78	1.05	0.18	0.11	-24.9	-28.8	5,936	N/A	N/A	N/A	N/A	N/A	N/A	N/A
Boltodden	Helvetiafjellet Fm	S5-FW	Coaly shale	5.66	0.65	1.01	2.48	0.43	-25.5	-28.7	4,351	9.47	0.016	6.48	25.84	67.68	51.61	51.04
		S6-FW	Coaly shale	4.88	0.55	1.12	2.48	0.47	-25	-29.4	7,232	7.17	0.026	6.22	11.94	81.84	52.50	49.58

8 Synthesis

This chapter synthesizes the main findings in papers I-III and discusses the paleoenvironmental conditions and the effect of rifting/faulting during the Early Cretaceous period and its implication towards understanding deposition of Lower Cretaceous organic-rich units on the NCS. We also discuss the possible connection to global Oceanic Anoxic Events (OAEs), which has promoted accumulation of viable source rocks worldwide (e.g. Schlanger and Jenkyns, 1976; Jenkyns, 1980; Dorè et al., 1997; Jenkyns, 1999; Erba et al., 2004; Coccioni et al., 2006; Baudin and Riquier, 2014).

8.1 Basin configuration and its influence on organic-matter preservation

The configuration of a basin execute a first order control on the formation of organic-rich units, as the basin configuration can promote and influence the occurrence and nature of anoxic conditions, sedimentation rates, and productivity (Demaison and Moore, 1980; Demaison et al., 1983; Pedersen and Calvert, 1990; Katz, 2005). In rift basins, the subsidence rate, eustatic sea-level variations and the structural relief between depocenters and footwalls, have an effect on the circulation patterns of oceanic waters. Free and unlimited mixing of oxygenated water masses between the open ocean and the basin, will promote high biodegradation and limit water stratification. In contrast, in a more confined basin, evaporation rates could outpace the inlet of oxygenated waters, thus promoting water stratification and eventually anoxic bottom water conditions. In extensional regimes, the formation of rift-basins and its internal configuration with grabens, half-grabens and horsts will influence the circulation patterns of water masses relative to eustatic sea-level. In this subchapter, the main differences between the shallow and deep Cretaceous basins on the NCS is outlined.

The Vøring, Tromsø and Bjørnøya basins have a all a deep rifted configuration attributed to the Late Jurassic – Early Cretaceous rifting event (Faleide et al., 2015). The internal highs and conjugated margins of these basins formed local and regional sediments source areas which promoted high sedimentation rates, which presumably caused a dilution effect that effectively limited the possibility for the organic matter to accumulate to sufficient concentrations and thicknesses (Ibach, 1982; Bohacs et al., 2005). The occurrence of a potential source rock in these basins are dependent on the reduction of sedimentation input, which is controlled by paleobathymetric conditions and sediment fairways in the basin.

The shallower Hammerfest Basin and Fingerdjupet Subbasin, did not experience such severe sedimentation rates, as evident by their thinner and condensed Lower Cretaceous infill successions (see Paper I). These shallow basins were also more prone to stagnant water circulation, as they lack a deep-water connection to the deeper basins which can promote the establishment of convection cells. In addition, organic matter settling on the seafloor of the shallow basins had a shorter transit and closer proximity to the photic zone, which limits the exposure to oxidizers. Thus, if waters are relatively stagnant and if high primary productivity prevails, oxygen consuming bacteria degrading the organic matter could promote water stratification and anoxia (e.g. Arthur et al., 1987; Demaison et al.,

1983; Demaison and Moore, 1980; Demaison et al., 1983). This development was more likely to occur in the shallow basins compared to the more unrestricted deeper basins with high sedimentation rates.

In scenarios influenced by upwelling, anoxic conditions can develop on the margins of deep rift basins. In such cases, nutrient rich waters are supplied from the deep oceans and forced up against the margins of the basin. This may typically promote significant primary production in the photic zone where an oxygen minimum zone (OMZ) develops. This OMZ could extend towards the deeper basins but this depends on the deep-water circulation and inlet of oxygenated waters (Arthur et al., 1987). The occurrence of thin and condensed organic-rich units on the Halten Terrace (see Paper II), may indicate that an OMZ extended across much of the terrace. However, cross-shelf sedimentation transport, recurring oxygenated conditions, fault-related uplift, and subsequent erosion prohibited preservation of significant qualities of organic matter.

8.2 Lower Cretaceous organic-rich units, global anoxic events, and other controlling factors

Although this study does not include carbon or oxygen isotope data which is typically used to detect the signature of OAEs in the rock record (e.g. Arthur et al., 1987; Schlanger and Jenkyns, 1976; Jenkyns, 1980), some of the Lower Cretaceous organic-rich units documented in papers I and II appears, seems age-wise to correlate to OAEs that occurred in the Hauterivian, Barremian, early Aptian, and in the very latest Cenomanian. Increased TOC and Rock-Eval values are documented in these units, possibly strengthening this assumption (Fig. 8.2). The occurrence of these global OAEs is tied to major volcanism and the formation of Large Igneous Provinces (LIPs) but also active seafloor spreading causing a volume increase of mid-ocean ridges and thermal uplift of the seafloor (Schlanger and Jenkyns, 1976; Jenkyns, 1980). Consequently, the OAEs are associated with supra-regional transgressions and eustatic sea-level highstands (Haq et al., 1987; Miller et al., 2005). The chain of events involved to facilitate and initiate OAEs are outlined in Figure 8.1.

Volcanic outgassing associated with the development of the LIPs caused a substantial increase in the concentration of CO_2 in the atmosphere (Beil et al., 2020). On initiation, volcanic outgassing led to heighten global temperatures (Cavalheiro et al., 2021). However, after the outgassing, the abundance of CO_2 enhances organic productivity which boosted the atmospheric draw-dawn of CO_2, resulting in a cooling effect (Price and Nunn, 2010). Elevated primary production also involved increased consumption of dissolved oxygen by bacteria during decomposition, which results in expansion of anoxic and euxinic water layers (Fig. 8.1) (Arthur et al., 1987; Leckie et al., 2002). This caused a depletion of oxygen in the ocean and establishment of periodically global anoxic conditions (Arthur et al., 1987; Schlanger and Jenkyns, 1976; Jenkyns, 1980). The elevated primary production and the increased preservation potential during the short-lived OAEs, caused the accumulation and preservation of organic-rich sediments across large areas. The Cretaceous period have some of these supra-regional to global events recorded as organic-rich shales in the Hauterivian, Barremian, Lower Aptian and uppermost Cenomanian successions (Fig. 8.2). Bellow, follows a discussion on the occurrence of these events and the organic-rich units documented in this study.

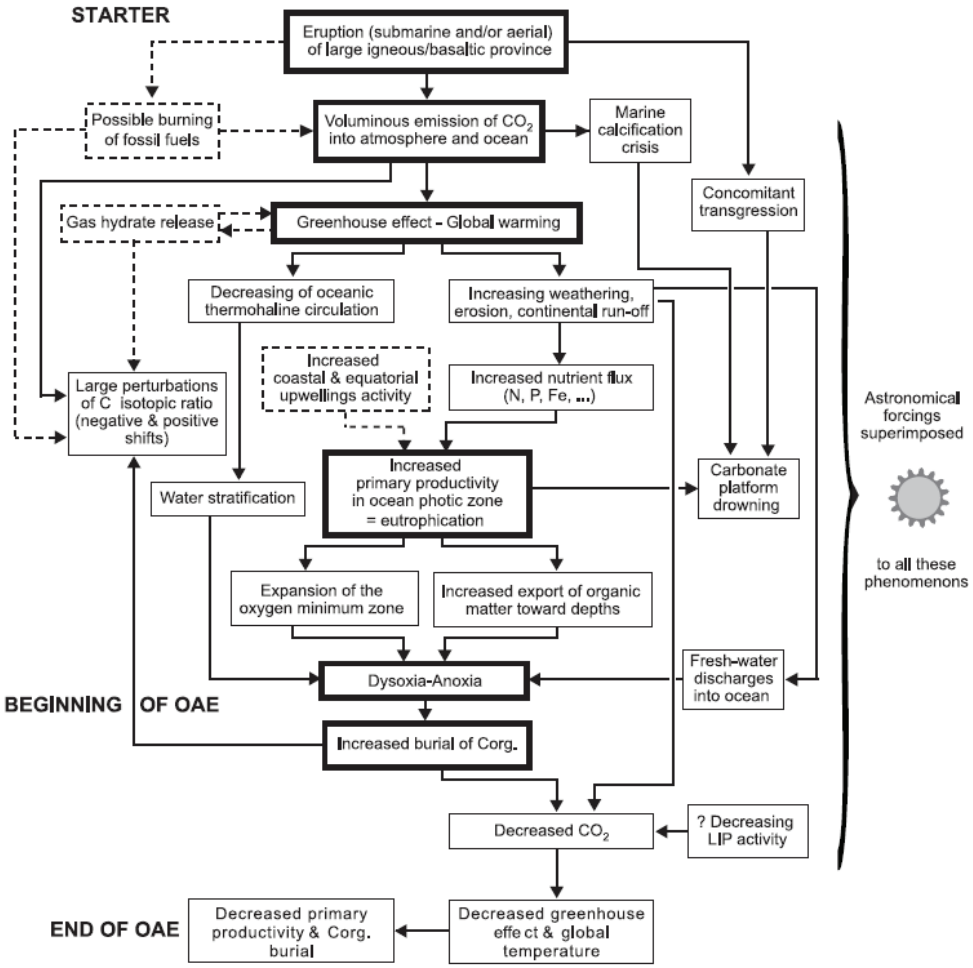

Fig. 8.1. A model displaying the chain of events leading up to anoxic oceanic conditions. The figure is taken from Baudin and Riquier, 2014.

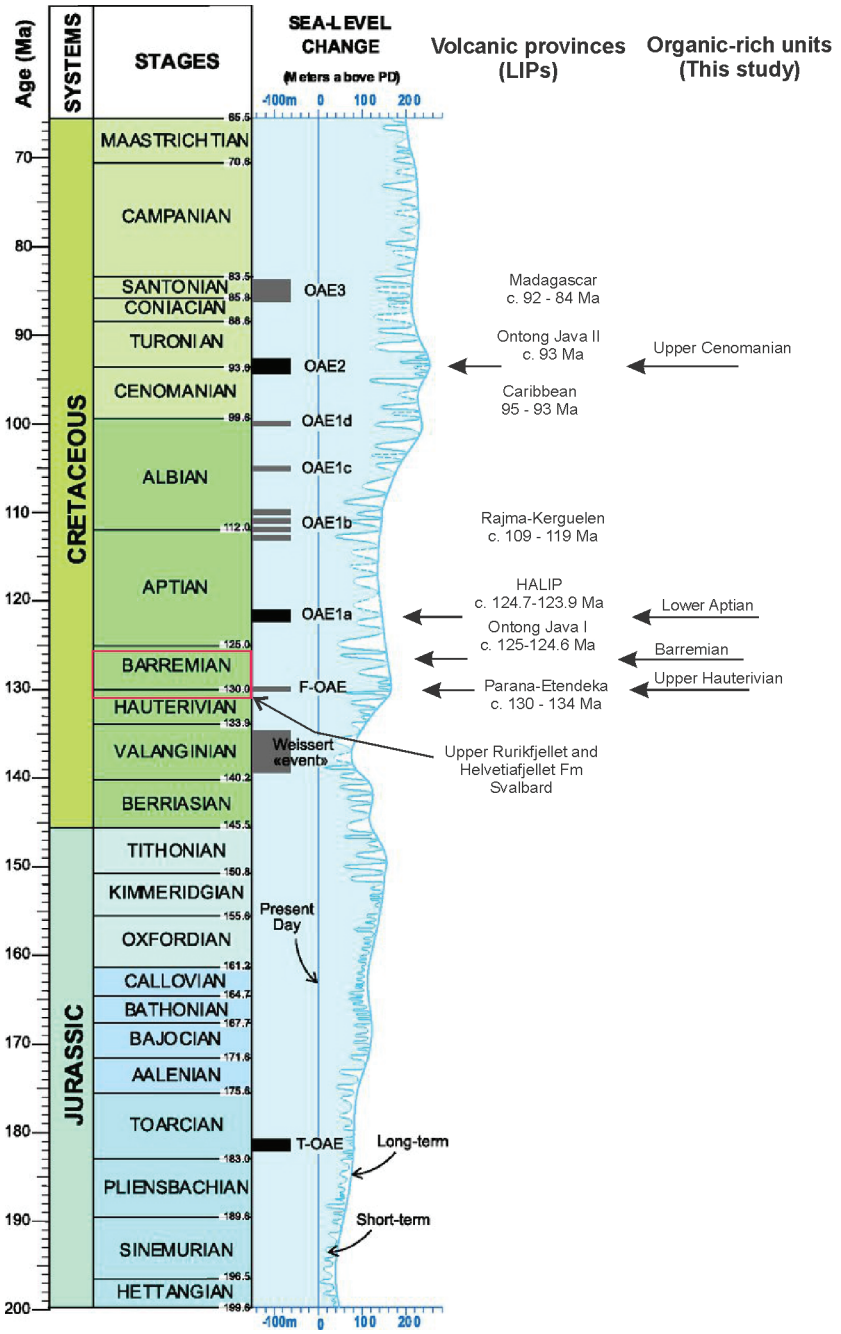

Fig. 8.2. Time scale with annotated Cretaceous OAEs, sea-level curve and occurrence of volcanic provinces (LIPs) and the organic-rich units of this study. The figure is modified after Baudin and Riquier, 2014. Timescale from Gradstein et al. (2012) Sea-level curve is from Haq et al., (1988; 2014). Timing and occurrence of the volcanic provinces are modified after Keller et al. (2021).

8.2.1 Hauterivian

An upper Hauterivian organic-rich unit was established to be present in the shallow Hammerfest Basin on the SW Barents Shelf (well 7120/6-3S and 7120/8-3). This unit display a kerogen Type II composition, testifying to its marine origin and to the occurrence of dysoxic to anoxic bottom water conditions (e.g. Demaison and Moore, 1983). This unit may be time-equivalent to organic-rich units

deposited in response to the so-called Faraoni event (see F-OAE in Fig. 8.2). Most documentation of the F-OAE derives from the Tethyan domain (Godet et al., 2006; Bodin et al., 2009; Baudin and Riquier, 2014). However, organic-rich sediments linked to the event have also been recorded in the Atlantic Ocean, the North Sea, and the Central Pacific region (Baudin and Riquier, 2014). The forcing of anoxic conditions during F-OAE was possibly induced by volcanic activity attributed the main phase of magmatic activity of the Paraná-Etendeka Large Igneous Province (Weissert and Erba, 2004; Erba et al., 2004; Baudin and Riquier, 2014). Another possibility is that the F-OAE is linked to the submarine magma production of the Tristan da Cunha plume, which was dated to c.127 Ma (Baudin and Riquier, 2014). Although temperatures were relatively low in Arctic during early Cretaceous times (Price and Nunn, 2010), elevated productivity was most likely ensured by outgassing during formation of the Paraná-Etendeka LIP, similar to the Tethyan pelagic basins.

There may be a correlation between the upper Hauterivian organic-rich unit and the F-OAE in the Hammerfest Basin. Our findings in Paper I, indicate that this organic-rich unit have similar Rock-Eval characteristics as the ones documented in different Tethyan pelagic basins (Baudin and Riquier, 2014). Although there is a possible connection, the occurrence of anoxia seems dependent on the structural confinement of the basin, as the upper Hauterivian organic-rich unit appear to have less or no potential (i.e. richness and quantity) outside the basin. Thus, the structural configuration and paleoenvironmental conditions that followed with the structural restriction must have played a key role in accumulating organic-rich sediments in the Hammerfest Basin.

Being on the speculative side, organic-rich sediments associated with the F-OAE could also be present in the central depocenter of the Fingerdjupet Subbasin. In contrast to the Hammerfest Basin, no exploration wells have encountered an upper Hauterivian organic-rich unit in this area. However, the seismic horizon presumably representing the Hauterivian organic-rich unit display similar characteristics in this depocenter as the one in the Hammerfest Basin (i.e. seismic horizon iuH; see Paper I). The structural configuration also displays similar characteristics, with a restricted downfaulted half-graben, where sediments thicken towards the main fault complex. On Svalbard, the time-equivalent strata are represented by the uppermost part of the Rurikfjellet Formation. These deposits which was deposited in an open marine environment under well oxygenated conditions and high sedimentation rates does not have any petroleum potential. In their isotope study of the Rurikfjellet Formation, Vickers et al. (2019) indicate an interval in the upper part of the unit which may correspond to the F-OAE, albeit the correlation does not appear very clear.

8.2.2 Barremian

The occurrence of black shales in late early Barremian have been documented in the Boreal Realm and described from the North Sea, the northeastern UK, and northern Germany (Mutterlose et al., 2009; Mulkoc and Mutterlose. 2010; Mutterlose et al., 2014; Wulff et al., 2020). These black shales are not tied to a specific OAE but appear to be linked to supra-regional anoxic bottom waters in an epicontinental basin system cf. Mutterlose et al. (2009; 2014) and Yilmaz et al. (2012). In Paper I, we presented the occurrence of an intra Barremian organic-rich unit in the fault-bounded depocenter of the Hammerfest Basin, SW Barents Shelf (i.e. wells 7120/6-3S and 7120/5-1). This organic-rich units are associated with an elevated gamma ray (GR) signature, often indicating the increased uranium content in organic rich deposits (Rider and Kennedy, 2011). In addition, the Barremian unit display

distinct peaks in TOC values and the Rock-Eval S2 parameter, which coincide with the negative reflector (seismic horizon IB; Hagset et al., 2022). A similar organic-rich unit could also be present in a more condensed variety in well 6407/1-3 on the mid-Norwegian margin (see IB in Fig. 2. of Hagset et al., 2023). On Svalbard, the occurrence of coals and coaly shales occur in the Barremian to lower Aptian succession of the Helvetiafjellet Formation (e.g. Midtkandal et al., 2007; Grundvåg et al., 2019). These organic rich deposits consist of a predominance of terrestrial organic matter with limited marine influence, and therefore holds a limited potential with respect to recognizing OAEs.

It could be speculated that the anoxic bottom water conditions associated with the black shales documented elsewhere in the Boreal Realm (Mutterlose et al., 2009; 2014) also extended into the SW Barents Shelf. However, there is currently no data to support this. It rather appears that the development of the Barremian organic-rich unit was dependent on the structural confinement in fault-bounded depocenters of the Hammerfest Basin. Despite the dens population of exploration wells in the Hammerfest Basin, no Barremian organic-rich units is documented outside this depocenter (Hagset et al., 2022, i.e. Paper I). This also the case on the mid-Norwegian margin, where most exploration wells on the more unrestricted Halten Terrace do not display any signs of a Barremian organic-rich unit.

8.2.3 Aptian

The early Aptian OAE1a event, is one of two OAEs that extended across the oceans at a global scale (Schlanger and Jenkyns, 1976; Jenkyns, 1980; Jenkyns, 2010). The formation of OAE1a can be correlated to the eruption of the Pacific Ontong-Java Plateau (Fig. 8.2) (Tejada et al., 2009). In addition, the development of the High Arctic LIP (HALIP) could also have contributed to the development of global oceanic anoxia. In Svalbard, the HALIP is manifested as mostly basaltic sills assigned to the Diabasodden suit (Dallmann et al., 1999). Corfu et al. (2013) determined the ages of mafic sills and felsic tuff on Svalbard. Their results indicate crystallization of the Diabasodden sill at 124 (+/-) 0.2 Ma, the Linnèvatn sill at 124.7 +- 0.3 Ma (with secondary younger titanite with the age of 123.9 (+-) 0.3 Ma. These ages appear to coincide with the occurrence of OAE1a (Fig. 8.2). Hence, substantial volcanic activity during the formation of the HALIP, could have regional implications with respect to deposition of lower Aptian organic-rich units on the NCS.

On the SW Barents Shelf the lower Aptian organic-rich unit in well 7321/9-1 was established to be an early mature source rock unit. The organic matter in this source rock exhibits a kerogen Type II composition and display high hydrogen and low oxygen content, indicating that the source rock is of high quality. This unit was deposited in shallow half-grabens in the transition from Fingerdjupet Subbasin to the Bjarmeland Platform. As such, the structural confinement of the basin yet again seems to be the main control for organic-rich units to develop.

On the mid-Norwegian margin, the lower Aptian organic-rich unit could occur on the Halten and Dønna terraces as condensed organic-rich units, or even more thicker units in smaller intra-shelf downfaulted segments. However, based on our investigation, their potential seems limited due to high sedimentation rates, erosion on the uplifted terraces, and reoccurring oxygenated condition. Signatures corresponding to the OAE1a also appear to be recorded in the deeper Vøring Basin (well 6608/2-1S; see Zastrozhnov et al., 2020).

On Svalbard, the OAE1a is recorded in an organic-rich mudstone unit in the lower part of the Carolinefjellet Formation in boreholes drilled in relation to the UNIS CO_2 storage project as well as in outcrops across most of the Lower Cretaceous outcrop belt on Spitsbergen (Midtkandal et al.,2016; Grundvåg et al.,2019). These organic-rich mudstones were deposited during a regional extensive flooding event on a restricted marine shelf that develop immediately after the retreat and drowning of the Helvetiafjellet Formation paralic system. The mudstone unit, which hold some source rock potential, appear to be gas condensate prone (Grundvåg et al., 2019). It may be speculated that the development of LIPs in the Pacific and in the Arctic might have contributed to the establishment of an eustatically high sea-level which forced the shoreline to retreat and thus promoted the establishment of shallow shelf conditions across the region, and increased atmospheric CO2 concentrations, which together caused widespread anoxia and deposition of organic-rich sediments even at high latitudes.

8.2.4 Cenomanian

The OAE2 is represented by organic-rich shales across an interval spanning the Cenomanian/ Turonian boundary and appear to be distributed on a global scale (Schlanger et al., 1987; Arthur et al., 1987; 1988; Beil et al., 2020). On the mid-Norwegian margin, the upper Cenomanian organic-rich unit (Fig. 8.2) have the greatest potential on the Halten Terrace and the Sklinna High, exhibiting a kerogen Type III-II composition. Thus, conforming to the model proposed by Arthur et al. (1987) where most of these organic-rich shales appear in shallow to intermediate water levels. The occurrence of OAE2 might be prolonged in coastal upwelling zones because of higher pre-existing productivity and well-developed midwater OMZ (Arthur et al., 1987). However, the relative sea-level high stand at the Cenomanian/Turonian boundary increased the extent and distribution of epicontinental shelf and shallow basins worldwide (Schlanger and Jenkyns, 1976). This would imply that larger areas of epicontinental shelfs, and basins was characterized by shallow water depths, which had high evaporation rates and surface water productivity, thus expanding the midwater OMZ (Arthur et al., 1987). Thus, the occurrence of the upper Cenomanian organic-rich unit appear to be less dependent on the structural confinement of a basin, but more on the global eustatic sea-level highstand and the occurrence of OAE2 on the mid-Norwegian Margin.

The oceanic deep-water circulation and productivity responded to the rapid transgressive development during the Cenomanian/Turonian transition (Arthur et al., 1987). Deep-water environments were most likely oxygenated but could experience short-lived anoxic conditions during more sluggish water circulation accompanied by the highest periods surface productivity which would intensify the OMZ (Arthur et al., 1987). However, although dysoxic to anoxic waters may have been induced, the massive sediment input, hindered the development and preservation of substantial amounts of quantities of organic matter associated with OAE2 in the deep Cretaceous basins on the NCS. Although, there is limited well data from the deeper segments of these basins, our current datasets indicate that the potential of this unit appear limited. This is especially evident on the SW Barents Shelf, where no exploration wells have yet encountered significant concentrations of organic matter at the Cenomanian/Turonian boundary interval.

In Svalbard and large parts of the wider Barents Shelf, middle to Upper Cretaceous strata are not present due to recurring uplift and glaciations during the Cenozoic (Dörr et al., 2012; Olaussen et al., 2022; Lasabuda et al., 2021).

9 Implications and concluding remarks

This study documents the lateral variability and potential of four Lower Cretaceous source rocks in the deep to shallow marginal basins along the SW Barents and mid-Norwegian shelves. These are the: upper Hauterivian, Barremian, lower Aptian and the upper Cenomanian organic-rich units. The distribution and development of these organic-rich units are mainly controlled by the occurrence of sub-oxic to anoxic conditions. These conditions could only develop sufficiently in structural confined settings, such as rift basins where the development of grabens and half-grabens occur. The occurrence of OAEs, eustatic highstand, and the relatively warm greenhouse climate promoted anoxic conditions in these restricted basins. The geochemical/Rock-Eval data indicates that there is a local petroleum potential in these fault bounded depocenters. This study has thus improved the understanding of changing conditions and basinal settings involved in the formation of Lower to middle Cretaceous organic-rich units, potentially reducing exploration risk in the frontier areas of the NCS.

9.1 Future research

Future research may focus on the link between the OAEs and the occurrence of organic-rich units on a regional scale, coupling the data from the exploration wells on the SW Barents Shelf to the excellent exposed outcrops on Svalbard. Such studies should utilize carbon and oxygen isotope methods along with biostratification. As such, the proposed study could potentially lay the groundwork for understanding global OAEs at higher latitudes. Furthermore, it may also elucidate the connection between the development of the HALIP and the deposition of organic rich sediments on the Barents Shelf.

Further research could also take on a more geophysical approach, involving rock physical modelling, seismic inversion, amplitude variation with offset (AVO) and 3D seismic attributes. This will allow to estimate the lateral variations in physical properties of the potential source rock units. The large spacing between the regional 2D seismic lines used in this study, makes it difficult to map the organic-rich units in detail. As such, the use of 3D seismic data could better determine the properties and lateral variability of potential source rock units on a smaller scale. The proposed study, could thus be a valuable contribution on the potential of Lower Cretaceous organic-rich units.

10 References

Arthur, M.A., Dean, W.E., Pratt, L.M., 1988. Geochemical and climatic effects of increased marine organic carbon burial at the Cenomanian/Turonian boundary. Nature 335 (6192), 714–717. https://doi.org/10.1038/335714a0.

Arthur, M.A., Schlanger, S.O., Jenkyns, H.C., 1987. The Cenomanian-Turonian Oceanic Anoxic Event, II. Palaeoceanographic controls on organic-matter production and preservation. In: Brooks, J., Fleet, A.J. (Eds.), Marine Petroleum Source Rocks. Geological Society, London, Special Publications. 26. Blackwell Scientific Publications, London, pp. 401–420

Baudin, F., Riquier, L., 2014. The Late Hauterivian Faraoni 'Oceanic Anoxic Event': an update. Bulletin de la Société Géologique de France; 185 (6): 359–377. https://doi.org/10.2113/gssgfbull.185.6.359

Beil, S., Kuhnt, W., Holbourn, A., Scholz, F., Oxmann, J., Wallmann, K., Lorenzen, J., Aquit, M., Chellai, E.H., 2020. Cretaceous Oceanic Anoxic events prolonged by phosphorus cycle feedbacks. Clim. Past 16, 757–782.

Blystad, P., Færseth, R.B., Larsen, B.T., Skogseid, J., Tørudbakken, B., 1995. Structural elements of the Norwegian continental shelf. Part II: the Norwegian Sea Region. Norwegian Petroleum Directorate Bulletin 8, 45p.

Bodin, S., Fiet, N., Godet, A., Matera, V., Westermann, S., Clément, A., Janssen, N.M.M., Stille, P., Föllmi, K.B., 2009. Early Cretaceous (late Berriasian to early Aptian) palaeoceanographic change along the northwestern Tethyan margin (Vocontian Trough, southeastern France): d13C, d18O and Sr-isotope belemnite and whole-rock records. Cretaceous Research 30, 1247-1262.

Bohacs, K.M., Jr, G.J.G., Carroll, A.R., Mankiewicz, P.J., Miskell-Gerhardt, K.J., Schwalbach, J.R., Wegner, M.B., Simo, J.A.T., 2005. Production, destruction and dilution–the many paths to source-rock development. Soc. Sediment. Geol. 82, 61–101.

Brekke, H., 2000. The tectonic evolution of the Norwegian sea continental margin with emphasis on the Vøring and More basins. Geological Society, London, Special Publications 167 (1), 327–378. https://doi.org/10.1144/gsl.sp.2000.167.01.13.

Brekke, H., Dahlgren, S., Nyland, B., Magnus, C., 1999. The prospectivity of the Vøring and Møre basins on the Norwegian continental margin. In: Fleet, A.J., Boldy, S.A.R. (Eds.), Petroleum Geology of Northwest Europe: Proceedings of the 5th Conference. Geological Society of London, pp. 231–246.

Brown, A. R., 2011. Interpretation of three-dimensional seismic data. Society of Exploration Geophysicists and American Association of Petroleum Geologists.

Cavalheiro, L., Wagner, T., Steinig, S., Bottini, C., Dummann, W., Esegbue, O., Gambacorta, G., Giraldo-G´omez, V., Farnsworth, A., Flögel, S., Hofmann, P., Lunt, D. J., Rethemeyer, J., Torricelli, S., Erba, E., 2021. Impact of global cooling on Early Cretaceous high pCO2 world during the Weissert Event. Nat. Commun. 12, 1–11. https://doi.org/10.1038/s41467-41021-25706-41460.

Cedeño, A., Ohm, S., Escalona, A., Marín, D., Olaussen, S., Demchuck, T., 2021. Upper Jurassic to Lower Cretaceous Source Rocks in the Norwegian Barents Sea, Part I: Organic Geochemical, Petrographic, and Paleogeographic Investigations.

Clayton, J. L., Swetland, P. J., 1978. Subaerial weathering of sedimentary organic matter. Geochim. cosmochim. Acta 42, 305-312

Coccioni, R., Luciani, V., Marsili, A., 2006. Cretaceous oceanic anoxic events and radially elongated chambered planktonic foraminifera: paleoecological and paleoceanographic implications. Palaeogeography, Palaeoclimatology, Palaeoecology 235, 66-92.

Corfu, F., Polteau, S., Planke, S., Faleide, J.I., Svensen, H., Zayoncheck, A., Stolbov, N., 2013. U–Pb geochronology of cretaceous magmatism on svalbard and Franz Josef land, Barents sea large igneous province. Geol. Mag. 150, 1127–1135.

Dalland, A., Worsley, D., Ofstad, K., 1988. A Lithostratigraphic scheme for the Mesozoic and Cenozoic succession offshore mid- and northern Norway. Norwegian Petrol. Direct. Bull. 4.

Dallmann, W.K., Dypvik, H., Gjelberg, J.G., Harland, W.B., Johannessen, E.P., Keilen, H.B., Larssen, G.B., Lønøy, A., Midbøe, P.S., Mørk, A., Nagy, J., Nilsson, I., Nøttvedt, A., Olaussen, S., Pcelina, T.M., Steel, R.J., Worsley, D.,

1999. Lithostratigraphic Lexicon of Svalbard: Review and Recommendations for Nomenclature Use. Norsk Polarinstitutt, Tromsø (318 pp.).

Dembicki, H., 2016. Practical Petroleum Geochemistry for Exploration and Production. Elsevier, p. 342.

Doré, A.G., 1995. Barents Sea geology, petroleum resources and commercial potential. Arctic 48, 207–221.

Doré, A.G., Lundin, E.R., Birkeland, Ø., Eliassen, P.E., Jensen, L.N., 1997. The NE Atlantic Margin: implications of late Mesozoic and Cenozoic events for hydrocarbon prospectivity. Petrol. Geosci. 3, 117–131.

Doré, A.G., Lundin, E.R., Jensen, L.N., Birkeland, Ø., Eliassen, P.E., Fichler, C., 1999. Principal tectonic events in the evolution of the northwest European Atlantic margin, 1. In: Geological Society, London, Petroleum Geology Conference Series, vol. 5. Geological Society of London, pp. 41–61.

Demaison, G.J., Hoick, A.J.J., Jones, R.W., Moore, G.T., 1983. Predictive source bed stratigraphy: a guide to regional petroleum occurrence. In: Proceedings of the 11th World Petroleum Congress, vol. 2. John Wiley & Sons, Ltd., London, p. 17.

Demaison, G.J., Moore, G.T., 1980. Anoxic environments and oil source bed genesis. AAPG (Am. Assoc. Pet. Geol.) Bull. 64, 1179–1209.

Dörr, N., Lisker, F., Clift, P.D., Carter, A., Gee, D.G., Tebenkov, A.M., Spiegel, C., 2012. Late Mesozoic–Cenozoic exhumation history of northern Svalbard and its regional significance: constraints from apatite fission track analysis. Tectonophysics 514–517, 81–92. http://dx.doi.org/10.1016/j.tecto.2011.10.007.

Erba, E., Bartolini, A., Larson, R.L., 2004. Valanginian Weissert oceanic anoxic event. Geology 32, 149-152.

Espitalié, J., Madec, M., Tissot, B., Mennig, J.J., Leplat, P., 1977. Source rock characterization method for petroleum exploration. Paper OTC (Offshore Technology Conference) 2935, 439–444.

Faleide, J.I., Bjørlykke, K., Gabrielsen, R.H., 2015. Geology of the Norwegian continental shelf. In: Bjørlykke, K. (Ed.), Petroleum Geoscience: from Sedimentary Environments to Rock Physics. Springer Berlin Heidelberg, Berlin, pp. 603–637.

Faleide, J.I., Gudlaugsson, S., Jacquart, G., 1984. Evolution of the western Barents Sea. Mar. Petrol. Geol. 1, 123–150.

Faleide, J.I., Vågnes, E., Gudlaugsson, S.T., 1993a. Late mesozoic-cenozoic evolution of the southwestern Barents Sea. Geol. Soc. Lond. Pet. Geol. Conf. Ser. 4, 933–950.

Faleide, J.I., Vagnes, E., Gudlaugsson, S.T., 1993b. Late mesozoic-cenozoic evolution of the south-western Barents Sea in a regional rift shear tectonic setting. Mar. Petrol. Geol. 10, 186–214.

Forsberg, A., Bjorøy, M., 1983. A sedimentological and organic geochemical study of the Botneheia Formation, Svalbard, with special emphasis on the effects of weathering on the organic matter in shales. In Bjorøy, M. et al. (edit.) Advances in organic geochemistry 1981,60-68. London: Wiley & sons Lid.

Færseth, R.B., Lien, T., 2002. Cretaceous evolution in the Norwegian Sea – a period characterized by tectonic quiescence. Mar. Petrol. Geol. 19, 1005–1027. https://doi. org/10.1016/S0264-8172(02)00112-5.

Gabrielsen, R.H., Færseth, R.B., Jensen, L.N., Kalheim, J.E., Riis, F., 1990. Structural elements of the Norwegian continental shelf. Part 1: the Barents Sea region. NPD Bull 6, 33.

Gawthorpe, R.L., Leeder, M.R., 2000. Tectono-sedimentary evolution of active extensional basins. Basin Res 12, 195–218.

Gjelberg, J., Steel, R.J., 1995. Helvetiafjellet formation (Barremian-Aptian), spitsbergen: characteristics of a transgressive succession. In: Steel, R.J., Felt, V.L., Johannesen, E.P., Mathieu, C. (Eds.), Sequence Stratigraphy on the Northwest European Margin. Elsevier, Amsterdam, pp. 571–593.

Godet, A., Bodin, S., Föllmi, K.B., Vermeulen, J., Gardin, S., Fiet, N., Adatte, T., Berner, Z., Stüben, D., van de Schootbrugge, B., 2006. Evolution of the marine stable carbon-isotope record during the early Cretaceous: a focus on the late Hauterivian and Barremian in the Tethyan realm. Earth and Planetary Science Letters 242, 254-271.

Gradstein, F.M., Anthonissen, E., Brunstad, H., Charnock, M., Hammer, O., Hellem, T., Lervik, K.S., 2010. Norwegian offshore stratigraphic lexicon (NORLEX). Newsl. Stratigr. 44, 73–86.

Gradstein, F.M., Ogg, J.G., Sschmitz, K., Ogg, G., 2012. The geologic time scale 2012, vol. 2. – Elsevier, Amsterdam, 1144 pp.

Grundvåg, S.-A., Jelby, M.E., Olaussen, S., Śliwińska, K.K., 2020. The role of shelf morphology on storm-bed variability and stratigraphic architecture, Lower Cretaceous, Svalbard. Sedimentology. 68, 196-237. https://doi.org/10.1111/sed.12791

Grundvåg, S.A., Jelby, M.E., Śliwińska, K.K., Nohr-Hansen, H., Aadland, T., Sandvik, S.E., Tennvassas, I., Engen, T., Olaussen, S., 2019. Sedimentology and palynology of the Lower Cretaceous succession of central Spitsbergen: integration of subsurface and outcrop data. Norw. J. Geol. 99, 253–284.

Grundvåg, S.A., Marín, D., Kairanov, B., Śliwińska, K.K., Nøhr-Hansen, H., Jelby, M.E., Escalona, A., Olaussen, S., 2017. The lower cretaceous succession of the northwestern Barents shelf: onshore and offshore correlations. Mar. Petrol. Geol. 86, 834–857.

Hagset, A., Grundvåg, S.A., Badics, B., Davies, R., Rotevatn, A., 2022. Tracing lower cretaceous organic-rich units across the SW Barents shelf. Mar. Petrol. Geol. 140, 105664.

Hagset, A., Grundvåg, S.-A., Badics, B., Davies, R., & Rotevatn, A., 2023. Deposition of Cenomanian – Turonian organic-rich units on the mid-Norwegian Margin: controlling factors and regional implications. Mar. Petrol. Geol. 149, 106102. *https://doi.org/10.1016/j.marpetgeo.2023.106102*

Haq, B.U., 2014. Cretaceous eustasy revisited. Global Planet. Change 113, 44–58. https://doi.org/10.1016/j.gloplacha.2013.12.007.

Haq, B.U., Hardenbol, J., Vail, P.R., 1987. Chronology of fluctuating sea levels since the Triassic (250 million years ago to present). Science 235, 1156–1166.

Ibach, L.E.J., 1982. Relationship between sedimentation-rate and total organic-carbon content in ancient marine-sediments. AAPG (Am. Assoc. Pet. Geol.) Bull. 66, 170–188.

IEA (2022), How to Avoid Gas Shortages in the European Union in 2023, IEA, Paris. https://www.iea.org/reports/how-to-avoid-gas-shortages-in-the-european-union-in-2023 License: CC BY 4.0

Jelby, M.E., Grundvåg, S.-A., Helland-Hansen, W., Olaussen, S., Stemmerik, L., 2020. Tempestite facies variability and storm-depositional processes across a wide ramp: towards a polygenetic model for hummocky cross-stratification. Sedimentology 67, 742–781.

Jenkyns, H.C., 1980. Cretaceous anoxic events - from continents to oceans. J. Geol. Soc. 137, 171–188.

Jenkyns, H.C., 2010. Geochemistry of oceanic anoxic events. Geochem. Geophys. Geosyst. 11. http://dx.doi.org/10.1029/2009GC002788.

Jenkyns, H.C., 1999. Mesozoic anoxic events and palaeoclimate. Zbl. Geol. Paläontol. 943–949, 1997

Kairanov, B., Escalona, A., Norton, I., Abrahamson, P., 2021. Early cretaceous evolution of the Tromsø basin, SW Barents Sea, Norway. Mar. Petrol. Geol. 123, 104–714.

Katz, B., 2005. Controlling factors on source rock development—a review of productivity, preservation, and sedimentation rate. Soci. Sed. Geol. 82, 7–16.

Keller, G., Nagori, M.L., Chaudhary, M., Nallapa Reddy, A., Jaiprakash, B.C., Spangenberg, J.E., Mateo, P., Adatte, T., 2021. Cenomanian – Turonian sea-level transgression and OAE2 deposition in the Western Narmada Basin, India. Gondwana Res. 94, 73–86. https://doi.org/10.1016/j.gr..2021.02.013.

Lasabuda, A.P.E., Johansen, N.S., Laberg, J.S., Faleide, J.I., Senger, K., Rydningen, T.A., Patton, H., Knutsen, S.M., Hanssen, A., 2021. Cenozoic uplift and erosion of the Norwegian Barents Shelf-A review. Earth Sci. Rev. 217, 103609.

Leckie, R.M., Bralower, T.J., Cashman, R., 2002. Oceanic anoxic events and plankton evolution: biotic response to tectonic forcing during the mid-Cretaceous. Paleoceanography 17, 1–29.

Leith, T.L., Weiss, H.M., Mørk, A., Århus, N., Elvebakk, G., Embry, A.F., Brooks, P.W., Stewart, K.R., Pchelina, T.M., Bro, E.G., Verba, M.L., Danyushevskaya, A., Borisov, A.V., 1993. Mesozoic hydrocarbon source rocks of the

Arctic region. In: Vorren, T.O., Bergsager, E., Dahl-Stamnes, A., Holter, E., Johansen, Å., Lie, Å., Lund, T.B. (Eds.), Arctic Geology and Petroleum Potential. Elsevier, Amsterdam, pp. 1–25.

Lerch, B., Karlsen, D.A., Seland, R., Backer-Owe, K., 2017. Depositional environment and age determination of oils and condensates from the Barents Sea. Petrol. Geosci. 23, 190–209.

Løseth, H., Wensaas, L., Gading, M., Duffaut, K., Springer, M., 2011. Can hydrocarbon source rocks be identified on seismic data? Geology 39, 1167–1170.

Marín, D., Escalona, A., Śliwińska, K.K., Nohr-Hansen, H., Mordasova, A., 2017. Sequence stratigraphy and lateral variability of Lower Cretaceous clinoforms in the southwestern Barents Sea. AAPG (Am. Assoc. Pet. Geol.) Bull. 101, 1487–1517.

Marín, D., Escalona, A., Grundvåg, S.A., Nohr-Hansen, H., Kairanov, B., 2018a. Effects of adjacent fault systems on drainage patterns and evolution of uplifted rift shoulders: the Lower Cretaceous in the Loppa High, southwestern Barents Sea. Mar. Petrol. Geol. 94, 212–229.

Marín, D., Escalona, A., Grundvåg, S.A., Olaussen, S., Sandvik, S., Śliwińska, K.K., 2018b. Unravelling key controls on the rift climax to post-rift fill of marine rift basins: insights from 3D seismic analysis of the Lower Cretaceous of the Hammerfest Basin, SW Barents Sea. Basin Res 30, 587–612.

Marín, D., Helleren, S., Escalona, A., Olaussen, S., Cede˜no, A., Nøhr-Hansen, H., Ohm, S., 2020. The Middle Jurassic to lowermost Cretaceous in the SW Barents Sea: interplay between tectonics, coarse-grained sediment supply and organic matter preservation. Basin Res. 33 (2), 1033–1055. https://doi.org/10.1111/bre.12504.

Matapour, Z., Karlsen, D.A., 2017. Ages of Norwegian oils and bitumen based on agespecific biomarkers. Petrol. Geosci. 24, 92–101. https://doi.org/10.1144/ petgeo2016–119.

Midtkandal, I., Nystuen, J.P., 2009. Depositional architecture of a low-gradient ramp shelf in an epicontinental sea: the lower Cretaceous of Svalbard. Basin Res. 21, 655–675. http://dx.doi.org/10.1111/j.1365-2117.2009.00399.x.

Midtkandal, I., Nystuen, J.P., Nagy, J., 2007. Paralic sedimentation on an epicontinental ramp shelf during a full cycle of relative sea-level fluctuation; the Helvetiafjellet Formation in Nordenskiöld Land, Spitsbergen. Nor. J. Geol. 87, 343–359.

Midtkandal, I., Svensen, H.H., Planke, S., Corfu, F., Polteau, S., Torsvik, T.H., Faleide, J. I., Grundvåg, S.A., Selnes, H., Kurschner, W., Olaussen, S., 2016. The aptian (early cretaceous) oceanic anoxic event (0AE1a) in svalbard, Barents Sea, and the absolute age of the barremian-aptian boundary. Palaeogeogr. Palaeocl. 463, 126–135.

Miller, K.G., Kominz, M.A., Browning, J.V., Wright, J.D., Mountain, G.S., Katz, M.E., Sugarman, P.J., Cramer, B.S., Christie-Blick, N., Pekar, S.F., 2005. The Phanerozoic record of global sea-level change. Science 310, 1293-1298.

Mitchum, R.M.J., Vail, P.R., Sangree, J.B., 1977. Seismic stratigraphy and global changes of sea-level, part 6: stratigraphic interpretation of seismic reflection patterns in depositional sequences. In: Payton, C. (Ed.), Seismic Stratigraphy – Applications to Hydrocarbon Exploration, vol. 26. Mem. - Am. Assoc. Pet. Geol., pp. 117–133.

Mulkoc, M., Mutterlose, J., 2010. The Early Barremian warm pule and the Late Barremian cooling: a high-resolution geochemical record of the boreal realm. Palaios, 25, 14-23.

Mutterlose, J., Pauly, S., & Steuber, T., 2009. Temperature controlled deposition of early Cretaceous (Barremian–early Aptian) black shales in an epicontinental sea. Palaeogeography, Palaeoclimatology, Palaeoecology, 273(3-4), 330-345.

Mutterlose, J., Bodin, S., & Fähnrich, L., 2014. Strontium-isotope stratigraphy of the Early Cretaceous (Valanginian–Barremian): implications for Boreal–Tethys correlation and paleoclimate. Cretaceous Research, 50, 252-263.

Nemec, W., Steel, R.J., Gjelberg, J., Collinson, J.D., Prestholm, E., Øxnevad, I.E., 1988. Anatomy of collapsed and re-established delta front in Lower Cretaceous of Eastern Spitsbergen: gravitational sliding and sedimentation process. AAPG Bull. 72, 454–476.

Ohm, S.E., Karlsen, D.A., Austin, T.J.F., 2008. Geochemically driven exploration models in uplifted areas: examples from the Norwegian Barents Sea. AAPG (Am. Assoc. Pet. Geol.) Bull. 92, 1191–1223.

Olaussen, S., Grundvåg, S-A., Senger, K., Anell, I., Betlem, P., Birchall T., Braathen, A., Dallmann, W., Jochmann, M., Johannessen, E. P., Lord G., Mørk, A., Osmundsen, P. T., Smyrak-Sikora, A. and Stemmerik, L., 2022. The

Svalbard Carboniferous to Cenozoic Composite Tectono-Stratigraphic Element. Geological Society, London, Memoirs, 57 (1), M57-2021-36. https://doi.org/10.1144/M57-2021-36.

Olaussen, S., Larssen, G.B., Helland-Hansen, W., Johannessen, E.P., Nøttvedt, A., Riis, F., Rismyhr, B., Smelror, M., Worsley, D., 2018. Mesozoic strata of Kong Karls land, svalbard, Norway; a link to the northern Barents Sea basins and platforms. Norw. J. Geol. 98 (4), 1–70. https://doi.org/10.17850/njg98-4-06.

Onderdonk, N., Midtkandal, I., 2010. Mechanisms of collapse of the cretaceous Helvetiafjellet Formation at kvalvågen, eastern spitsbergen. Mar. Petrol. Geol. 27, 2118–2140.

Parker, J.R., 1967. The jurassic and cretaceous sequence in spitsbergen. Geol. Mag. 104, 487–505.

Pedersen, T.F., Calvert, S.E., 1990. Anoxia vs productivity - what controls the formation of organic-carbon-rich sediments and sedimentary-rocks. AAPG (Am. Assoc. Pet. Geol.) Bull. 74, 454–466.

Peters, K.E., 1986. Guidelines for evaluating petroleum source rock using programmed pyrolysis. AAPG (Am. Assoc. Pet. Geol.) Bull. 70, 318–329.

Peters, K.E., Cassa, M.R., 1994. Applied source rock geochemistry. In: Magoon, L.B., Dow, W.G. (Eds.), The Petroleum System - from Source to Trap. AAPG, pp. 93–120.

Price, G.D., Nunn, E.V., 2010. Valanginian isotope variation in glendonites and belemnites from the Arctic Svalbard: transient glacial temperatures during the Cretaceous greenhouse. Geology 38, 251-254.

Prosser, S., 1993. Rift-related linked depositional systems and their seismic expression. Geological Society, London, Special Publications, 71(1), 35-66.

Rider, M.H., Kennedy, M., 2011. The Geological Interpretation of Well Logs, third ed. Rider-French, Scotland.

Rotevatn, A., Kristensen, T.B., Ksienzyk, A.K., Wemmer, K., Henstra, G.A., Midtkandal, I., Grundvåg, S.-A., Andresen, A., 2018. Structural inheritance and rapid rift-length establishment in a multiphase rift: the East Greenland rift system and its Caledonian orogenic ancestry. Tectonics 37, 1858–1875. https://doi.org/10.1029/ 2018TC005018.

Saller, A., Lin, R., Dunham, J., 2006. Leaves in turbidite sands: the main source of oil and gas in the deep-water Kutei Basin, Indonesia. AAPG (Am. Assoc. Pet. Geol.) Bull. 90, 1585–1608.

Sattar, N., Juhlin, C., Koyi, H., Ahmad, N., 2017. Seismic stratigraphy and hydrocarbon prospectivity of the lower cretaceous Knurr sandstone lobes along the southern margin of Loppa high, Hammerfest basin, Barents Sea. Mar. Petrol. Geol. 85, 54–69.

Scotese, C.R., Song, H., Mills, B.J.W., van der Meer, D.G., 2021. Phanerozoic paleotemperatures: the earth′s changing climate during the last 540 million years. Earth Sci. Rev. 215, 103–503.

Schlanger, S.O., Arthur, M.A., Jenkyns, H.C., Scholle, P.A., 1987. The Cenomanian- Turonian Oceanic Anoxic Event, I. Stratigraphy and distribution of organic carbon-rich beds and the marine δ13C excursion. Geol. Soc. Lond. Spec. Publ. 26 (1), 371–399. https://doi.org/10.1144/GSL.SP.1987.026.01.24.

Schlanger, S.O., Jenkyns, H.C., 1976. Cretaceous oceanic anoxic events: causes and consequences. Geol. Mijnbouw 55, 179–184.

Seldal, J., 2005. Lower Cretaceous: the next target for oil exploration in the Barents Sea? Petrol. Geol. Conf. Proceed. 231–240.

Serck, C.S., Faleide, J.I., Braathen, A., Kjølhamar, B., Escalona, A., 2017. Jurassic to early cretaceous basin configuration(s) in the Fingerdjupet Subbasin, SW Barents Sea. Mar. Petrol. Geol. 86, 874–891.

Smelror, M., Petrov, O.V., Larssen, G.B., Werner, S., Norway, G.S.o., 2009. Geological history of the Barents Sea: atlas. Geological Survey of Norway 1–135.

Steel, R.J., Worsley, D., 1984. Svalbard's post-Caledonian strata e an atlas of sedimentational patterns and palaeogeographic evolution. In: Spencer, A.M. (Ed.), Petroleum Geology of the North European Margin. Norwegian Petroleum Society. Graham and Trotman Ltd, pp. 109–135.

Tejada, M.L.G., Suzuki, K., Kuroda, J., Coccioni, R., Mahoney, J.J., Ohkouchi, N., Sakamoto, T.,Tatsumi, Y., 2009. Ontong Java Plateau eruption as a trigger for the early Aptian oceanic anoxic event. Geology 37, 855–858. http://dx.doi.org/10.1130/G25763A.1.

Tissot, B., Welte, D., 1984. Petroleum Formation and Occurrence 219. Springer Verlag, New York, p. 699.

Vail, P., 1987. Seismic stratigraphy interpretation using sequence stratigraphy, part I, seismic stratigraphy interpretation procedure. In: Bally, A. (Ed.), Atlas of Seismic Stratigraphy, vol. 1. AAPG Studies in Geology, pp. 271-310.

Veeken, P.C.H., 2007. Seismic Stratigraphy, Basin Analysis and Reservoir Characterisation. Elsevier, Amsterdam. p. 453.

Vickers, M. L., Price, G. D., Jerrett, R. M., Sutton, P., Watkinson, M. P., & FitzPatrick, M. (2019). The duration and magnitude of Cretaceous cool events: Evidence from the northern high latitudes. GSA Bulletin, 131(11-12), 1979-1994.

Weissert, H., Erba, E. 2004: Volcanism, CO_2 and palaeoclimate: a Late Jurassic-Early Cretaceous carbon and oxygen isotope record. J. Geol. Soc. 161, 695-702

Way, R., Ives, M. C., Mealy, P., & Farmer, J. D., 2022. Empirically grounded technology forecasts and the energy transition. *Joule*, *6*(9), 2057-2082.

Wulff, L., Mutterlose, J., & Bornemann, A., 2020. Size variations and abundance patterns of calcareous nannofossils in mid Barremian black shales of the Boreal Realm (Lower Saxony Basin). Marine Micropaleontology, 156, 101853.

Yilmaz, I.O., Altiner, D., Tekin, U.K., Ocakoglu, F., 2012. The first record of the “Mid-Barremian” Oceanic Anoxic Event and the Late Hauterivian platform drowning of the Bilecik platform, Sakarya Zone, western Turkey. Cretac. Res. 38, 16–39.

Zastrozhnov, D., Gernigon, L., Gogin, I., Planke, S., Abdelmalak, M.M., Polteau, S., Faleide, J.I., Manton, B., Myklebust, R., 2020. Regional structure and polyphased Cretaceous-Paleocene rift and basin development of the mid-Norwegian volcanic passive margin. Mar. Petrol. Geol. 115.